CONTROLLED DRUG DELIVERY FROM BIOMATERIALS USED FOR CARDIAC REPAIR

by

Devin Max Nelson

B.S. Biomedical Engineering, University of Utah, 2007

Submitted to the Graduate Faculty of the

Swanson School of Engineering in partial fulfillment

of the requirements for the degree of

Doctor of Philosophy

University of Pittsburgh

2012

UNIVERSITY OF PITTSBURGH

SWANSON SCHOOL OF ENGINEERING

This dissertation was presented

by

Devin Max Nelson

It was defended on

November 7, 2012

and approved by

Sanjeev Shroff, PhD, Professor, Departments of Bioengineering and Medicine

Steven Little, PhD, Professor, Departments of Chemical and Petroleum Engineering, Bioengineering, and Immunology

Kacey Marra, PhD, Professor, Departments of Surgery and Bioengineering

Kimimasa Tobita, MD, Professor, Department of Developmental Biology

Dissertation Director: William R. Wagner, PhD, Professor, Departments of Surgery, Bioengineering, and Chemical and Petroleum Engineering

CONTROLLED DRUG DELIVERY FROM

BIOMATERIALS USED FOR CARDIAC REPAIR

Devin Nelson, PhD

University of Pittsburgh, 2012

The continued risk of death due to heart failure has spurred the advancement of biomaterials-based treatments for cardiac repair, two of which are the application of a cardiac patch or intramyocardial material injection. The inclusion of signaling molecules in these materials can improve the treatment results; however, appropriate molecule delivery is not trivial. This research presents the broad application of therapeutics from both a patch and injectable system to demonstrate how system properties influence drug delivery and how these systems may be engineered to provide added benefit in the desired application.

We demonstrated the ability to release a gene-inducing molecule, Rheoswitch ligand 1 (RSL1), from a biodegradable elastomer that has been used as a cardiac patch. Not only was bioactive RSL1 released over an extended period, the ability to differentially load scaffolds with RSL1 allowed for spatial patterning of gene expression in cells cultured on the scaffold surface, which has implications for creating complex 3D tissues in vitro. This same elastomeric material was able to release bioactive insulin-like growth factor 1 (IGF1) and hepatocyte growth factor (HGF) in vitro. The complex release behavior of IGF1 into saline was replaced by a much simpler release profile during simulated in vivo degradation, demonstrating that the implant environment must be considered when studying drug delivery behavior.

A strong, thermoresponsive and degradable hydrogel was developed for intramyocardial injection. We showed the release rates of a model protein from this gel, or from protein-loaded microparticles inside the gel, could be controlled by changing the material composition. The combination of hydrogel with microparticles delivered two proteins in a sequential manner. We

further used this system to release bioactive basic fibroblast growth factor (bFGF) followed by IGF1 in vitro. Injection of the unloaded polymer into infarcted rat hearts was able to improve the remodeling process for at least 16 weeks. While increased tissue bFGF and IGF1 were demonstrated following injection of growth factor-loaded gels, there were no clear benefits seen from protein inclusion. This points to the primary ability of the hydrogel alone to benefit cardiac function and cellular environment and warrants further investigation.

TABLE OF CONTENTS

LIST OF TABLES

LIST OF FIGURES

NOMENCLATURE

α-SMA – alpha smooth muscle actin
BDI - 1,4-diisocyanatobutane
bFGF – basic fibroblast growth factor
BSA – bovine serum albumin
CABG – coronary artery bypass grafting
DAPI – 4’,6-diamidino-2-phenylindole
DMEM – Dulbecco’s modified eagle medium
DMSO – dimethyl sulfoxide
ECM – extracellular matrix
EcR – ecdysone receptor
EDA – end-diastolic area
EF – ejection fraction
EPO – erythropoietin
ESA – end-systolic area
FAC – fractional area change
FDA – Food and Drug Administration
FS – fractional shortening
GFP – green fluorescent protein
HEMA – hydroxyethyl methacrylate
HFIP - hexafluoroisopropanol
HGF – hepatocyte growth factor
HUVEC – human umbilical vein endothelial cells
IGF1 – insulin-like growth factor 1
LAD – left anterior descending artery

LV – left ventricle

LVEF – left ventricular ejection fraction

LVEDD – left ventricular end-diastolic diameter

LVEDP – left ventricular end-diastolic pressure

LVESD – left ventricular end-systolic diameter

MI – myocardial infarction

MIC – mean inhibitory concentration

MAPLA – methacrylate polylactide

MeHA – methacrylated hyaluronic acid

MEM – minimum essential medium

MHC – myosin heavy chain

MPEG-PCL-MPEG – methoxy polyethylene glycol–poly (caprolactone)-(dodecanedioic acid)–poly(caprolactone)-methoxy polyethylene glycol

Mn – number average molecular weight

MSC – mesenchymal stem cell

MW – molecular weight

NIPAAm – N-isopropylacrylamide

PBS – phosphate buffered saline

PCL – polycaprolactone

PDGF – platelet derived growth factor

PEG – poly(ethylene glycol)

PEUU – poly(ester urethane)urea

PLA – poly(lactic acid)

PLCL – poly(lactic-co-ε-caprolactone)

PTFE – poly(tetrafluoroethylene)

RA - RheoActivator

RAD16-II – AcN-RARADADARARADADA-CNH2 (where R=arginine, A=alanine, D=aspartate)

RXR – retinoid X receptor

RGD – arginine-glycine-aspartate

RGE – arginine-glycine-glutamate

RR1 – RheoReceptor-1

RSL1 – RheoSwitch ligand 1

SAP – self-assembling peptide

SDF1 – stromal cell derived factor 1

SIS – small intestinal submucosa

SMC – smooth muscle cell

TCPS – tissue culture polystyrene

THF - tetrahydrofuran

TIPS – thermally induced phase separation

TnI – troponin I

VEGF – vascular endothelial growth factor

YIGSR – tyrosine-isoleucine-glycine-serine-arginine

PREFACE

Research in bioengineering is often only possible thanks to the efforts of people extending across many disciplines. Without a doubt, what has been accomplished in my research has been because of the tireless, coordinated effort and expertise of many people from different specialties. It is with great pleasure and humility, therefore, that I have the opportunity to acknowledge those that have been so crucial to this work and to my own development.

I would like foremost to thank Dr. William R. Wagner for being a patient and dedicated dissertation advisor. His level of professionalism is unparalleled. He has taught me how to think and how to plan, from the small details to the big picture, in a way that has allowed me to reach my goals. I know the lessons I have learned from him will positively influence my entire professional career.

To my committee members Dr. Sanjeev Shroff, Dr. Kimimasa Tobita, Dr. Kacey Marra, and Dr. Stephen Little, I am tremendously grateful. They have willingly provided valuable guidance and direction throughout my studies and always had my best interests in mind.

I owe gratitude to the many current and former members of the Wagner Lab that have been invaluable in my research and have become valued friends along the way. Of those I would like to say a special thank you to Dr. Zuwei Ma. He taught me how to become the scientist and engineer I wished to be. He was unbelievably patient and encouraging, even as he spent countless hours helping develop my skills. A special thanks is also due to many gifted surgeons; namely, Dr. Kazuro Fujimoto, Dr. Ryotaro Hashizume, Dr. Tomo Yoshizumi, and Dr. Hongbin Jiang. From surgery to histology and more, their expertise and support made this work possible.

A special thanks to Cory Leeson for providing so much work, insight and skill to these projects. Thank you also to Dr. Yi Hong, Dr. Huili Fu, Dr. Sang Ho Ye, Nick Amoroso, Dr. Antonio D'Amore, Megan Jamiolkowski, Yang Zhu, Anna Blakney, Phillip Choi, Jill Andersen,

and Dr. Rick Koepsel for applying your abundant talents to this research. To Priya Baraniak, who took me under her wing and has been an outstanding mentor, thank you. Joshua Woolley deserves special recognition for his continued support, counsel, and friendship that I have taken advantage of since my first day in the lab. I could not have done much of this without the help and friendship of Vera Kucharski, who had answers to many of the important questions, not least of which was, “When is Dr. Wagner back in town?”

The Artificial Heart Program staff deserve acknowledgement for providing me opportunities to further develop myself as an engineer. In the lives of those treated in the program I was constantly reminded why I started on this path.

On a personal note I would like to thank my church community over these years of graduate school. There have been too many to name that have supported me and my family along the way. I valued your daily Christ-like care and love.

I find myself at a loss for words to express my gratitude to my family during my graduate career. Thank you to my parents, my siblings, and all my in-laws for your love, support and prayers. Your confidence in me was frequently a source of strength and encouragement. Of course, my deepest gratitude goes to my dear wife, Karah, for being my foundation during these years. My heart overflows when I think of the way she sacrificed for me and our children, put up with me when I was being difficult, celebrated my successes, and was always there to support and love me as I strived to reach this goal. Thank you for letting me bore you with reports of new polymer chemistry techniques, controlled-release studies, and in vivo results. Finally, my children have been my strongest motivation. Thank you Joshua and Kambree for believing that I can do anything. Thank you for being understanding when work kept me away from home more than we all would have liked sometimes. Your smiling faces brightened all my hardest days. And thank you to my new baby girl, due in just a few weeks, for again reminding me what this is all for. I can’t wait to tell you all about it!

Funding for this research was provided by the Commonwealth of Pennsylvania and National Institutes of Health grants #HL069368, #T32-HL076124, and #HL105911.

1.0 INTRODUCTION

1.1 SIGNIFICANCE

(Note: A majority of this chapter was previously published as: Nelson, D.M., Z. Ma, K.L. Fujimoto, R. Hashizume, and W.R. Wagner. Intra-myocardial biomaterial injection therapy in the treatment of heart failure: materials, outcomes and challenges. Acta Biomaterialia 2011;7(1):1-15)

It is estimated that a new coronary attack will be experienced by 785,000 Americans annually, while 470,000 will have a recurrent attack.[1] This number of myocardial infarctions (MIs) increases by 20% when one adds silent occlusive events, unrecognized by the individual and often asymptomatic until more extensive tissue damage is incurred.[1, 2] Coronary artery disease and MI provide the underlying etiology in 2 out of 3 cases of heart failure, the widespread, end stage condition that draws heavily on health care resources. Currently 5 million Americans have been diagnosed with heart failure and 670,000 more patients are identified each year, which leads to $33.7 billion in annual direct costs.[1, 3]

The deterioration of patients with ischemic cardiomyopathy is driven by the progressive remodeling in left ventricular (LV) architecture occurring after MI. This is the result of stages of necrosis and fibrosis that lead to cell death, breakdown of extracellular matrix, and scar formation following ischemia. Initially, this remodeling is required for maintenance of cardiac output in the face of decreased pumping capacity but ultimately it leads to LV dysfunction and heart failure, even in the absence of a recurrent ischemic event.[4, 5] Even with current optimal therapy, mortality in end-stage heart failure amounts to 20–50% per year and it is arguable that

there has been little to no improvement in the prognosis for patients with heart failure over the past several decades.[6, 7]

A diverse array of treatment methods and technologies has been developed in an attempt to alleviate the morbidity and mortality associated with cardiac failure.[8] Interventional procedures that seek to revascularize the myocardium through coronary artery bypass grafting and coronary stent placement have become both common and effective when performed early following an MI – though the benefits of such interventions are not as clear in late presenting patients.[9-11] Cardiac pacing in appropriate patients has been shown to increase the energy efficiency of the heart.[12] Pharmacological regimens are useful to improve systolic performance and decrease workload.[13, 14] The gold standard for those with end-stage heart failure remains cardiac transplantation, but donor hearts far outstrip the number of people who could benefit from transplantation.[15] To address this need, ventricular assist device implantation can take over the pumping function of the ventricle by independently circulating blood in late stage heart failure patients. [16, 17] Biomaterials development has played a critical role in the creation of medical devices for advanced heart failure treatment, from membrane oxygenator microporous hollow fibers, to stents and stent coatings, prosthetic heart valves, pacing leads, and many other devices. Important areas of cardiovascular biomaterials research and development for treating heart failure that have grown during the past decade include delivery of materials to the epicardium in the form of a cardiac patch and direct biomaterial injection into the myocardium.[18] Results in these areas demonstrate that the mechanical effects that may be achieved with appropriate biomaterial application may be beneficial independent of any cellular components.

1.2 MECHANICAL APPROACHES TO HEART DISEASE

Myocardial infarction sets off a series of complicated processes that alter the cellular, structural and mechanical properties of the heart.[4, 19, 20] Not only does the heart lose systolic capacity due to a decrease in the amount of functional myocardium after MI, simple geometric changes that take place in remodeling also play a role in heart failure progression. As pumping efficiency decreases, blood backs up in the LV leading to increased intraventricular pressures contributing

to LV dilation – **Figure 1**. While the initial dilation following infarction is believed to be a coping mechanism by which cardiac output can be maintained through the Frank-Starling mechanism, it has been shown that over time the cardiomyocytes lose the ability to respond with increased contractility when stretched, resulting in a dilated, underperforming ventricle.[21] Ventricular dilation in terms of LV sphericity, and particularly LV volume is strongly linked to poor outcomes following MI.[22, 23] This remodeling involves a host of biomechanical processes which alter the local mechanical environment and cellular milieu leading to changes in cardiac performance.

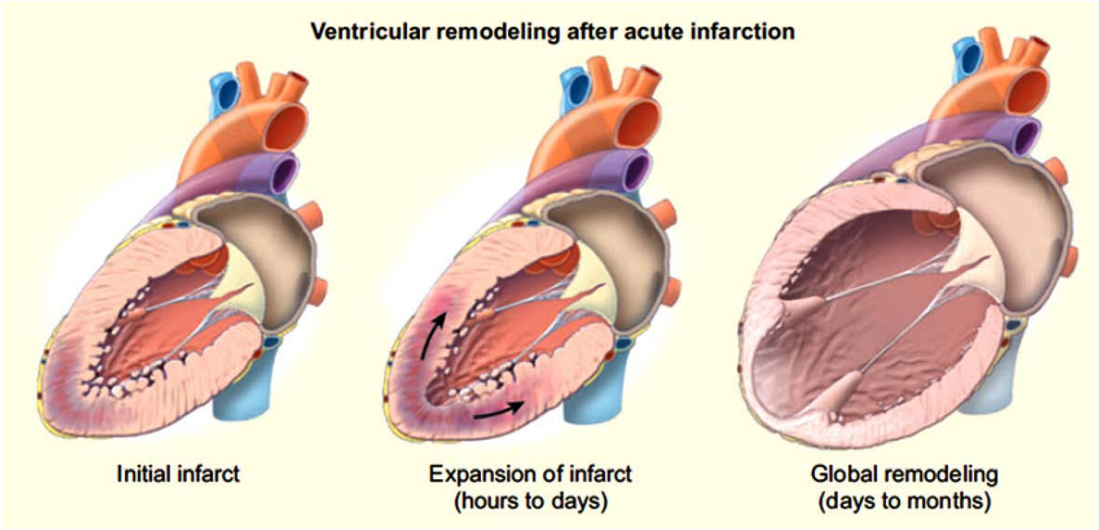

.

Figure 1. Ventricular dilation associated with progressive heart failure. After the initial insult, infarct expansion and ventricular wall thinning contribute to further ventricular remodeling, ultimately causing increased intraventricular pressure and decreased cardiac output (from [8])

Pathological LV dilation is propagated through a positive feedback loop with LV wall stress.[4, 24] This stress is the preload against which the cardiomyocytes must contract during systole. As this stress increases their strain to high levels, the cardiomyocytes lose the capacity to shorten effectively, leading to further stretching and continued decreases in cardiac pumping efficiency, quantified as the ejection fraction (EF). The physics behind this unfortunate positive feedback system can be explained in part by the Law of Laplace, where the stress in the wall of a

round chamber (T) is directly related to the pressure in the chamber (P), the radius of curvature (R), and the thickness of the wall (h), as shown in **Equation 1**. During the ventricular remodeling process following an MI, changes in the local and global mechanical environments causes pressure and radius to increase and the LV free wall to thin. This increases the cardiac wall stress, which ultimately leads to more dilation, thinning, and stress. The heart can proceed down a pathway towards end-stage heart failure where transplantation, hospice care, or ventricular assist device implantation are the only options.

$$T = \frac{PR}{h} \tag{1}$$

Many treatments exist that use mechanical approaches to discourage cardiac dilation, restore geometry, and reduce ventricular wall stress and thinning.[25] Cardiac restraint devices such as the CorCap (Acorn Cardiovascular Inc) and HeartNet (Paracor Medical Inc) employ Dacron and nitinol wraps, respectively, to provide physical support for the failing ventricular wall – **Figure 2**.[26-29] Experimental devices such as the Myosplint (Myocor Inc) and CardioClasp (CardioClasp Inc) force a dilated ventricle into two smaller lobes to reduce the intraventricular radius and thereby decrease wall stress.[30, 31] Advanced surgical procedures such as endoventricular patch plasty (the Dor procedure) and partial left ventriculectomy (the Batista procedure) physically restructure a spherical, dilated ventricle into a more natural elongated shape.[32, 33] These methods have demonstrated limited clinical efficacy in both acute and chronic heart failure patients. One reason for the lack of complete success of these devices may include their inability to address the underlying damage to the native tissue. Even when a restraint device is able to prevent dilation, the myocardium can continue to thin and cardiomyocyte death and tissue fibrosis will not be completely halted.

As the limitations to cardiac restraint devices have been recognized in recent years, other approaches wherein biomaterials interact more actively with the native myocardium and encourage tissue repair have been investigated. The two treatments that have been shown to be of most value for this approach are the implantation of a cardiac patch on the epicardium or injection of a material directly into the myocardial wall. Both of these approaches are under active investigation with many types of materials being applied in an effort to elucidate the material parameters that will provide the most benefit when employed. Understanding what has

been done in both the patch and material injection literature is critical to moving forward in this relatively nascent field of research.

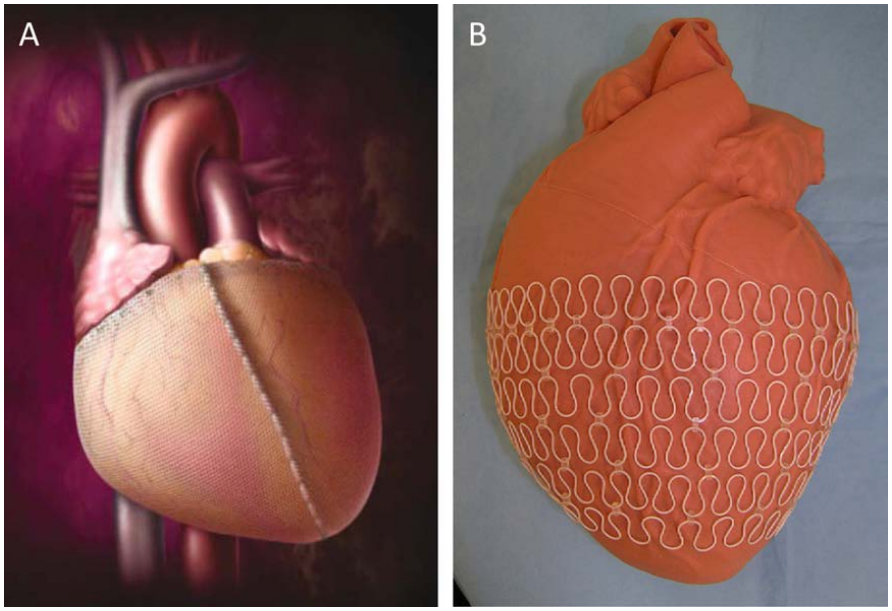

Figure 2. Cardiac restraint devices are used as a means to limit ventricular dilation following MI. The CorCap device (A) uses a Dacron woven mesh to maintain ventricular dimensions whereas the HeartNet (B) surrounds the ventricle in an elastic nitinol metal wrap. (A from [29] and B from [27]).

1.3 CARDIAC PATCH IMPLANTATION

1.3.1 Biological Materials

An important subset of commonly utilized biomaterials is derivatives of natural materials produced by biological systems. Examples of biological materials that are commonly employed for implants include collagen, fibrin and extracellular matrix (ECM) derivatives. These materials have been applied in a variety of physiological environments because they often have acceptable levels of biocompatibility without significant processing, and are readily accessible to clinicians

and researchers. Thus, it is not surprising that early studies evaluating biomaterials as a cardiac patch have employed these materials.

While various biological materials have been used as a cardiac patch following myocardial infarction, few of these materials are used individually for the purpose of providing mechanical support and aiding in regeneration. The primary material that has been explored as a patch is collagen, though usually in conjunction with cellular delivery which will be discussed later. Porous collagen scaffolds without cells were implanted immediately after cryoinjury in rats – **Figure 3**.[34] The scaffolds were all but degraded 60 days after implantation and demonstrated significant angiogenesis and arteriogenesis in the scaffold region. While patches were heavily infiltrated with macrophages, no cardiomyoblasts or cardiomyocytes, and few cells staining positive for cardiac stem cell markers, were observed. The functional role that the observed angiogenesis had on cardiac function remains to be explored in this model. In a similar study however, there was no detectable benefit to collagen patch implantation immediately after left anterior descending artery (LAD) ligation in rats.[35] While angiogenesis was mildly spurred by patch implantation there was no benefit in terms of contractile behavior or remodeling. Besides a mild improvement in intraventricular pressures, a similar lack of benefit was seen when gelatin, a derivative of collagen, was used as a patch material.[36] These results suggest collagen to be an inadequate material for this application.

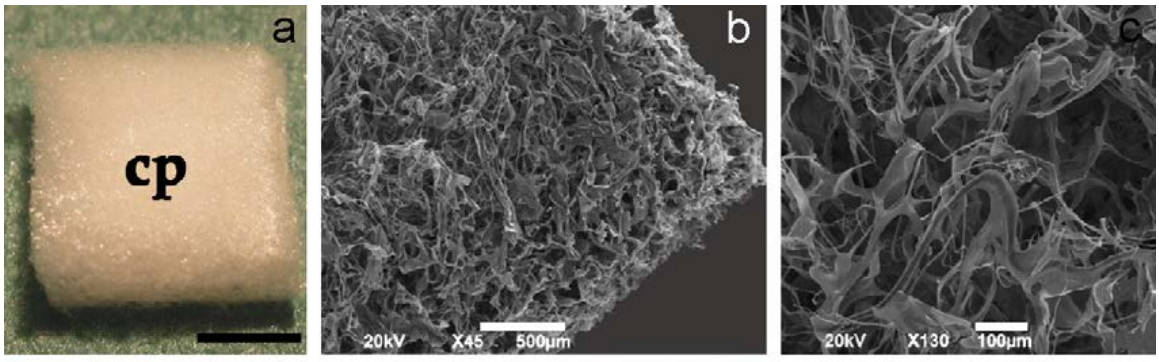

Figure 3. Optical (a) and SEM (b,c) images of an acellular cardiac patch (cp) made from collagen. The high porousity and fiber structure of the collagen are apparent. (From [34]).

A similar lack of effect was seen when fibrin patches were applied to the heart in a porcine ischemia reperfusion injury. There was no significant benefit to functional performance or histological assessment compared to control infarcted animals.[37] When a fibrin material bound to poly(ethylene glycol) (PEG) was used it showed a mild ability to prevent infarct expansion though this did not translate to functional improvements.[38] The reason for the lack of effect may be related to many factors including mechanical environment or lack of biological activity.

A sheet of decellularized ECM of porcine small intestinal submucosa (SIS) was used by Tan et al as a patch on 4 week old infarcts in rabbits.[39] The material was shown to have good integration into the host myocardium, be infiltrated with macrophages and fibroblasts, and show new collagen deposition after 4 weeks. This may have contributed to the increased angiogenesis and wall thickness shown after patch implantation compared to control animals. Importantly, the function of hearts receiving the SIS patch was also significantly better than controls. This was demonstrated by an improved EF, decreased dilation, and lower LV end diastolic pressure (LVEDP).

Krupnick et al investigated the application of a scaffold combining both biological and synthetic components to make a patch for full-thickness myocardial replacement following ventriculectomy.[40] The patch consisted of a solution of type I rat tail collagen, Dulbecco's Modified Eagle's Medium (DMEM), horse serum, and Matrigel which is poured into a poly(lactic acid) (PLA) porous, non-woven mesh and allowed to gel. This scaffold is then attached to a poly(tetrafluoroethylene) (PTFE) sheet which facilitates the patch attachment to the myocardium. It was demonstrated that this construct could be successfully implanted with good proximity between native myocardium and the patch. The presence of the patch was able to increase ventricular volumes as desired. The behavior of this scaffold as a long-term substitute for the myocardium following ventriculectomy is yet to be explored though the increased biological activity from collagen and Matrigel, as well as the degradation of the scaffold components, may make this a more appealing option than PTFE alone – the current material of choice for this procedure.

1.3.2 Synthetic Materials

Materials that can be designed and synthesized in the laboratory from primary building blocks offer some advantages over those adapted from biological systems. In particular, every stage of material synthesis is under control of the engineer, allowing for material generation to meet specific design objectives, such as degradation, mechanical, and biocompatibility properties. A trade-off for this control is that synthetic materials are generally more likely to trigger inflammatory and foreign body responses that can be avoided for some minimally processed natural materials. Introducing biomolecules into the design process and utilizing labile synthetic materials that degrade into non-toxic components can potentially minimize the undesired effects associated with permanent foreign body implantation.

Many synthetic materials have been approved for use in various surgical applications and devices. For example, materials such as PTFE and PET have been employed in vascular grafts for many years with significant success. Degradable materials such as PLA have revolutionized suture technology. While usually employed with a cellular component, these kinds of established synthetic materials represent the majority of materials that have been used for cardiac patches.

The use of a slow degrading, highly porous polyurethane patch has been explored both in short-term and long-term implants.[41, 42] Rats were implanted two weeks after infarction by permanent ligation of the LAD. Following patch application it was found that results for patched animals were nearly identical to sham animals who received no treatment, when looking at EF, dilation, and LV pressure generation. Whereas sham animals had significantly worse function 6 months after sham treatment, patch animals had regressed to the same deteriorated state by 9 months. Over the course of a one-year follow-up there was some angiogenesis in the patch but no evidence of patch degradation.

In contrast, Fujimoto et al showed that a quicker degrading poly(ester urethane)urea (PEUU) patch with greater elasticity was shown to halt LV functional deterioration when sutured onto the epicardium 2 weeks after infarction – **Figure 4**.[43] This material prevented further dilation and was associated with the formation of a new smooth muscular layer in the infarct zone, possibly due to the stress shielding provided by the patch. Additionally the global mechanics of the LV stress-strain relationship was closer to native myocardium after patch

implantation than infarct control animals. Further investigation of the new smooth muscle cells in the infarct zone showed they co-expressed proteins α-SMA, α-actinin, cardiac troponin T, connexin 43, and genes Nkx-2.5 and GATA-4.[44] This expression was shown to be similar to cells in the embryonic rat heart during development and designate these cells to be on a myocardial lineage. While the benefit of material implantation was also manifest by increased reserve in dobutamine stress testing, there was no evidence that the smooth muscle cells take on an adult cardiomyocyte contractile phenotype. This same material was also applied as a full thickness patch for reconstruction of a right ventricular outflow graft defect.[45] This patch material allowed significant cellular infiltration and was completed degraded at the 3 month endpoint leaving behind only native tissue in the sealed defect. By comparison, non-degradable PTFE patch controls showed no cellular infiltration and had increased inflammation throughout the study. Taken together, these results suggest that material properties of degradation time and mechanics may play important roles in the success or failure of a particular patch material.

Polyester patch materials have also been employed as cardiac patches with mixed results. For example, poly(glycolide-co-ε-caprolactone) was implanted as a cardiac patch 1 week after an ischemia reperfusion injury in rats.[46] At the 4 week echocardiography assessment these patches showed significantly better fractional shortening (FS), left ventricular end diastolic diameter (LVEDD), LV end systolic diameter (LVESD), and LVEDP than saline control groups. Importantly, the results were the same as patches that had been loaded with stem cells. On the contrary, poly(lactic-co-ε-caprolactone) (PLCL) patches showed no improvements over saline control animals 4 weeks after implantation in a rat cryoinjury model.[47] While functional and geometric parameters were not improved by placement of the patch there was evidence of increased expression of cardiomyocyte proteins myosin heavy chain (MHC) and troponin I (TnI) in the infarct zone. It is interesting to note the differences in these two studies considering the general similarity between materials used. This highlights the need for further investigation into what material properties and deployment techniques may provide the greatest benefit in this therapy.

Overall it appears that the material that is used in a cardiac patch can influence the outcomes seen after treatment. While biological materials may have inherent biocompatibility, they seem generally unable to provide much benefit when used alone as a cardiac patch. The

highly variable results that can be seen when similar materials are applied points to the need for further research in this field. Synthetic materials have been able to show some good improvements to cardiac function after implantation. It may the mechanical properties of some of these materials or it may the inflammatory response that comes with their use that provides cell infiltration and support to the failing ventricle. As will be shown presently, the combination of a patch with signaling molecules may augment the results shown with patch alone for some materials.

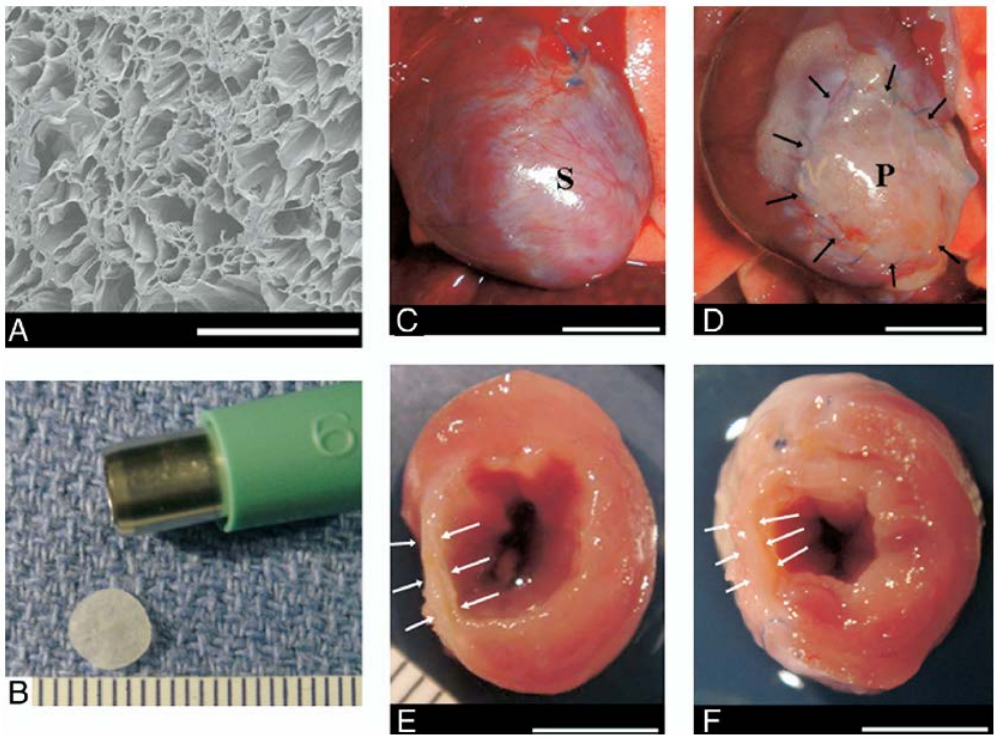

Figure 4. Electron micrograph of a porous polyester urethane urea material used as a cardiac patch (A). Macroscopic image of patch before implantation (B). Representative images, 8 weeks after implantation, of the anterior view of infarction control (C) and patched (D) hearts. The cross-sectional view of both groups is shown in E and F, respectively. Black arrows point to the implanted patch, and white arrows indicate the infarcted anterior wall. Scale bar: 500 µm in A, 1 mm in B, 55 mm in C to F. P = the patch implanted area; S = the infarcted scar. (From [43])

1.3.3 Cardiac Patch Materials Including Drug Delivery

There has been significant research into direct injection of growth factor solutions into the heart for therapeutic angiogenesis, including in human clinical trials.[48-50] However, the controlled release of signaling molecules from scaffolds for the cardiac patch application has received notably less attention. What reports do exist suggest that inclusion of signaling molecules in the cardiac patch can be beneficial and warrants further investigation. In one report, the release of 1.5 μg of basic fibroblast growth factor (bFGF) from alginate patches was studied. The left coronary artery of rabbits was permanently ligated followed by immediate application of an alginate epicardial patch. This patch was mostly degraded at the 4 week endpoint suggesting nearly all of the growth factor would have been delivered by that time. While the data on cardiac function under rest conditions was not better for patches with bFGF compared to those without, staining of CD31 positive cells did show increased angiogenesis when bFGF was present. The presence of growth factor also trended towards smaller infarcts. When hearts were stressed by norepinephrine those that received the patch or the patch with bFGF had better pressure responses in the LV than control animals.

In the case of stromal cell derived factor 1 (SDF1), which has been shown to be upregulated after infarction in the heart and is responsible for stem cell recruitment, controlled release may be beneficial following MI.[51, 52] Zhang et al. used a PEGylated fibrin that bound SDF1 as a cardiac patch immediately following infarction in a mouse model.[38] In vitro characterization showed that the SDF1 was completely released within 10 days and was equivalently bioactive to unbound SDF1. In vivo it was shown that the number of ckit+ cells was higher at 2 and 4 weeks after implantation in the SDF1 patch group compared to direct injection of SDF1. It is notable that there were more ckit + cells after one week in the SDF1 injection group, followed by a steep decline in later weeks. This shows the longer term benefits of the controlled release mechanism compared to direct injection of growth factor. The SDF1 patch groups also had an improved EF after 4 weeks compared to controls and patch without the growth factor, demonstrating the functional benefits of this approach.

1.4 BIOMATERIAL INJECTION

The use of biomaterials for cardiac repair has primarily focused on applications where the material is anchored to and interacts with the outer edges of the myocardium to provide support. Incorporating the material completely within the heart wall is an alternative approach where direct contact with cardiac cells occurs as the material acts as a bulking agent for the heart wall. Generally, materials are delivered through direct epicardial injection at distinct locations in and around the infarct leading to focal points of biomaterial presence – **Figure 5**. Current methods for direct injection have required sternotomy or thoractomy, though thorascopic or intravascular procedures could be feasible to decrease procedure-related morbidity. Not only may the injected material alter the mechanical environment upon injection, but appropriate biomaterials can have biological functions that encourage cardiac repair. Functions such as angiogenesis, cardiomyocyte protection, and stem cell recruitment may be another primary means to improve the efficacy of material injections for treating heart disease.

In 2006, a report by Wall et al. utilized a finite element model to evaluate the theoretical effect on cardiac wall stress of injecting a noncontractile biomaterial into the LV wall.[53] The injected volume changes the LV geometry by increasing the wall thickness, thus lowering local wall stress. The simulation showed that injection of a volume 4.5% of the total LV wall volume and with a stiffness 20% of the natural LV tissue into the infarct border zone could decrease the wall fiber stress in the border zone by 20% compared to a control simulation in which there was no injection – **Figure 6**. The mechanical simulation also showed that this attenuating effect on LV wall stress increased with the injection volume and modulus of the injected material.

Importantly, while this model demonstrated a slight increase in EF following material injection, a more precise measure of global cardiac function, namely stroke volume divided by LV end-diastolic pressure, was unchanged. This disparity results from the fact that EF is computed from geometric factors and thus changes in ventricular geometry from the presence of material can cause higher EF calculations without real functional improvement. Because EF is a common clinical metric of heart performance it is advisable to confirm perceived improvements to EF with other measures of function. Reductions in cardiac wall stress computed after material injection have been corroborated by recent finite element modeling where mean myofiber stress

for the entire LV can be reduced by 15% and 5% at end-diastole and end-systole, respectively, depending on number and configuration of injection sites. [54] These finite element models, in conjunction with an understanding of the Law of Laplace, provide the theoretical basis for growing interest in injectable biomaterials to treat cardiac failure.

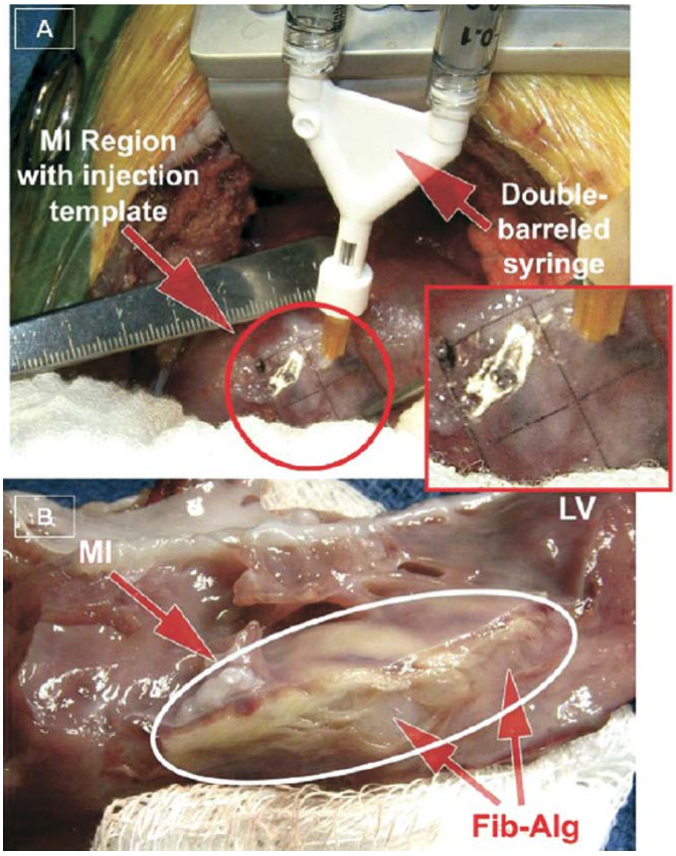

Figure 5. Direct epicardial injection of a fibrin–alginate composite into porcine myocardium. (A) Using a grid template, material was injected from a double-barreled syringe to distinct points across the infarcted area. (B) A myocardial cross section reveals the material present as amorphous compartments at the injection sites. (From [55]).

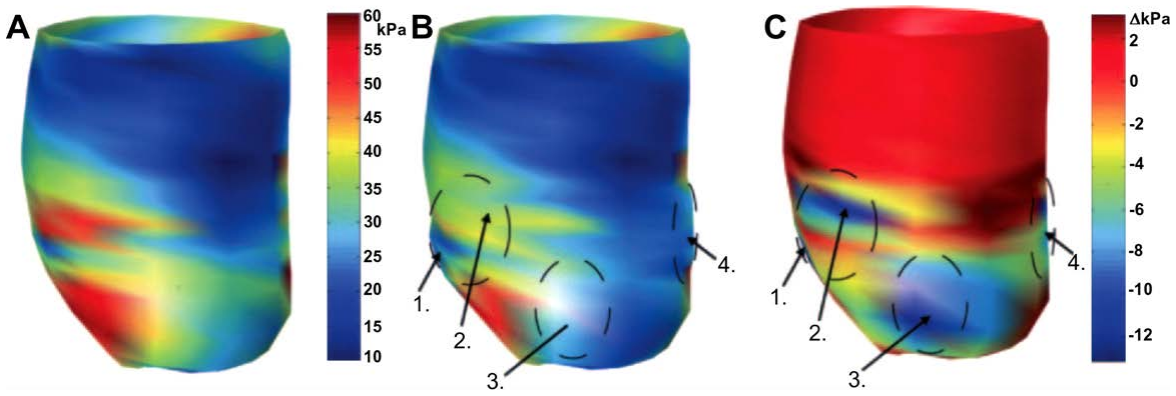

Figure 6. Representation of mid-wall ventricular fiber stress as a function of position in the heart. (A) Wall stress with an apical infarct (red is higher stress localized near the infarct). (B) Wall stress with injection of a theoretical gel material at four different numbered locations peripheral to the infarct region. (C) The difference in the previous two images. A marked reduction in wall stress is seen due to injection therapy (cooler colors representing reduced stress). (From [53]).

1.4.1 Biological Materials

Inherent in the application of materials to intramyocardial injection therapy is the ability to pass the material through a small needle. Examples of biological materials that are amenable to injection delivery include collagen, gelatin, fibrin and alginate. These materials have been investigated extensively and thus the processing parameters needed to change material properties is well understood. This provides a framework to change the injectability and mechanical properties of these materials for this application.

1.4.1.1 Alginate

Alginate, a linear block copolymer of (1-4)-linked β-D-mannuronate and α-L-guluronate residues, is bioinert and does not support cell attachment.[56] However, modifications to alginate, such as introduction of the cell binding sequence arginine-glycine-aspartate (RGD), can significantly improve attachment.[56, 57] The material properties of alginate, especially mechanical strength and degradation rate have been extensively studied leading to a good understanding of methods to adjust these properties[58]. Increasing alginate concentration in solution increases mechanical strength but also increases solution viscosity, which may be undesirable when material injection is desired. However, it has been demonstrated that a mixture

of high and low molecular weight (MW) chains can lead to a relatively high elastic shear modulus of 10-24 kPa while still maintaining a low viscosity of less than 2 Pa s.[59] Variations in alginate composition and ionic makeup can vary the elastic modulus of the gel widely from 5 to 55 kPa.[60, 61] The same characteristics of alginate that influence mechanical properties, such as molecular weight, also influence the degradation time of the gel. To further tailor degradation time alginate polymer chains can be partially oxidized by reaction with sodium periodate, which ultimately provides hydrolysable bonds to speed degradation.[62] Alginate has been used in both drug delivery and tissue engineering applications with marked success.[56-58, 63, 64]

Landa et al. aimed to study the ability of alginate to improve LV remodeling and function when injected as a bulking agent into the myocardium. [65] They compared the results of injecting 150 μL of alginate (MW 30 kD) solution into both recent (7 days after) and old (8 weeks after) infarcts. Eight weeks after material injection into recent infarcts LV geometry was improved in the biomaterial group in the form of increased LV wall thickness and attenuated LV dilation compared to control hearts that received a saline injection. The improvements in old infarcts were less pronounced demonstrating the greater difficulty in rescuing a chronically infarcted heart. Using a biotin-labeled alginate, histological sections were able to accurately track material degradation in vivo. One hour after injection alginate occupied 45% of the infarct area, but this decreased to 6% after six weeks. Of particular note, material injection was compared to injection of $1x10^6$ neonatal cardiomyoctyes in saline with similar or better results in all measures for material injection alone. In other reports alginate was able to show significantly improved cardiac function in terms of fractional area change (FAC) or fractional shortening compared to saline injection controls. The improvements in FAC and FS associated with alginate injection were demonstrated for as many as 5 to 8 weeks after injection, and even in a chronic infarct model where injections occur several weeks after infarction. [66, 67]

A mixture of alginate polymers with molecular weights of 125 kD and 5 kD at a ratio of 75:25 High MW: Low MW was injected in the peri-infarct region of rat hearts 7 days after coronary ligation.[68] The histological evaluation showed the inert properties of alginate, as the material was unable to increase capillary density or α-actin positive smooth muscle cell (SMC) density 28 days after injection. In this material 1% of the alginate sugar residues were oxidized by incubation with sodium periodate, to increase the material degradation rate. In vivo only a

third of all hearts showed any material left at the 28 day endpoint – and then only in small fragments. The lack of angiogenesis in this study after alginate injection has not been universally observed. Other studies have reported that plain alginate injection into the myocardium can cause mild increases in capillary and arteriole density and myofibroblast infiltration. [55, 65, 66, 69, 70] The direct cause of the increased cell population is not completely understood but may be related to the alginate creating a healthier microenvironment through stress shielding. Alternatively, the inflammatory response to the foreign body injection may similarly have triggered increases in local cellular content. For cardiac biomaterials injection studies in general it is difficult to separate the underlying cause of the observed effects. While mechanical effects are most commonly hypothesized, the material-related inflammatory response is potentially contributing in concert or independently.

In order to improve upon results from cardiac injection of alginate alone by facilitating greater cellular infiltration into the material, the cell adhesion peptides RGD and tyrosine-isoleucine- glycine-serine-arginine (YIGSR) have been introduced into the polymer backbone.[66, 70] While in vitro studies confirmed that these peptide sequences allowed for improved cell attachment, functional and histological results with peptide-modified alginate have been mixed. For example, Yu et al. reported that 2 days after injection, both unmodified alginate and RGD-alginate showed mild improvements in FS and wall thickness but after 5 weeks no functional difference was seen between peptide-modified and plain alginate. However, there was a significant increase in arteriole density after 5 weeks in the RGD-alginate compared to plain alginate and saline injected control animals, indicating some local biological effect. While these results would suggest that the cell adhesion sequence may be beneficial for angiogenesis, a report by Tsur-Gang et al. showed that injection of alginate modified with both RGD and YIGSR peptides was not able to cause improved function or increase angiogenesis compared to unmodified alginate or alginate with a nonsense arginine-glycine-glutamate (RGE) peptide attached. Even though RGD/YIGSR-modified alginate showed the lowest blood vessel density compared to plain and RGE alginate, it was still able to maintain scar thickness. It is unknown why there was not a stronger cellular response in the RGD/YIGSR alginate group but the authors speculate that the modification, which involved 0.2% of uronic acid monomers, may have been inadequate or that the peptides were not well exposed to surrounding cells.

Another interesting approach to encourage cell infiltration into alginate was the blending of polypyrrole with alginate.[69] Polypyrrole, though mechanically brittle, may be particularly advantageous for cardiac injection because of its ability to conduct electrical signals and encourage endothelial cell growth.[71] Injection of 0.025% w/v polypyrrole with alginate led to significantly higher arteriole density than injection of alginate alone. The authors reasoned that increased cell attachment to polypyrrole, as was demonstrated in vitro, as well as improved electrical conductivity through the infarct region may have encouraged cell growth and arteriole formation.

While the most common delivery site for injectable biomaterials is through an epicardial approach, a recent report demonstrates that intracoronary injection of appropriate materials may be possible without detrimental side effects. An alginate-calcium solution was injected intravascularly into the left anterior descending artery of pigs post-MI through a coronary catheter.[72] The vasculature in the injured myocardium becomes leaky after infarction, allowing the alginate polymer to diffuse across the permeable endothelium into the extravascular space. While the alginate solution is unable to gel in the vasculature due to inadequate calcium ion concentration, within the myocardium the calcium concentration is adequate to allow ionic crosslinking and gel formation throughout the myocardial wall – **Figure 7**. Different volumes of alginate solution were injected and results studied for 60 days. It was demonstrated that the volume injected was related to the measured benefit, as injection of 2 ml had better outcomes than 1 or 4 ml. It is not clear what volume is optimal for cardiac injection therapy but this report suggests that an optimal range may be desired wherein there is enough material to provide mechanical benefit but without impinging on diastolic expansion. In this study, even though the material was completely removed by the 2 month endpoint, improvements to FS and wall thickness remained. This method allows for diffuse delivery noninvasively but may lead to other concerns. For example many patients with heart failure also have co-morbidities such as diabetes and peripheral vascular disease.[73] Damaged blood vessels from these conditions may allow for alginate deposition and gelation in undesired locations, the effects of which are not known. It will be necessary for appropriate controls to prove efficacy, or appropriate patient selection to make this a clinically feasible approach.

Figure 7. Two hours after intracoronary injection of alginate the material had migrated from the vascular space and was found throughout the myocardial wall in a porcine model. The presence of this material led to increased wall thickness, which persisted after the material had degraded 6 weeks later. (From [72]).

1.4.1.2 Fibrin

Fibrin, which has been used as a biomaterial in a broad array of applications for decades, has been reviewed extensively.[74-76] A fibrin "glue" or fibrin "sealant" aims to reproduce the final steps of the coagulation cascade which forms a three dimensional cross-linked fibrin network. This occurs when fibrinogen is cleaved by thrombin into fibrin monomers that self-assemble and are subsequently cross-linked by factor XIIIa. In commercially available fibrin sealants such as Tisseel (Baxter Healthcare) or Crosseal (Ethicon Inc) the reactive components that form the fibrin clot come in contact only upon injection through a double-barreled syringe. One of the solutions consists of fibrinogen mixed with anti-fibrinolytic agent aprotinin, while the other solution contains thrombin, factor XIIIa and calcium ions. The deposited fibrin, which is digested by the enzyme plasmin, is usually completely degraded within days to weeks depending on implant location and the concentration of aprotinin. The material properties of these sealants depend on the starting solution compositions. For example, increasing the thrombin concentration increases clotting speed and also leads to stronger networks. A high fibrinogen concentration (70 mg/ml) can provide an elastic modulus up to 40 kPa compared to 10 kPa for a low concentration (30 mg/ml).[77] Importantly, fibrin sealants have been FDA approved in certain applications as a sealant or to aid hemostasis, allowing ready access in most operating rooms.

Fibrin injected into rat hearts following creation of an infarct by ischemia-reperfusion injury has been shown to yield positive results.[67, 78-81] Injection of 50 μL of fibrin into one site in week-old infarcts prevented wall thinning and maintained FS over 5 weeks after injection, even though the material is resorbed within 2 weeks.[78, 82] In contrast, injection into 5 week-old infarcts did not improve FS 5 weeks after fibrin injection.[67] After injection of fibrin infarct size, as measured by the ratio of infarcted LV area to total LV area, is consistently reduced compared to negative control studies. Arteriole density, but not capillary density, was increased after fibrin injection compared to bovine serum albumin injection, and importantly it was proven that the new arterioles formed were found within the infarct zone, were functional, and were connected to the existing vasculature. [80, 81] Since arteriole formation was consistently associated with fibrin injection, but functional improvement was not, improvements to the vasculature alone do not appear to be sufficient for improving long-term function.

A report of myocardial injection in a large animal model involved fibrin injection into infarcted porcine hearts.[55] Researchers injected 200 μL of a composite of fibrin with gelatin-grafted alginate into each of 25 points on a grid across the infarct area. While the report did not demonstrate functional improvement the researchers did show increased posterior wall thickness for one week following injection and infarct expansion was prevented for two weeks after injection. Likely due to the presence of alginate in the fibrin clot, material was still detected at three weeks. While limited conclusions can be drawn from this study, it is notable as one of the first reports of biomaterial injection therapy applied to a large animal model.

1.4.1.3 Chitosan

Chitosan, a cationic polymer derivative of chitin, has been used in biomedical, tissue engineering, and drug delivery applications because of its general biocompatibility, capacity to form porous structures and gels, and tunable degradation rate.[83, 84] While being soluble in acidic aqueous solutions through protonation of its many amine groups, neutralization of chitosan aqueous solutions to a pH exceeding 6.2 systematically leads to the formation of a hydrated gel-like precipitate.[85] Chitosan aqueous solutions can be transformed from purely pH-dependent solutions into temperature-controlled pH-dependent chitosan solutions by mixing with polyol salts bearing a single anionic head, such as glycerol-, sorbitol-, fructose- or glucose-

phosphate. Conjugation of hydrophobic groups such as hydroxybutyl to the hydroxyl and amino reactive sites of chitosan can also confer temperature-responsive properties. [86] Thermal responsiveness allows chitosan to be optimized for injection, with achievable elastic moduli over 5 kPa reported after gelation.[85]

A thermally responsive chitosan formed by mixing chitosan with β-glycerol phosphate and hydoxyethyl cellulose has been injected into infarcted rat hearts one week after an ischemia-reperfusion injury. Injection of the material, which was almost completely degraded by 4 weeks, was shown to improve FS and decrease dilation to the same extent as injection of stem cells alone, and better than saline injections alone.[87] A new material developed by Yeo et al. combined an azidobenzoic acid-modified chitosan with an acryloyl-PEG-RGDS to make a photocrosslinkable gel for use in injection therapy.[88] The material was able to form a gel in situ after two minutes of UV irradiation and had a shear modulus up to 370 Pa. This material was shown to support cell growth at a level comparable to tissue culture polystyrene and was able to release VEGF in vitro for more than 24 days. While not yet studied in vivo, this material does represent the growing interest in enhanced material properties through improved material design for the field of cardiac injection.

1.4.1.4 Extracellular Matrix and Derivatives

Extracellular matrix-derived materials are generally comprised of structural proteins such as collagen, laminin, fibronectin, and vitronectin, as well as an array of glycosaminoglycans, and are specific to their tissue source. ECM is naturally bioactive, is important in cell signaling and in the case of cardiac ECM, plays an important role in the inflammation and remodeling process following MI. [89, 90] Because cells are naturally inclined to interact well with ECM it is often used as scaffolding for tissue engineering applications.[91] Degradation speed of these materials is determined by the cellular milieu in vivo and factors such as concentration and extent of cross-linking. For example, gelatin, a denatured derivative of collagen, is much weaker and degrades quicker than its parent molecule.[92] The mechanical strength of injectable ECM derived materials is generally low. For example, the storage modulus, as determined by parallel plate rheometry, of injectable collagen is in the range of 20 to 80 Pa. Matrigel (Beckton & Dickenson),

an ECM gel generated by mouse sarcoma cells, is comprised primarily of collagen and has a modulus of 30 to 120 Pa.[93, 94]

Gelatin has been injected into infarcted rat hearts but without improvement to function or histology after 4 weeks.[95] Gelatin was present in half the hearts after 2 weeks in vivo but was completely absent after 4 weeks of injection. Collagen has had slightly better results.[96] Injection of 100 μL of collagen at a single point in the infarct zone led to a higher EF than saline injection 6 weeks after treatment. Surprisingly the injected material did not allow for cell infiltration or angiogenesis, and thus seemed to behave similarly to the native collagen-rich infarcted tissue. The increased EF may have been a consequence of the increased wall thickness that was observed after injection. In contrast, Huang et al. were able to show improved myocardial angiogenesis and myofibroblast infiltration into injected collagen.[81] The reason for these disparate results could be related to the infarct model. No angiogenesis or cell infiltration was seen when injection occurred one week after infarction, whereas there was cell infiltration if injected after just 30 minutes of ischemia. This result may further indicate the difficulty in salvaging late-stage diseased tissue and reflect the importance of timing in therapeutic application.

Injection of Matrigel was able to form a collagen-fiber network that ran parallel to that of the host myocardium and integrated with native collagen.[97, 98] For ischemic hearts Matrigel injection was able to improve FS and wall thickening 4 weeks after treatment. While the application of Matrigel clinically is questionable due to its tumor cell source, ECM from a variety of animal tissues are routinely applied in a variety of settings and are of interest in cardiac applications. For injection therapy, a mechanically ground digest of ECM from small intestinal submucosa was hydrated and injected into infarcted rat hearts.[99] The ECM material was able to improve function and decrease remodeling in the 6 week follow-up compared to infarct controls. As was hypothesized, the ECM material increased cell infiltration into the infarct zone. There was a significant increase in myofibroblasts, macrophages, and importantly, c-kit positive cells. ECM-injected hearts had substantially more stem cell factor and VEGF present. This study demonstrates a relatively high level of regeneration in the form of stem cell recruitment and muscle repair that can be elicited by biologically active ECM, and sets the stage for future work using similar materials.

Under the belief that ECM of a certain tissue type is going to best facilitate regeneration of that tissue, many groups are interested in using tissue-specific ECM materials for tissue engineering. In a pilot study, Singelyn et al. injected a hydrogel made of digested porcine cardiac ECM into healthy rat hearts.[100] Animals were sacrificed 11 days after injection to demonstrate that the ECM was still present and in morphology similar to intact decellularized cardiac ECM. Both in vivo and in vitro results showed that SMCs and endothelial cells migrate to and infiltrate the ECM biomaterial. The ability to use pericardial ECM for cell injection has also been recently demonstrated.[101] This tissue source is important as it may allow for injection of autologous ECM. Both human and porcine pericardial ECM gels supported arteriole formation within the injected material in healthy rat hearts and a few c-kit+ precursor cells to be recruited around the material. These studies demonstrate the potential that ECM materials may have for this application, although without results from injection into injured hearts, more detailed conclusions cannot be made.

1.4.1.5 Comparative Studies

Unfortunately, only a few studies have directly compared different types of materials for cardiac injection.[67, 81] In these studies the specific differences in material properties can be more directly linked to outcomes since all other study parameters are held constant. In one report, fibrin, collagen, and Matrigel were each injected 1 week after an ischemia-reperfusion injury into separate groups of rats. While lacking data on cardiac function, this study did show that for all three materials there was a similar increase in myofibroblast infiltration, capillary density, and arteriole density compared to saline injection. In another report, by comparing alginate to fibrin injection the importance of material residence time may be demonstrated.[67] Two days after injection both of these materials caused similar increases to wall thickening, decreased intraventricular diameters, and increased FS – **Figure 8**. After five weeks however, the fibrin-injected hearts no longer maintained improved function despite largely preserving LV wall thickness. Alginate on the other hand improved FS, albeit at levels less than was shown at 2 days. An obvious difference between groups was that the alginate was still present in substantial amounts after 5 weeks, whereas fibrin was completely resorbed. The continued presence of a material that may provide physical support in this case appears to be more advantageous.

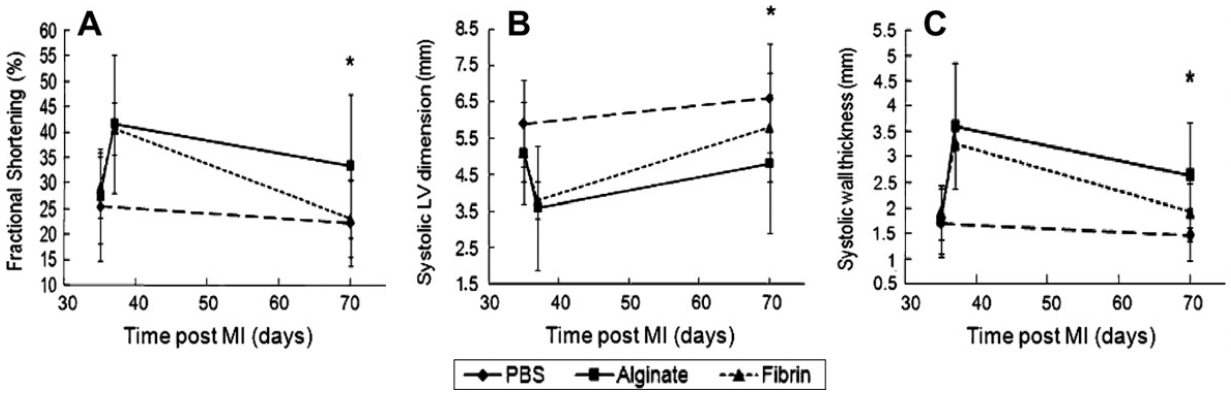

Figure 8. Comparison between injection of fibrin or alginate into 5-week-old infarcts in rats. Two days after injection both materials demonstrated equivalent improvements to FS, (A) LV dimension (B) and wall thickness. (C) Five weeks after treatment the fibrin group lost much of the advantage seen at 2 days, whereas alginate retained a significant improvement (*p < 0.05). (From [67]).

A recent study aimed to evaluate the how mechanical strength of the injected material can influence outcomes following cardiac injection.[102] Methacrylated hyaluronic acid with 30% (MeHA Low) and 60% (MeHA High) methacrylate substitution were injected into ovine infarcts and crosslinked in situ. While the two materials demonstrated similar degradation rate, cellular response, and tissue distribution the storage modulus of the MeHA High group was over 3 times higher than that of the MeHA Low group. In vivo, the stronger material allowed less infarct expansion and LV dilation compared to the weaker material. Functionally, MeHA High was associated with better EF than MeHA Low after 8 weeks, especially under cardiac stress testing. By evaluating the functional effects of manipulating a specific material property, in this case mechanical strength, this comparative study provides further guidance for future material development.

1.4.2 Synthetic Materials

As stated above, there are specific advantages to using synthetic materials that revolve around the engineer's ability to control material properties to meet the desired specifications. The requirement for the material to be injectable can present a significant level of complexity to material design. Approaches that involve in situ polymerization or crosslinking are often

associated with high cytotoxicity making them unattractive for in vivo applictions. Because of this, self-assembling and temperature-responsive materials make up the majority of injectable synthetic materials used for cardiac application. Controlling the proclivity for self-assembly and the transition temperature of thermoresponsive materials becomes the main focus of material scientists in designing and implementing these materials. Further, controlling these parameters while simultaneously controlling properties such as mechanical strength and degradation rate, makes both the difficulty and the potential versatility of using these materials apparent.

1.4.2.1 Self-Assembling Peptides

Nature is replete with examples of materials that self-assemble to create larger structures. Materials ranging from lipids to proteins can form complex shapes with minimal outside influence so long as the appropriate complementarities exist between building blocks. Engineers have long sought to utilize self-assembling behavior to build materials on a small scale.[103, 104] For example, peptides with specifically placed amino acid sequences can self-assemble into macroscopic materials that have been shown to support cell growth and have been considered as injectables for cardiac wall therapy.[105, 106]

Peptides with the amino acid sequence AcN-RARADADARARADADA-CNH_2 (RAD16-II), which form a nano-fibrous 3D gel, have been studied extensively for cardiac injection to repair the myocardium after MI. Injection of 10 µL of this gel into a non-infarcted LV free wall showed significant host cell infiltration including endothelial cells and cells that exhibit some cardiac-specific markers even though the peptide sequence did not possess any cell recruitment signals.[107] However, injection of 80 µL of the same material into sham animals in a similar study showed a temporary decline in FS and LVESD before returning to normal levels after 2 months.[108] This indicates that while this material may be advantageous on a cellular scale, the addition of the non-contractile material in a healthy heart may have a transient negative effect on systolic function in healthy animals. For the more relevant infarction model, RAD16-II nanofiber injection into a rat heart immediately after coronary ligation has not been able to improve cardiac function, geometry, or histology compared to MI control groups.[108-110] The lack of improvement has not been investigated but may be the result of too little material being injected and a material that is not mechanically robust. These results led to significant

modifications of this material to act primarily as both a drug delivery and cell delivery vehicle with very promising results to be discussed later.

1.4.2.2 Synthetic Hydrogels

Because of their high water content and diffusivity, among other properties, hydrogels have been investigated as implantable biomaterials across a broad range of regenerative medicine applications.[111] One challenge for synthetic hydrogels for cardiac injection application is controlling the formation of hydrogel structure in situ following injection. While very weak hydrogels may be forced through a needle, the material strength may be inadequate for such a mechanically taxing environment as the myocardium, and mechanical modeling discussed earlier suggests that a more mechanically robust material may be beneficial. Several material design strategies may be employed to confront this issue: in situ cross-linking [112], photo-induced polymerization [113], self-assembly[114] and thermally responsive hydrogels[115].

A solution of α-cyclodextrin and methoxy polyethylene glycol–poly (caprolactone)-(dodecanedioic acid)–poly(caprolactone)-methoxy polyethylene glycol (MPEG–PCL–MPEG) triblock polymer (α-cyclodextrin/MPEG–PCL–MPEG) has the ability to self-assemble into a hydrogel.[116] This gelation is posited to occur by two mechanisms. First, the MPEG-PCL-MPEG polymer chain may be able to thread through the center of α-cyclodextrin rings to form microcrystal complexes. Second, micellization of the PCL blocks can further add physical cross links within the hydrogel network. This polymer solution can form a hydrogel within a few minutes at room temperature and then will degrade in accordance with PCL block hydrolysis. Injectability is obtained by separating the α-cyclodextrin solution from the MPEG-PCL-MPEG solution using a double barreled-syringe. Injection of this material into new or old infarcts in rabbits and rats has been able to show significant improvements in LVESD and LVEDD one month after infarction.[117, 118] FS was reported at 56% in the hydrogel injection group compared to only 37% in the saline injection group after 4 weeks in rabbits. Contrary to other studies, improvements in geometry and function were not present two days after injection but were so after one month. This indicates that presence of the material alone may not be the cause of enhancement. Rather, it appears the body's longer-term reaction to this material generates the benefits. Indeed the LV wall thickness is increased after a month largely due to more collagen

deposition. Interestingly, functional improvements could not be linked to increased blood flow to the infarcted area as there was no difference in blood vessel density between hydrogel and saline injection groups.

Because injected material acts as a mechanical support, it may be beneficial for the material to remain in situ indefinitely. To this end a non-degradable, in situ polymerized PEG hydrogel has been investigated for cardiac injection after MI.[119] Despite the often perceived inert nature of PEG hydrogels there was substantial macrophage response to the material throughout the 3 month follow-up. The benefits seen after injection – increased wall thickness and modestly attenuated dilation – only persisted during the first 4 weeks. By 3 months the hydrogel injection group had regressed to a cardiac geometry and function similar to the saline treated control group. In this case a long-remaining material did not provide long-term benefit, but rather appeared to only introduce a focal point for chronic inflammation. Indeed, hydrogel injection into sham operated hearts showed a significant reduction in FS at 3 months which may point to the damaging role that chronic inflammation can play. The authors also suggest that while PEG may be an adequate mechanical support initially, as the heart continues to dilate the wall stresses eventually become more than the PEG hydrogel can support and so remodeling continues unchecked.

Thermoresponsive materials that transition from sol to gel near body temperature are frequently employed for tissue engineering and drug delivery applications because their transitional properties make them easy to deliver and manipulate.[120] N-isopropylacrylamide (NIPAAm) is one of the most studied thermoresponsive molecules. Poly-NIPAAm (pNIPAAm) chains can be dissolved in water below their transition temperature of 32°C, but precipitate to form a hydrogel upon warming to body temperature. Disadvantages to using pNIPAAm are related to its inability to degrade in vivo as well as its apparent structural similarity to toxic acrylamides. However, copolymerization of NIPAAm with degradable polymers can create a material that is thermoresponsive, biodegradable, and lacking observed cytotoxicity.[121, 122] It is also feasible to incorporate protein-reactive mers in NIPAAm-based copolymers to allow for covalent attachment of ECM components and growth factors [121, 123] and to incorporate enzymatically labile peptide cross-links [124] and adhesive peptide sequences [125].

Fujimoto et al. developed a degradable, thermally responsive copolymer of NIPAAm, acrylic acid, and hydroxyl-ethyl methacrylate-poly(trimethylene carbonate) (HEMAPTMC).[126] The sol-gel transition of this polymer occurred around 33°C, forming a hydrogel with a mechanical stiffness of 20 kPa, and a degradation time greater than two months in vivo. The sol-gel transition of this material and subsequent elasticity is demonstrated in **Figure 9**. Using a chronic rat infarction model, injection of this material around the infarct prevented the progression of cardiac dilation and remodeling. In addition to cellular infiltration in the material, histological evaluation of the LV wall 8 weeks after injection also showed the formation of a layer of smooth muscle next to the remaining material. This muscle layer expressed proteins associated with a contractile phenotype, though the direct effect of the smooth muscle layer on overall LV contractility was not assessed. This phenomenon was similar to that found after alginate injection and may be the result of reduced ventricular wall stress altering the remodeling pathway away from a largely fibrotic result – **Figure 10**.

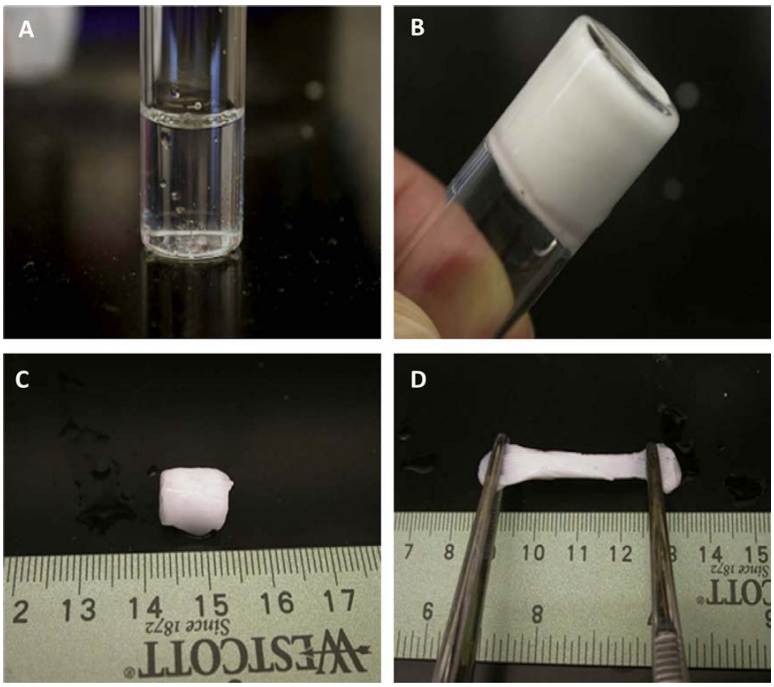

Figure 9. Demonstration of the thermal properties of NIPAAm–co-AAc–co-HEMAPTMC hydrogel. (A) Aqueous polymer solution at 4 °C, (B) gel formation after 30 s incubation in a 37 °C water bath, (C) after 10 min the gel continued to shrink and stiffen, leading to (D) a mechanically robust material with some elastic behavior. (From [126]).

A similar approach to the NIPAAm-based thermally responsive material above was investigated by Wu et al., who synthesized a hybrid biological-synthetic gel with PCL-grafted dextran chains that were subsequently copolymerized with NIPAAm monomer to form large branched copolymer chains.[127] Gel formation above 32°C led to a material with a storage modulus between 100 and 1500 Pa. Dextran cleavage in vivo led to breakdown and removal of the copolymer from the injection site within about 1 month. A volume of 200 µL of this material was injected into 4-day old infarcts in rabbits.[128] After 4 weeks, echocardiography showed that EF and LVEDD were significantly better in the material injection group compared to the saline injection group. While no material was evident in the histology at 4 weeks, the LV wall was substantially thicker. No analysis was done to determine if increased thickness was due to cell infiltration or more collagen deposition.

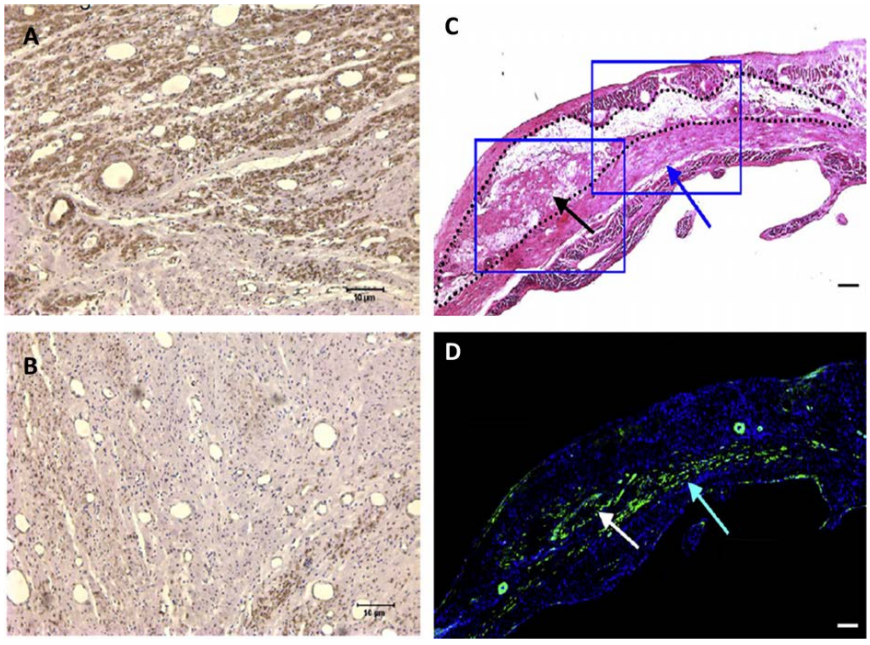

Figure 10. Histological evaluation of myocardium following material injection. Intracoronary injection of alginate (A) led to substantial growth of myofibroblasts that stained positive for smooth muscle a-actin (brown) in the infarct. (B) Direct epicardial injection of a thermally responsive NIPAAm copolymer led to a smooth muscle layer (C) (blue arrows) beneath the material that stained positive for smooth muscle actin (D) (green stain). (Left panels from [72], scale bar 10 µm; right panels from [126], scale bar 100 µm).

Adaptation of an off-the-shelf material for use in cardiac injection was seen when Radiesse (Bioform Medical Inc) was injected into ovine infarcts.[129] Radiesse is a soft tissue filler made up of calcium hydroxyapatite microspheres suspended in a gel-like solution of water, carboxymethyl cellulose, and glycerin. This material is typically used in cosmetic procedures and has been shown to increase local collagen production after injection.[130] Injection of a total of 1.3 ml of Radiesse at 20 uniformly distributed locations within the infarct area led to improved cardiac function within 15 minutes. The improvements were primarily the result of transforming the dyskinetic myocardium into akinetic tissue. Study of the ejection fraction in local regions of the myocardium demonstrated that apical and midventricular ejection fractions immediately improved after material injection contributing to the global improvement seen in EF. Four weeks after injection, improvements were seen compared to saline controls, although the benefits seen immediately after injection were attenuated and cardiac dilation continued.

1.4.3 Injectable Materials Including Drug Delivery

To build upon the results of material injections alone and to further encourage cardiac regeneration and functional improvements, many groups have sought to combine material injections with the controlled release of growth factors or other bioactive molecules. The injected material can serve as a depot for sustained biomolecule delivery, while also acting to protect these agents and thus extend their half-life in vivo.

It has been shown that VEGF and platelet derived growth factor (PDGF) play important roles in vessel formation.[131] While VEGF is important in the early stages of angiogenesis, PDGF is crucial to stabilize and mature the new vascular network. Thus it has been shown that sequential delivery of VEGF followed by PDGF can cause larger, more mature vasculature to develop in an ischemic region.[132] The differing natural affinity of alginate to VEGF and PDGF can lead to a level of sequential dual delivery of these growth factors from this material.[68] In vitro, about 50% of the VEGF is released from alginate during the first day compared to only 10% of the PDGF, though both show about 80% release by 4 weeks. In the infarcted myocardium, this sequential dual growth factor delivery translated to increased capillary density and α-actin SMC positive vessels compared to delivery of either factor

individually. While EF and LVEDD were not changed after growth factor delivery, the researchers do show that the systolic velocity time integral – a measure of displacement of the myocardium during contraction – did improve significantly compared to saline injections and compared to single factor delivery.

Because it has been shown that high local doses of angiogenic factors such as VEGF can have deleterious effects Christman et al. aimed to deliver a plasmid coding for pleiotrophin with the fibrin glue injected into an infarcted rat heart.[80] While no studies were performed to demonstrate transfection efficiency or overall levels of pleiotrophin production in the infarct zone, it was shown that hearts which received 250 μg of pleiotrophin with fibrin glue had an 80% increase in arteriole density compared to those receiving pleiotrophin delivered in saline. Using a microbead perfusion assay it was shown that the neovasculature was functionally connected to the native vessel network. No data for cardiac function were presented in this study to determine if the increased vasculature translated to improved LV pumping capacity.

Similarly, bFGF was delivered with gelatin injection into infarcted myocardium.[95] Delivery of 20 μg of bFGF either with saline or with gelatin lead to increases in arteriole density, capillary density, and fewer TUNEL-positive cells than injection of material without bFGF over 4 weeks. However, bFGF in gelatin consistently suggested a stronger effect than bFGF in saline. The only functional improvement was an increase in FS transiently at two weeks in the bFGF with gelatin which reverted back to a level similar to the saline control by 4 weeks. This again demonstrates that improvements in cardiac function cannot necessarily be directly associated with improvements on a cellular level though it may be a necessary beginning.

The hormone erythropoietin (EPO) has been found to inhibit cell apoptosis and increase neovasculature formation in ischemic tissue but may lead to increased risk of thromboembolic complications as well. Synthetic hydrogel α-cyclodextrin/MPEG-PCL-MPEG was used as delivery vehicle for EPO when injected into recent rat infarcts.[118] In vitro it had been shown that bioactive EPO is released from the biomaterial in a mostly linear fashion with 40% released after one week. In vivo, western blotting confirmed the presence of EPO both in and around the injected material after one week. There was a significant increase in the recruitment of CD 34+ cells and neovascularization, and decrease in apoptosis when EPO was delivered with the hydrogel compared to delivery of EPO with saline, injection of hydrogel alone, or injection of

saline. Importantly in this study the EPO-containing hydrogel group also showed improvements to cardiac geometry, FS and left ventricular end-systolic pressure that mirrored the histological improvements.

The largest body of research related to protein delivery with a biomaterial for cardiac injection involves self-assembling peptides (SAPs). Insulin-like growth factor 1 (IGF1), PDGF, and SDF1 have all been incorporated into SAPs with promising results.[108-110, 133] PDGF has a natural affinity for SAPs at approximately 1 ng/μg material, leading to a steady in vivo release over 2 weeks. This is a large improvement over free PDGF in saline injections, which is all but removed by 3 days. Delivery of 8 ng of PDGF with nanofibers showed improved FS over 4 months, decreased caspase-3 activation, and decreased apoptosis in the infarct region but did not increase myocardial cell proliferation, neovascularization, or regional blood flow.[108, 109] IGF1 within SAPs is also delivered over 2 weeks in vivo due to native peptide-growth factor affinity. However, in an attempt to increase the retention time of IGF1, nanofibers and IGF1 were both biotinylated and tethered together by streptavidin – **Figure 11**.[133] This binding kept IGF1 present at the injection site for longer than 84 days. Because IGF1 was associated with the nanofibers it was not free to diffuse out of the material. Thus, only cells that infiltrated the boundaries of the material showed the Akt signaling activation that IGF1 elicits. While the IGF1 was retained for a long duration and appeared to be bioactive it did nothing to improve FS, LVEDD, or wall thickness over a 3 week follow up period.

Finally, specially designed SDF1 was produced that was resistant to MMP cleavage to improve its half-life in vivo.[110] Fusion proteins of the resistant SDF1 and the RAD16-II nanofiber sequence were synthesized, allowing direct SDF1 incorporation into the SAPs. Using a cleavage sequence for MMP-2 as the spacer sequence between SDF1 and RAD16-II allowed for release of SDF-I only in the presence of MMP-2, which is a method of stimuli-responsive drug release. SAPs containing SDF1 fusion proteins delivered to injured myocardium elicited significant improvements in EF and left ventricular end systolic volume 28 days after injection. Stem cell recruitment, capillary density and arteriole density were also significantly improved after delivery of fusion protein nanofibers compared to nanofibers alone or nanofibers with free SDF1.

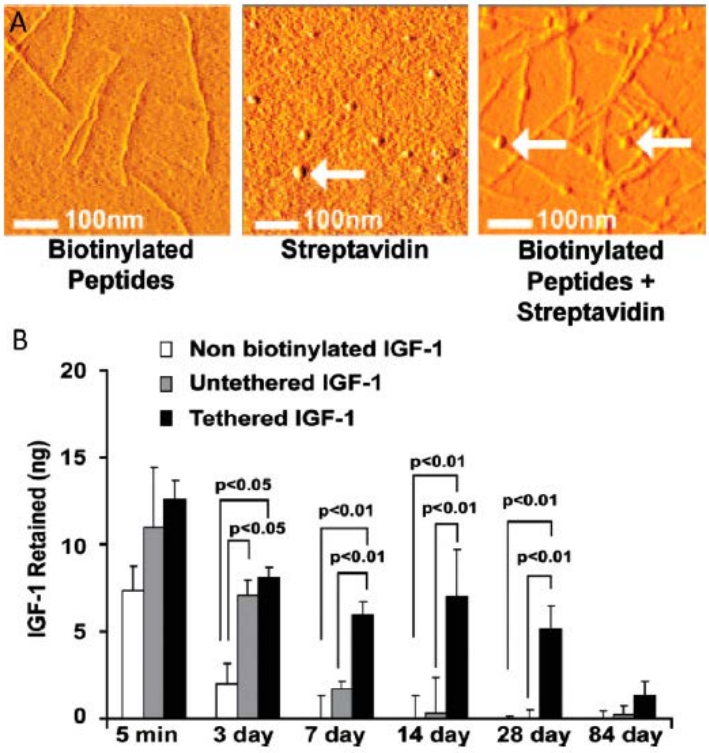

Figure 11. Atomic force microscopy (A) of biotinylated peptide nanofibers (left), streptavidin (center) and streptavidin-bound biotinylated peptides (right) creating a beads-on-a-string appearance. IGF1 was biotinylated and bound to biotinylated peptides through streptavidin (B). This attachment dramatically slows the release of IGF1 from the SAP environment compared to IGF1 that is not biotinylated or not tethered by streptavidin. (From [115], image copyright 2006 National Academy of Sciences, U.S.A.)

Taken together, the results reported to date suggest that delivery of SAPs combined with growth factor delivery may have the ability to improve cardiac function. Furthermore, methods to increase drug retention time, such as using fusion proteins, appear to be worthwhile to improve therapeutic efficacy. It should also be noted that in all studies involving SAPs the material was injected within 1-2 minutes of coronary artery occlusion, which decreases the clinical relevance of the results. Further studies are necessary wherein more myocardial damage is allowed to occur before an intervention is performed as is generally the case in patients presenting with myocardial infarctions and ischemic cardiomyopathy.

In reviewing the use of materials alone or as a delivery vehicle for drugs some notable general trends appear. First, injection of hydrogel materials can improve cardiac function and

histology over injection of saline. Second, injection of material provides similar or better results than injection of only growth factors in solution, when considering comparative studies. Third, combining material with growth factors often improves upon the benefits seen when material is injected alone. From a practical perspective, however, it may be that obtaining cardiac benefits by material delivery alone is the most attractive therapy for clinical translation because it avoids the regulatory burden associated with pharmaceutical-associated strategies. While the promise of adding appropriate drugs to a material is significant, ultimately the risk-benefit of adding this further complexity to intramyocardial biomaterial injections will need to be evaluated as these technologies advance.

1.5 LIMITATIONS AND CHALLENGES

In both patch and injection therapy, by reviewing the current literature it is difficult to determine which material properties and deployment techniques are most advantageous. For example, the volume of material injected into rat myocardium has varied between tens and hundreds of μL in different studies, which likely impacts the results regardless of material. Further, the number and location of these injections, whether a single injection directly in the middle of the infarct or multiple injections around the border zone, vary between studies. It is reasonable to assume, as was demonstrated in numerical modeling studies, that the volumes and locations will have an effect on outcomes.[53, 54] Delivery of material to the border zone may be better positioned to encourage regeneration from the healthier peripheral tissue than material injected in the center of the infarct. Looking at injection from another dimension, endocardial and epicardial injection approaches each have potential risks and benefits. The coupling of injection therapy with functional imaging is an area of promise, where the injection sites might be optimized and delivery of appropriate volumes achieved safely.

Likewise, these same considerations relating to size, placement, and material properties of a cardiac patch may be important in understanding the successes and failures of that technique. Some synthetic materials are able to provide elastic mechanical strength to the heart and a support for engrafted cells which may be beneficial after injury, however these materials

may lack the biocompatibility desired for longer-term regeneration. The extent of remodeling is also influenced by the types and concentration of drugs and cells that are delivered with the materials, adding a significant layer of complexity when trying to understand the mechanisms of benefit. Different cell types have shown different capacities to survive and integrate in host tissue when delivered from a patch or by injection.

Another major limitation to drawing general conclusions from data surrounding biomaterial treatments to heart disease involves the myriad infarction models employed. Many different scenarios are represented wherein hearts are treated between minutes to weeks after infarction. The ability to improve cardiac remodeling following deployment of a patch or injection of material is likely related to the duration between injury and treatment. It is reasonable to assume that delivery of material immediately after injury, as is done in many of the animal models discussed above, would provide the most benefit as it has the highest likelihood of improving the damaging mechanical and cellular milieu that leads to negative remodeling. Early deployment, however, is clinically problematic as patients will never be available for immediate treatment at the onset of injury. Recent data also suggest that delivery of materials that are enzymatically degradable immediately after infarction may not be as beneficial as when delivered later.[134] Thus data on later stage infarction treatment are of particular value and relevance. In particular, treatment within one week after infarction may be the most clinically relevant as it follows the clinical flow often seen with patients. These patients often present to the hospital within a day of the onset of symptoms and are then stabilized and monitored until more advanced cardiac procedures are performed in the subsequent days. Treatment during this intermediate stage may also bolster the injured tissue before significant and lasting geometric remodeling have occurred, thus providing more benefit than if the patch or injection therapy was administered at later times. As noted above, a number of patients undergo silent cardiac events and may present to the hospital long afterwards and so studying the delivery of material in the later stages of cardiac remodeling is also relevant. However, it may be more difficult to obtain positive results from later-stage material delivery due to the substantial damage that will have occurred by this time.

The type of infarction, such as a sustained occlusion or an ischemia-reperfusion event, and the location and extent of the blockage may also influence recoverability. On top of this,

underlying co-morbities, which would be encountered in the patient population (e.g. diabetes, valvular disease) would further confound conclusions drawn from current animal models. A further important variable between studies is that the materials used often have different mechanical properties and degradation times, even if they are from similar starting molecules. It was suggested by several studies that residence time in the tissue may have a role in maintaining improvements. Finally, as few studies follow the outcomes for periods beyond a few months, the long-term benefits of these treatment approaches are not known.

As the field involving biomaterials treatments for cardiovascular disease develops it will be necessary to conduct more comparative studies to elucidate which of the many material design variables provide functionally relevant cardiac improvements. It remains difficult to parse out what benefits are derived from changes exclusively in the mechanical environment of the LV and what benefits are a result of cardiac remodeling occurring concurrently, and likely dependently, in the ventricular wall. Furthermore, the potential positive and negative impact of the local inflammatory and phagocytic activity associated with material degradation is not clear. While there is evidence to suggest that ongoing inflammation from a non-degradable hydrogel injection is counter-productive [119], others have suggested that the inflammatory response may be beneficial, stimulating acute angiogenesis and potentially positively impacting the remodeling result [126, 135].

1.6 FUNDAMENTALS OF DRUG DELIVERY

As discussed above, the inclusion of important signaling molecules such as DNA, small peptides, and proteins can be important in the overall function of an implanted material. The presence of the biomaterial carrier is particularly important given that bolus injection of a drug free in solution leads to rapid clearance of the drug from the injection site, but extended periods of bioactivity over the tissue remodeling period in situ are desirable.[136] For example, It has been shown that when a solution of free bFGF is injected directly into the myocardium only 16% remains after one hour.[137] Contrariwise, the amount of bFGF remaining at the injection site 72 h after injection was roughly 30% when the factor was incorporated into gelatin microspheres – a

15x increase compared to free bFGF injection at that time point. Because the rate of drug delivery from a biomaterial carrier may ultimately determine the success or failure of the implant, in vitro characterization of drug delivery systems is always warranted before being used in vivo.

The complexities of drug delivery kinetics from a biomaterial carrier are significant and can vary depending on many system parameters such as material composition, material processing, carrier degradation rate, drug physicochemical properties, and drug loading – **Table I** (adapted from [138]).[139-142] The combination of these and other parameters leads to an overall release profile of drug that can be generally categorized into different types. Many systems demonstrate simple diffusion-controlled delivery characterized by a burst release of near-surface drug, a subsequent fast diffusion period, and ending with lower release rates as the agent is exhausted – **Figure 12A**. This is especially common for hydrogel systems due to their high water content, which provides drugs a relatively easy diffusion path out of the matrix. In the case of biodegradable materials a two-stage release profile can be observed. In this profile, after an initial burst a significant amount of drug remains trapped in the carrier until adequate degradation of the material occurs, at which point the remaining drug diffuses out quickly – **Figure 12B**. For many applications the ideal release profile would be one of constant delivery at a defined rate that doesn't change over time. This is referred to as a linear or zero-order release profile – **Figure 12C**. So long as the drug can be made to release from the matrix at a therapeutic rate, this type of carrier system could deliver drugs without the peaks and troughs in drug concentrations seen in other systems. However, the difficulty in developing this kind of system is often high and requires a fine balance of system properties.

Table I. Design Criteria from Hydrogels in Drug Delivery Formulations

Design criteria	Design variables
Transport properties	Molecular weight and size of protein
Molecule diffusion	Molecular weight of polymer
	Crosslinking density
	Polymer-protein interactions
	Hydrogel degradation rate
	Additional functionalities
Physical Properties	Polymer/crosslinker/initiator concentrations
Gelling mechanisms	Temperature, pH, ionic strength
Stimuli-responsiveness	Concentration of responsive groups
Structural properties	Molecular weight of polymer
Biodegradability	Mechanical strength
	Concentration of degradable groups
Biological Properties	Cytotoxicity of the hydrogel
Biocompatibility	Cytotoxicity of degradation products
	Capsule formation

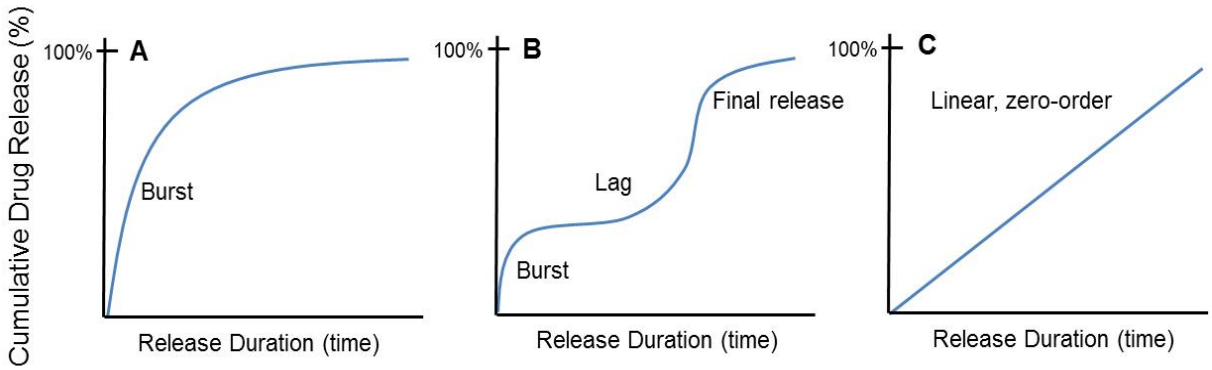

Figure 12. Typical drug release profiles in controlled release formulations. Diffusion-controlled systems show a large burst release early followed by slowing release until drug exhaustion (A), degradable materials can often provide levels of high release rate separated by a lag phase (B), and zero-order release is characterized by steady release rates throughout the release period (C).

Extensive mathematical modeling has been applied to various drug delivery systems in order to describe the release rates of a given drug from a given matrix. There are many excellent reviews which catalogue these various models.[138, 143-145] From an engineering standpoint these models are most useful if they can be linked directly to physical parameters of the drug delivery system which can be purposefully controlled. This allows the models to be more predictive than simply descriptive and thus guides system fabrication. For example, Guo et al have developed a model for polyurethane-coated stents incorporating variables for polymer degradation rate and polymer swelling rate. In this way, experimental data of degradation and swelling, when put into the model, are adequate to predict release without having to run the full release experiment.[146] Recently Rothstein et al have made significant improvements in this predictive modeling approach within the limits of certain bulk and surface degrading materials.[141, 147] Their model allows the user to specify what release profile is desired and then provides the necessary characteristics of the system - such as polymer molecular weight, matrix size, polymer degradation rate, including various processing methods - that will provide that profile. This promising area of research is the natural continuation to earlier work in drug delivery and is useful for newer systems that are increasingly complex and have stricter design requirements.

There are additional considerations when studying drug delivery systems that need to be investigated. While many studies and models are good at quantifying and describing early stages of release behavior, most studies of drug release behavior from new materials do not extend beyond a few weeks, meaning that the complexities of the release kinetics may be left unobserved. The duration of release will also be influenced by the physiologic environment that the system will be used in. Changes in drug delivery rates may arise from the flow, mechanical forces, and biodegradation seen at the site of the implanted drug delivery system. Thus trying to duplicate the in vivo environment for controlled release experiments may be useful. For example, whereas enzymes have been routinely used to investigate polyurethane biodegradation, reports of the use of enzymes in the context of controlled release are scarce.[148, 149]

Various therapeutic molecules have a relatively short half-life in vivo due to physiologic processes such as renal clearance, proteolysis, and non-specific binding.[150, 151] It is generally understood that drugs gain a level of protection from degradation when protected within a

carrier, thus increasing the effective half-life. However, the microenvironment of the carrier, and the processing necessary to load the drug, can also contribute to a loss of bioactivity of the drug. For example, protein denaturation can occur through mechanisms such as adsorption to the material surface or hydrolysis by acidic environments.[152, 153] Processing of drug-loaded materials may require the use of organic solvents, high temperatures, or reactive chemicals that may denature loaded proteins.[154] Many strategies have been employed to prevent denaturation of loaded proteins. Neutralizers can be used to prevent a buildup of acidic byproducts during material degradation, excipients such as BSA may help protect proteins from harsh microenvironments, and polymers such as poly(ethylene glycol) can be covalently attached to drugs to protect them.[155-157] Taken together the challenges in developing a drug delivery system to meet the end-user needs require a significant understanding and pairing of the principles of controlled release and biomaterial science.

1.7 OBJECTIVES

As has been discussed above, both cardiac patch and intramyocardial material injection are the most promising of biomaterials-based treatments for treating heart failure. The demonstrated ability of specific materials to encourage regeneration and improve function warrants their continued investigation. As has been shown previously, both implantation of a PEUU patch and injection of a NIPAAm-based hydrogel were able to halt detrimental dilation and wall thinning and encourage angiogenesis and tissue growth. PEUU has been used due to its strong and elastomeric mechanical properties that would be relevant to a cardiac environment. NIPAAm-based gels have been useful because of their rapid transition and the ability to tune their chemistry to provide relatively strong mechanical properties compared to other injectable hydrogels. In both cases their degradation rate appears to provide support for an extended period. In both cases the material was associated with positive responses in the absence of delivering any endogenous biosignaling molecules. That previous work becomes the foundation upon which the current work is built. The literature in this field is full of examples where inclusion of a drug in the material was able to improve upon the results of the material alone. Thus, the main goal of this research was to build upon the results of patch or injection therapy from PEUU or NIPAAm-

based gels by adding appropriate drugs and studying their release. Because controlled release properties can be dramatically different between different materials and different kinds of drugs, one primary aspect of this work was to study the release properties and control points for each drug/material system, all the while investigating drug activity and ultimate efficacy of the system as a whole.

1.7.1 Objective #1: Spatial control of gene expression in a cardiac patch

As discussed previously, PEUU that is processed into a porous structure by a thermally-induced phase separation technique has been shown to be beneficial as a cardiac patch following myocardial infarction. In the first specific aim of this research, PEUU was studied for its ability to release a small molecular weight gene-inducing molecule, rheoswitch ligand 1 (RSL1), in a controlled and spatially specific manner. We hypothesized that RSL1 could be released from PEUU in a bioactive manner. The ability for cells grown on RSL1-loaded PEUU films or porous scaffolds, similar to what is used as a cardiac patch, to uptake the inducer and express a gene of interest was studied. By spatially patterning the location of RSL1 in the scaffold we aimed to cause cells grown on the surface of the scaffold to express the gene of interest in the corresponding patterned arrangement. Such a system would have the unique ability to independently control local cell behavior towards developing complex three dimensional tissues.

1.7.2 Objective #2: Controlled growth factor delivery from PEUU patches

Previous results of the application of a PEUU cardiac patch were acquired in the absence of any pharmacological agent in the material. It is likely that the inclusion of growth factors within the patch that are relevant to cardiac regeneration may be able to aid in the healing process and improve upon the previous results. Before future in vivo application, however, we aimed to study the delivery two growth factors that are relevant for cardiac repair – IGF1 and hepatocyte growth factor (HGF) – from PEUU patches in vitro. Due to the activity of inflammatory cells it is well understood that after implantation material degradation is increased compared to degradation of the material in saline. We first aimed to study the ability of the patch to release bioactive IGF1 and HGF from porous PEUU scaffolds. After determining the protein delivery rates in the typical

saline environment, we aimed to better approximate the delivery rates of the proteins from the scaffolds in vivo by employing an esterase enzyme to our in vitro release media that would degrade the PEUU in a timeframe similar to what is seen in vivo. Characterizing the material during this degradation process was also studied to link the hypothesized in vivo drug delivery rates to the changes in material properties over time. This type of study, which encourages better understanding of the release behavior in the implant environment would be valuable in all controlled release applications.

1.7.3 Objective #3: Controlling the drug delivery properties of an injectable gel

We have previously shown that a thermally responsive injectable hydrogel based on N-isopropylacrylamide can prevent cardiac remodeling and maintain cardiac function following injection into infarcted myocardium. As discussed above, reports suggest that concomitant delivery of growth factors can improve upon the benefits seen from materials alone. We developed a new thermoresponsive poly(NIPAAm)-based hydrogel material with stronger mechanical properties and slower degradation. We aimed to determine how it can be loaded with model protein bovine serum albumin and how that protein is subsequently released. Specifically, the ability to control the delivery of this protein by modifications to the polymer composition or by incorporation of protein-loaded microparticles into the hydrogel was investigated. The ability to release two different protein populations at different rates was also explored in this system. This research provided a basis for moving to functional growth factor delivery to the myocardium.

1.7.4 Objective #4: Characterization and in vivo application of a protein-loaded gel for cardiac repair

After development of the hydrogel to release two different model proteins in a sequential manner, we sought to study how functional growth factors bFGF and IGF1 would be released from this system and if they would maintain their bioactivity upon release. The rationale was to provide a system wherein bFGF would be delivered primarily early after injection with IGF1 release coming later as the microparticles degraded. Both the in vitro and in vivo release rates of

these proteins were investigated. The effect of intramyocardial injection of the new thermoresponsive hydrogel was investigated over a 16 week period. In addition to injection of the material alone, animals were divided into groups to receive injection of gel loaded with bFGF, IGF1-loaded PLGA microparticles, or both bFGF and IGF1-loaded microparticles. The ability of growth factors to improve upon results of unloaded gel were investigated by cardiac function, geometry, and histological milieu.

2.0 SPATIAL CONTROL OF GENE EXPRESSION BY LOCAL MOLECULE DELIVERY IN A PEUU DEGRADABLE SCAFFOLD

2.1 INTRODUCTION

(Note: This chapter was previously published as: Baraniak, P.R., D.M. Nelson, C.E. Leeson, A.K. Katakam, J.L. Friz, D.E. Cress, Y. Hong, J. Guan, W.R. Wagner. Spatial control of gene expression within a scaffold by localized inducer release. Biomaterials 2011;32(11):3062-71.)

The inherent complexity associated with the structure of a tissue poses a major design challenge to engineering strategies for tissue repair and regeneration. Embryogenesis demonstrates the commitment of cells to multiple lineages in a well-regulated spatial and temporal manner, and differentiated cells must perform specific functions in synchrony to form a functional tissue or organ structure. Growth factor gradients and spatial patterning of gene expression not only direct cell differentiation, but also regulate processes such as vascularization and wound repair [158-165]. Therefore, tissue engineered constructs capable of spatially and temporally controlling cell behavior may more closely mimic the natural tissue microenvironment, thereby resulting in more successful *ex vivo* development of functional tissues and in situ tissue repair and regeneration.

Controlling the location and timing of biomolecule delivery from tissue engineering scaffolds has been the subject of many reports in the literature. Scaffolds have been used for the sustained delivery of numerous growth factors [68, 158, 166], and the spatial organization of growth factors on substrates has been achieved through a number of fabrication processes to modulate cell behavior including proliferation, differentiation, and migration in vitro [167-175]. In lieu of growth factor presentation, natural and synthetic polymers have also being used for controlled non-viral gene delivery [176-178]. Inducing cells to express a gene of interest can effectively alter local cell behavior and function leading to, for example, neovascularization following myocardial infarction or cell death in a tumor [80, 179]. Adsorption of DNA to

specific regions of a tissue engineered construct is also under investigation to encourage cells to express different genes depending on their location in the scaffold. Some of this work has been aimed at mimicking the organization of motor and sensory neurons in a spinal cord bridge following injury with promising results [180-182].

Inducer molecules capable of regulating gene expression in specific cell populations have thus far proven effective in basic science and preclinical studies [183-186]. One such inducible gene expression system is based on a modified version of the ecdysone-responsive gene expression system which mimics the action of 20-hydroxyecdysone, a steroidal hormone which regulates genes necessary for metamorphosis in *Drosophila melanogaster* [187-189]. In this gene expression system, which uses a non-steroidal analog of 20-hydroxyecdysone as the inducer ligand, transcription is repressed in the absence of inducer, however, when the ligand is added to the system, it binds to the receptor and induces gene expression over a broad range of concentrations and in a dose-dependent manner. High induction potential coupled with very low basal expression makes this an attractive gene expression system. The use of such regulatable gene expression systems has many advantages relative to traditional DNA delivery approaches. First, because all cells used in these applications are stably transfected with the gene of interest prior to use, the problem of low transfection efficiency from delivering plasmid in situ is circumvented. Second, because the inducer molecules provide a direct method to regulate both the level and timing of gene expression, these systems offer the potential for greater control. Third, a well-designed inducer will have no effect on cells that lack the transfected plasmid, thus assuring a response only in the designated cells.

The objective of this study was to combine the benefits of local controlled release with a gene expression system to provide spatial control of gene expression in a tissue engineered construct. To our knowledge, this approach has not been investigated previously, and is a potential step towards generating complex tissue architectures without the need for direct DNA delivery. To this end, the ability to achieve controlled release of an inducer ligand in an active form over extended periods of time was demonstrated from a biodegradable poly(urethane). Two-dimensional polymer films and three-dimensional porous scaffolds were fabricated with spatially-defined regions containing or omitting ligand. Cells stably transfected with a gene

under control of the inducer ligand were seeded onto biomaterials variably loaded with inducer, and spatial patterning of gene expression was achieved.

2.2 MATERIALS AND METHODS

2.2.1 Gene expression system

The inducible gene expression system (RheoSwitch, Intrexon Corp) was composed of an engineered nuclear receptor and a highly specific synthetic ligand inducer – **Figure 13a**. In *Drosophila melanogaster* 20-hydroxsyecdysone allows gene expression by binding to a nuclear receptor heterodimer consisting of an ecdysone receptor (EcR) and a retinoid X receptor (RXR). The RheoSwitch system uses a hybrid EcR (RheoReceptor-1, RR1), composed of the ligand binding domain of EcR fused to the yeast GAL4 binding domain. RR1 binds to RheoActivator (RA), which fuses the ligand binding domain of RXR with the activation domain of viral transactivator VP16. The RR1-RA bipartite holoreceptor has also been engineered to bind to the 5X RE (contains 5 copies of the GAL4 response element) promoter and induce gene expression only in the presence of the non-hormonal, synthetic inducer ligand RheoSwitch Ligand 1 (RSL1, N-(2-ethyl-3-methoxybenzoyl)-N´-(3,5-dimethylbenzoyl)-N´-tert-butylhydrazine) (MW 382.5) – **Figure 13b.** Briefly, cells were stably transfected with both the pNEBR-R1 and pNEBR-X1 plasmids (New England Biolabs), which constitute the RheoSwitch system. pNEBR-R1 constitutively produces RA and RR1 under control of the ubiquitin B and ubiquitin C promoters, respectively. Once formed the holoreceptor regulates transcription of the gene of interest which was cloned into the pNEBR-X1 expression vector. For the selection and generation of stable cell lines pNEBR-R1 and pNEBR-X1 plasmids also provide neomycin and hygromycin resistance, respectively. In the absence of inducer ligand, the holoreceptor binds with negative regulatory cofactors to the 5X RE promoter, preventing transcription. However, when present, inducer tightly and selectively binds to the holoreceptor, changing the conformation of and activating the receptor protein so that it releases bound negative regulatory cofactors, resulting in a highly induced transcriptional state. The level of gene expression can be controlled by adjusting the concentration of inducer ligand present [189].

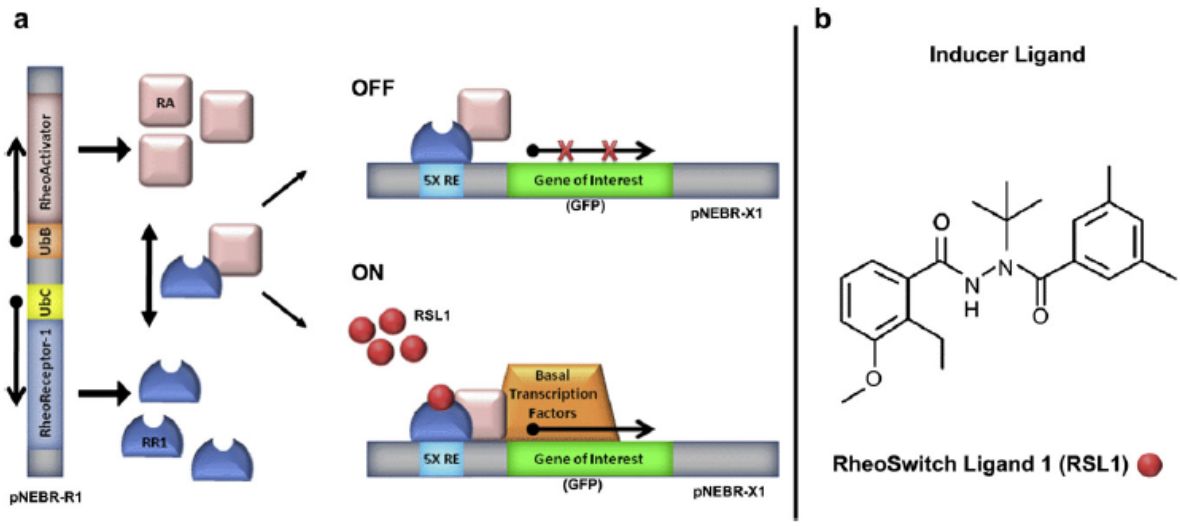

Figure 13. Modified ecdysone-responsive gene expression (RheoSwitch) system (a) and chemical structure of the RSL1 inducer ligand (b). Plasmid pNEBR-R1 uses ubiquitin B (UbB) and ubiquitin C (UbC) promoters to constitutively express proteins RheoActivator (RA) and RheoReceptor-1 (RR1), respectively. RR1and RA form a bipartite holoreceptor that binds the 5X RE promoter sequence on plasmid pNEBR-X1, which contains the gene of interest (green fluorescent protein, GFP). When bound to inducer ligand RSL1, the holoreceptor exchanges bound negative regulatory cofactors for positive cofactors, allowing high transcription rates of GFP.

A B16 murine melanoma cell line was obtained from Intrexon Corporation. These cells were stably transfected with both the pNEBR-R1 and pNEBR-X1 plasmids. pNEBR-X1 plasmids were cloned to express a reporter gene, green fluorescent protein (GFP), in the presence of inducer ligand. Cells were maintained on tissue culture polystyrene (TCPS) in growth medium (RPMI-1640 supplemented with fetal bovine serum, gentamycin, G418 sulfate, non-essential amino acids, and beta-mercaptoethanol), and varying amounts of RSL1 ligand (1-5 µM final concentration) were added directly to growth medium in order to induce gene expression. After 48 hrs, cells were fixed with 2% paraformaldehyde for 10 minutes, and nuclei were stained with Hoechst dye (1:100 in phosphate buffered saline [PBS]) or 4',6-diamidino-2-phenylindole (DAPI, 1:100 in PBS). Cell nuclei and GFP expression were visualized using fluorescent microscopy.

2.2.2 Polyurethane synthesis

Poly(ester urethane) urea based on PCL diol (MW 2000, Aldrich), butane diisocyanate (BDI, Fluka), and putrescine (Aldrich) was synthesized in a two-step solution polymerization as previously reported – **Figure 14**. [190]. Briefly, PCL in dimethyl sulfoxide (DMSO) was stirred with BDI in DMSO. A catalyst, stannous octoate, (Aldrich) was added, and the reaction was allowed to continue at 80°C for 3 hrs. Putrescine in DMSO was then added to the pre-polymer solution, and the reaction was allowed to continue at room temperature for 12-18 hrs. The stoichiometry of the reaction was 2:1:1 BDI:PCL:putrescine. PEUU was precipitated in distilled water and immersed in alcohol to remove unreacted monomers. Finally, polymer was dried under vacuum at 50°C for 4-5 days in order to completely remove solvent.

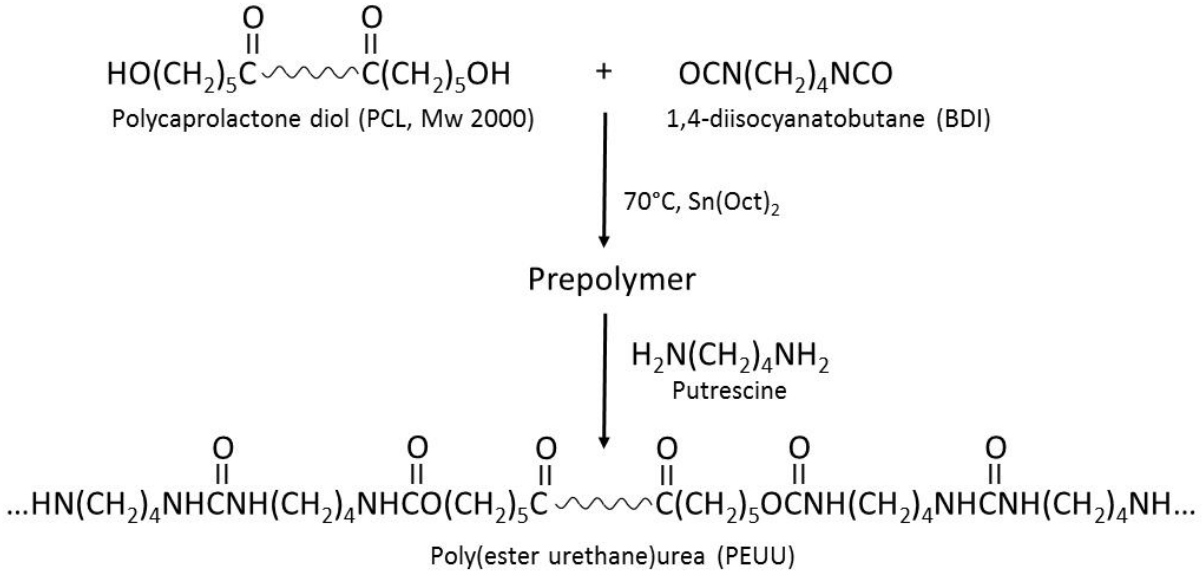

Figure 14. Synthesis of PEUU. Poly(caprolactone) diol reacts with 1,4 diisocyanatobutane to form the prepolymer. The final product is formed by chain extension of prepolymer with putrescine.

2.2.3 Preparation of RSL1-loaded PEUU films

RSL1-loaded PEUU films were fabricated using a solvent casting method. PEUU was dissolved in DMSO at 80°C to obtain a 2 wt% polymer solution. Predetermined amounts of RSL1 (reconstituted in DMSO) were added to polymer solutions (0-150 μM final ligand concentration), and 0.5 ml polymer solution was cast into each well of 24 well culture plates or glass vials for gene expression and ligand release studies, respectively. PEUU films were dried under vacuum at 50°C prior to the initiation of experimental protocols.

2.2.4 RSL1 release kinetics

RSL1-loaded PEUU films were incubated in vitro at 37°C in 1 ml release fluid (90% v/v PBS and 10% v/v acetonitrile) in order to determine ligand release kinetics. A solubility enhancer, in this case acetontrile, was required in the release fluid to encourage sink conditions for the hydrophobic RSL1 [140, 191]. Releasate was collected and stored at -20°C at pre-determined time points and was replaced with fresh release fluid. A ligand standard curve was obtained by adding known concentrations of RSL1 to releasate collected from polymer films that were not loaded with ligand and by assaying absorbance using UV spectrometry (Lambda 2, Perkin Elmer) at 250 nm. Absorbances at 250 nm for releasate collected from RSL1-loaded PEUU films (n=4) were compared to the ligand standard curve to determine the amounts of RSL1 released over time.

2.2.5 Degradation of PEUU films

Degradation of PEUU films was determined over time by measuring the intrinsic viscosity of polymer films dissolved in hexafluoroisopropanol (HFIP). Films were soaked in either PBS or a solution of 90% v/v PBS with 10% v/v acetonitrile. Degradation fluid was replaced weekly. At designated time points over one year, polymer films (n=3) soaked in each degradation fluid were

collected, dried, and dissolved in HFIP to a concentration of 1.5 mg/ml. Polymer solutions were put into a modified Ubbelohde viscometer (Ace Glass Inc.), and the time for solution to travel between markings was measured and compared to the time for pure HFIP solvent. These data were used to determine the intrinsic viscosity of polymer solutions using a single-point calculation as a representation of polymer chain degradation [192].

2.2.6 Bioactivity of released RSL1

The bioactivity of released RSL1 was determined by the ability of the ligand to induce GFP expression in B16 cells plated on TCPS. For short-term bioactivity studies (3 week endpoint), 24 well tissue culture plates containing PEUU films (n=4) loaded with 0-10 μM RSL1 were incubated in 1 ml B16 growth medium per well at 37°C. Growth medium was removed at pre-determined time points from polymer films and transferred to B16 cells on 24 well tissue culture plates. For long-term (greater than 3 weeks) bioactivity studies, films (n=4) loaded with high RSL1 content (25, 75, 150 μM) were prepared. Releasate from polymer films was dried in a vacuum oven at 50°C overnight to remove acetonitrile and subsequently reconstituted in 4 ml B16 growth medium per sample prior to transfer to B16 cells on 24 well plates. In order to visualize cells and quantify gene expression, cell monolayers were fixed with 2% paraformaldehyde and stained with nuclear dye 48 hrs after treatment with released RSL1. Cells were visualized (at least 4 fields) for nuclear staining and GFP expression using fluorescent microscopy, and the percentage of GFP-positive cells was quantified.

2.2.7 Gene expression on PEUU cell-seeded films

Polymer films containing varying concentrations of RSL1 ligand (0-10 μM) were cast into 24 well glass bottom plates (MatTek Corporation), and B16 cells (1000 cells/cm^2) were plated directly onto PEUU films in 1 ml growth medium per well. Growth medium was exchanged every 3-4 days for a period of three weeks. At pre-determined time points, cells were fixed with 2% paraformaldehyde and stained with a nuclear dye. Cells were visualized for nuclear stain and GFP expression using confocal fluorescent microscopy, and the percentage of GFP-positive cells was quantified.

2.2.8 Spatial control of gene expression on PEUU films

A 2 wt% PEUU solution in DMSO was obtained as described. RSL1 ligand was added to half of the polymer solution to yield a 10 μM final ligand concentration. Droplets (20 μLs each) of PEUU with RSL1 and PEUU without RSL1 were pipetted onto glass microscope slides in a spatially-defined pattern and allowed to dry under vacuum at 50°C – **Figure 20a**. Once solvent was evaporated, another droplet was placed on top of the existing one. In total, five droplets of polymer solution (i.e. 5 x 20 μLs) were placed at each spot on each microscope slide. Various configurations of droplets were tested to optimize spatial control. Slides were incubated overnight in 10 ml PBS to remove surface-bound RSL1 and then sterilized under UV light for 20 min. B16 cells were plated onto slides (1000 cells/cm^2) and cultured in Petri dishes in 10 ml growth medium for up to 72 hrs with culture medium exchanged every 24 hrs. At pre-determined time points, slides were fixed with 2% paraformaldehyde and stained with a nuclear dye. Cells were visualized for nuclear stain and GFP expression using confocal fluorescent microscopy, and the percentage of GFP-positive cells was quantified.

2.2.9 Fabrication of PEUU scaffolds with localized RSL1 loading

A two-step salt-leaching processing method was used to obtain porous PEUU scaffolds. Polymer was dissolved in 1 ml HFIP (35% w/v PEUU) and 1000 μM RSL1, mixed with 5 g NaCl (particle size 75-100 μm), forming a paste-like material, and tightly packed into a small diameter (6 mm inner diameter) cylindrical glass mold. The newly formed scaffold was immediately pushed out of the glass mold and exposed to air overnight to allow solvent evaporation. The dried scaffold was then placed in the center of a larger cylindrical glass mold (inner diameter 13 mm), and a polymer and salt mixture identical to that described above, but without RSL1, was packed around the small-diameter scaffold, creating a concentric scaffold with an RSL1-containing core and an outer ring without RSL1. The concentric scaffold was removed from the mold, and solvent was again evaporated. The final scaffold was cut into disks (0.75 mm thickness, 13 mm diameter), and salt was leached from constructs by soaking in deionized water for 30 min immediately before seeding with cells. For comparison, porous scaffolds without any RSL1 or with RSL1 through the entire scaffold were also synthesized and seeded with B16 cells.

Scaffold disks were visualized using a JEOL 9335 field emission gun scanning electron microscope (JEOL, Peabody MA) to confirm porous structure and continuity between concentric scaffold regions.

2.2.10 Spatial control of gene expression within PEUU scaffolds

Stably transfected B16 cells were seeded onto porous PEUU disks with spatially defined RSL1 loading in order to demonstrate the ability of the constructs to elicit spatially defined gene expression. Scaffolds were sterilized under UV light for 20 min, and cells were seeded onto scaffolds at a density of 2 $x10^6$ cells/scaffold using a filtration seeding method [193]. Cell-seeded scaffolds were then statically cultured in 6-well TCPS plates containing 8 mls/well B16 growth medium for up to 7 days with media exchanged every 3-4 days. Scaffolds were also cultured in a transmural perfusion system to reduce near-surface RSL1 in the fluid phase [194]. At days 3 and 7, scaffolds were fixed with 2% paraformaldehyde, stained with nuclear dye, and mounted onto slides. For each scaffold (n=3), nuclear dye and GFP expression were visualized using fluorescent confocal microscopy, and 10 images were captured from each of the inner and outer regions. The percentage of cells expressing GFP was quantified for each image. One representative scaffold was selected to be imaged in its entirety in a mosaic fashion. Additionally, a Matlab computer program (Mathworks) was written to quantify the location-dependent color intensity of the fluorescent images in order to obtain a quantitative measure of spatial control of gene expression. Specifically, the intensity of the green signal (GFP) was normalized to the intensity of the blue signal (nuclear dye) (G/B ratio) and averaged along a 4 mm thick horizontal band across the center of the scaffold.

2.2.11 Statistical methods

Statistical analyses were performed by one-way ANOVA with Tukey post-hoc testing of differences at specific times of interest using SPSS software. Linear regression was used to describe the dose-dependent response of GFP expression to RSL1 loading dose in films or culture medium. Differences in GFP expression between inner and outer regions of concentric scaffolds were compared using a student's t-test with $p<0.05$ considered significant.

2.3 RESULTS

2.3.1 Gene expression by media manipulation

Stably transfected B16 cells cultured in growth medium in the absence of RSL1 ligand did not express GFP. GFP expression, however, was evident in cells cultured in growth medium containing varying concentrations of ligand (1-5 uM) 48 hrs post-RSL1 administration – **Figure 15**. The percentage of cells expressing GFP was 16.6 ± 4.4, 32.5 ± 3.0, 44.0 ± 15.0, and 63 ± 7.0% for 1, 2, 3, and 5 µM RSL1, respectively (R^2 = 0.981).

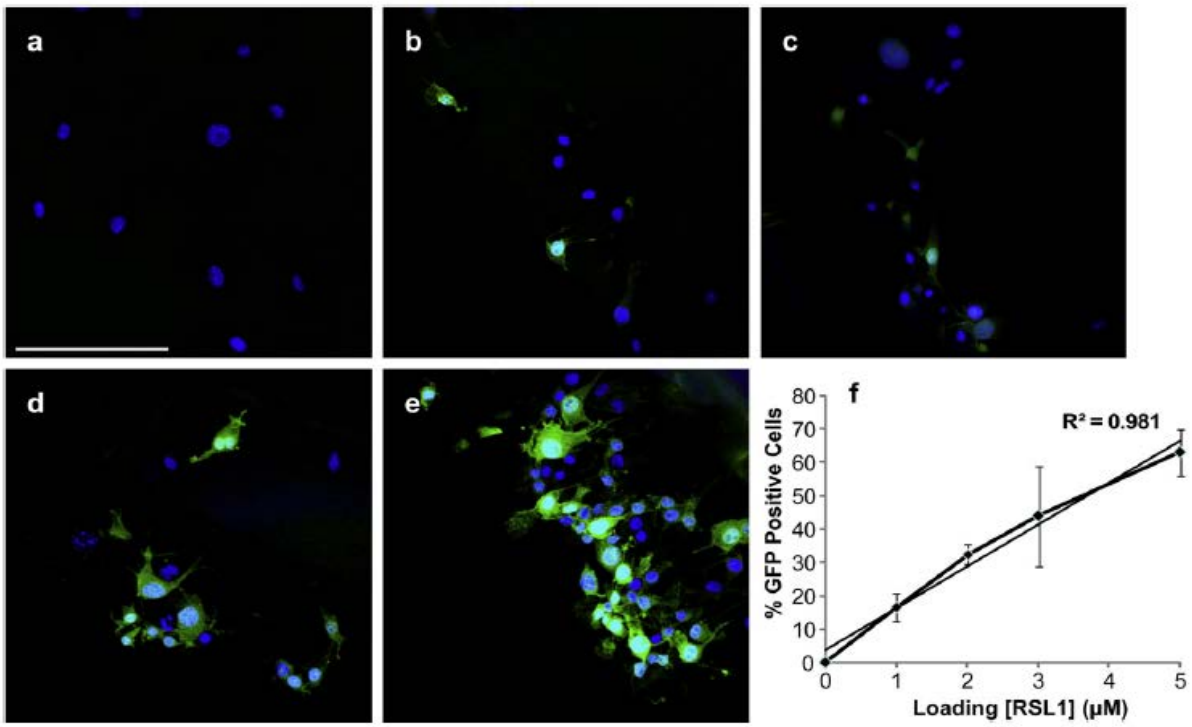

Figure 15. Gene expression control by culture medium manipulation. At 48 hrs post-RSL1 administration, cells in growth medium without ligand did not express GFP (a), while cells in growth medium containing 1, 2, 3, and 5 µM ligand (b-d, respectively) expressed GFP with increasing frequency in a linear fashion (f). Scale bar = 200 µm.

2.3.2 Sustained release of RSL1 from PEUU films

Solvent casting of PEUU into 24 well TCPS plates yielded approximately 50 µm-thick polymer films. PEUU films loaded with 25, 75, or 150 µM RSL1 demonstrated a two-phase in vitro release profile with a small burst release of ligand accounting for less than 10% of loaded RSL1 during the first week of incubation followed by near zero-order release kinetics over the next 10 months. A total of 65-80% of loaded RSL1 was released after 10 months in vitro with approximately 1-3% of RSL1 steadily released per week regardless of the initial ligand loading dose – **Figure 16**. Degradation of PEUU films, as determined by the decrease in polymer viscosity over 1 year, was not different when films were soaked in PBS with 10% v/v acetonitrile compared to pure PBS. After just one week of soaking in each medium polymer intrinsic viscosity was 2.49 ± 0.03 and 2.51 ± 0.08 dL/g for films in PBS and in PBS with acetonitrile ($p>0.1$), respectively. These values decreased to 2.03 ± 0.14 and 1.91 ± 0.08 dL/g after 1 year ($p>0.1$). Additionally, RSL1 solubility in PBS/acetonitrile fluid far exceeded the total loading doses used in the films studied.

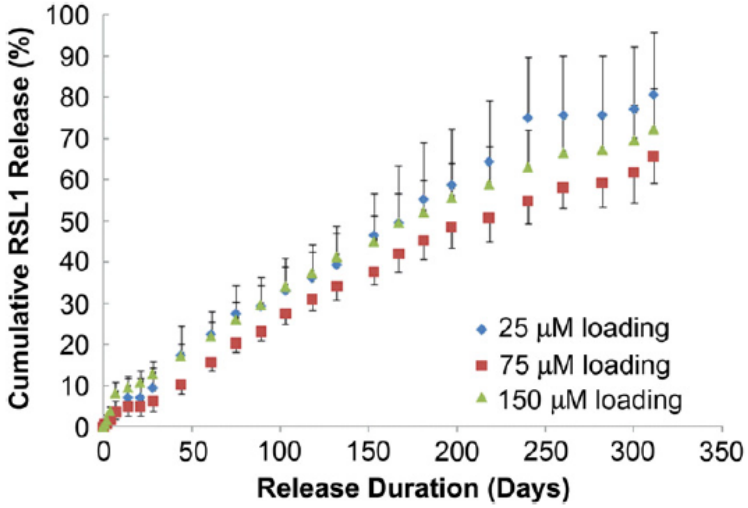

Figure 16. Release of RSL1 from PEUU films in vitro. Films had initial loading concentrations of 25, 75, and 150 µM RSL1.

2.3.3 Bioactivity of released RSL1

For short-term studies, cells cultured in releasate from all RSL1-loaded PEUU films expressed GFP 48 hrs post-treatment, while cells in releasate from PEUU films without ligand did not. Additionally, dose-dependent gene expression (R^2=0.99) was evident in cells cultured in releasate collected over a three week period from polymer films containing as little as 0-5 µM RSL1 – **Figure 17**. For long-term studies, releasate collected from films loaded with high concentrations of RSL1 (>25 µM) was able to induce GFP expression in B16 cells for extended periods of time, with the duration of effective gene expression increasing with increasing RSL1 loading concentration – **Figure 18**. Gene expression levels were similar between all three concentrations until 300 days, at which point differences in scaffold loading doses had a significant effect on the percentage of GFP expressing cells ($p<.001$ between each of the loading doses). By 300 days in vitro, releasate from 25 µM-loaded films appeared to lose the ability to effectively induce GFP expression in adherent cells, while releasate from 75 µM- and 150 µM-loaded films maintained gene induction ability to at least 355 days, the longest timepoint studied. At this time, however, gene expression was reduced compared to earlier time points.

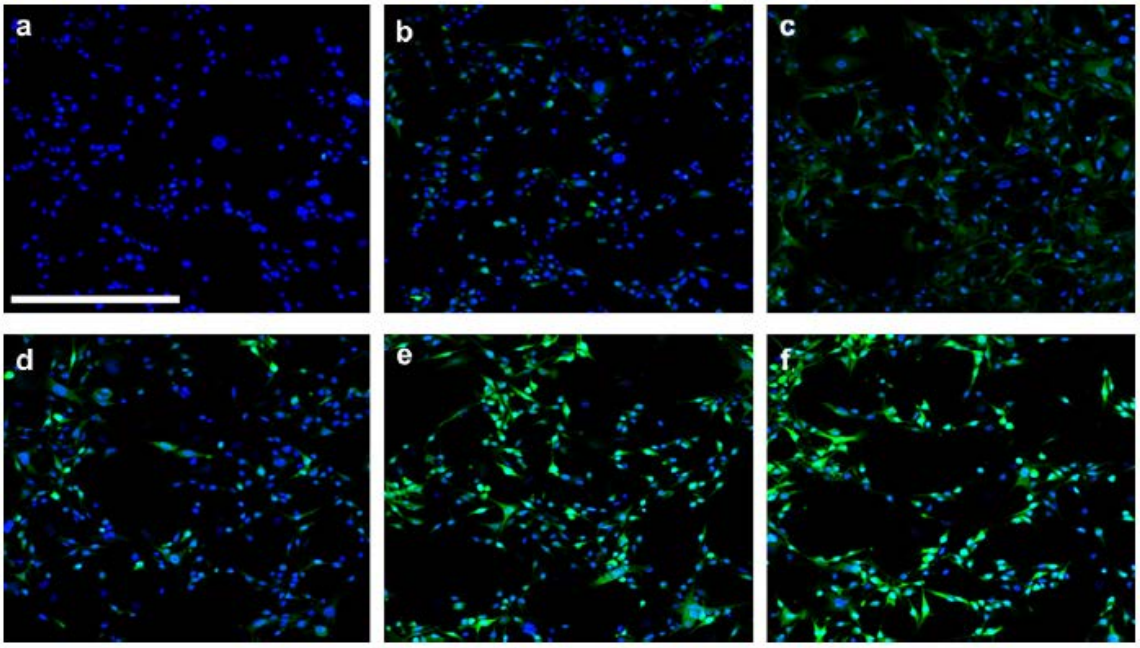

Figure 17. Gene expression in cells treated with release medium from PEUU films containing (a) 0 µM, (b) 1 µM, (c) 2 µM, (d) 3 µM, (e) 4 µM, and (f) 5 µM RSL1. Scale bar = 500 µm.

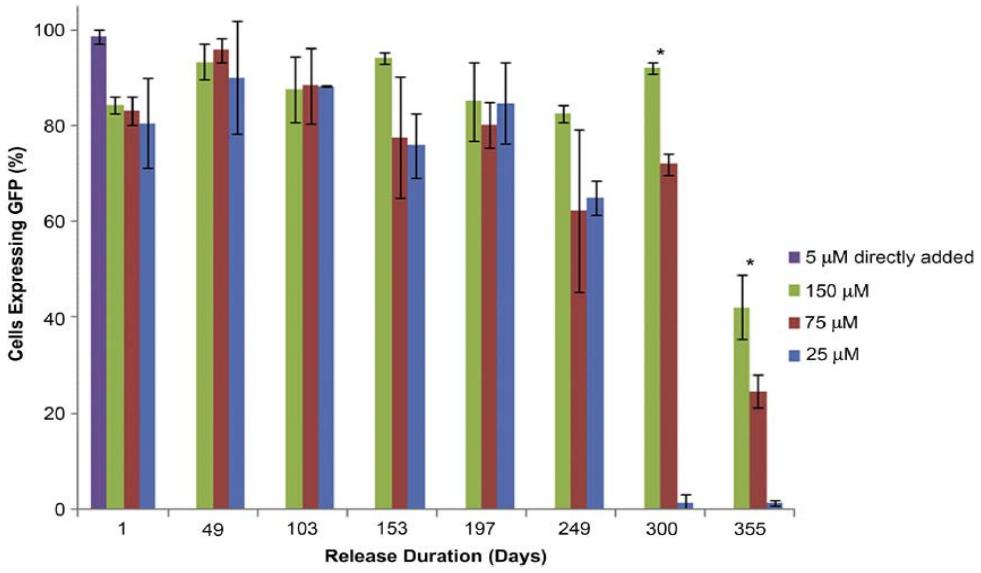

Figure 18. Long-term bioactivity of released RSL1. Release fluid from films loaded with 25, 75, or 150 µM RSL1 at designated time points was able to cause GFP expression in cultured B16 cells. * denotes p<.001 between each of the 3 concentrations.

2.3.4 Gene expression from PEUU films

B16 cells cultured directly on PEUU films containing 1-10 µM RSL1 expressed GFP for up to 21 days in vitro, while cells cultured on films without ligand did not express GFP. Furthermore, cells cultured on films containing 0-5 µM RSL1 demonstrated dose-dependent GFP expression (R^2=0.99) over this 3 week period, as evidenced by an increasing percentage of GFP-positive cells with increasing ligand loading concentration – **Figure 19.** While 75.2 ± 9.0% of cells on PEUU films loaded with 5 µM RSL1 expressed GFP, an increase in the GFP-positive cell fraction was not seen in cells cultured on PEUU films loaded with 7 µM (72.2 ± 7.8%) and 10 µM (76.1 ± 8.3%) RSL1.

2.3.5 Spatial control of gene expression on PEUU films

All cells expressed GFP 24 hrs after being plated onto microscope slides containing distinct regions of polymer with and without RSL1, regardless of the configuration of PEUU droplets. At

48 and 72 hrs after cell seeding, however, cells in regions where polymer contained RSL1 ligand expressed GFP, whereas cells in regions where ligand was not added to the polymer did not express GFP – **Figure 20b**.

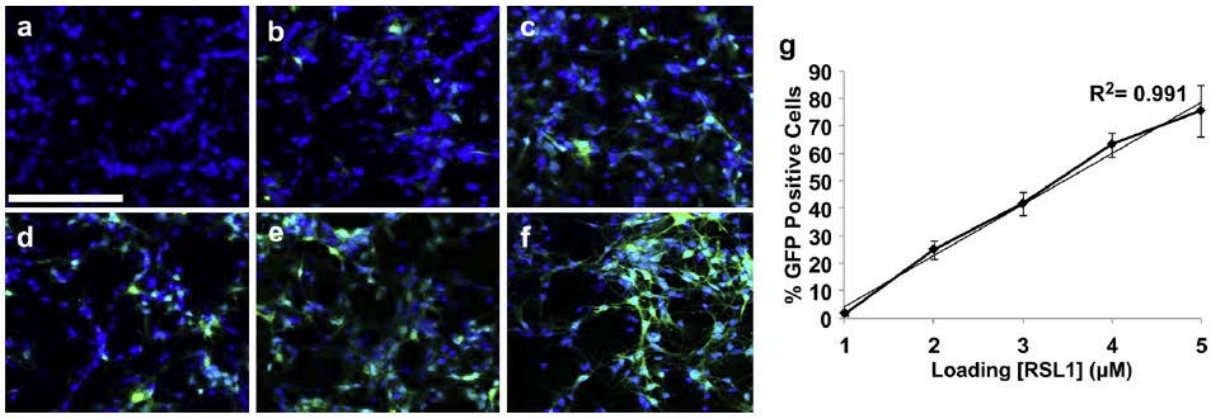

Figure 19. Gene expression on PEUU films containing (a) 0 μM, (b) 1 μM, (c) 2 μM, (d) 3 μM, (e) 4 μM, and (f) 5 μM RSL1. (g) Dose-dependent GFP expression is preserved when cells are maintained on polymer films. Scale bar = 500 μm.

2.3.6 Spatial control of gene expression on PEUU scaffolds

Porous scaffolds with or without RSL1 were successfully fabricated using the salt leaching technique. After 72 hrs of cell culture, cells were found on the surface and interior of PEUU scaffolds either with or without RSL1 ligand. Cells cultured in scaffolds without RSL1 did not express GFP, while cells cultured in scaffolds with ligand expressed GFP. Concentric porous scaffolds generated with an interior region containing RSL1 were successfully generated – **Figure 21a**. Electron microscopy revealed that the inner and outer regions were fused well at their interface (white arrows **Figure 21b**). Material continuity between the regions was further demonstrated by manual stretching of these scaffolds. The scaffold disks did not separate at the boundaries between inner and outer regions, but acted as a continuous material **Figure 21c**.

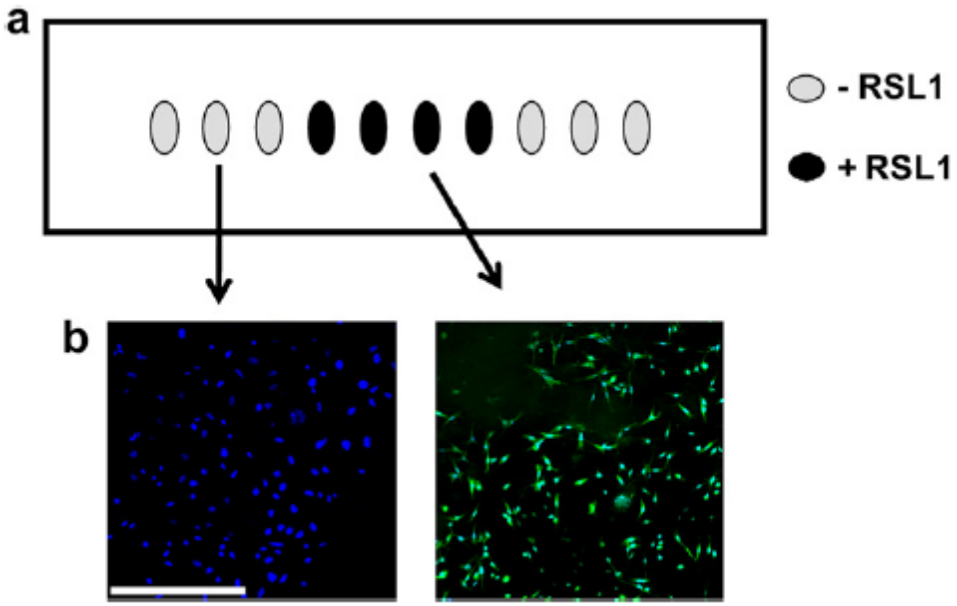

Figure 20. Spatial control of gene expression on PEUU films. (a) Typical slide layout for 2-dimensional spatial control experiments. (b) Cells on all regions of slides containing PEUU without ligand (grey) did not express GFP (left), whereas cells on all regions of slides containing PEUU loaded with RSL1 (black) clearly expressed GFP (right), demonstrating spatial control of gene expression on 2-dimensional PEUU films. Scale bar = 500 µm

Cells were evident throughout the concentric scaffolds after 72 hrs of static culture – **Figure 22a-c**. Cells in the center of the scaffold predominately expressed GFP; however, some GFP positive cells were evident in the non-RSL1 outer ring of the scaffold, radiating outward from the RSL1-containing core. The extent of high GFP expression in non-RSL1 regions varied by location around the scaffold core, in some areas being largely confined to the center and in other areas extending >1 mm away from the core. Additionally, the same level of spatial control over gene expression could be maintained up to seven days in static culture. The percentage of cells expressing GFP in the inner and outer regions of the scaffold after 3 days of culture was 87 ± 2.5% and 14 ± 2.6%, respectively ($p<.001$). The normalized G/B ratio of image intensity data across the center of the scaffold demonstrated the general localization of GFP expression to the middle of the scaffold, and GFP expression levels rapidly decreased the further cells were from

the RSL1-containing core – **Figure 22d**. Use of the transmural perfusion system led to fewer cells present on the scaffolds and markedly less GFP expression overall.

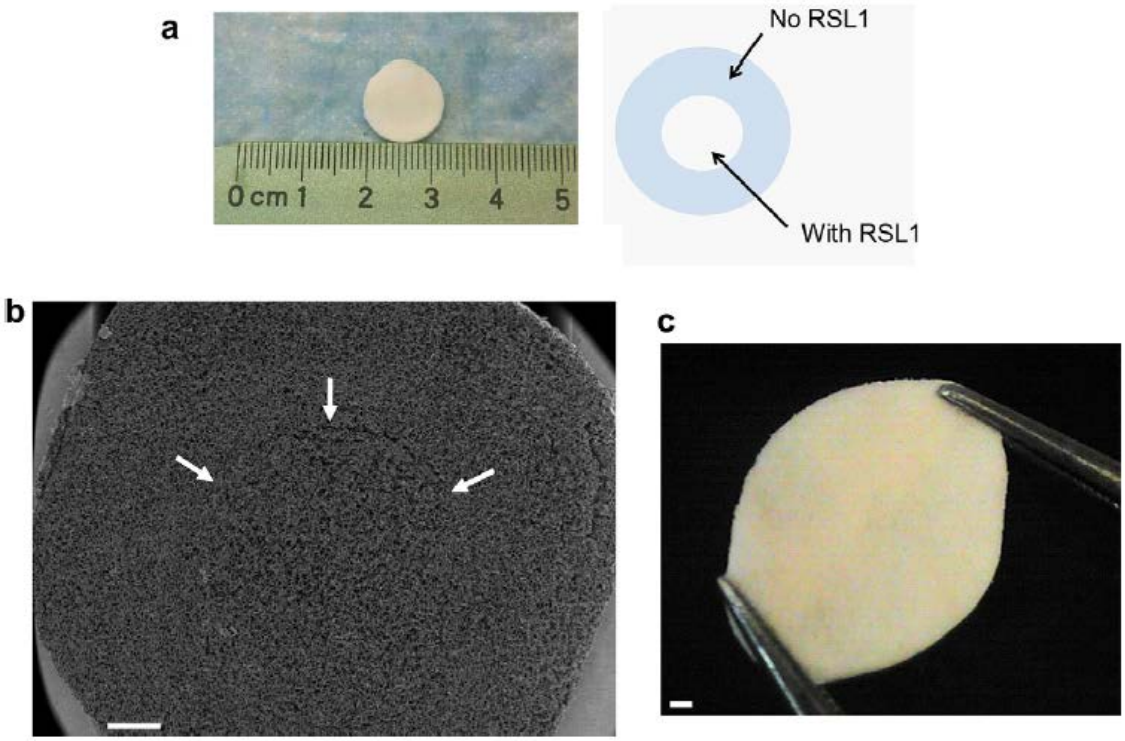

Figure 21. Macroscopic and scanning electron micrograph of porous scaffold differentially loaded with RSL1. (a) RSL1 was added to a center core of the material whereas no RSL1 was present in the outer ring, (b) Scanning electron micrograph of the boundary between RSL1-containing core and RSL1-free outer ring. White arrows delineate boundary between regions. (c) Mechanical stretching of the scaffold seen in (a) reveals continuity between concentric regions. Scale bar = 1 mm.

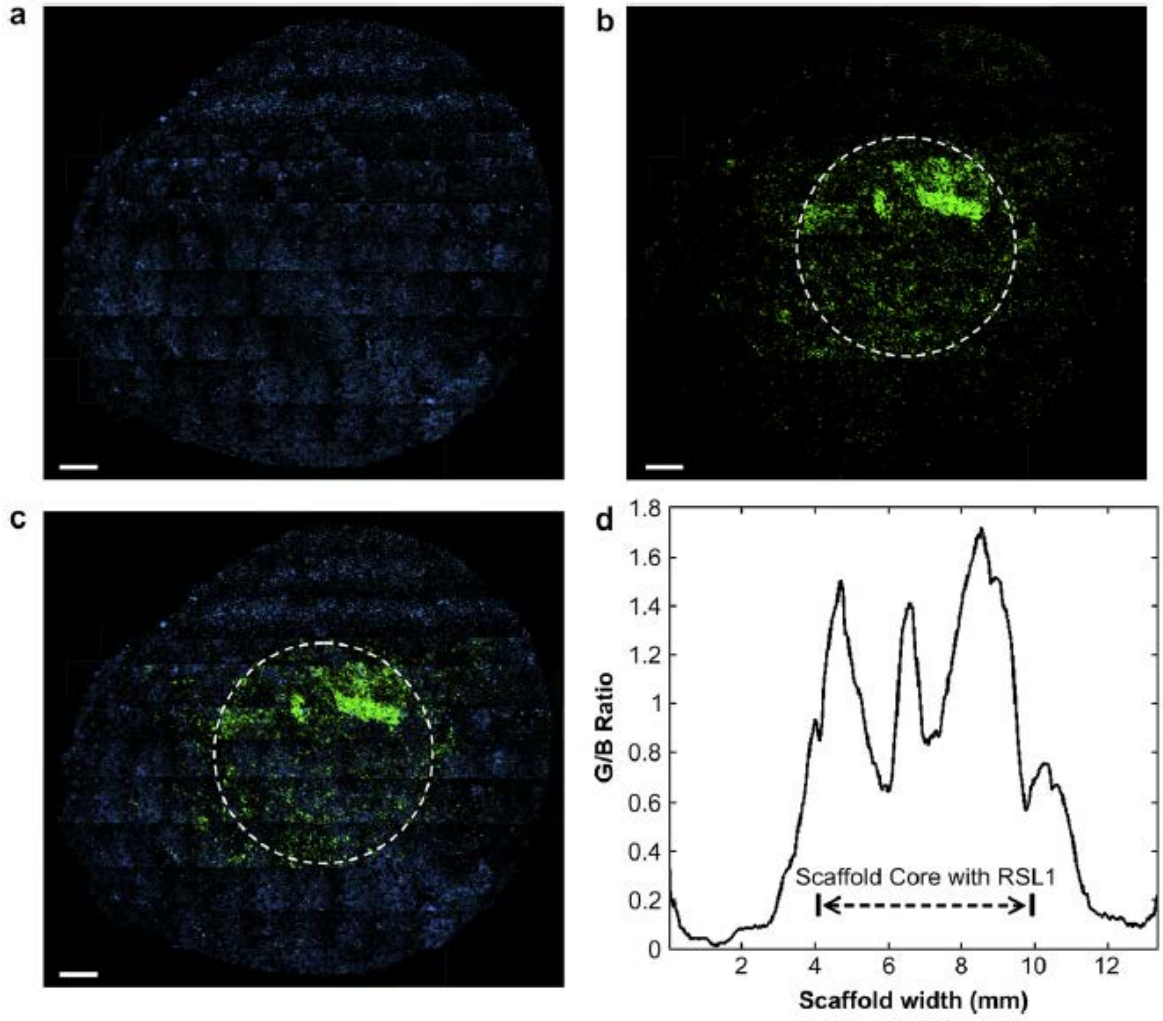

Figure 22. Spatial control of gene expression within 3D PEUU scaffolds. GFP expression was concentrated in the inner region of the scaffold where RSL1 inducer was present. (a) Blue - DAPI nuclear staining only, (b) green - GFP expression only, and (c) combined image showing localization of both cells and GFP expression. Dashed white circle represents boundary between inner and outer scaffold regions. Scale bar = 1 mm. (d) Ratio of green to blue (G/B) fluorescence signal with respect to location across center of scaffold, demonstrating spatial control of gene expression.

2.4 DISCUSSION

Gene-regulating systems that utilize an inducer molecule to regulate the timing and level of gene expression have proven effective in various applications [183-186, 189, 195]. Not only do these systems eliminate the need for DNA delivery in situ, the inducer molecules are more stable than plasmids, lending themselves to easy incorporation into biomaterials with the potential for maintained bioactivity for extended release. The present study explored the potential for spatiotemporal regulation of gene expression through the use of a biodegradable, elastomeric polyurethane scaffold as a controlled-release system for the delivery of one such inducer molecule, RSL1.

Biodegradable polyurethane scaffolds have been explored for a variety of soft tissue engineering applications including blood vessel, myocardial, cartilage, and abdominal wall reconstruction [43, 45, 196-200]. Linear thermoplastic elastomers are particularly advantageous because they can be easily blended and processed with biomolecules for controlled release applications [148, 201]. In the current report, scaffolds were synthesized using a salt-leaching technique since it provided a simple method to fabricate porous scaffolds containing RSL1 in a step-wise process with good continuity between neighboring regions. Further, this method did not require a liquid phase solvent extraction step which might allow premature release of incorporated ligand.

The release characteristics of RSL1 from PEUU films were studied over an extended period in vitro. Release studies were performed under a solution consisting of 10% v/v acetonitrile to simulate sink conditions for the hydrophobic RLS1 inducer. This release medium also proved attractive because it did not influence polymer degradation and subsequently, release rates. The small burst release and subsequent linear release profile of ligand was likely due to the interaction of the hydrophobic RSL1 molecule with hydrophobic regions of the PEUU polymer. It is understood that such positive interactions between drug and carrier can influence drug release kinetics and has been demonstrated in other drug-delivery systems [140, 202]. Furthermore, the lack of porosity in PEUU films may lead to release rates slower than that which would be seen from porous scaffolds.

The diffusion of the RSL1 ligand seems to play an important role in the ability to spatially control gene expression. Varying the spatial patterning of droplets on microscope slides for 2D control had no effect on the spatially-defined gene expression. Rather, spatial control of gene expression in 2D films could be achieved only during the second phase of ligand release in static culture because the initial burst release from areas of film containing RSL1 sufficiently spread throughout the culture medium to cause GFP expression in cells on regions without RSL1. This limitation was less pronounced with three-dimensional scaffolds in static culture. Ligand from the center of the scaffold was not adequate to cause all cells on the scaffold to express GFP. However, the presence of some GFP-positive cells in the non-RSL1-containing region may have been due to the diffusion of the inducer molecule laterally from regions of high RSL1 content to regions of low RSL1 content. The functional consequence of high levels of GFP expression extending about 1 mm out from the scaffold core may be insignificant if larger scaffolds are involved. In contrast, dynamic culture of cell-seeded scaffolds, using a transmural perfusion system [194], did not achieve high levels of GFP expression regardless of cell location on the scaffold, and it is postulated that this was due to RSL1 being washed away from cells too rapidly (i.e. before they could take up ligand to initiate transcription). As such, while the use of static culture was limited in that it may have allowed RSL1 diffusion to trigger GFP expression in bordering non-RSL1 regions, its use led to higher GFP expression overall. Appropriate dynamic culture systems may be explored more fully for the potential to control molecule diffusion while allowing for RSL1 uptake into cells. Other material-based techniques may be employed to control ligand diffusion, for example forming a polymer film around the inner core to discourage lateral RSL1 diffusion or cell migration to the outer regions. Diffusion of ligand at a scaffold implant location in vivo may also vary depending on the local tissue environment. Areas with high mass transfer, for example on the luminal side of a blood vessel, may behave differently than other areas.

It has been demonstrated that the activation of just a few genes of interest can cause both precursor and adult cells to differentiate to specific lineages [203-207]. While outside the scope of the current research, it is reasonable to postulate that if precursor cells are loaded with multiple genes which are under control of an inducer ligand, and which cause differentiation to a specific lineage, then those cells would differentiate automatically once in the location of a scaffold loaded with the inducer. For example, cardiac fibroblasts transfected with genes

GATA4, Mef2c, and Tbx5 under control of an inducer ligand may automatically reprogram to cardiomyocytes in the location of a scaffold containing the inducer ligand [203]. Additionally, it has been shown that spatiotemporal control of biochemical signals plays a role in influencing appropriate chondrogenesis [208, 209]. Particularly, articular cartilage has a complex three dimensional arrangement wherein the size and shape of chondrocytes, and the content and type of collagen and proteoglycans varies from the subchondral bone to the articulating surface. Using spatial gene expression through an inducer system may more closely generate this multifaceted by encouraging cellular differentiation or localized growth factor and extracellular matrix production.

A similar approach may be useful in various cardiovascular applications. Blood vessels have a particular spatial arrangement of endothelial and smooth muscle cells, collagen, and elastin that is crucial to proper function. Currently, synthetic vascular grafts are being fabricated in a stepwise processes using thermally induced phase separation or electrospinning that could give distinct inner and outer layers of material that may be similar to what is seen in native vessels.[210] Loading each layer of the synthetic scaffold with specific inducers that could influence transfected cells, one could encourage growth of an endothelial layer in the inner region and a smooth muscle layer with high collagen production in the outer layer, for example. This is even more feasible when considering, in the case of electrospinning, that cells can be simultaneously electrosprayed during scaffold fabrication.[211] By applying both inducer-loaded materials and stably transfected cells, any layered geometry could be constructed with each layer being composed of the desired cells to respond to a desired inducer. In the realm of a cardiac patch, loading of channels through the patch material with inducer ligands in a geometry that resembles a vascular network may help to vascularize implantable scaffolds. Specifically, the inducer might encourage transfected cells that infiltrate the material to become the smooth muscle and endothelial cells necessary for blood vessels. Various molecules that are known to encourage cell differentiation for development of vascular networks could be employed.[212-214] As a vascularized network would be critical in the generation of new myocardial tissue, an approach that guides such network development may be highly useful. The appreciation of such approaches is gaining momentum as shown by recent publication of research using other inducers, cell types, and materials.[215]

These types of complex architectures are found throughout the body including in the gastrointestinal tract, spinal column, and bone. Even more advanced scaffold systems may be envisioned wherein different cell types are loaded with different gene expression systems, the inducer ligands for which have been independently loaded into specific regions of a single scaffold. In this way both cell types could be cultured in the scaffold together, yet each will only perform a designated behavior in the location of release for their specific inducer ligand. Cells not in contact with their ligand would remain in their original state or subject to endogenous influences. Overall, such approaches may be promising for the development of a desired tissue type from precursor or adult cells in a three dimensional configuration which is patterned at the time of scaffold fabrication.

While the in vitro data of this report demonstrate the potential for extended periods of controlled release of a bioactive inducer ligand, performing in vivo studies to evaluate the duration of the gene expression effect for extended periods is a logical next step. Polymer degradation will be accelerated in vivo and will be accompanied by local inflammatory phenomena. The inducer ligand release might be accelerated, or potentially the ligand bioactivity might be compromised at extended periods. Data from the in vivo administration of RSL1 does not suggest acute lability, however [216]. A more appropriate cell type would also likely be pursued for in vivo studies. B16 cells were utilized here for their ease of handling and expansion. Use of a cell whose functionality could be altered in a clinically relevant manner by the expression of a specific gene could be pursued. Furthermore, while B16 cell attachment and growth was qualitatively evident throughout the scaffolds and no reduction in cell numbers was noted over the culture period used in this study, the viability and proliferation of clinically-relevant cell populations will need to be examined with further assessment of the therapeutic potential for this type of scaffold system.

2.5 CONCLUSIONS

A polymer scaffold system capable of spatially controlling gene expression in cells in vitro without local DNA delivery has been demonstrated. The biodegradable elastomeric polyurethane

employed released an inducer ligand over an extended period while maintaining ligand bioactivity. This scaffold system may ultimately provide a means to precisely control progenitor cell commitment in a spatially-defined manner in vivo for soft tissue repair and regeneration including in cardiac biomaterial therapies.

3.0 CONTROLLED RELEASE OF IGF1 AND HGF FROM A BIODEGRADABLE POLYURETHANE SCAFFOLD

3.1 INTRODUCTION

(Note: This chapter was previously published as: Nelson, D.M., P.R. Baraniak, Z. Ma, J. Guan, N.S. Mason, and W.R. Wagner. Controlled release of IGF-1 and HGF from a biodegradable polyurethane scaffold. Pharmaceutical Research 2011;28(6):1282-93.)

The influence of substrate mechanical properties on cell proliferation, differentiation, and extracellular matrix production is increasingly appreciated.[217, 218] As such, more attention is being paid to the mechanical properties of candidate scaffolds for tissue engineering and regenerative medicine applications in an effort to improve functional outcomes. Historically, synthetic polymers used for cardiovascular replacement and repair have included non-degradable polymers such as poly(ethylene-terephthalate) and poly(tetrafluoroethylene) and tissue engineering approaches have frequently employed common polyesters such as poly(lactide), poly(glycolide), and their copolymers.[219] However, these polymers are relatively stiff and not mechanically similar to native cardiovascular tissue.

Polyurethanes as a class of polymers are attractive for soft tissue applications because of their ability to exhibit elastic behavior generally similar to many soft tissues and to be able to do so through physical crosslinking. To this end, biodegradable, elastomeric polyurethanes have been developed using a variety of techniques to introduce lability [190, 220-222], and these materials have been investigated in several locations in vivo, including both vascular and myocardial applications.[43, 210] In the case of biomolecule delivery from polyurethane scaffolds, agents such as growth factors and adhesion molecules have been incorporated in order to enhance cellular infiltration into and survival within scaffolds and to direct the differentiation of endogenous and exogenous stem cell populations in situ.[201, 223-227]

Of particular interest for controlled release applications in myocardial tissue engineering is IGF1, which has been implicated in many physiological processes including tissue growth, protection and repair. Specifically, IGF1 has been linked to several pathways in skeletal muscle formation and regeneration [228] and is expressed during the early and middle stages of muscle repair.[229-231]. Following myocardial infarction, IGF1 has been shown to stimulate hypertrophy and prevent cardiomyocyte death, thereby attenuating ventricular dilation.[232] Another growth factor that plays both a protective and reparative role in cardiac muscle is HGF.[233-235] It has been shown to be antifibrotic, proangiogenic, and also recruit stem cells when delivered to the heart.[233, 236, 237] However, the therapeutic use of these growth factors is limited by their short half lives in vivo.[238, 239] Thus, the sustained delivery of IGF1 or HGF coupled with the attractive mechanical properties of a biodegradable, elastomeric polyurethane scaffold may prove more advantageous for myocardial or skeletal muscle repair and regeneration than the administration of growth factor or polymer matrix alone.

The objective of the current study was to synthesize and process a biodegradable, elastomeric poly(ester urethane)urea material with the ability to incorporate and release bioactive IGF1 and HGF. Porous PEUU scaffolds were fabricated using a thermally induced phase separation technique, and growth factors were directly incorporated into scaffolds during preparation. The long-term in vitro release kinetics of IGF1 from scaffolds were investigated in PBS and in the presence of the enzyme lipase to simulate in vivo degradation. The bioactivity of released IGF1 was confirmed with in vitro cell assays. HGF was also loaded into PEUU scaffolds, and while controlled release kinetics were not evaluated, it was also shown to maintain bioactivity upon release.

3.2 MATERIALS AND METHODS

3.2.1 Biodegradable poly(ester urethane)urea (PEUU) synthesis

PEUU based on polycaprolactone diol (MW=2000, Aldrich), BDI (Aldrich), and putrescine (Aldrich) was synthesized in a two-step solution polymerization as previously reported – **Figure**

14.[190] In brief, a 15 wt% solution of PCL in DMSO was stirred with a 5 wt% solution of BDI in DMSO under argon gas. Stannous octoate, the catalyst, was added, and the reaction allowed to continue at 80°C for three hr with constant stirring. After this time, the prepolymer solution was removed from heat and allowed to cool to room temperature. Putrescine in DMSO was then added dropwise, with constant stirring, to the prepolymer solution, and the reaction allowed to continue at room temperature for 12-18 hr. The stoichiometry of the reaction was 2:1:1 BDI:PCL:putrescine. The PEUU solution was precipitated in distilled water and immersed in isopropanol to remove unreacted monomers. Finally, the polymer was dried under vacuum at 50°C.

3.2.2 Fabrication of three-dimensional, growth factor-loaded PEUU scaffolds

Three-dimensional, porous PEUU scaffolds were fabricated by a thermally induced phase separation (TIPS) method.[240] Following synthesis, PEUU was dissolved in DMSO at 80°C to make 5 or 8 wt% polymer solutions. Insoluble, cross-linked polymer was removed by centrifugation at 250xg, and PEUU solution was once again heated to 80°C. Hot polymer solution was injected into a cylindrical glass mold (inner diameter 10 mm) capped with rubber stoppers. The mold was immediately placed at -80°C for 3 hr. The cylinder end caps were then removed, and the mold was transferred to 200-proof ethanol for 3-7 days at 4°C for solvent extraction. Solvent extraction was considered complete once the polymer scaffold detached from the edges of the glass mold. Following DMSO removal, scaffolds were placed in water overnight to remove ethanol and reconstitute pore structure. Finally, the scaffolds were vacuum-dried for 24 hr. Electron microscopy was used to verify porous scaffold morphology.

To fabricate growth factor-loaded scaffolds, IGF1 and HGF (R&D Systems) were first reconstituted in PBS in an excess of bovine serum albumin (BSA) (1:100, wt:wt) to stabilize the protein. Solutions containing growth factor and BSA were then snap-frozen in liquid nitrogen and vacuum-dried for 48 hr. Dried proteins with salts were mixed with DMSO to make IGF1 and HGF stock solutions at a concentration of 25 µg/ml. Growth factor in DMSO was added to the polymer solution at 80°C under rapid stirring for 15 s to make protein homogenous in solution, after which the solution was injected into a cylindrical glass mold and immediately transferred to

-80°C. ^{125}I-IGF1 was synthesized following previously published methods.[241] IGF1 and ^{125}I-IGF1-loaded scaffolds contained 2.5 mg of BSA and a final IGF1 concentration of 500 ng/ml in PEUU solution. HGF-loaded scaffolds contained 2.5 mg of BSA and a final HGF concentration of 250 ng/ml of PEUU solution. Scaffolds were also fabricated without growth factor, but with BSA.

3.2.3 Mechanical testing of PEUU scaffolds

Scaffolds with and without growth factor were snap frozen in liquid nitrogen and cut into 500 μm-thick discs. In order to demonstrate similarity to scaffolds previously reported [201] , tensile properties were measured on an MTS Tytron^{TM} 250 MicroForce Testing Workstation (10 mm/min crosshead speed) according to ASTM D638-98. Five samples were tested for each scaffold.

3.2.4 Degradation of PEUU scaffolds

BSA-loaded scaffold disks were weighed and then immersed in PBS with or without 2 μL lipase enzyme solution (Sigma Aldich, 100 units/ml final concentration) at 37°C. At specified time points, scaffolds (n=3) were collected, dried, and weighed. After collecting the data for each time point the studied scaffolds were discarded. The mass of dry scaffolds at each time point was compared to the starting dry mass of the sample. Release fluid was changed at regular intervals in order to maintain a constant pH and to keep an active concentration of enzyme present. Differential scanning calorimetry (DSC) of scaffold disks (n=3) at different stages of enzymatic degradation over 1 week, or without enzyme over 2 weeks, was completed using a Thermal Analyst 2000 (TA Instruments) DSC 2910 differential scanning calorimeter. Scaffold disks were heated from -100°C to 80°C at a heating rate of 10°C/min.

3.2.5 Quantification of growth factor release from PEUU scaffolds

Release kinetics for PEUU scaffolds containing ^{125}I-IGF1 were determined in vitro. Scaffold disks (750 µm thickness, 10 mm diameter) were placed in test tubes and incubated in release media consisting of either 2 ml PBS or 2 ml PBS + 100 U/ml lipase enzyme per well at 37°C. Releasate was collected at pre-determined time points and replaced with 2 ml of fresh release media. The calculation of pretin release at every time point was adjusted to account for the radioactive decay of I^{125} which is 59.6 days. These studies extended for up to a 440 day period. Growth factor release was determined by quantifying the radioactivity of the release fluid using a gamma counter (Auto Gamma II, Perkin Elmer).

3.2.6 Verification of bioactivity of released growth factor

The bioactivity of IGF1 released from scaffolds without lipase enzyme was measured by a cell mitogenicity assay, employing Balb/3T3 cells (a mouse embryonic fibroblast cell line, R&D Systems) and MG-63 cells (a human osteosarcoma cell line, R&D Systems). These cell types were selected due to their documented dose-dependent proliferation in response to IGF1 treatment.[242, 243] Preliminary studies involving direct addition of IGF1 to these cells over a range from 0-200 ng/ml showed a maximum growth response for both cell types at 150 ng/ml IGF1. Thus, this concentration was used as the standard for comparison in bioactivity assays. The bioactivity of released HGF was measured by a cell motogenic assay, and human umbilical vein endothelial cells (HUVECs) were selected due to their documented motogenic response to HGF.[244] Scaffold disks (500 µm thickness, 10 mm diameter) with and without growth factor loading were placed into wells of 24 well tissue culture plates in cell basal media (Minimum Essential Medium (MEM) for MG-63 cells and DMEM for Balb/3T3 cells, both without fetal bovine serum). Basal medium from wells containing scaffolds was collected at pre-determined time points over three weeks, sterile-filtered, and kept frozen at -20°C until transfer to cells.

Balb/3T3 and MG-63 cells were plated at 1 x 10^4 cells/cm^2 in each well of 24 well TCPS plates in cell growth medium (MEM or DMEM supplemented with 10% fetal bovine serum and penicillin and streptomyocin). Prior to growth media exchange with polymer releasate (basal

medium), cells were treated overnight with 1 µl/ml colcemid (Sigma Aldrich) to synchronize cell cycle. Cells were then washed with PBS to remove traces of colcemid and fed with the appropriate polymer releasate. Four days following releasate treatment, cell numbers were indirectly quantified using a colorimetric assay for mitochondrial activity (MTT assay).[243] MTT results were qualitatively confirmed by visual cell inspection. Cell numbers for cells cultured in releasate were normalized to cells maintained in growth media.

HUVECs were plated at 1 x 10^4 cells/cm^2 in each well of 6 well TCPS plates in growth medium (Endothelial basal medium, Lonza Inc). An in vitro wound healing assay was used to confirm the motogenic effect of HGF on cells.[244] Briefly, once cells had grown to confluence, a cell scraper was used to create a wound down the center of each well of the 6 well plate. Cells were then washed with PBS to remove cell debris from the wound and treated with polymer releasate. A live-cell imaging system from Automated Cell Technology (ACT) was used to image cells at 10 min intervals over a four day period. Cell motility was quantified in terms of cell velocity (using ACT software) and cell migration into the wound (using NIH ImageJ software).

3.2.7 Statistical analyses

Data are reported as mean ± standard deviation. All statistical analyses were performed using SPSS software. For cell proliferation, mass loss, and protein release studies t-tests were used for evaluation of differences between 2 sets of data. For cell motility studies, mechanical properties, and protein release data involving 3 or more data sets, data were analyzed by ANOVA with Tukey post-hoc testing for specific differences between various degradation solutions. Significance was defined as $p < 0.05$.

3.3 RESULTS

3.3.1 Mechanical properties of PEUU scaffolds

TIPS scaffolds fabricated without the addition of any biomolecules (BSA or growth factors) had tensile strengths of 0.61±0.15 MPa. Scaffolds containing BSA alone had tensile strengths of 0.43±0.04 MPa, and scaffolds containing BSA and growth factor (IGF1 or HGF) had tensile strengths of 0.32±0.18 MPa ($p>0.05$).

3.3.2 Degradation of PEUU Scaffolds

Scaffolds incubated in PBS did not demonstrate significant mass loss over the time period studied – **Figure 23**. In the presence of lipase scaffold mass loss was substantially accelerated, with both polymer concentrations losing nearly half their mass over the first two days. With enzyme present 5 wt% scaffolds lost more mass over the first week compared to 8 wt% scaffolds with 38.9 ± 11.5% and 60.2 ± 2.5% mass remaining, respectively ($p<0.05$). Polymer degradation was nearly complete after 8 weeks. Morphologically, scaffolds maintained an organized pore

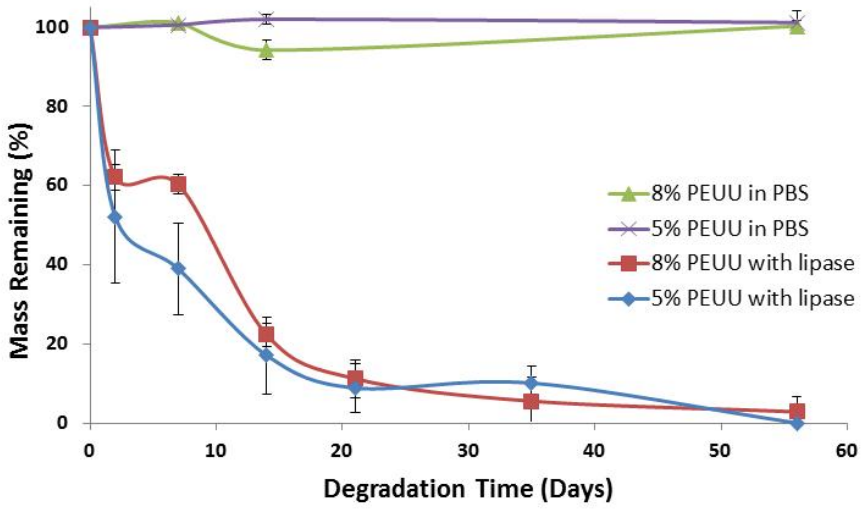

Figure 23. The mass loss of PEUU scaffolds was determined over time for 5 and 8 wt% scaffolds soaked in PBS or with 100 units/ml lipase enzyme. * denotes $p<0.05$ between scaffold polymer concentrations.

structure, and after one week of incubation with lipase the polymer surfaces were noticeably broken apart – **Figure 24**.

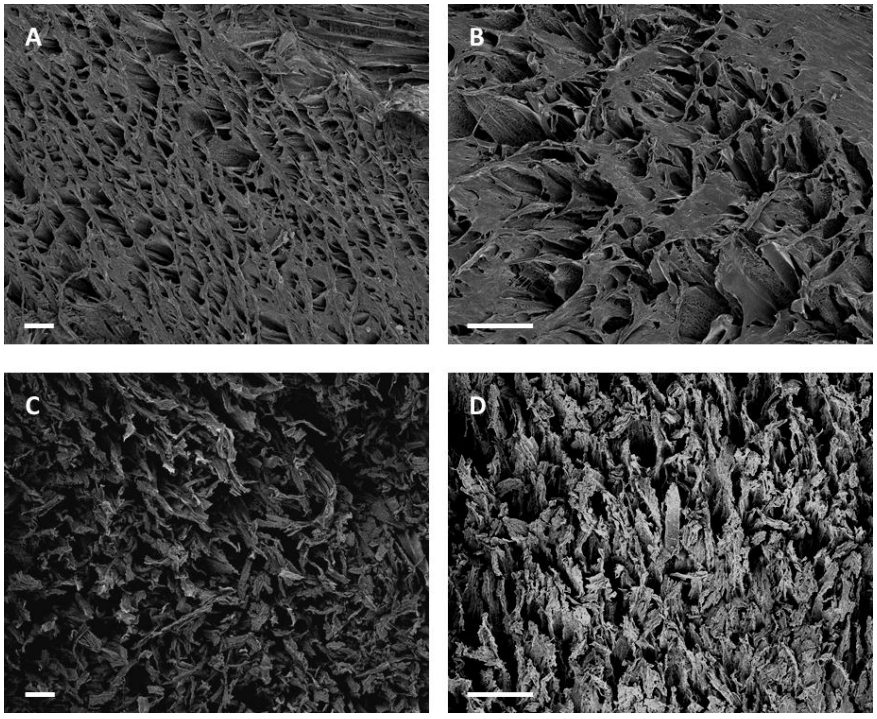

Figure 24. Electron micrographs of TIPS scaffolds (5wt% A and C, 8 wt% B and D) incubated in PBS (top panels) or lipase solution (bottom panels) for 1 week. Scaffolds maintained an organized pore structure after one week in PBS. After one week of incubation with lipase, scaffold surfaces were noticeably broken apart. Scale bar = 100 µm.

DSC confirmed the degradation of scaffolds in the presence of enzyme. The melting temperature (T_m) for original scaffolds was around 50°C for both 5 wt% and 8 wt% scaffolds – **Figure 25 and Table II**. During degradation a significantly lower second melting peak grew near 30°C as the primary peak weakened. By 7 days the original peak was gone in 5 wt% scaffolds though it continued to persist in 8 wt% scaffolds. Scaffolds in PBS did not show a significant change in T_m after 2 week.

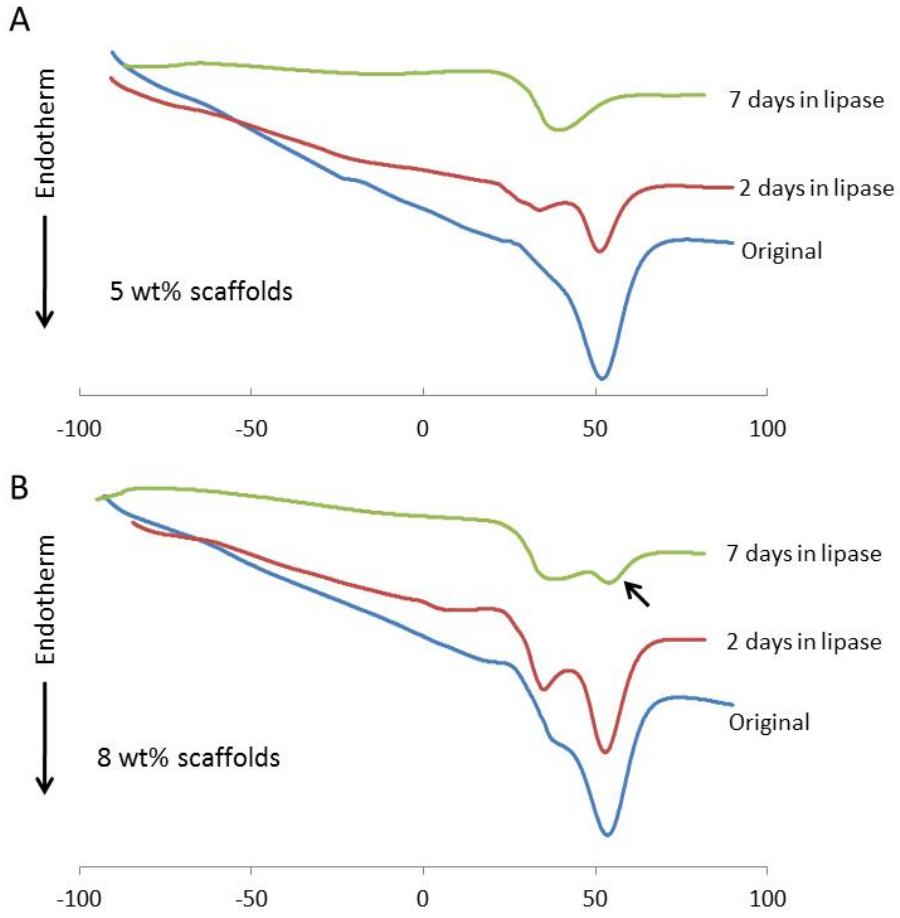

Figure 25. DSC heating curves of 5 wt % (A) and 8 wt% (B) scaffolds during degradation with lipase enzyme. In all situations the initial primary melting temperature near 50°C is lost as a new substantial peak near 30°C is formed. Scaffolds with 8 wt% PEUU maintain the first peak for 7 days (black arrow) suggesting a slower degradation than 5 wt% scaffolds which have lost that peak by 7 days.

Table II. Melting Temperature of Polymer Scaffolds

Scaffold wt%	Incubation Conditions	Primary Peak (°C)*	Secondary Peak (°C)*
5 wt%	Original	51.0 ± 1.3	-
	2 days in lipase	51.3 ± 0.2	36.2 ± 2.2†
	7 days in lipase	34.4 ± 4.6†	-
	14 days in PBS	54.1 ± 0.8	-
8 wt%	Original	52.6 ± 1.3	-
	2 days in lipase	53.1 ± 0.7	36.3 ± 2.4†
	7 days in lipase	35.3 ± 3.1†	53.8 ± 0.02
	14 days in PBS	54.8 ± 0.2	-

*data presented as mean ± standard deviation

†$p<0.05$ compared to original Tm of same wt% scaffolds

3.3.3 IGF1 Release from PEUU scaffolds

Before samples were utilized in the release kinetics study, a substantial amount of IGF1 had already been lost from the cylindrical scaffolds during DMSO extraction in ethanol. In particular, 8 wt% scaffolds lost 15% of loaded protein during this step compared to 50% for 5 wt% scaffolds. Thus, the starting mass of IGF1 in 8 wt% and 5 wt% scaffolds was 46.8 ± 7.5 and 22.5 ± 4.1 ng/scaffold, respectively. Once TIPS scaffold disks were immersed in PBS the initial burst release occurred over 48 hr, the extent of which was dependent on polymer concentration. Scaffolds with 8 wt% and 5 wt% polymer showed a burst release of 21.0 ± 1.0% and 10.3 ± 0.4 %, respectively ($p<0.001$) – **Figure 26A and Table III**. Following the burst release, there was an extended period of slow, steady protein release from scaffolds, termed latent phase I, and the release rate in this phase was faster in 5 wt% scaffolds (0.80%/week) than 8 wt% (0.39%/week) scaffolds ($p<0.001$). Following latent phase I, a period of more rapid release occurred, labeled diffusion phase I, wherein 10-30% of protein was released. Observationally, the scaffolds showed distinct, moderate swelling at this point but maintained their shape. Upon handling, a qualitative reduction in modulus was noted. The initial burst, latent I, and diffusion I phases were followed by a second period of steady protein release (termed latent phase II) and then a second

stage of accelerated protein release (termed diffusion phase II) from the scaffolds. Protein release after this point was very low for both polymer concentrations (latent phase III). Neither scaffold released all incorporated protein during the study, but radioactivity measurements confirmed that residual incorporated protein still resided within the polymer scaffolds, both types of which remained in a single piece throughout the study.

As is apparent in **Figure 26A** and **Table III**, the rate of protein release varied depending on the phase of the release profile and the initial polymer mass fraction. The rate of IGF1 release decreased for each subsequent latency phase. For example, during latent phase I in 5 wt% scaffolds, IGF1 released at 0.80%/week compared to 0.53%/week and 0.14%/week for the second and third latency periods, respectively ($p<.001$ between groups). The release rates in 8 wt% scaffolds followed a similar pattern but were consistently lower than for the 5 wt% scaffolds during these same latent phases at 0.39, 0.35, and 0.08%/week respectively ($p<.001$ between groups). The 8 wt% scaffolds consistently demonstrated longer latent periods. For example, the latent phase I lasted over 20 weeks compared to 10 weeks for 5 wt% scaffolds. Interestingly, diffusion I and diffusion II phases lasted similar amounts of time for both scaffold mass fractions. The diffusion I stage released more protein in 5 wt% scaffolds than 8 wt% scaffolds ($30.3 \pm 3.9\%$ vs. $11.9 \pm 2.1\%$, $p<.001$) but the diffusion II stage release was the opposite with less release from 5 wt% scaffolds ($17.5 \pm 2.9\%$ vs. $32.6 \pm 4.7\%$, $p<.001$) than the 8 wt% counterparts.

Scaffolds incubated with lipase enzyme released protein much faster than those without enzyme, with more than 90% of IGF1 being released after 9 weeks for both polymer concentrations – **Figure 26B**. The distinct release phases observed with scaffolds in PBS were not apparent when enzyme was present. However, a noticeable attenuation of release rate was demonstrated in 8 wt% scaffolds compared to 5 wt% scaffolds during specific early time points. Specifically, IGF1 release was slower in 8 versus 5 wt% scaffolds between days 1-2 ($2.1 \pm 0.8\%$ vs. $7.5 \pm 1.8\%$ respectively, $p<.05$), days 2-4 ($4.0 \pm 1.6\%$ vs. $10.4 \pm 0.5\%$, $p<.05$), and days 4-7 ($7.6 \pm 1.4\%$, vs. $13.1 \pm 2.1\%$, $p<.05$).

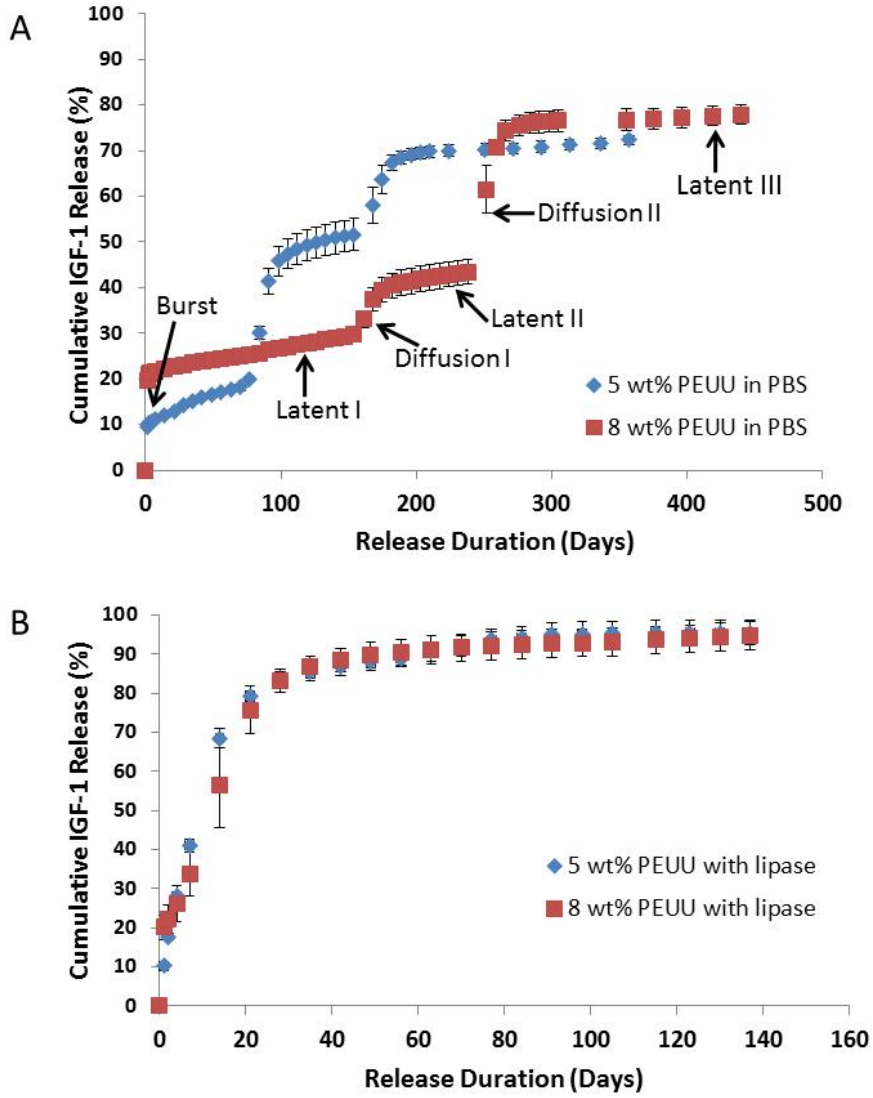

Figure 26. A) Scaffolds in PBS demonstrated a tri-phasic release profile for IGF1 over the time period studied. Alternating periods of slow, steady protein release (latent phases) and more rapid release (diffusion phases) followed an initial burst release. B) Both scaffold types incubated with 100 units/ml lipase enzyme released IGF1 at a much faster rate than those without enzyme.

Table III. IGF1 Release Kinetics

5 wt% PEUU Scaffolds					
Release Phase	**Phase Begin (Day)**	**Phase End (Day)**	**Phase Duration (Day)**	**Release Rate (%/week)***	**Total IGF-1 Release (%)***
Burst	0	2	2	--	10.3 ± 0.41
Latent I	2	70	68	0.80 ± 0.04	7.8 ± 0.38
Diffusion I	70	112	42	--	30.3 ± 3.91
Latent II	112	154	42	0.53 ± 0.03	3.2 ± 0.16
Diffusion II	154	196	42	--	17.5 ± 2.89
Latent III	196	--	--	0.14 ± 0.02	--
8 wt% Scaffolds					
Release Phase	**Phase Begin (Day)**	**Phase End (Day)**	**Phase Duration (Day)**	**Release Rate (%/week)***	**Total IGF-1 Release (%)***
Burst	0	2	2	--	21.0 ± 1.0
Latent I	2	147	145	0.39 ± 0.01	8.1 ± 0.22
Diffusion I	147	189	42	--	11.9 ± 2.10
Latent II	189	238	49	0.35 ± 0.02	2.4 ± 0.15
Diffusion II	238	284	46	--	32.6 ± 4.71
Latent III	284	--	--	0.08 ± 0.01	--

*data presented as mean ± standard deviation

3.3.4 Bioactivity of released IGF1 and HGF

MG-63 and Balb/3T3 cells treated with releasate from IGF1 containing scaffolds collected between days 0-7 and days 7-14 exhibited a significant increase in proliferation compared to those treated with degradation solutions from scaffolds without growth factor ($p<0.05$) – **Figure 27**. Cellular proliferation was comparable to that for cells treated with 150 ng/ml IGF1. Specifically, cells treated with day 0-7 releasate from scaffolds containing IGF1 exhibited a 2.0-fold (MG-63) and 2.1-fold (Balb/3T3) increase in cell number compared to cells treated with releasate from scaffolds without growth factor. Cells treated with day 7-14 releasate from scaffolds containing IGF1 exhibited a 1.6-fold (MG-63) and 1.7-fold (Balb/3T3) increase over

cells in releasate from scaffolds without growth factor. No significant difference in cell proliferation was seen between cells treated with releasate collected between days 14-21 from either set of scaffolds. For HGF, following treatment with the day 0-7 and day 14-21 polymer releasate from scaffolds containing HGF, endothelial cells grew into and repopulated the wound area more extensively than those maintained in growth medium or in releasate from scaffolds without growth factor ($p<0.05$) – **Figure 28**. Day 7-14 releasate was not collected to evaluate.

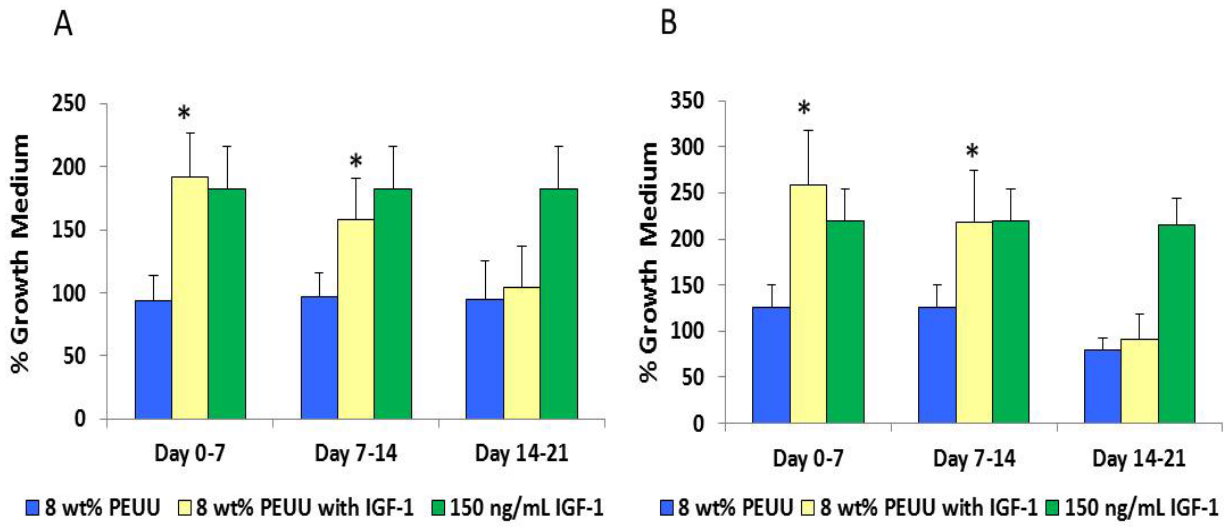

Figure 27. MG-63 (A) and Balb/3T3 (B) cells cultured in releasate from polymer containing IGF1 showed greater cell metabolic activity (as an index of cell number) compared to cells cultured in releasate from polymer without growth factor (*$p<0.05$). IGF1 added at 150 ng/ml to releasate from polymer without growth factor served as a positive control.

3.4 DISCUSSION

The release profiles of drugs from biodegradable elastomers vary widely depending on material composition and processing. Biodegradable thermoset elastomers based on ε-caprolactone and D,L-lactide have been processed with solid drug particles to form an osmotically-driven drug delivery device that delivers drug in a zero-order fashion.[139, 245, 246] The release rates in this system can be altered by changing the molecular weight of the prepolymer or the amount of excipient included with the drug. In another report ascorbic acid was incorporated into the backbone of a thermoplastic polyurethane and released only after hydrolysis of ester bonds.[227]

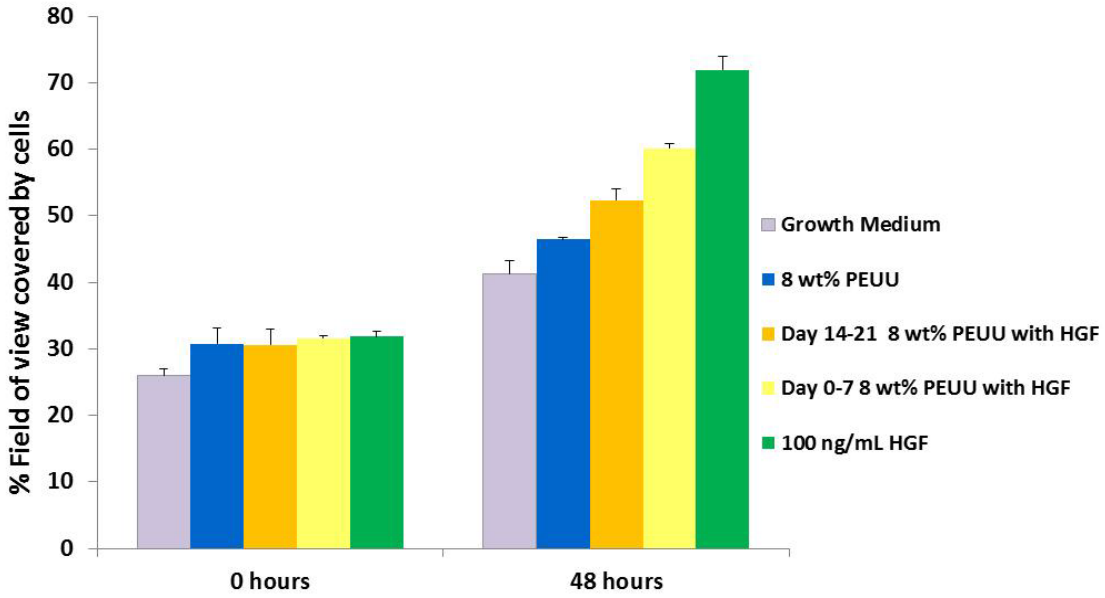

Figure 28. HUVECs maintained in releasate from scaffolds containing HGF grew into and repopulated the artificial wound area more extensively than those maintained in growth medium or in releasate from scaffolds without growth factor (*p<0.05). HGF added at 100 ng/ml to releasate from polymer without growth factor served as a positive control.

This led to a slow release rate initially which increased substantially over time in a way that corresponded with bulk polymer degradation. Many other biodegradable elastomers release molecules in a diffusion-controlled manner characterized by high initial release rates that quickly taper off.[142, 224, 247] One such group, a family of injectable biodegradable polyurethanes, has been of particular interest due to their ability to crosslink in situ to form porous polymer scaffolds in a way that does not substantially decrease the bioactivity of incorporated drugs. These systems generally show a high initial release that plateaus after a few days with 50-90% of drug being released depending on the drug loading mechanism and type of drug being delivered.[223, 248] Despite the fact that some members of this family are relatively slowly degrading (~30% mass loss over 36 weeks), release studies do not extend beyond a few weeks. This prevents understanding the mechanisms involved over time in a slow-degrading polyurethane and how the remaining 10-50% of protein is released from the system. In studying the long-term release kinetics of protein from PEUU, as has been done here, more insight may be gained toward developing extended release approaches for polyurethane systems.

IGF1 release from this biodegradable porous scaffold system demonstrated a multi-phasic release profile. There are a number of drug delivery systems that follow a biphasic drug release profile characterized by two separate stages of quick drug release separated by a latency phase.[138, 140, 249] The first phase of quick drug delivery occurs as drug is released that is either close to the surface or can easily diffuse out of the bulk of the material. Following this, delivery is slow in the latency phase until material degradation becomes adequate to loosen the scaffold and allow trapped drug to quickly diffuse out. The current report demonstrates a release profile wherein there are three distinct occurrences of rapid, diffusion-controlled release. Importantly, because the quantitative studies of IGF1 release used radiolabeled protein, the release kinetics observed may be different from what actually occurs when non-labeled IGF1 is released, as in the case of the bioactivity studies. As the scaffolds for both studies were made with identical protocols and loading concentrations, the protein released at each stage would likely be similar. However, variation may arise due to potential differences between IGF1 and ^{125}I-IGF1 and processing variability.

While the exact mechanisms of the complex release mechanism are not clear and warrant further investigation, it is likely that the phase segregated nature of PEUU plays a role. First, both hard and soft segments may act independently in relation to degradation and drug release. Additionally, PCL is known to contribute significant crystallinity to polyurethanes, the gradual breakdown of which can be delayed even in the presence of enzyme.[220, 250] It is possible that degradation follows a multi-step process where amorphous soft segment, crystalline soft segment, and hard-segment degradation occur separately with each stage influencing drug delivery. This hypothesis is supported by the DSC data which show a change in Tm during degradation. The transition from a Tm near 50°C to one near 30°C in the presence of lipase shows that the crystal structure of the polymer is being altered, particularly to a Tm below body temperature. In the case of the lower Tm, crystal structures would largely be melted above 37°C which could loosen the polymer network and allow more protein to be released. It may be that one of the diffusion phases seen for protein release from scaffolds in PBS is the result of a transition from the higher Tm to the lower one. Additionally, the delayed loss of the initial melting peak for 8 wt% scaffolds agrees well with the slower mass loss and slower protein release that was demonstrated during enzymatic degradation of 8 wt% scaffolds compared to 5 wt%.

The differences in protein release between 5 wt% and 8 wt% scaffolds illustrate the influence that polymer mass fraction had on drug release. First, 5 wt% scaffolds lost more protein in the solvent extraction step of scaffold processing, meaning these scaffolds had a lower loading efficiency. Second, the delivery rates of protein from 5 wt% scaffolds were consistently higher and occurred at earlier time points than for 8 wt% scaffolds. This phenomenon may be attributed to the smaller mass fraction of PEUU in the 5 wt% scaffold disks, which led to more free volume for molecular diffusion out of the scaffold and less material that required degradation. Both polymer mass fractions, however, exhibited slower release rates for IGF1 than had been shown previously when bFGF was released from similar scaffolds.[201] The reason for this difference is not clear but may be related to differences in the affinity of IGF1 and bFGF to the polymer or the slower polymer degradation that was present here compared to the previous study. While no significant mass loss was seen in the scaffolds in PBS over the time period studied, in the presence of enzyme, scaffolds with 8 wt% polymer had attenuated mass loss, particularly in the first week compared to those with 5 wt% polymer. This difference in enzymatic degradation between 5 and 8 wt% scaffolds was noticeable in the release profiles where the rate of IGF1 release was significantly lower between days 1 and 7 for the 8 wt% scaffolds.

The biodegradation of polyurethanes is a complex process that has received significant attention in recent decades.[251] Hydrolytically labile bonds in the soft segment provide the most common mechanism of degradation. It has been shown that both oxidative and enzymatic processes encouraged by inflammatory cells may speed polymer breakdown in vivo.[252, 253] Two common esterase enzymes produced by macrophages that have been utilized in vitro to simulate in vivo soft-segment biodegradation mechanisms are cholesterol esterase and lipase.[149, 250, 252-254] The ability of cells and enzymes to degrade polyurethanes is dependent on many factors including hard and soft segment chemical composition, size, surface morphology and mechanical environment.[253, 255-257] These studies illustrate that numerous complex processes are involved in biomaterial degradation, which cannot be fully replicated in vitro.

The enzyme concentration in this report was chosen for its ability to provide a degradation rate that corresponded to scaffold break down over approximately 8 weeks, similar

to what is histologically observed in vivo when a similar scaffold disk was implanted as a cardiac patch.[43] The release profile exhibited when scaffolds were incubated with lipase demonstrated that for in vivo environments where material degradation was accelerated, release rates were markedly different than in the PBS environments often used for in vitro controlled release studies. The rapid rate of polymer degradation in the presence of enzyme made for protein release kinetics that appeared more like the simple diffusion controlled systems discussed earlier, which was substantially different from the multiple phasic release profile seen in the PBS. Therefore, these data emphasize that researchers should consider the working environment when characterizing controlled release from biodegradable matrices, a practice not regularly seen in the literature.

Linear thermoplastic elastomers have an advantage over thermoset elastomers in that drugs can be readily incorporated during processing and in a way that does not risk drug inactivation during polymer crosslinking. In the current research, protein bioactivity was studied over the first three weeks of drug delivery. It is unclear if the loss of measurable cellular response to IGF1 between day 14-21 was from a loss of bioactivity or simply due to the low protein release during that time period as seen in the release profile. The latter case would suggest that released protein was of insufficient concentration to influence cell behavior in the assay used, which might be corrected with a higher initial loading dose of protein. Additionally, it has been shown that growth factors incorporated into thermoset degradable elastomers can maintain bioactivity over at least 3 weeks [245], suggesting that longer-term maintenance of bioactivity is feasible.

One limitation of the current research deals with understanding the maintenance of protein bioactivity during scaffold processing and throughout the release duration. To determine changes in bioactivity the amount of protein released from a scaffold needs to be quantified and then the functionality of that protein would be tested. However, in this report two distinct experiments were employed to study IGF1 release – quantitative release kinetics using radiolabeled protein and bioactivity of non-labeled released protein. Both were needed due to an inability to quantify non-labeled IGF1 using enzyme-linked immunosorbent assays (ELISA) and other spectrophotometric techniques. The inability to detect both IGF1 and HGF protein with these techniques may be related to the presence of polymer degradation products or

conformational changes to the protein which would prevent binding of the monoclonal antibody in the ELISA sandwich assay. In particular, the TIPS processing involved mixing protein in organic solvent and brief exposure to high temperatures – both factors that could damage the loaded protein. In order to preserve bioactivity, BSA was added in excess to protect the protein of interest as has been done previously.[157] Importantly, in spite of any presumed destruction of protein or changes to protein binding in the ELISA, enough protein remained bioactive over the three week studied to elicit the expected results on cell behavior in vitro.

One basis of controlled release formulations is that while proteins generally have a short half-life in vivo, their sequestration in a polymeric scaffold can act to protect them in vivo to prevent rapid degradation. An important finding in this research is that maintaining protein bioactivity for long durations as would be necessary for in vitro release studies may be irrelevant given the much faster release seen in conditions that mimic the in vivo environment. In the experiments using lipase, protein delivery was nearly complete after only 9 week compared to nearly 15 months for studies without lipase.

The ideal duration of IGF1 delivery that would be desired is dependent on the drug delivery application. For example, in the case of cardiac ischemia, rapid delivery of IGF1 in the days following injury has been shown to rescue injured myocardium.[133] However, in the case of slowly-progressing, chronic degenerative diseases such as inherited cerebellar ataxia [258] or diabetes [259], therapeutic options to treat severely debilitating symptoms are currently limited by the short in vivo life-span of peptide molecules and the need to administer drugs to patients on a daily basis. In such cases, controlled-release formulations leading to sustained improvements in patient symptoms and/or disease conditions allows for more convenient dosage and increased compliance with treatment.

Scaffold processing was also noteworthy for its role in determining protein loading efficiency in PEUU scaffolds. The final step of scaffold synthesis using TIPS involved DMSO solvent extraction. This step required 3-7 days of soaking in ethanol during which time a substantial amount of protein was lost to the solvent. While this method was necessary to create the mechanically robust, porous scaffolds studied here, other techniques such as salt-leaching may be considered which do not have a lengthy liquid-phase solvent extraction step. The short duration required to remove salts from thin scaffold disks in water (<20 minutes) may lead to

less protein loss in solution initially, even in spite of the higher solubility of protein in water compared to ethanol. Regardless of processing technique it is important to have a uniform distribution of protein throughout the scaffold. In this report disks cut from locations throughout the initial cylindrical scaffold were used in the release experiments. The narrow standard deviation in the protein release kinetics among all disks suggests a homogeneous distribution of protein throughout the cylindrical scaffolds.

Tissue engineering often seeks to combine appropriate scaffolding materials with important signaling molecules to encourage healthy tissue regeneration. It has been demonstrated that the controlled delivery of IGF1 and HGF from biomaterials in the context of ischemic myocardium has been influential in cardiac repair.[133, 260] These studies, however, utilize biomaterials that provide minimal mechanical support in a setting where such support may be advantageous. A mechanically robust, elastomeric scaffold similar to the one studied here was able to prevent further cardiac deterioration after its application as a surface patch following myocardial infarction.[43] Combining the benefit of this temporary mechanical support system with growth factor delivery might act to abrogate disease progression and encourage functional tissue repair in injured myocardium more effectively than either system independently.

3.5 CONCLUSIONS

A biodegradable elastomeric PEUU scaffold system was characterized for its ability to be loaded with and deliver growth factors (IGF1 and HGF) of clinical relevance. Cellular assays confirmed that the bioactivity of IGF1 and HGF was maintained during scaffold processing and for at least the early period of drug delivery. The kinetics of IGF1 release over a period up to 440 days demonstrated a complex triphasic profile. Much of this complexity was lost and replaced by a single phase release profile when enzyme was present to simulate in vivo scaffold degradation. The ease of processing associated with this thermoplastic biodegradable elastomer for both scaffold formation and drug loading makes this material an attractive option for soft tissue applications where both drug delivery and appropriate mechanical support are desired.

4.0 EXTENDED AND SEQUENTIAL DELIVERY OF PROTEIN FROM INJECTABLE THERMORESPONSIVE HYDROGELS

4.1 INTRODUCTION

(Note: This chapter was previously published as: Nelson, D.M., Z. Ma, C.E. Leeson, and W.R. Wagner. Extended and sequential delivery of protein from injectable thermoresponsive hydrogels. Journal of Biomedical Materials Research Part A 2012;100A(3):776-785.)

The unique versatility of injectable biomaterials has led to their use in many biomedical applications including tissue engineering and drug delivery.[261, 262] One primary advantage of this class of materials is that material injection may avoid the morbidity associated with the large incisions required for implantation of a pre-formed material.[263] N-isopropylacrylamide (NIPAAm) has been incorporated into many biomaterials due to its favorable sol-gel behavior.[115, 121, 124, 125, 264-266] Below its lower critical solution temperature (LCST) of 32°C, an aqueous solution of polyNIPAAm is liquid and can be injected through a small diameter needle. Upon reaching body temperature the polymer solution undergoes a sol-gel transition, thus forming a hydrogel in situ. Important functional properties such as mechanical strength, biodegradability, and cellular responsiveness have been imparted to NIPAAm-based injectable materials by copolymerization with specific monomers and peptides.[124, 125, 265-268] These materials have been developed for many potential applications including cartilage, bone, spinal cord and cardiac repair, as well as for drug delivery. [123, 125, 126, 264, 269-271]

Growth factor delivery has become an important tool in tissue engineering.[272] The delivery method is particularly important given that bolus solution injection leads to rapid removal of the growth factor from the injection site and extended periods of bioactivity over the tissue remodeling period in situ are desirable.[136] Hydrogels and microparticles are two delivery vehicles that have been widely studied for controlled drug release.[273, 274] Combining

both systems is a promising method under recent investigation to gain greater control over protein delivery rates. For example, it has been shown that putting drug-loaded microparticulates inside a hydrogel network can influence the rate of drug delivery from the microparticulates.[275-279] Additionally, combining microparticles of different compositions, where each particle type is loaded with a different growth factor, in the same hydrogel network is one way to allow for delivery of multiple drugs at rates independent of each other.[280] A variation on this theme, wherein one growth factor is loaded into microparticles that are inside the gel while another growth factor is dispersed in the gel phase, provides another means of controlling delivery rates.[280, 281] The value in delivering multiple versus individual growth factors on tissue response has been demonstrated in angiogenesis and bone growth.[64, 282] Further, independently controlling the rate at which each protein is delivered may allow for sequential delivery of factors, which has also been shown to be beneficial in some settings.[68, 283, 284] In angiogenesis new blood vessels must sprout and then mature with appropriate cellular components. This process may be achieved by sequential delivery of biomolecules such as vascular endothelial growth factor followed by either platelet-derived growth factor or sphingosine 1-phosphate.[68, 136, 284] Simultaneous delivery of these protein combinations does not elicit the same level of regeneration.

The objective of this study was to develop a thermoresponsive, biodegradable hydrogel system that would be capable of protein release from two distinct reservoirs – one where protein was attached to the hydrogel backbone, and one where protein was loaded into biodegradable polyester microparticles mixed into the hydrogel. A recently developed biodegradable and injectable NIPAAm-based biomaterial[265] was modified to allow direct protein conjugation. Poly(lactide-co-glycolide) microparticles generated by double emulsion processing were utilized to form the microparticulate protein carriers. The model protein bovine serum albumin (BSA) was delivered for extended periods from the modified thermoresponsive hydrogels, and distinct populations of labeled BSA were delivered from modified hydrogels embedded with microparticles to demonstrate sequential protein release. In addition, the effects of modifying the hydrogel to enable controlled release were examined in terms of thermoresponsive behavior.

4.2 MATERIALS AND METHODS

4.2.1 Materials

All chemicals were purchased from Sigma-Aldrich unless otherwise stated. NIPAAm was purified by recrystallization from hexane and vacuum-dried. HEMA was purified by vacuum distillation. Lactide was purified by recrystallization from ethyl acetate. Benzoyl peroxide (BPO), polylactide-co-glycolide (PLGA), sodium methoxide ($NaOCH_3$), poly(vinyl alcohol) (PVA), acrylic acid (AAc), N-hydroxysuccinimide (NHS) and methacryloyl chloride were used as received. Iodinated bovine serum albumin (^{125}I-BSA) (Perkin-Elmer) and fluorescein isothiocyanate or Texas Red labeled BSA (FITC-BSA and TexR-BSA, Molecular Probes) were used as received.

4.2.2 Material synthesis

4.2.2.1 Synthesis of methacryloxy N-hydroxysuccinimide (MANHS)

MANHS was synthesized by dropping 20 g methacryloyl chloride into a solution of NHS (20 g) and triethylamine (22 g) in 350 ml dichloromethane under stirring at 0°C followed by reaction overnight at room temperature. After a filtration process to remove the precipitate, the solution was washed with water 3 times and the organic phase collected by centrifugation and dried over anhydrous $MgSO_4$. Dichloromethane solvent was removed by rotary evaporation and the solid product was purified by flash chromatography to obtain a white solid, with a yield of 85%. Synthesis was verified by ^{1}H NMR spectrum (in $CDCl_3$): C$\underline{H}_2$=(6.43ppm, 1H, s), C$\underline{H}_2$=(5.90ppm, 1H,s) , -NCOC$\underline{H}_2$C$\underline{H}_2$CON-(2.88pm, 4H,s), -C$\underline{H}_3$(2.08ppm, 3H,s).

4.2.2.2 Synthesis of methacrylate polylactide (MAPLA)

MAPLA was synthesized as reported previously – **Figure 29**.[265] Polylactide-monomethyl ether (HOPLA-OCH_3) was synthesized by ring opening polymerization by dissolving lactide in dichloromethane to which $NaOCH_3$ initiator in methanol was added. After 2 h of reaction at 0°C,

the polymer solution was rinsed with 0.1 M HCl and deionized water, the organic phase was dried with $MgSO_4$ and removed by rotary evaporation. MAPLA was formed by dropping methacryloyl chloride in an HOPLA-OCH_3 solution in dichloromethane containing triethylamine, followed by reaction overnight at 0°C. Following reaction, precipitates were removed, the organic phase was dried and removed by rotary evaporation, leaving raw MAPLA product. MAPLA was purified by flash chromatography. NMR confirmed the synthesis of MAPLA with an average of 2.8 PLA units per MAPLA monomer.

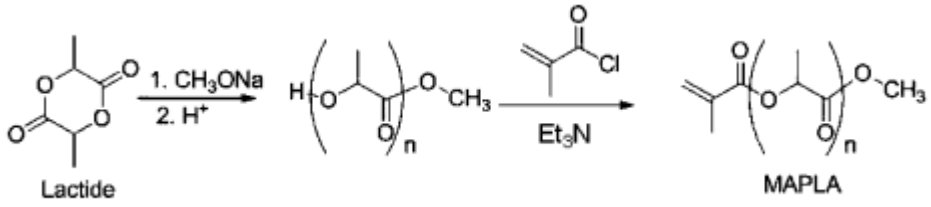

Figure 29. Synthesis scheme for methacrylate polylactide (MAPLA)

4.2.2.3 Synthesis of poly(NIPAAm-co-HEMA-co-MAPLA)

Poly(NIPAAm-*co*-HEMA-*co*-MAPLA) copolymers with or without MANHS were synthesized by free radical polymerization – **Figure 30**. Monomers, NIPAAm (6 g, 0.053 mol), HEMA, and MAPLA at a molar ratio of 80/10/10 were dissolved in 200 ml of 1,4-dioxane containing 160 mg BPO. The polymerization was carried out at 70°C for 24 h under argon atmosphere. The copolymer was precipitated in hexane and further purified by precipitation from tetrahydrofuran (THF) into diethyl ether and vacuum-dried. For inclusion of MANHS the molar feed ratio for NIPAAm, HEMA, MAPLA, and MANHS was 80/9/10/1, respectively. An additional copolymer was synthesized that incorporated 1 mol% AAc as a means to increase the degradation rate of the copolymer. The molar feed ratio for this copolymer was 80/8/10/1/1 NIPAAm/HEMA/MAPLA/MANHS/AAc.

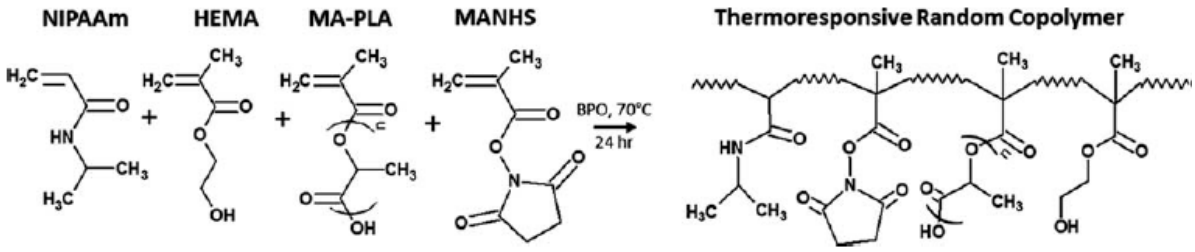

Figure 30. Synthesis scheme for a thermally responsive copolymer containing protein-reactive MANHS.

4.2.2.4 Synthesis of PLGA microspheres

PLGA microspheres with a lactide:glycolide ratio of 75:25 (Mw 66-107 kD) were synthesized using a water-in-oil-in-water (W/O/W) double emulsion technique.[277] FITC-BSA or ^{125}I-BSA was mixed with unlabeled BSA at a ratio of 1:10 and dissolved in 0.02x PBS to make a final total BSA concentration of 1 mg/ml . Initially, 200 mg of PLGA was dissolved in 4 ml dichloromethane. After all PLGA was dissolved, 200 µL of BSA solution was added to the dissolved PLGA and vortexed for 1 min. This primary emulsion was immediately added to 60 ml of 2% PVA that was stirring at 1000 rpm, to generate the W/O/W emulsion. After 5 min, the stirring speed was reduced to 600 rpm and an additional 80 ml of 1% PVA solution was added. After stirring for 6 h to allow dichloromethane evaporation, the microspheres were collected by centrifugation, rinsed with DI water and freeze-dried.

4.2.3 Copolymer characterization

Copolymer molecular weight was determined by gel permeation chromatography (Waters Breeze System). The copolymers were dissolved in tetrahydrofuran at 1 mg/ml and elution time was used to determine molecular weight by comparison to a poly(methyl methacrylate) standard. LCST values were determined by measuring the optical density of the material at 500 nm wavelength over a temperature range from 2 to 24°C. The LCST of the 80/9/10/1 copolymer without protein, with low protein content (BSA at 0.2 wt% of polymer), high protein content (20

wt%), and with microspheres (10 wt%) was determined (n=4 each group). The temperature at which the absorbance reached half of its maximum value was taken as the LCST, and was determined using a custom Matlab (MathWorks) program.

Hydrogel degradation was studied by quantifying the mass loss of samples at 37°C in PBS over time. PBS was changed frequently to maintain a constant pH throughout degradation. Samples (n=3 each) were collected at specific time points and lyophilized. The mass remaining in each sample was compared against the initial dry mass to determine percent mass loss. Hydrogel and microsphere morphology was viewed with scanning electron microscopy.

The change in mechanical properties of the hydrogels during sol-gel transition was characterized on a TA instrument rheometer (AR2000). Solutions of the 80/9/10/1 copolymer(16.7 wt % in PBS), with or without the inclusion of PLGA microparticles (10 wt%), were placed between two parallel plates and a temperature sweep from 5 to 35 °C (heating rate of 4 °C/min) was applied. The shear storage modulus G' and the loss modulus G'' were recorded as a function of temperature at a fixed strain of 2% and a frequency of 1 Hz.

4.2.4 In vitro protein release studies

4.2.4.1 Protein release from hydrogels

Copolymer was dissolved in PBS at 4°C at a concentration of 16.7 wt% and loaded with protein at a concentration of 100 µg/ml. For the 80/9/10/1 copolymer, protein was present in the PBS to be available to react with MANHS groups as the polymer dissolved – **Figure 31A**. For the 80/10/10 copolymer, protein was added to the solution after dissolving polymer. Gelation occurred by injecting 0.5 ml polymer solution into 1 ml of 37°C PBS. Samples ($n \geq 4$ for each gel type) were maintained in a water bath at 37°C and releasate was collected and replaced with fresh PBS at desired time points. ^{125}I-BSA was used for these release studies and the amount of protein released was determined by a gamma counter (Auto Gamma II, Perkin Elmer).

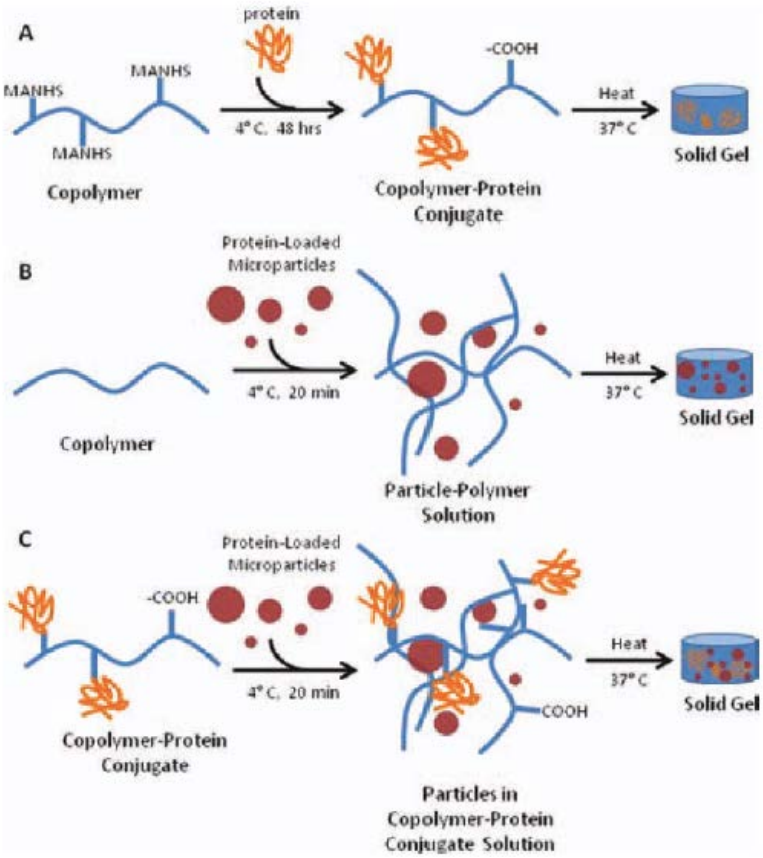

Figure 31. Approaches to protein loading in thermally responsive hydrogels. A) Protein is mixed with reactive copolymer to form protein-polymer conjugates in solution before hydrogel formation. B) Protein-loaded microspheres are mixed with copolymer solution before heating. C) Combination of (A) and (B) where one protein population is reacted with the copolymer in solution to form protein-polymer conjugates followed by mixing with microparticles loaded with a second protein population prior to thermally induced gel formation.

4.2.4.2 Stability of protein linkage to hydrogels

To determine the stability of the protein-polymer linkage, hydrogels with and without MANHS were loaded with ^{125}I-BSA and thermally cycled. Hydrogel solutions (n=4) were gelled at 37 °C for 3 h, released protein was collected, and gels were redissolved at 16.7 wt% at 4 °C. This process was repeated five times and released protein was measured after each cycle.

4.2.4.3 Protein release from microspheres

For studies involving PLGA microspheres, microspheres were either free in PBS or were contained within the hydrogel network –**Figure 31B**. For inclusion inside the gel, microspheres were added to aqueous polymer solutions and mixed for 30 min until homogeneous, at which point the solution was heated to form the gel. For these studies ^{125}I-BSA was encapsulated in the microspheres and release quantified by a gamma counter (n=4 for each group).

4.2.4.4 Conformational stability of released protein

The conformation of the released protein was assessed by circular dichroism (CD) spectroscopy as previously reported.[285, 286] FITC-BSA released from hydrogels without MANHS was collected after 3 h of gelation and concentrated using a centrifuge filter (Millipore) with a 50 kD molecular weight cutoff to remove interfering soluble polymer chains. FITC-BSA encapsulated in PLGA microparticles was collected using a method described previously.[285] Specifically, protein-loaded PLGA microparticles (75 mg) were dissolved in 1 ml dichloromethane to which 4 ml of deionized water was added. The solution was sonicated for 90 min at 25 °C and centrifuged at 2000 x g for 10 min. The aqueous phase was decanted and the BSA was concentrated in a centrifuge filter. All protein solutions were measured using a Jasco J-810 spectropolarimeter, and compared against stock FITC-BSA.

4.2.4.5 Dual protein release from microspheres inside hydrogel

Release of two distinct protein populations, FITC-BSA and TexR-BSA, was studied. TexR-BSA was allowed to react with the 80/9/10/1 copolymer in PBS to form a protein-polymer conjugate followed by addition of microspheres encapsulating FITC-BSA to the polymer solution. After mixing until microspheres were homogeneous, the solution (n=4) was heated to 37°C for gelation to occur – **Figure 31C**. Protein concentration in the releasate from the hydrogel was measured by a fluorescence microplate reader (SpectraMax M2, Molecular Devices) with excitation/emission wavelengths of 495/520 nm and 594/615 nm for FITC-BSA and TexR-BSA, respectively. In all experiments measured levels of radioactivity or fluorescence were compared against standard curves to determine concentration.

4.2.5 Statistics

Protein release rates during specific phases in the release profile were compared between polymer types using unpaired t-tests. Where three or more groups were being compared, one-way ANOVA was used. To determine differences between hydrogel compositions during thermal cycling two-way ANOVA was applied. Tukey's post hoc test was used in conjunction with each ANOVA. Statistical significance was defined as $p<0.05$.

4.3 RESULTS

4.3.1 Characterization of thermoresponsive copolymers

Thermoresponsive hydrogels were successfully synthesized with yields >75%. The 80/10/10 copolymer had a M_n of 22K with a polydispersity index (PDI) of 1.6. The M_n and PDI of the 80/9/10/1 copolymer was 26K and 1.5, respectively. All copolymers were able to form bulk gels upon heating to 37°C. Representative thermal transition profiles are shown in **Figure 32** with quantification of the LCST values in **Table IV**. Although altering the LCST as much as 5°C, the presence of protein or PLGA microspheres did not interfere with the polymer's ability to form a gel below body temperature. The presence of microparticles increased the turbidity of the polymer solution leading to a smaller relative change in optical density upon heating, but the final gel appeared similar to those without microparticles. Likewise, the addition of microparticles did not have an effect on the mechanical properties of the hydrogel above or below the LCST. The maximum of the shear storage and loss moduli for the hydrogel without microparticles was 10290 Pa and 21940 Pa, respectively. Similarly, the maxima of these same parameters for the hydrogel with microparticles was 10720 Pa and 22620 Pa, respectively – **Figure 33**.

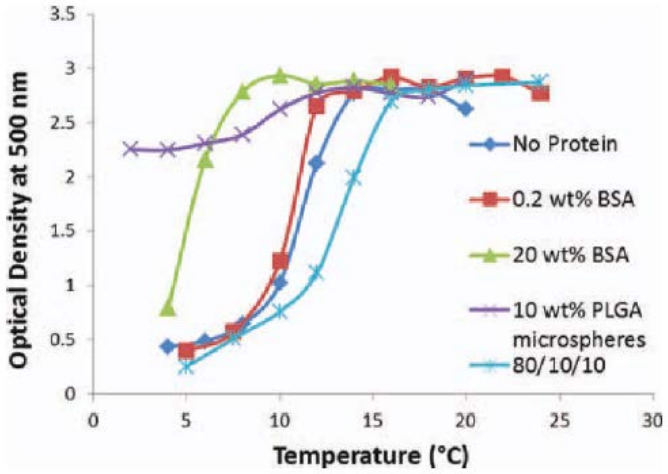

Figure 32. Representative optical absorption curves of hydrogel solutions with various protein and microparticle additives as solutions are heated.

Table IV. LCST of Hydrogels

Hydrogel	Additive	Transition Temperature (°C ± SD)
80/9/10/1	None	11.0 ± 0.1
	0.2 wt% BSA	10.5 ± 0.1
	20 wt% BSA	5.4 ± 0.3
	10 wt% PLGA microspheres	9.2 ± 0.6
80/10/10	none	12.4 ± 0.4

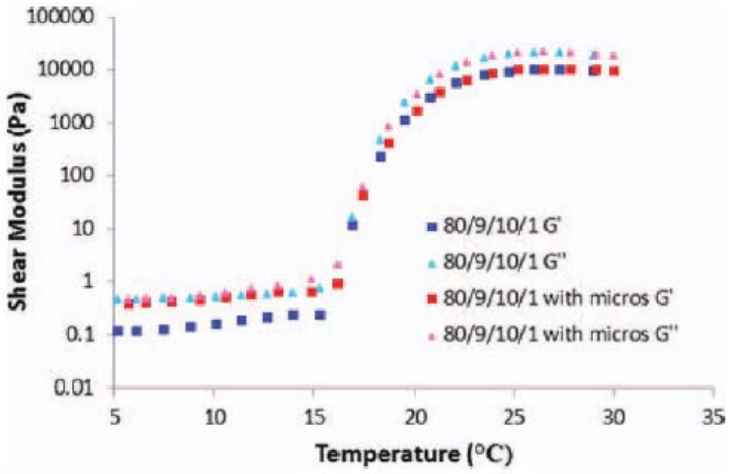

Figure 33. Shear mechanical properties during heating of the 80/9/10/1 hydrogel with or without the inclusion of microparticles in the gel network. The presence of microparticles did not alter the mechanical properties of the hydrogel.

The degradation of the copolymer, which occurs as hydrolysable MAPLA side chains are cleaved leaving a more hydrophilic polymer chain that becomes soluble at 37°C, is complete after approximately 4 to 6 months. The inclusion of 1 mol% MANHS increased the degradation rate of the copolymer as shown in **Figure 34**. However, the degradation profile remained similar to the 80/10/10 copolymer wherein mass loss was slow in the first few months of gel formation followed by a rapid loss of mass as MAPLA side chains were cleaved to increase hydrophilicity and allow solubilization at 37°C.[265]

4.3.2 Protein release from hydrogels

The BSA release profile for 80/10/10 (no MANHS, protein mixed), 80/9/10/1 (1% MANHS, protein reactive), and 80/8/10/1/1 (1% MANHS and 1% AAc, protein reactive) copolymers are shown together in **Figure 35**. For ease of comparison, release profiles were separated into distinct phases and rates were quantified using previously reported methods – **Table V.**[280] The loading efficiency was here defined as the amount of protein remaining after the 3 h necessary for the complete stabilization of hydrogel size and water content.[265] Protein release was relatively quick during the burst release phase from 3 to 24 h. Following the burst there was a

period of continued high diffusion rates (phase I, days 1 to 7) followed by slower release (phase II, weeks 1 to 6). Hydrogel degradation became more prominent as time progressed leading to higher release rates in phase III (week 6 until 98% of protein was released).

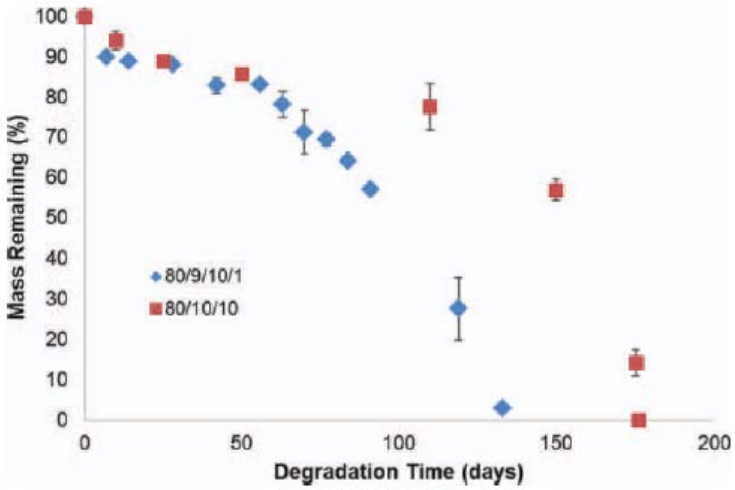

Figure 34. Mass loss curves for hydrogels with and without the MANHS linker. Incorporation of 1 mol% MANHS increased the polymer degradation rate. Data for 80/10/10 hydrogel reproduced from [265].

The loading efficiency increased from 22.0 ± 2.1% in the 80/10/10 hydrogel up to 44.6 ± 6.9% when 1 mol% of MANHS was present ($p<0.05$). The 80/9/10/1 hydrogel showed significantly higher release rates in phases I, II, and III compared to the 80/10/10 hydrogel ($p<0.05$ each phase) and demonstrated a more linear release profile. The presence of hydrophilic AAc sped polymer degradation and displayed near zero order release kinetics such that the release rates in phases I, II, and III were not significantly different from each other ($p>0.05$), although in all phases they were higher than the 80/10/10 copolymer ($p<0.05$ each phase). In hydrogels without AAc, BSA continued to be released for over 3 months in vitro, whereas the duration of release was shortened to 2 months in the copolymer with hydrophilic AAc. After the burst phase the copolymer without MANHS released protein at a slow rate until polymer degradation became more substantial after 60 days.

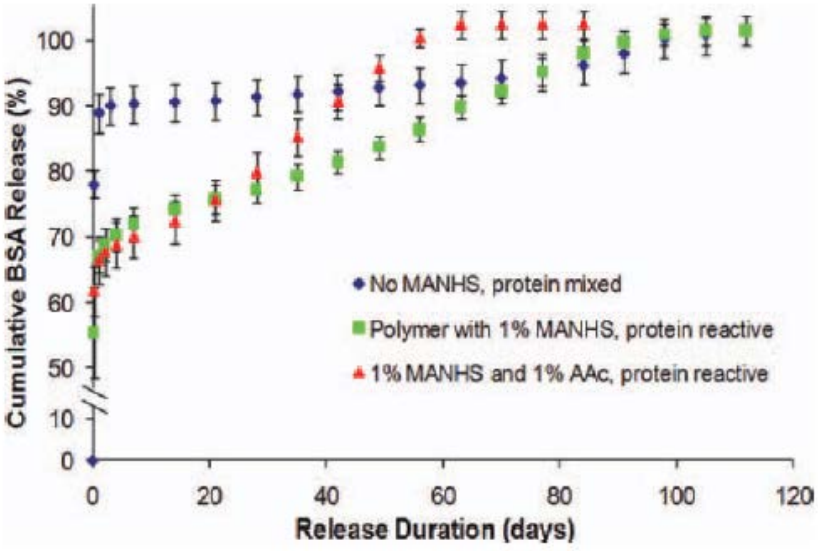

Figure 35. In vitro BSA release from hydrogels with different compositions. Polymers with protein-reactive MANHS showed higher loading efficiency and more constant release rates than copolymers without. Addition of hydrophilic AAc increased the rate of protein delivery.

Table V. In Vitro BSA Release Kinetics from Hydrogels

Hydrogel	Loading Efficiency (%)	Burst (%)	Phase I (%/wk)	Phase II (%/wk)	Phase III (%/wk)
80/10/10	22.0 ± 2.1	10.9 ± 1.6	1.61 ± 0.32	0.37 ± 0.05	0.82 ± 0.04
80/9/10/1	44.6 ± 6.9*	11.7 ± 6.3	5.81 ± 0.73*	1.88 ± 0.29*	2.77 ± 0.32*
80/8/10/1/1	38.3 ± 3.9*	4.8 ± 1.3*	4.05 ± 1.18*	4.14 ± 0.32*	4.86 ± 1.33*

* Denotes p<.05 compared to 80/10/10 hydrogel during same phase

The influence of MANHS on protein retention within the hydrogel is demonstrated in **Figure 36**. More protein remained after each thermal cycle in hydrogels with MANHS compared to those without ($p<0.05$). The percent of protein lost from the preceding thermal cycle is presented in **Table VI**. Hydrogels without MANHS lost a significantly greater percentage of their remaining protein at each subsequent cycle compared to hydrogels with the MANHS linker ($p<0.05$).

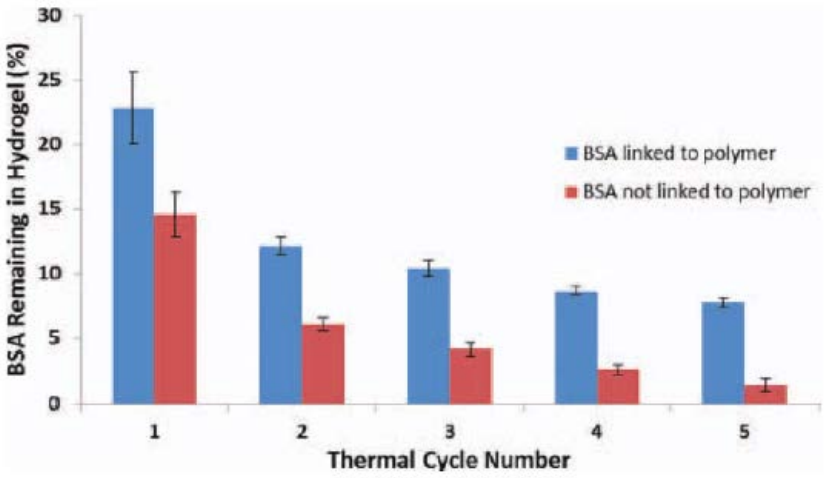

Figure 36. Protein remaining in hydrogels during repeated thermal cycling. Hydrogels incorporating the MANHS linker retained more protein after each cycle than hydrogels without linker.

Table VI. BSA Lost After Each Thermal Cycle

Cycle Number	Not Linked (% ± SD)	Linked (% ± SD)*
Cycle 1	85.4 ± 1.7	77.1 ± 2.8
Cycle 2	57.8 ± 5.6	46.4 ± 5.3
Cycle 3	30.9 ± 5.3	14.0 ± 1.4
Cycle 4	36.6 ± 2.7	16.7 ± 2.5
Cycle 5	46.0 ± 14.0	10.9 ± 2.8

* denotes $p<0.05$ for all cycles compared to not linked

4.3.3 Protein release from PLGA microspheres

BSA-loaded PLGA microspheres were synthesized with an average diameter of 34 ± 30 µm and could be easily incorporated into the hydrogel networks – **Figure 37**. Microspheres free in PBS demonstrated a substantial early-stage protein release – **Figure 38** and **Table VII**. The burst

release, which included all release during the first 24 h, for microspheres in PBS was 17.4 ± 5.4% compared to 6.6 ± 1.0% when microspheres were entrapped in hydrogel ($p<0.05$). During the remainder of the first week (phase I) release rates were 16.9 ± 2.5% and 6.6 ± 1.2%, respectively ($p<0.05$). The release rate of BSA from microspheres inside the hydrogel was higher than the PBS counterparts only during phase III as polymer degradation became more substantial.

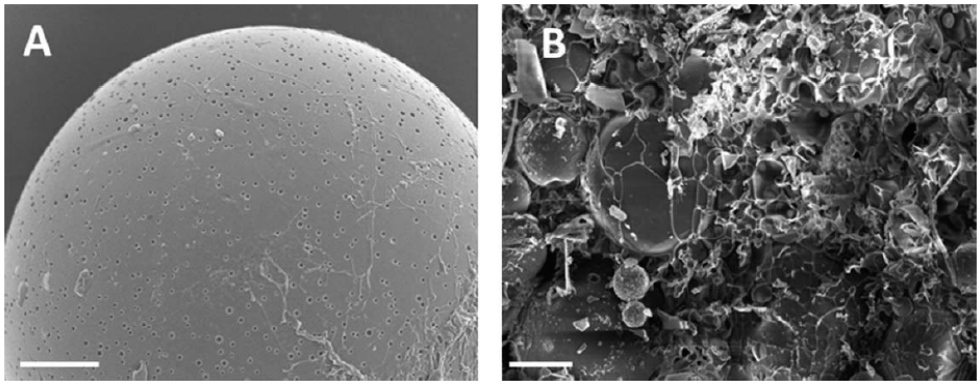

Figure 37. Scanning electron micrographs showing dehydrated structure of A) PLGA microparticle (scale bar = 5 µm) and B) PLGA microparticles embedded in the hydrogel polymer network (scale bar = 20 µm).

CD spectroscopy of protein encapsulated in PLGA microparticles and protein released from the hydrogels is shown in **Figure 39**. The spectra of both BSA released from hydrogels and BSA encapsulated in microparticles are similar to native FITC-BSA. Each has minima near 208 and 222 nm and increased ellipticity below 200 nm, characteristic of the largely alpha-helical BSA.[286]

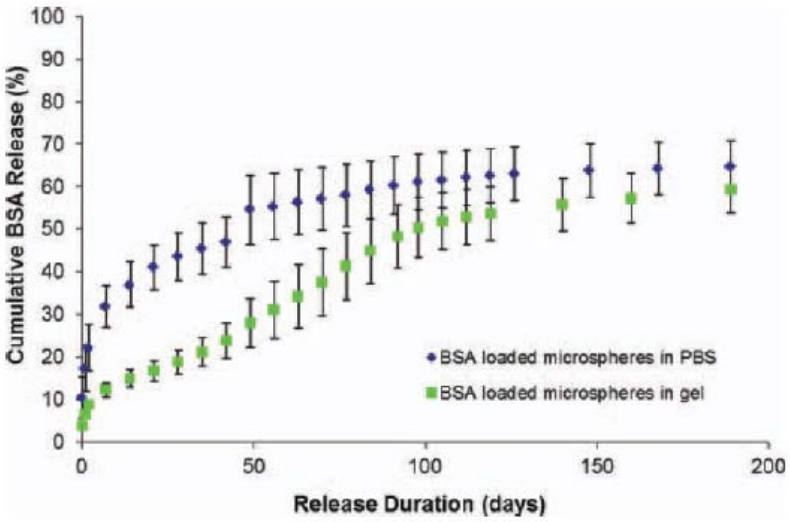

Figure 38. BSA release from microspheres in PBS and mixed into hydrogel network. Protein release was delayed when microspheres were entrapped in the hydrogel.

Table VII. In Vitro BSA Release Kinetics from Microspheres

Microsphere Environment	Burst (%)	Phase I (%/wk)	Phase II (%/wk)	Phase III (%/wk)
Microspheres in PBS	17.4 ± 5.4	16.9 ± 2.5	2.99 ± 0.31	1.13 ± 0.05
Microspheres in 80/10/10 gel	6.6 ± 1.0*	6.6 ± 1.2*	2.33 ± 0.58	2.27 ± 0.18*

* denotes $p<0.05$ compared to microspheres in PBS during same phase

4.3.4 Sequential protein release from microspheres embedded within the hydrogel

The release of two differently labeled BSA proteins (FITC-BSA and TexR-BSA) from the same hydrogel samples using the MANHS-containing polymer with microspheres together showed sequential protein release – **Figure 40**. TexR-BSA, which was in the gel phase, showed a large release initially, whereas during the same early time points FITC-BSA release from entrapped PLGA microspheres was relatively slow. Specifically, in the first 3 week 54.2 ± 3.1% of TexR-BSA was released compared to 17.9 ± 5.4% of FITC-BSA. Over the next 10 week TexR-BSA

release averaged 1.6%/week whereas FITC-BSA release gradually accelerated from an average of 1.4%/week up to a high of 3.7%/week.

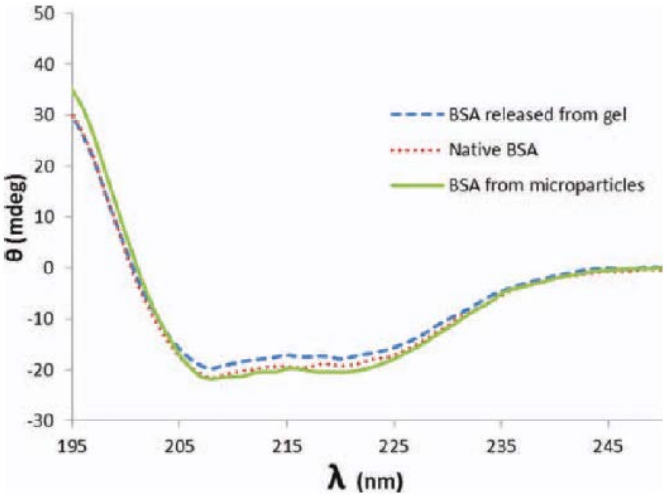

Figure 39. CD spectroscopy of native BSA compared to BSA encapsulated in PLGA microparticles and BSA released from hydrogels without MANHS. Spectra demonstrate that protein conformation is not altered by this polymeric drug delivery system.

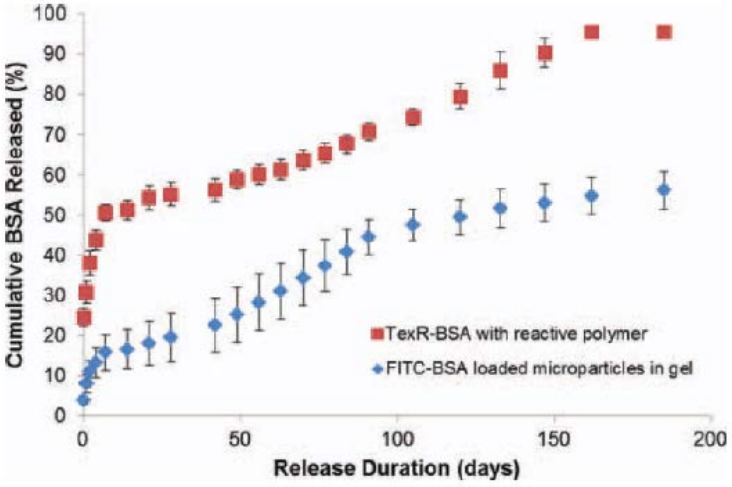

Figure 40. Sequential release of distinct BSA protein populations. A majority of TexR-BSA was released from the reactive polymer system during the first three weeks compared to the delayed release of FITC-BSA from microspheres inside the hydrogel.

4.4 DISCUSSION

Of the many applications of injectable materials in tissue engineering, one of recent focus in the literature is that of material injection into the myocardium following ischemic injury.[287] An appropriate biomaterial, upon injection into the heart wall, may act as a bulking agent to mechanically support the weakened myocardium or as a focal point for tissue remodeling and angiogenesis. These benefits have been shown using a number of injectable synthetic and biological materials. It has been reported that intramyocardial injection of a NIPAAm-based material with similar design features as the one presented in the current report was able to halt deleterious cardiac remodeling following ischemic injury.[126] Use of the current injectable material in this same application would also be feasible. Another treatment for cardiac disease of clinical interest has been therapeutic angiogenesis, which aims to increase collateral blood flow and attenuate ischemic damage by delivering pro-angiogenic proteins to ischemic myocardium. Of the clinical trials that have investigated cardiac therapeutic angiogenesis, the longest and most substantial benefit was seen when basic fibroblast growth factor was delivered to the heart in sustained release capsules compared to direct intracoronary infusion.[48, 288] Studies using animal models have also confirmed the potential for improved cardiac function when pro-angiogenic factors are released in a controlled fashion in the heart wall.[68, 95, 289] In this report we have sought to combine these two beneficial effects by developing an injectable, biodegradable material capable of serving as a bulking agent with controlled release capabilities.

The developed thermoresponsive polymer system was amenable to molecular design changes that resulted in predictable effects on protein delivery. For example, addition of just 1 mol% MANHS consistently improved the loading efficiency of this system and allowed more protein to be delivered over an extended duration in a more linear fashion. Additionally, inclusion of 1 mol% AAc predictably increased the degradation rate of the polymer allowing the protein to be delivered over a shorter duration and in a near zero order fashion. These features may allow for a more specific release profile to be engineered depending on the hypothesized drug delivery needs of the target biological environment.

The addition of microspheres to the system provided another means to control the timing of protein delivery and allow for multi-factor release in a sequential manner. PLGA was chosen

for microsphere synthesis because of a hypothesized affinity of the hydrophobic PLGA to associate with the hydrophobic MAPLA and NIPAAm residues of the copolymer. This interaction appeared to exist as the microparticles were not excluded from the hydrogel during phase transition. Likewise, the fact that the mechanical properties were not altered by the inclusion of microparticles in the gel network may be a manifestation of a favorable interaction between these two moieties. Release profiles from protein-loaded microspheres suggested that only about 60% of the loaded protein was released. However, measurements of the sample tubes at the end of the experiments demonstrated that 100% of protein was released, but the remaining 40% of the protein was adsorbed onto the inner surface of the polypropylene tubes, making it unavailable for measurement in the collected fluid samples.

It was apparent that the initial release of protein was delayed when the microspheres were entrapped in the hydrogel versus being free in PBS. While releasing some protein in the first few weeks, acceleration of the delivery rate did not occur until after 6 week. The extent of the delay may be related to the degradation rate of PLGA used, which would constitute another control point in this delivery system. For example, PLGA with lower molecular weight or higher PLA content would lead to faster degradation and potentially quicker release. Additionally, the W/O/W fabrication technique used in this study produces a dense inner structure and porous surface on the microparticles, which also plays a role in the release profile. Particle morphology is influenced by many different processing parameters and has been shown to influence drug delivery rates.[290-292] In particular, surface porosity will lead to a larger burst release than would be seen from a nonporous surface. The high polymer volume fraction of the dense internal structure provides a more tortuous diffusional path that would favor a more extended release compared to hollow particles, which lose all encapsulated drug once the outer shell is breached. Thus, processing of the microparticles may provide yet another control mechanism for drug release.

It is clear that the sequential nature of the current drug delivery system does not follow a strict on-off mechanism wherein all of one protein is delivered before all of another. Indeed, in both the hydrogel and the microparticle system there is continued release throughout the duration of the study. However, a strict sequential delivery may not be necessary to see desired biological effects. Previous studies have shown a beneficial biological outcome when growth factors are

delivered in a sequential manner similar to the one shown in the current report.[68, 283, 293] For example, Ruvinov et al. demonstrated different rates of IGF1 and HGF release from an alginate gel.[293] Similar to the current report, the growth factors were both continuously released from the gel but with one releasing faster than the other. Nevertheless, the sequential nature was adequate to elicit an improved biological response. One advantage of the current system is that the release profile of each of the two components – hydrogel and microsphere – could be independently manipulated, allowing each drug to be released in a desired profile to meet the perceived biological need.

The thermoresponsive hydrogels reported were able to deliver protein, with or without protein-reactive moieties in the backbone, for a period in excess of 3 months. This contrasts with many hydrogel systems which, because of their high water content, are associated with quick molecular diffusion.[138] Previous studies have shown that the equilibrium water content of the 80/10/10 hydrogel is near 45%.[265] This relatively low water content was associated with a more collapsed gel structure with smaller pore sizes and thus likely lower aqueous convection rates for protein release. In conjunction with this, the large size of the model protein BSA (MW 66 kD) may inhibit its quick release from the gel. This size effect has been shown in polyNIPAAm hydrogel systems previously.[294, 295]

The presence of MANHS in the 80/9/10/1 hydrogels consistently improved loading efficiency compared to 80/10/10 hydrogels – an effect attributed to the putative linkage of the protein to the polymer backbone. The occurrence of this linkage is also supported by the protein loss data during hydrogel thermal cycling. Presumably protein that is not bound to the hydrogel will be lost more quickly as the gel solubilizes and reforms, with the collapse of the gel pushing unbound protein out. Accordingly, hydrogels undergoing thermal cycling retained protein to a greater extent when MANHS was present compared to those without the linker. Because more protein remains in the gel after formation there is subsequently more protein to be released over time, and it appears to be released in a more linear fashion.

Protein bioactivity is a primary concern for any drug delivery system. Synthesis of the PLGA microparticles involved a W/O/W emulsion technique that includes the possibility of protein denaturation by various mechanisms.[152] CD spectroscopy confirmed that BSA

encapsulated in microparticles maintained its native confirmation following synthesis, as compared to the changes in ellipticity that would occur following denaturation.[286] Likewise, BSA released after 3 h from 80/10/10 hydrogels did not exhibit a conformational change. One potential concern associated with the protein-reactive hydrogel approach would be the effect that polymer-protein conjugation could have on protein bioactivity. Covalent attachment of polymers, specifically poly(ethylene glycol), to protein therapeutics is an established method being used clinically to improve protein half-life in vivo for better pharmacokinetics.[155] However, it has been shown that uncontrolled conjugation can lead to a decrease in activity of the therapeutic if the polymer chain blocks protein active sites or influences protein conformation.[296] Each protein that would be conjugated to this polymer would require a bioactivity assessment to define the impact of conjugation. Should conjugation prove detrimental, a more careful linking strategy could be pursued by different conjugation chemistries, analogous to the approaches used for pharmaceutical PEGylation.

4.5 CONCLUSIONS

Injectable, biodegradable polymers with thermoresponsive properties were synthesized and characterized as a drug delivery system. These hydrogels were able to release model protein BSA in a controlled manner extending 3 months. Modification of the polymer backbone, specifically inclusion of a protein-reactive MANHS group, led to higher protein loading in the gel during thermal transition. Further, addition of hydrophilic AAc to the polymer increased the drug delivery rate as predicted. The presence of both MANHS and AAc led to a more linear protein release profile than from hydrogels without these monomers. Protein-loaded microspheres entrapped in the hydrogel network during gel formation released protein in a delayed fashion relative to microspheres in saline. Neither protein conjugation nor microsphere presence interrupted the ability of the copolymer to transition from sol to gel when warmed to body temperature, thus maintaining the injectability of this system. Combining both systems provided a sequential release of two distinct protein populations where the majority of protein associated with the gel phase was released before protein loaded into microparticles. Thus, this

composite material combines the advantages of injectability, degradability, extended release, and sequential release into a single delivery system.

5.0 INVESTIGATION OF A STRONG, BIODEGRADABLE HYDROGEL WITH CONTROLLED PROTEIN DELIVERY FOR INTRAMYOCARDIAL INJECTION

5.1 INTRODUCTION

Intramyocardial biomaterial injection therapy continues to be an area of significant research involving materials of both biological and synthetic origins, generally with promising results.[287, 297] It has been noted previously that the material properties may play a role in the overall benefit seen following injection. These properties include material degradation rate, bioactivity, and mechanical strength.[53, 119, 298-300] It has been demonstrated, for example, that materials that degrade too quickly (<6 week) and those that are non-degradable both lead to decreased function similar to saline control groups at study end points. Likewise, theoretical models and empirical data suggest that stronger materials may have a greater benefit than weaker materials, though the upper limits on mechanical strength have not been investigated. It has also been postulated that appropriate cell infiltration into the injected material may be important in eliciting sustainable improvements to cardiac function. While studying the effects of these material properties it is important to provide adequate follow-up time after injection to see the lasting effects of the therapy. Few published studies extend beyond 2 months, making long-term efficacy difficult to assess.

Another area that has shown promise to improve material injection therapy is the inclusion of appropriate growth factors with the material for controlled release at the injection site. Growth factors that have received the most focus to-date are those with known proangiogenic properties such as bFGF, VEGF, PDGF and HGF.[136, 237, 301-305] IGF1 has also been used due to its known benefits in the myocardium including influencing cell size and metabolism, decreasing apoptosis, improving contractility, and encouraging cardiac stem cell

proliferation.[236, 306, 307] It has recently been demonstrated that controlled release of two or more growth factors, in some cases in a sequential manner, can have benefits beyond what is seen from single factor delivery.[68, 293, 308] For example, the delivery of complementary proteins sequentially has been shown to be more beneficial in angiogenesis than simultaneous delivery, presumably because it mimics the body's own regenerative healing mechanisms.[284, 309] Finally, in an approach that delivers the myriad growth factors and cytokines that are released from activated platelets, a gel made of 10% v/v plasma, after injection into rats immediately after infarction, reduced the damage of infarction compared to controls.[308]

As discussed previously we have reported on the benefits of injecting a N-isopropylacrylamide (NIPAAm)-based thermally responsive hydrogel in infarcted rat hearts and have subsequently developed a stronger material with a slower degradation time which may be more beneficial in cardiac injection therapy.[126, 265] We reported on the drug delivery properties of this new material by studying the release of model protein BSA. Specifically, this system allowed for two proteins to be delivered in a sequential fashion. The aim of that research was to develop and understand a system that could be used with functional growth factors for cardiac regeneration. We hypothesize that primary bFGF delivery to the heart may be able to encourage early angiogenesis, thus establishing a healthier microenvironment in the damaged muscle. Following this, delivered IGF1 may be able to encourage cardiac stem cell and cardiomyocyte proliferation at the newly-vascularized injection site.

This report shows the effects of intramyocardial injection of a biodegradable material with higher mechanical strength and a longer degradation time than has been published previously. After presenting the in vitro characterization of growth factor delivery from this gel, we further test the effect that delivery of bFGF, IGF1 or both from the hydrogel has on cardiac function and histology. In all cases the follow-up after injection continues for 16 weeks to determine longer-term effects of this therapy.

5.2 MATERIALS AND METHODS

5.2.1 Materials

All chemicals were purchased from Sigma-Aldrich unless otherwise stated. NIPAAm was purified by recrystallization from hexane and vacuum-dried. 2-Hydroxyethyl methacrylate (HEMA) was purified by vacuum distillation. Benzoyl peroxide (BPO), lactide, poly(lactide-co-glyoclide), sodium methoxide (NaOCH3), poly(vinyl alcohol), and methacryloyl chloride were used as received. IGF1 and bFGF (Peprotech) and ^{125}I-bFGF (Perkin Elmer) were reconstituted according to manufacturer instructions. Protein extraction buffer (Bioo Scientific) and ELISA assays (R&D Systems) were used as received.

5.2.2 Material Synthesis

5.2.2.1 Synthesis of methacrylate polylactide (MAPLA)

MAPLA was synthesized as reported above – **Figure 29**.[265] After dissolving lactide in dichloromethane to which $NaOCH_3$ initiator in methanol was added, polylactide-monomethyl ether (HOPLA-OCH_3) was synthesized by ring opening polymerization. The reaction persisted for 2 hr at 0°C, after which the polymer solution was rinsed with 0.1 M HCl and deionized water. The organic phase was next dried with $MgSO_4$ and then removed by rotary evaporation. HOPLA-OCH_3 was dissolved again in dichloromethane with added triethylamine. MAPLA was formed by dropping methacryloyl chloride into this solution and allowing reaction overnight at 0°C. Following reaction, precipitates were removed, the organic phase was dried and removed by rotary evaporation, leaving raw MAPLA product. MAPLA was purified by flash chromatography. NMR confirmed the synthesis of MAPLA with an average of 2.9 PLA units per MAPLA monomer.

5.2.2.2 Synthesis of poly(NIPAAm-co-HEMA-co-MAPLA)

Poly(NIPAAm-*co*-HEMA-*co*-MAPLA) copolymer was synthesized by free radical polymerization – **Figure 41**. Monomers, NIPAAm (6 g, 0.053 mol), HEMA, and MAPLA at a

molar ratio of 80/10/10 were dissolved in 200 ml of 1,4-dioxane containing 220 mg BPO. The polymerization was carried out at 70°C for 24 hr under an argon atmosphere. The copolymer was purified by repeated precipitations in hexane, diethyl ether, and warm DI water. The final product was freeze-dried before being dissolved in cold PBS at 15 wt% for use in all studies.

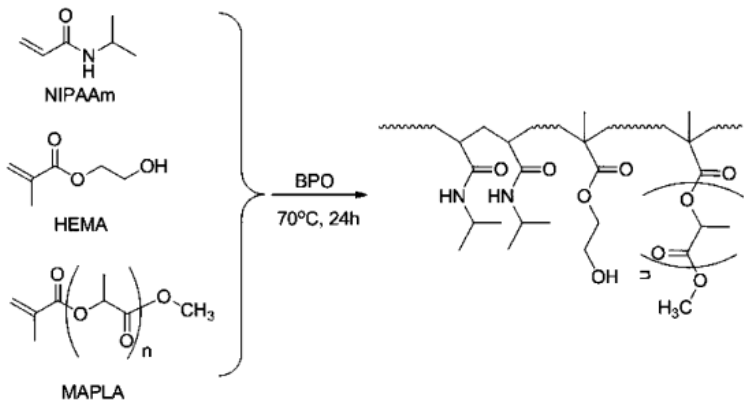

Figure 41. Schematic of poly(NIPAAm-co-HEMA-co-MAPLA) copolymer synthesis (from [288])

5.2.2.3 Synthesis of PLGA microspheres

PLGA microspheres with a lactide:glycolide ratio of 75:25 (Mw 66-107 kD) were synthesized using a water-in-oil-in-water (W/O/W) double emulsion technique.[277] IGF1 was mixed with unlabeled BSA at a ratio of 1:10 and dissolved in 0.02x PBS to make a final total BSA concentration of 1 mg/ml. Initially, 200 mg of PLGA was dissolved in 4 ml dichloromethane. After all PLGA was dissolved, 200 µL of IGF1 solution was added to the dissolved PLGA and vortexed for 1 min. This primary emulsion was immediately added to 60 ml of 2% PVA that was stirring at 1000 rpm, to generate the W/O/W emulsion. After 5 min, the stirring speed was reduced to 600 rpm and an additional 80 ml of 1% PVA solution was added. After stirring for 6 h to allow dichloromethane evaporation, the microspheres were collected by centrifugation, rinsed with DI water and freeze-dried. The IGF1 content of the PVA and DI water supernatants was determined by ELISA to calculate loading efficiency of IGF1 in the particles.

5.2.3 Copolymer characterization

Copolymer molecular weight was determined by gel permeation chromatography (Waters Breeze System). The copolymer was dissolved in tetrahydrofuran at 1 mg/ml and elution time was used to determine molecular weight by comparison to a poly(methyl methacrylate) standard. LCST values were determined by measuring the optical density of the material at 500 nm wavelength over a temperature range from 2 to 24°C. The temperature at which the absorbance reached half of its maximum value was taken as the LCST, and was determined using a custom Matlab (MathWorks) program.

5.2.4 In vitro growth factor release studies

5.2.4.1 In vitro quantification of growth factor release

For quantification of the bFGF release rate from hydrogels, ^{125}I-bFGF was loaded into 15 wt% gel solutions alone, or after being premixed with either BSA (1:350 bFGF:BSA molar ratio) or BSA and heparin (1:350 BSA, 1:1000 bFGF:heparin). These samples were gelled in PBS at 37 °C and releasate was periodically collected and measured with a gamma counter (Auto Gamma II, Perkin Elmer) to determine the amount of bFGF released at each time point. For quantification by ELISA and to determine growth factor bioactivity, hydrogel solutions loaded with 16 ug/ml bFGF or 1 ug/ml IGF1 in loaded microparticles were injected in 0.25 ml aliquots into 24 well plates containing 37 °C basal media (EMEM, Lonza). At designated time points the media was removed and replaced. A portion of the removed supernatant was used for determination of released growth factor concentration with ELISA (R&D Systems). The remaining media was stored at -80 °C until being used for bioactivity studies.

5.2.4.2 In vitro growth factor bioactivity

Rat smooth muscle cells were cultured at 5 x 10^3 cells per well in a 96 well plate in culture medium (DMEM, 5% fetal bovine serum, penicillin and streptomycin). After 24 hr the cell culture media was removed and replaced with serum-free supernatant from the growth factor release studies. Cells were cultured with the supernatant for 48 hrs, at which point a mitochondrial assay (CellTiter 96 Aqueous One, MTS, Promega) was used to determine cell

number. Visual inspection qualitatively confirmed the results from the MTS assay. Results from the assay were compared against cells grown in basal media without serum.

5.2.5 In vivo hydrogel injection studies

5.2.5.1 Chronic rat infarction model

Adult female Lewis rats (Harlan Sprague Dawley) weighing 200–250 g were used. The protocol followed National Institutes of Health guidelines for animal care and was approved by the University of Pittsburgh's Institutional Animal Care and Use Committee. Anesthesia was induced with 3.0% isoflurane inhalation followed by intubation and respiratory support with a rodent volume-controlled mechanical ventilator. Electrocardiogram and tail cuff blood pressure measurements were used to monitor vital signs in all animals. A left thoracotomy was performed to expose the heart after which the proximal left anterior descending coronary artery was ligated with a 7–0 polypropylene suture. The creation of myocardial ischemia was verified by regional cyanosis and ST segment elevation and the incision was closed in layers with 4–0 continuous silk sutures.

5.2.5.2 Poly(NIPAAm-co-HEMA-co-MAPLA) hydrogel injection

Two weeks after induction of myocardial infarction, the rats were anesthetized and evaluated with echocardiography to measure infarct size in terms of the percentage of scar area (akinetic or dyskinetic regions) compared to the LV free wall area. Rats with infarcts greater than 25% of the LV free wall were randomly divided into 5 groups: those that would receive plain hydrogel injections (hydrogel group, n=8 for all groups), control PBS injections (PBS group), hydrogel with 25 ug/ml bFGF (gel+bFGF group), hydrogel with 1 ug/ml IGF1 in PLGA microparticles (gel+IGF1 group), and hydrogel with 25 ug/ml bFGF and 1 ug/ml IGF1 in PLGA microparticles (gel+bFGF/IGF1 group). The infarcted anterior surface of the rat heart was exposed through a left thoracotomy. For rats receiving hydrogel injection a total volume of 400 ul of hydrogel solution in PBS was injected into the apical, proximal, lateral, and septal wall regions bordering the infarct as well as into the center of the infarct (5 injections, 80 µL per region). For a rat in the PBS group, 400 µL PBS was injected into the same locations with the same volumes. The incision was closed in layers with 4–0 silk continuous sutures for both groups.

5.2.5.3 Echocardiography

Echocardiography was performed immediately before injection (pre-injection time point – 2 weeks post-infarction), as well as 4, 8, 12 and 16 weeks after injection. To perform the procedure, rats were anesthetized with isoflurane inhalation. Standard transthoracic echocardiography was performed using the Acuson Sequoia C256 system with a 13-MHz linear ultrasonic transducer (Acuson Corporation) in a phased array format. The LV short axis view was studied using B-mode measurements. The end-systolic (ESA) and end-diastolic (EDA) inner LV areas were measured by outlining the endocardial surface. LV FAC was calculated as, FAC = [(LVEDA - LVESA)/LVEDA] x 100%. All measurements were taken using Scion Image software (Scion Image).

5.2.5.4 In vivo growth factor retention

To test the residence time of bFGF and IGF1 in the heart, animals for each treatment group above were injected two weeks following MI as described. At 5 minutes, 2 days, and 2 weeks after injection 3 animals from each group were euthanized and their complete hearts were immediately extracted and snap frozen in liquid nitrogen. The LV free wall of each heart was excised and digested using a tissue homogenizer and protein extraction solution followed by gentle mixing for 2 hr at 4 °C. Samples were centrifuged for 10 minutes and the supernatant was decanted. Growth factor concentration in the supernatants was determined by ELISA. Healthy hearts and PBS-injected hearts were similarly digested and tested for use as controls.

5.2.5.5 Histology

Rats were sacrificed for detailed histological analysis of the hearts 16 weeks after injection. Animals were anesthetized, and the heart was exposed and arrested by injection into the apex of 2 ml of a hypothermic arresting solution including 10 U/ml of heparin. The excised hearts were fixed in 2% paraformaldehyde for 2 hr before being embedded in optimal cutting temperature compound (Tissue-Tek) and frozen at -80° C. LV tissues were serially sectioned to a thickness of 8 mm in the LV transverse direction. Hematoxylin and eosin (H&E) staining and immunohistochemical staining were performed with antibodies against alpha-smooth muscle actin (a-SMA, Sigma), CD 68 (Serotec), and CD 163 (Serotec). Nuclei were stained with DAPI

(Sigma). For quantification of the immunohistochemical staining, each LV from 5 different animals was photographed at 10 different microscopic fields at 200x magnification.

5.2.6 Statistical Analysis

Where three or more groups were being compared, one-way ANOVA was employed. To determine if changes in LV variables over time varied among the experimental groups, a two-way repeated-measures ANOVA was used which determined the effects of treatment, time, and treatment-by-time interaction. The REGWQ post hoc test was used when the necessary assumptions were met. When there were unequal sample sizes or lack of homogeneity of variance Gabriel's test and the Games-Howell test were used, respectively. Statistical significance was defined as $p < 0.05$.

5.3 RESULTS

5.3.1 Material characterization

Poly(NIPAAm-co-HEMA-co-MAPLA) was successfully synthesized with properties similar to what has been reported previously.[265] Specifically, the Mn was 34.1 kD, Mw was 67.1 kD, and PDI was 1.96, with a transition temperature of 13 °C.

5.3.2 In vitro growth factor release

Quantification by ELISA of bFGF and IGF1 release in vitro was unsuccessful as no appreciable amount of growth factor was detected. However, the release rate of ^{125}I-bFGF from the hydrogels is shown in – **Figure 42**. During the initial gelation, which lasts approximately 3 hr, there was significant release of bFGF from the gels. The extent of that initial loss was influenced by the presence of excipient with the protein. The release at 3 hr for plain bFGF was nearly identical to the release when BSA was also present, with 41.5 ± 1.1% and 40.9 ±1.2% released, respectively.

When heparin was also combined with BSA and bFGF the amount released after 3 hr nearly doubled to 80.0 ± 2.8% ($p<0.05$). Release profiles from the hydrogel after this early release was similar and characterized by a slow, steady release over many weeks.

The cellular assays showed that the bFGF and IGF1 released from gels retained bioactivity over many weeks as demonstrated by increased rat SMC proliferation – **Figure 43**. Cell proliferation data show a peak of bFGF bioactivity during the first 2 weeks of release with little effect beyond 6 week. The effect of IGF1 was seen from the first time points to a period extending beyond 3 months. The peak effect observed for IGF1 bioactivity came after 4 weeks. These data demonstrate both the bioactivity of released growth factors as well as the difference in release rate of these two proteins from their respective carriers.

5.3.3 In vivo growth factor retention

The ability of growth factor to be retained at the cardiac injection site in vivo is shown in **Figure 44 and Table VIII**. Hearts injected with the bFGF-loaded gel demonstrated a 590-fold, 10-fold and 2-fold increase of bFGF content 5 min, 2 days and 2 weeks after injection, respectively, compared to injection of gel without growth factor at the same time points. Similarly, there was a 7-fold, 3-fold and 4-fold increase in detected IGF1 for hearts receiving hydrogel mixed with IGF1-loaded microparticles. There was no difference in detectable bFGF or IGF1 between infarct control and plain hydrogel injection.

Table VIII. Retention of Injected Growth Factors in Myocardium

Injection Fluid	LV bFGF content (ng)		
	5 min	2 day	2 wk
Healthy	2.03 ± 0.77		
Saline	5.26 ± 0.74	3.39 ± 0.40	6.15 ± 2.80
MAPLA only	4.04 ± 1.57	5.30 ± 0.32	5.51 ± 1.24
MAPLA with bFGF	2378 ± 404*	50.4 ± 13.1*	12.5 ± 4.32*
MAPLA with IGF1-loaded microparticles	4.14 ± 1.20	4.52 ± 1.31	6.35 ± 1.26
Injection Fluid	LV IGF1 content (ng)		
	5 min	2 day	2 wk
Healthy	0.32 ± 0.14		
Saline	0.19 ±0.09	0.23 ± 0.02	0.27 ± 0.12
MAPLA only	0.34 ± 0.22	0.30 ± 0.06	0.13 ± 0.10
MAPLA with bFGF	0.40 ± 0.14	0.28 ± 0.05	0.41 ± 0.02
MAPLA with IGF1-loaded microparticles	2.28 ± 0.46*	0.80 ± 0.08*	0.55 ± 0.06*

*p<0.05 vs gel injection at same time point

5.3.4 In vivo injection results

5.3.4.1 Effects of cardiac injection on cardiac function

Compared to pre-injection, FAC was significantly reduced in hearts injected with PBS after 16 weeks – **Figure 45**. By contrast, there was no significant decrease in FAC for any hearts receiving hydrogel injection. The presence of growth factors did not improve upon results seen from injection of the plain hydrogel. Overall there was a significant difference in FAC between all gel and PBS injection groups at 16 weeks.

Cardiac dilation was markedly improved after gel injection compared to saline controls – **Figure 46**. The ESA and EDA of hearts receiving plain hydrogel was 0.42 ± 0.15 and 0.62 ± 0.13, respectively, compared to 0.70 ± 0.10 and 0.88 ± 0.11 for hearts injected with saline ($p<0.05$). There was no difference in dilation when the hydrogel was loaded with growth factors

compared to hydrogel without these factors. In all cases the dilation was statistically larger at 16 weeks for all experimental groups than at baseline ($p<0.05$). In the case of gel-injected groups, the majority of the change occurred in the first 4 weeks, and subsequently there was no significant difference for either of these parameters over time from 4 to 16 weeks. In comparison, following saline injection the area at end systole and diastole continued to increase at each time point.

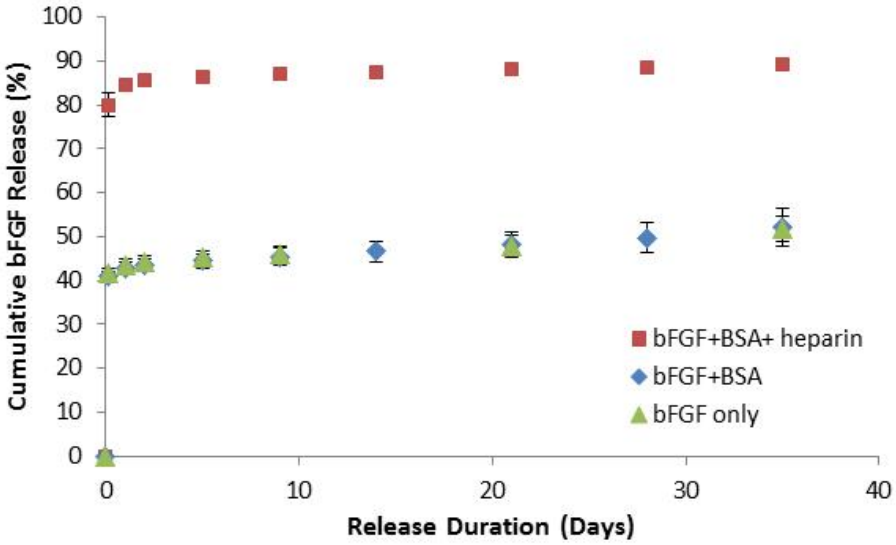

Figure 42. Release profiles of ^{125}I-bFGF from poly(NIPAAm-co-HEMA-co-MAPLA) hydrogels. The presence of heparin allowed more bFGF to be released during gel formation.

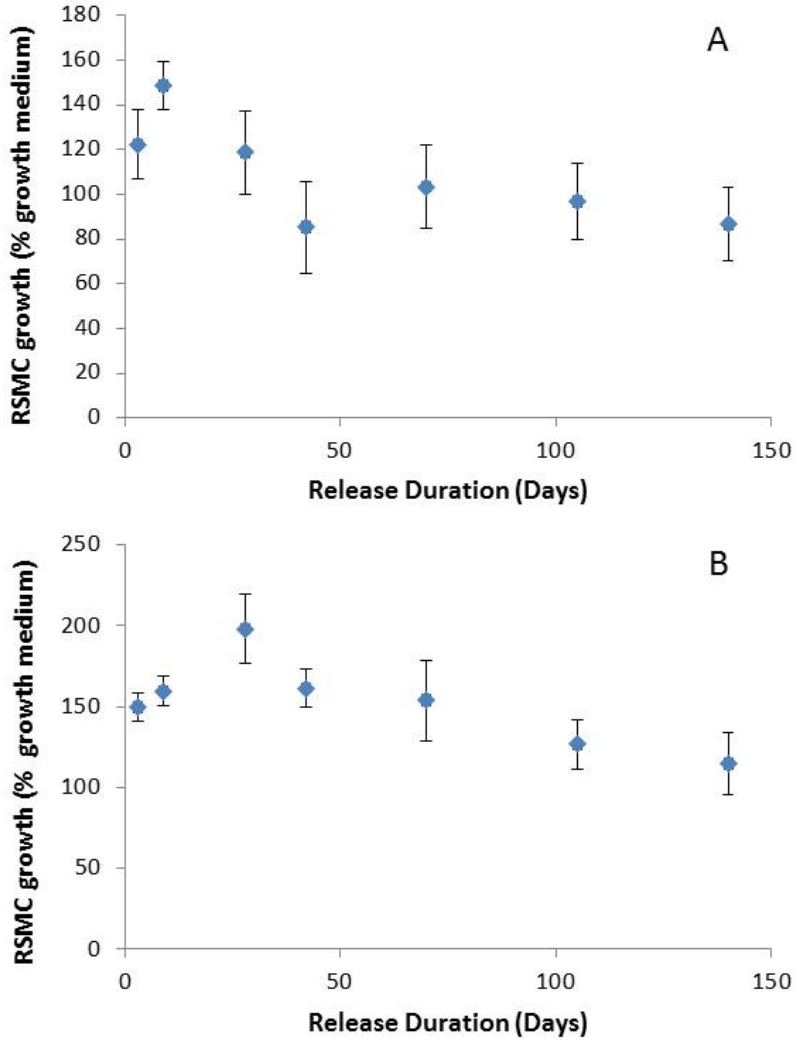

Figure 43. Proliferation of rat smooth muscle cells in response to bFGF released from the hydrogel (A) or IGF1 released from microparticles inside the hydrogel (B). bFGF release caused proliferation in the first few weeks of release whereas IGF1 caused proliferation over a longer time with a peak after four weeks.

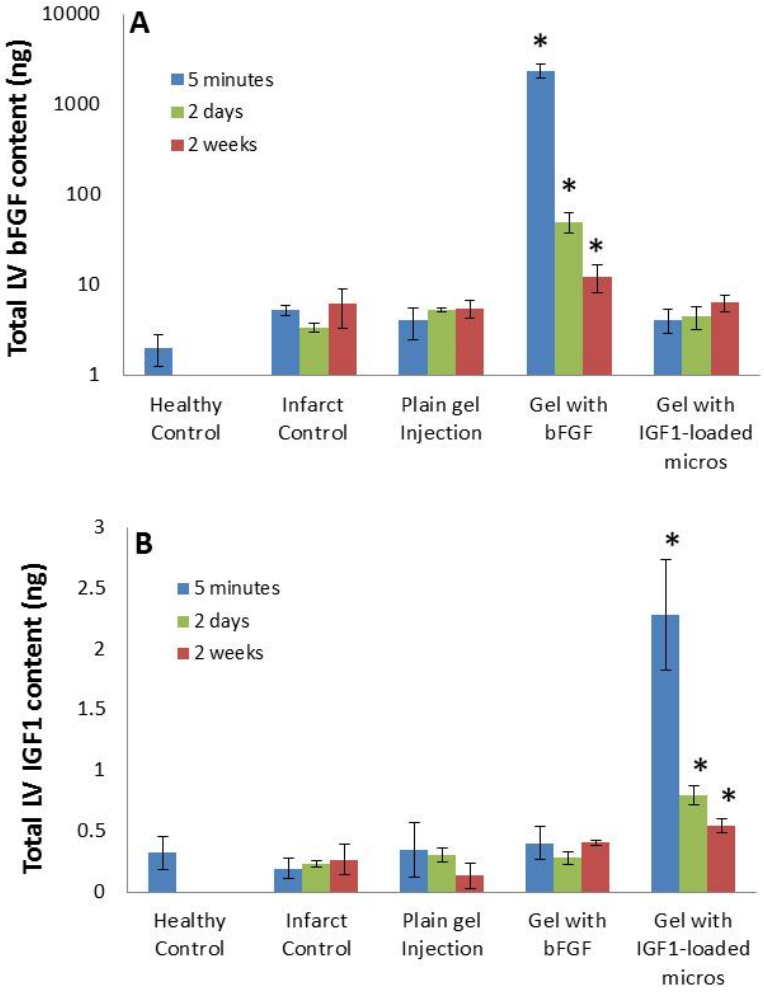

Figure 44. Total content of bFGF (A) and IGF1 (B) in the left ventricular free wall of rat hearts injected with either bFGF-loaded hydrogel or hydrogel loaded with microparticles encasulating IGF1, respectively. Increased levels for both growth factors are shown up to 2 weeks after injection. *denotes significance compared to injection of plain gel.

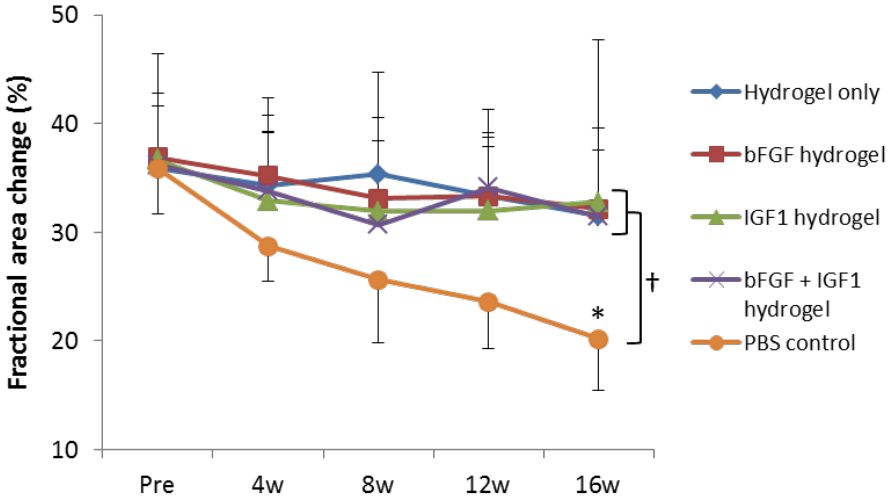

Figure 45. Effect of gel injection on fractional area change 16 week after treatment. Gel injection prevented the worsened function observed in hearts receiving saline injection. Addition of growth factors did not improve upon the results of the plain hydrogel. *denotes a significant change from pre-injection, † denotes differences between groups over time.

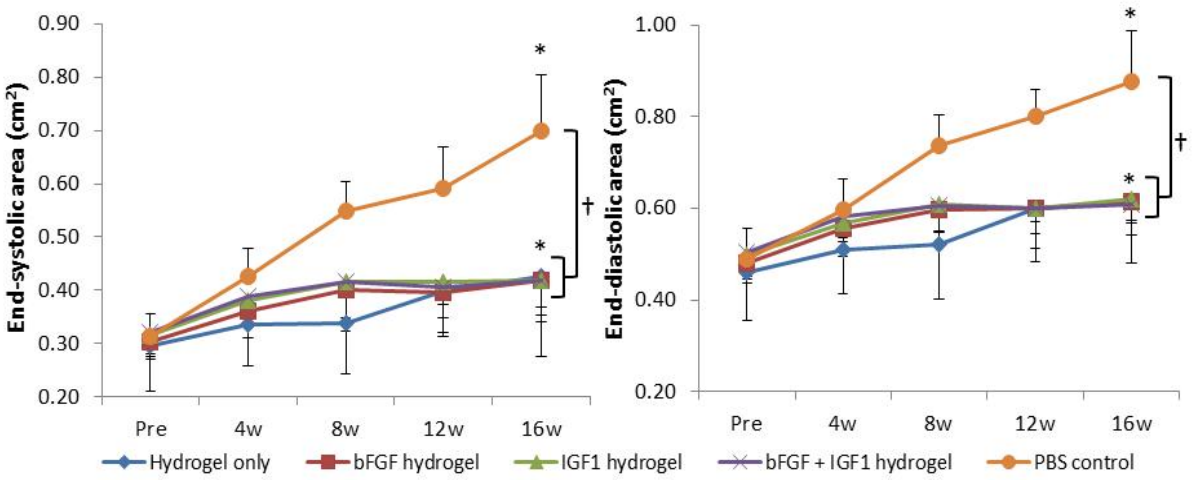

Figure 46. Measurements of dilation in hearts receiving injection of hydrogels with or without growth factors. *denotes a significant change from pre-injection, † denotes differences between groups over time.

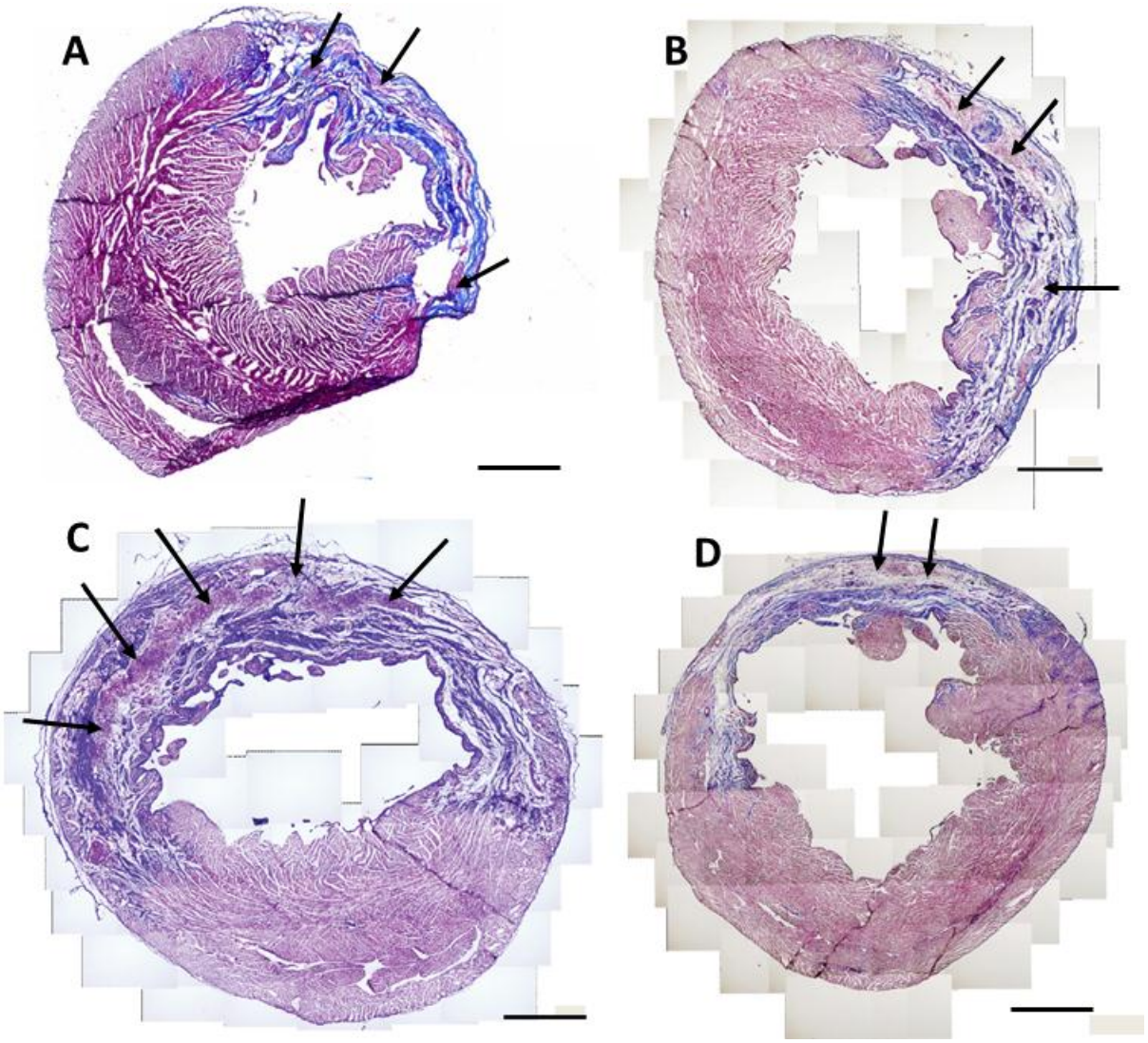

Figure 47. Histological view of cardiac cross-section 16 weeks after injection of plain material (A), or material loaded with bFGF (B), IGF1-loaded microparticles (C), or both (D). Arrows point to residual hydrogel infiltrated with cells. Scale bars = 500 µm

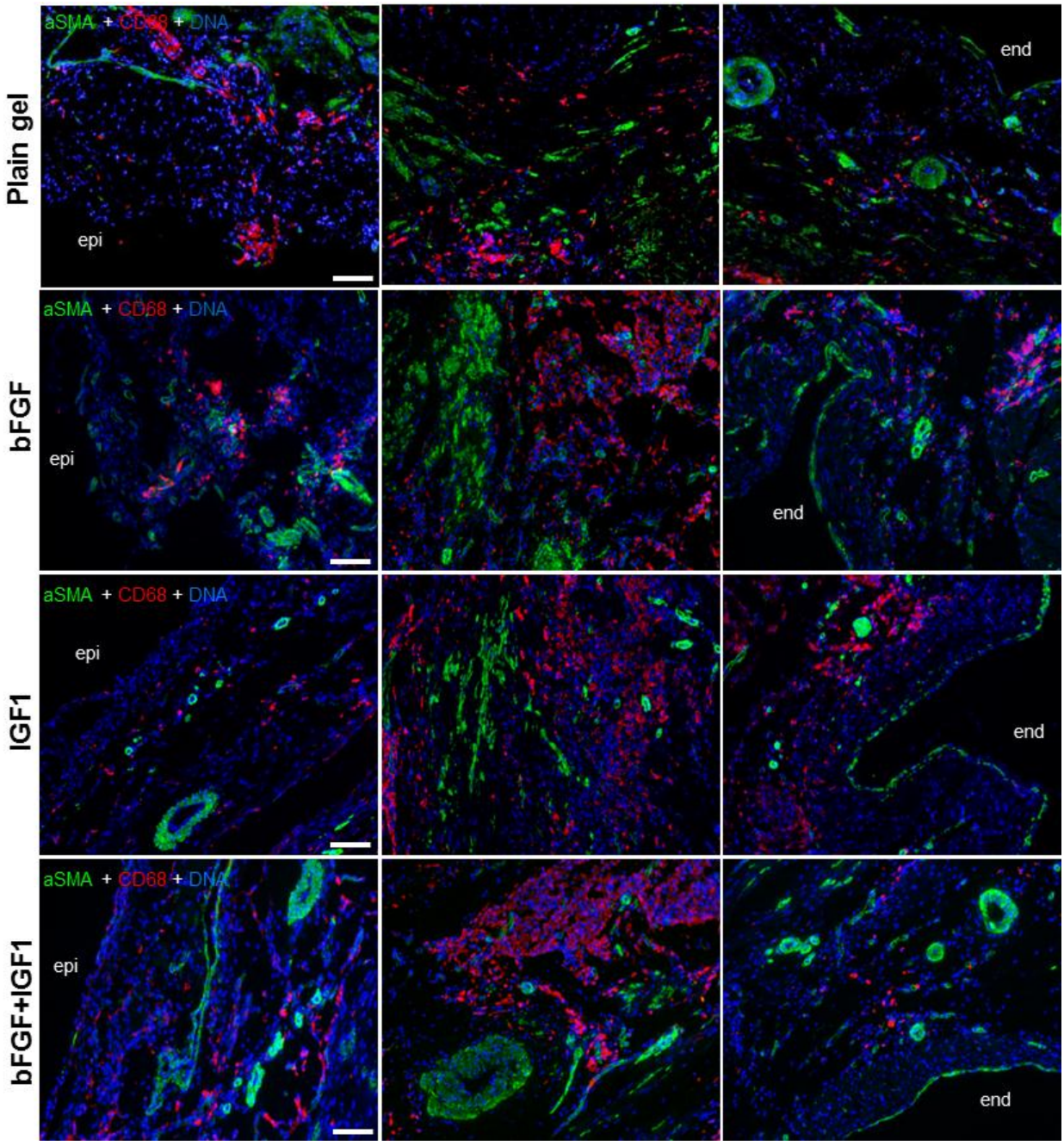

Figure 48. Representative images of αSMA (green), macrophage (red) and DNA (blue) staining from hearts receiving injection of hydrogel with and without growth factors. There is marked infiltration of macrophages and presence of smooth muscle cells, especially in the mid-wall. Scale bar = 100 µm

Table IX. Quantification of Immunohistochemical Staining of Infarct Zones in Hearts

Hydrogel Type	Nuclei (per HPF)	αSMA (x10,000 pixels per HPF)	CD68 (x10,000 pixels per HPF)	CD163 (x10,000 pixels per HPF)	Vessels (per HPF)	Arterioles (per HPF)
Plain gel	126 ± 34	3.6 ± 1.8	3.4 ± 0.6	2.0 ± 0.5	4.1 ± 0.9	0.3 ± 0.1
Gel + bFGF	136 ± 28	6.0 ± 3.0	5.1 ± 2.7	3.5 ± 1.2	3.8 ± 0.7	0.7 ± 0.4
Gel + IGF1	216 ± 79	4.0 ± 1.2	3.9 ± 1.7	3.5 ± 1.4	3.1 ± 0.8	0.5 ± 0.4
Gel + bFGF + IGF1	157 ± 55	3.9 ± 1.6	3.6 ± 2.5	2.8 ± 1.7	5.1 ± 2.0	0.7 ± 0.4

HPF = high-power field

5.3.4.2 Effect of injection on cardiac histology

Representative cross-sections of hearts explanted after 16 weeks showed regions where the material was still present and infiltrated with cells – **Figure 47**. Immunohistochemical evaluation of the LV walls at 16 weeks showed that all hearts injected with hydrogel showed a large number of αSMA-positive cells in the injected material and neighboring infarct regions, and both vessel and arteriole formation – **Figure 48**. Even at this late endpoint the material was clearly infiltrated by macrophages including those of an M2 phenotype. There was no significant difference in the amount of angiogenesis or cell infiltration at 16 weeks following injection of hydrogels with or without different growth factors – **Table IX**.

5.4 DISCUSSION

The continued development of intramyocardial biomaterial injection therapy requires that the mechanisms by which benefits are obtained following injection be further elucidated. Many parameters may contribute to successful treatment, including timing and location of injections, distribution of material in the heart wall, and physical and biological properties of the injected material. Moreover, the long-term benefits of this treatment will need further investigation before it can become a clinical reality. This report discusses application of a material that has been designed specifically for the cardiac environment as seen by its increased mechanical strength,

relatively slow degradation time, and the ability to delivery growth factors in a controlled way. The effects of treatment with this material have been observed for 4 months after injection.

Quantification of the growth factor released in vitro could not be completed by ELISA due to an inability to detect the released protein. Instead, using ^{125}I-bFGF it was shown that the release profile was similar to what has been previously shown with BSA from this material, particularly the significant release during the first 3 hrs of gel formation followed by slow release afterwards. It was interesting to note that when growth factor was loaded into the gel in the presence of BSA it released at the same rate as when it is loaded by itself, however when heparin is mixed into the solution nearly twice as much protein is released during gelation. This suggests that there may be a significant interaction of the protein with the polymer chains in the gel that is disrupted once heparin, which can bind bFGF, is added. A strong interaction between the polymer and the growth factors may partially explain why ELISA is unsuccessful at detecting the proteins. The polymer-protein interaction may cause conformational changes that prevent binding in the sandwich assay but yet still allow it to maintain a level of bioactivity as seen by its ability to affect in vitro cell proliferation. This observation highlights the vulnerability that sensitive growth factors may have to biomaterial carriers and the need to consider appropriate protective excipients with the protein.

Injection of the plain poly(NIPAAm-co-HEMA-co-MAPLA) in 2 week-old infarcts is remarkable for the ability to maintain cardiac function for at least 16 weeks after injection. During this time the material demonstrated significant cellular infiltration and growth of αSMA-positive cells throughout the infarct zone. The presence of these smooth muscle-like cells was likewise observed following injection of a similar thermoresponsive gel which also had relatively strong mechanical properties and degraded over a few months in vivo.[126] Interesting research into the biological response following application of a strong and elastomeric degradable epicardial patch has also shown a similar αSMA-positive zone near the implant. That muscular zone was shown to be similar to the myocardium during fetal growth and differentiation and may be a sign that the observed cells are on a pathway of tissue regeneration. The exact mechanisms that are involved in the growth and survival of these muscle cells near the injected material are unknown but may be related to a combination of appropriate cellular infiltration, material degradation, and mechanical support.

An interesting observation in this study was the lack of additional benefit to either cardiac function or cellular environment when either or both growth factors were included in the material. The amounts of growth factor that were delivered were similar to amounts that have shown benefits in other intramyocardial injection studies.[133, 293, 303, 304] It was observed that the tissue had elevated levels of both bFGF and IGF1 for at least two weeks following injection, which demonstrates that growth factor was being locally released at the site of injury. In vitro, the bioactivity of growth factors released from the gel was demonstrated by cellular proliferation assays. Because the in vivo environment will likely cause a faster rate of drug delivery than in vitro studies, the exact rates of delivery and the profile of the sequential release of bFGF and IGF1 cannot be determined. While the increase in IGF1 in the digested LV tissue was mostly gone by 2 weeks it is likely that more IGF1, which may not have been removed from the particles during tissue digestion, remained loaded in the microparticles to be released slowly over a longer term.

These results may provide important information about the mechanisms by which benefits are observed following injection. It is well known that a myriad of inflammatory processes are at work following injection of a material, especially a synthetic one, into the body.[310, 311] One aspect of that response is the recruitment of macrophages to the site of injury, which are known to excrete many cytokines and growth factors that aid in new ECM formation and angiogenesis.[312] We demonstrated that macrophage infiltration to the site of injury was pronounced, even 16 weeks after injection. Many of these cells stained positively as those of a M2 phenotype which encourages tissue regeneration as opposed to scar formation.[311, 313] It may be that a continued release of angiogenic and pro-healing factors from these cells at the implant site is adequate to provide robust angiogenesis that is not further augmented by endogenous delivery of these factors from the material.

The degradation rate of the material is also a likely contributor to the overall success of this material, especially as it relates to the cellular environment at the injection site. It has been shown previously that the benefits of material injection seen soon after delivery can be altogether lost if the material degrades too quickly.[67] On the other hand, non-degradable materials, whether they are infiltrated with cells or not, do not provide any long-term benefits.[119, 300] The material used in this research is one that degrades in vivo over approximately 4-5 months.

This time frame will be intimately tied to the cellular response. Because the material is not permanent it does not undergo fibrous encapsulation and chronic inflammation. However, it does remain long enough to maintain cell recruitment to the injection site where the cells may provide continued positive tissue remodeling as described above. While the exact timing of degradation in the cardiac environment remains to be determined there is evidence that a duration beyond 2 months should be considered if the material is also providing mechanical support.[299] The support provided during that time, and the slow shifting of load-bearing responsibilities to the newly formed tissue may also play a role in the overall health and function of the cellular environment.

The inability of growth factor delivery to improve the functional results with hydrogel delivery is not unprecedented. Whereas in many cases intramyocardial delivery of a growth factor with a biomaterial has shown functional improvements, in other reports the benefits are seen only histologically in terms of cellular milieu and vascularization. For example, Shao et al demonstrated that delivery of a bFGF gelatin showed a higher EF than injection of material alone 2 weeks after treatment but the increase was not maintained to 4 weeks despite higher vascular density, decreased infarct expansion and fewer TUNEL-positive cells throughout the study.[95] Likewise delivery of IGF1 tethered to self-assembling peptides demonstrated bioactivity in the form of cellular Akt signaling, but was unable to improve functional or geometric cardiac parameters.[133] There have also been studies that identify the positive histological effect seen after injection of extracellular matrix materials – known to contain growth factor signaling molecules.[100, 101, 314] However, benefits to cardiac function remain to be proven in these studies. Again, these results point to the complexity in understanding exactly how benefit is achieved in intramyocardial biomaterial injection.

5.5 CONCLUSIONS

A strong, slowly-degrading hydrogel was injected into infarcted rat hearts. The material was able to prevent worsened cardiac function for a period of at least 16 weeks. The injected material exhibited marked infiltration of macrophages and was associated with angiogenesis in the infarct

zone. Cells staining positive for αSMA were found throughout the infarct region near the injected material. Growth factors bFGF and IGF1 were successfully loaded into the gel directly or in polyester microparticles. Despite demonstration that injected growth factor was present at elevated levels in the LV for at least two weeks after injection, and that released growth factor was bioactive in vitro, there was no effect on cardiac function or histology following injection of growth factor-loaded gels compared to the gel without growth factor. These results suggest that the mechanisms by which benefit is achieved may involve a multitude of factors, the investigation of which is of critical importance to see the successful development of intramyocardial biomaterial injection therapy.

6.0 CONTINUED RESEARCH AND FUTURE DIRECTIONS

The data and results presented in the previous sections provide useful information that adds to the scientific knowledge of controlled release, especially for cardiovascular applications. It also lays the groundwork for more and exciting research that will continue to advance the field. Such work that continues beyond the specific aims of this dissertation will be shown presently. This work deals with controlled release systems, intramyocardial injection therapy, and the development of related biomaterials for cardiovascular and other applications.

6.1 OTHER APPROACHES TO GROWTH FACTOR DELIVERY

6.1.1 Introduction

When considering the results following growth factor loaded hydrogel injection into infarcted rat hearts, the lack of functional benefits is noteworthy and deserves further investigation. As has been discussed above there may be numerous mechanisms to describe these data. It is important to keep in mind that the ELISA assays were unable to detect the protein that was released from the gel. Additionally, the large change in the amount of protein released in vitro after 3 hr when bFGF was delivered alone compared to when bFGF was mixed with heparin, suggests a possible interaction between bFGF and the polymer chains that may be influencing protein conformation. While it was noted that the bioactivity is retained to a degree sufficient to elicit a cellular proliferation response, it is possible that some protein is no longer functional. What specifically may be happening at the molecular level is unknown but it is possible that other proteins do not have this same susceptibility to conformational change or loss of activity.

VEGF is a growth factor with similar proangiogenic effects as bFGF. This protein has been shown to play a prominent role in angiogenesis during embryogenesis and its controlled delivery can help preserve damaged ischemic tissue in adults.[50, 315, 316] The delivery of plasmid DNA coding for VEGF or delivery of the endogenous protein have both been shown to aid in angiogenesis following myocardial infarction.[305, 317] We tested the ability to quantify VEGF released from the gel using ELISA and measure its bioactivity. We did this as a potential replacement for bFGF for future studies. Preliminary results suggest that VEGF may be more compatible with this hydrogel system.

6.1.2 Methods

Similar to the methods reported above, VEGF was loaded into 15 wt% poly(NIPAAm-co-HEMA-co-MAPLA) gel solutions at a concentration of 1 ug/ml and allowed to gel at 37 °C in basal cell culture media (EGM-2, Lonza) with low serum content (0.5% v/v). The releasate was collected at predetermined time points and split into portions for ELISA measurement of growth factor content and for use in cellular proliferation assays. Human umbilical vein endothelial cells (HUVECs) were plated in full serum media in a 96 well plate at 5,000 cells per well. After one day of growth the media was replaced with releasate from gels loaded with VEGF or from control gels with no growth factor. After 3 days of growth in this media the cell number was counted with a hemocytometer.

6.1.3 Results and discussion

VEGF release was successfully quantified by ELISA measurements – **Figure 49A**. The release profile demonstrated a diffusion-controlled system characterized by high amounts of release early and decreasing release at later times. The released VEGF increased proliferation of HUVEC cells similar to what was seen by direct loading of VEGF into culture media – **Figure 49B**. The releasate collected for at least 4 weeks was able to increase proliferation.

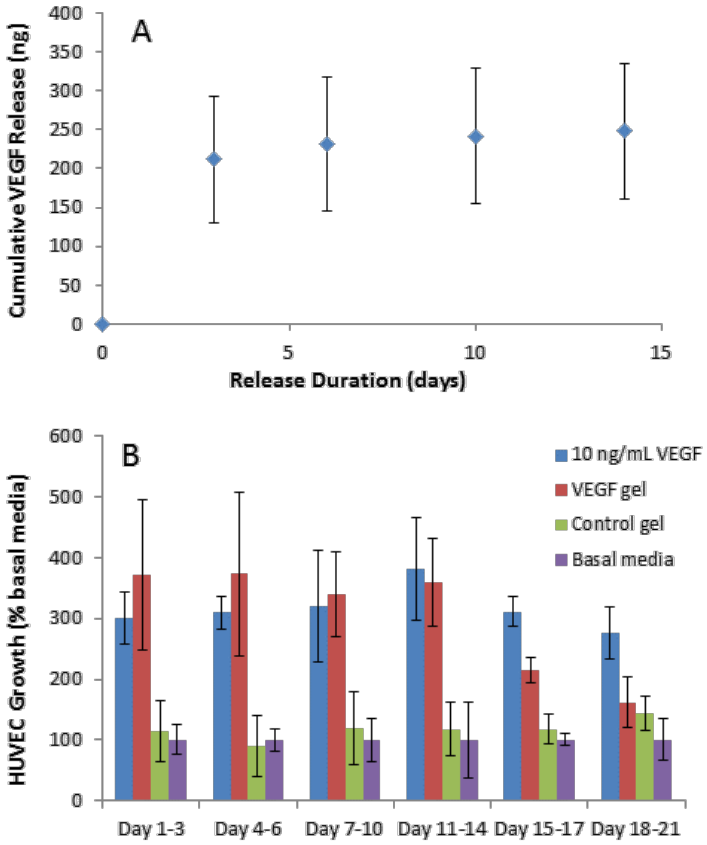

Figure 49. VEGF release from poly(NIPAAm-co-HEMA-co-MAPLA hydrogel. Released VEGF was detected by ELISA (A) and was bioactive as demonstrated by increased proliferation of HUVECs when grown in releasate (B).

These results show that VEGF can be released from poly(NIPAAm-co-HEMA-co-MAPLA) hydrogels in a way that is detectable with the ELISA sandwich assay and retains protein bioactivity. While the mechanisms by which bFGF was not detectable and VEGF was detectable has not been explored, these results show that the individual components of a drug delivery system can be important. This data suggest a potential path forward when considering the release of proangiogenic growth factors from the hydrogel. Simple in vivo tests may be appropriate to confirm the functionality of this drug delivery system before moving to future cardiac studies. For example, subcutaneous injection of the VEGF-loaded gel in rats may provide a more certain guarantee of bioactivity than in vitro tests and could be used as a reference in the event that growth factor-loaded gel injection to the heart was again unable to change the biological response.[318]

In conjunction with testing different signaling molecules, other delivery mechanisms may be worth exploring. Here we use direct-loading and microparticle encapsulation methods to deliver the growth factors. The number and properties of microparticle systems that have been used are many, and it may be that those using different materials or fabrication methods can do more to protect loaded proteins.[153, 273] If the growth factors are in greater need of protection then other techniques such as PEGylation, which has been reviewed elsewhere, could be explored.[155, 296, 319] Likewise other types of drugs may be appropriate in the cardiovascular application. For example, plasmid DNA either free or housed in a viral or synthetic vector could be explored.[320]

6.2 LARGE ANIMAL HYDROGEL INJECTION

6.2.1 Introduction

The use of injectable materials to treat heart disease has mostly been focused on small animal models to-date. Moving to larger animals is advantageous not only because of the increased relevance to final human application, but also because some of the technical difficulties associated with trying to inject into a small muscle mass is reduced. For example, the thickness of an infarcted rat LV wall can be less than 1 mm, and injecting a material into that space without puncturing through the wall is technically challenging. The complications that are likely to be associated with misplaced material are serious and can include embolic stroke and death. The pig LV wall is at least 1 cm thick which makes breaching the LV cavity unlikely during injection. The greater tissue space will also allow for more control on locations and configurations of the injected material, which may eventually inform patient specific injection regimens.

Larger animals also provide more options for the method of delivering the material. One particular device, the HeartLander, has been developed as an epicardial, semi-autonomous robot that can scale the surface of the heart and make injections at designated locations.[321, 322] This approach is obviously not possible in the small animal model due to size limitations, but in a

large animal such as the pig further development of this robotic system becomes feasible. Other approaches of delivery which rely on endovascular access to the heart are also not feasible in small animals. Pilot studies that involve injection of an alginate material into the lumen of the coronary arteries, or injection of material from an endocardial approach are recently being explored.[72, 314] Injection that does not require open-chest surgery has significant potential for human applications because it should decrease patient morbidity and recovery time. Potential problems with endovascular delivery such as accidental embolization of the material in the blood stream still need to be addressed. By this it becomes obvious that research on large animals will provide the necessary foundation to develop technologies that will ultimately make injection therapy more effective for human patients.

We have conducted a pilot study of the use of the poly(NIPAAm-co-HEMA-co-MAPLA) material, without growth factors, into infarcted porcine hearts for short-term follow-up. The pilot study has been aimed at determining the proper surgical protocols and injection methods to ultimately direct the next stage of long-term porcine injection experiments.

6.2.2 Materials and Methods

6.2.2.1 Materials

The thermoresponsive poly(NIPAAm-co-HEMA-co-MAPLA) material was prepared as described above – **Figure 41**. Dry polymer was dissolved in sterile PBS and mixed with a solution of gadoteridol (ProHance, Company) MRI contrast agent to a final polymer concentration of 15 wt% with 25 mg/ml gadoteridol. The material was sterilized by UV radiation for 30 minutes and loaded into sterile 1 ml syringes to a volume of 200 µl per syringe.

6.2.2.2 Infarction and injection procedures

A posterior wall myocardial infarction was created in female Yorkshire pigs by 60 min balloon occlusion of the second branch of the left circumflex artery (LCx). Animals were sedated with isoflurane inhalation and intubated. Animals were monitored by oximetry and ECG and maintained on continuous infusion of amiodarone throughout the procedure. Successful occlusion was determined by angiography. Four animals in total were infarcted and injected.

Animals were returned to the operating room 6 days after myocardial infarction and again sedated and monitored. Injections of Pigs #1, #2, and #3 were completed without preoperative echocardiography to determine the location of infarction, but rather the infarct was assumed to be around the coronary artery that had been occluded. Echocardiographic viewing preoperatively was added for Pig #4. A left thoracotomy was performed to expose the heart. The gel solution was injected at 20 sites in a grid configuration over the infarct and border zones (200 µl/injection) using a 25 g needle. All syringes were kept on ice until used for injection. Blood pressure and ECG monitoring were used to track the hemodynamic stability of the animal during injection.

6.2.2.3 Assessment of injection

Within one week after material injection (1 day for Pig #2 and #3, 7 days for Pig #4) the animals were again sedated for MRI imaging using a full body 1.5T scanner. The heart was imaged using a modified look-locker inversion recovery (MOLLI) method before and after contrast injection. After MRI, the animals were sacrificed and hearts harvested for visual and histological evaluation.

6.2.3 Results and discussion

Occlusion of the LCx in all animals was successfully completed as shown by angiography and ECG – **Figure 50**. All animals survived the infarction and underwent injection of the thermoresponsive gel – **Figure 51**. No arrhythmias were noted in any of the animals during or following material injection. The first three pigs received material injection into the anterolateral LV wall, and Pig #4 was injected in the posterolateral LV free wall. After the chest was closed following material injection in Pig #1 the animal went into cardiac arrest and expired. Upon removal and sectioning of the heart it was observed that the gel had been properly injected and there were no obvious signs of having injected material into the ventricular lumen. It is believed this animal expired due to complications surrounding anesthesia in the presence of decompensated cardiac function.

Pigs #2 and #3 survived material injection and MRI imaging one day later. In these, as well as all other animals in this pilot study, the infarction zone could not be determined by visual inspection of the epicardium. The material was injected into the anteriolateral region of the LV where, based upon fluoroscopy films from the infarct procedure, it was believed the infarction was located. In both of these animals MRI analysis and the cross section of the LV after explant demonstrated that the material was not injected into the infarcted tissue – **Figure 52**. The actual infarct region was found to be in the posterior LV free wall.

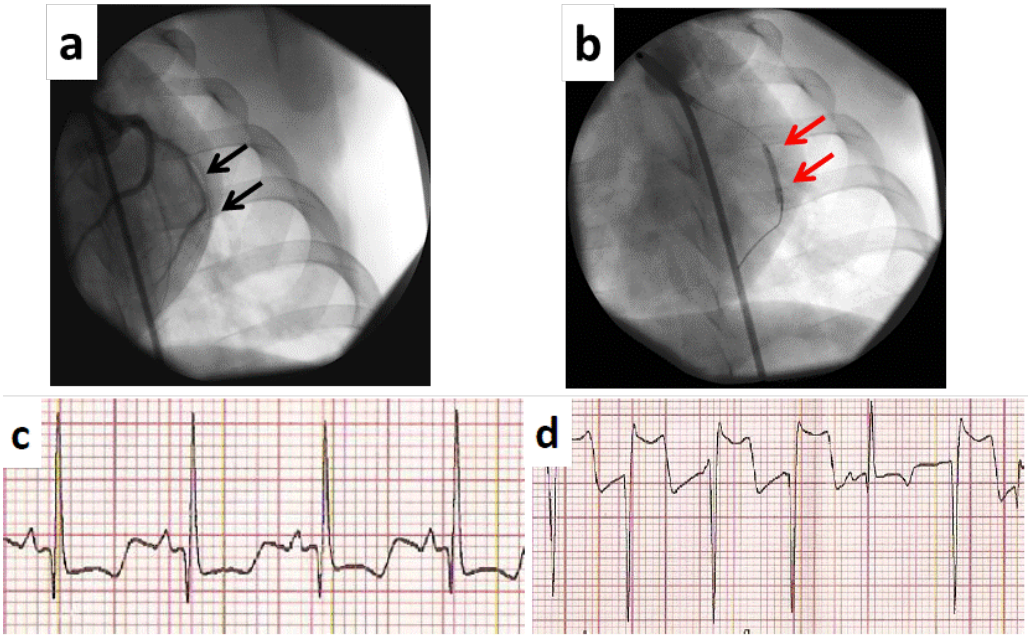

Figure 50. Radiographic images of the swine heart before (a) and during (b) 60 min occlusion of the LCx. Black and red arrows indicate the LCx, and occlusion balloon, respectively. Electrocardiographs pre-occlusion of the LCx (c) and post-occlusion (d) are shown. Elevated S-T segments were seen in lead I after occlusion.

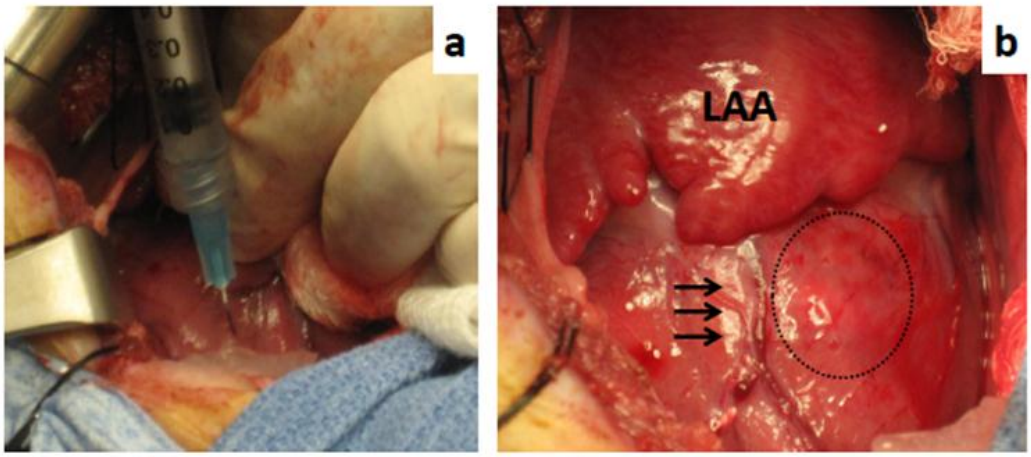

Figure 51. The hydrogel injection procedure (a) for Pig #2 and view of the heart after injection (b) show successful delivery of the material. Black arrows show the occluded coronary artery. The dotted circle outlines the region where hydrogel was injected. LAA denotes left atrial appendage.

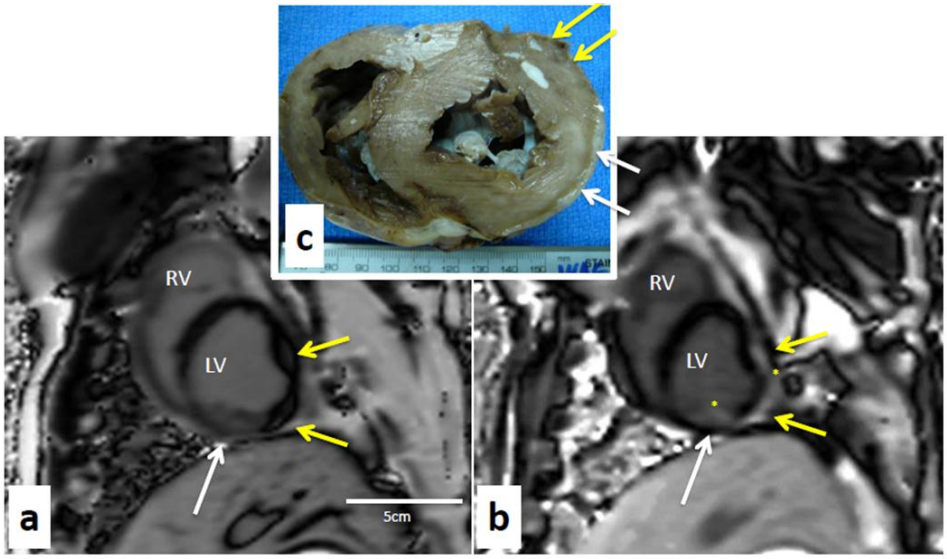

Figure 52. MRI images of the heart from Pig #2 before (a) and after (b) the MOLLI MRI imaging sequence. White arrows indicate the posterior wall infarction. Yellow arrows indicate presence of the hydrogel loaded with contrast agent. The high signal from the hydrogel is not enhanced in the post-MOLLI images as was seen in the infarct zone. Sectioning of the excised heart (c) confirms that hydrogel was not injected into the infarct zone, and agrees with the MRI images.

For Pig #4 echocardiography was performed prior to the injection procedure. This successfully confirmed location of the infarct zone to be in the posterolateral LV wall as was seen in the previous animals, and thus material delivery was focused on this region. Injection into the posterior wall proved more technically difficult as it required greater manipulation of the heart. While injection was still carried out successfully, it was necessary to take periodic breaks in between injections to allow the heart to rest and the heart rate to stabilize. In all cases the material was observed in the ventricular wall using MRI, and the MRI images agreed with what was observed upon sectioning the heart after explant – **Figure 53**. The presence of the contrast agent in the gel allowed visualization of the material location even when the MRI was done 1 week after injection as was the case for Pig #4.

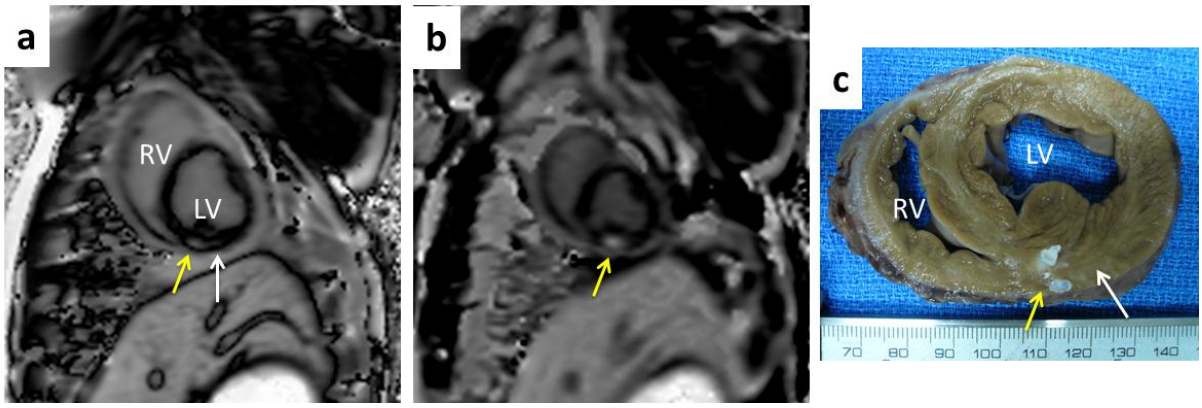

Figure 53. MRI images of the heart from Pig #4 before (a) and after (b) the MOLLI imaging sequence. White arrows indicate the posterior wall infarction. Yellow arrows suggest the presence of the hydrogel loaded with contrast agent. The high signal from the hydrogel does not change in the post-MOLLI images though it does in the surrounding infarcted tissue, indicating the material was accurately delivered into the infarcted myocardium. Autopsy confirmed that the material was successfully delivered to the posterior infarcted wall (c). RV = right ventricle, LV = left ventricle.

This pilot study injecting poly(NIPAAM-co-HEMA-co-MAPLA) into infarcted pig hearts demonstrates the early safety of this approach to treat heart disease. Of note is that the first animal did expire shortly after material injection. While there was no obvious evidence that the material was the cause, a more detailed autopsy would have been needed to completely rule out such a possibility. However, a surgical mortality of approximately 20% has been reported due to

the damaging and invasive nature of these procedures.[323] In all cases the material injection itself was without incident.

The ability to use imaging to improve the efficacy of this procedure is important. The material was observable in the MRI imaging, likely due to the presence of gadoteridol in the gel. The amount of this contrast agent that remains in the gel 24 hr after injection when the MRI imaging was done is not known, though based on previous drug delivery studies from this material it is likely that much of the agent was gone. Nonetheless, enough remained to provide a difference in appearance compared to the surrounding tissue under magnetic relaxation. This provides a useful way to see where the material has deposited relative to the infarct zone in living animals. It is unlikely, however, that this approach would be useful for long-term follow-up as the contrast agent will have been completely released from the gel and new tissue ingrowth into the material will change the magnetic appearance of that area of heart tissue. To address the inability to see the infarct zone visually during the injection procedure, echocardiography was introduced. This confirmed the presence of an infarct and guided the location of gel injection. This method of imaging each heart before injection provides a powerful means with which to personalize the treatment for each patient. A physician could map the infarct zone and provide material injection exactly to the regions that would benefit from it most.

This pilot study has provided the necessary information needed to inform long-term studies in pigs. The procedures on these first four animals have provided valuable information on the clinical flow of the pigs, the locations and methods of injection, and the necessity of imaging both before and after the procedure. The future group of animals, which will involve doing the same infarction and injection procedures, will be followed for eight weeks after injection to study longer-term effects of material injection.

6.3 THERMORESPONSIVE GELS FOR SHORT TERM THERAPEUTIC DELIVERY

6.3.1 Introduction

Much of the research described above is aimed at studying the delivery of drugs from an injectable hydrogel of poly(NIPAAm-co-HEMA-co-MAPLA). It was found that due to the thermal transition of the material, and in particular the large volume change from solution to solid gel, much of the incorporated drug is released during the first 3 hr of gelation. The extent of the initial release was shown to be dependent on the protein and the chemical composition of the material. The subsequent release also followed a general profile of slow release until material degradation became significant after many weeks. The reason for the slow, long-term release is likely due to the low water content of 45% and the collapsed polymer network following transition as shown in **Figure 54**.[265] There are many cardiovascular and other applications that may require the delivery of drugs on a faster scale or where material collapse may not be advantageous.

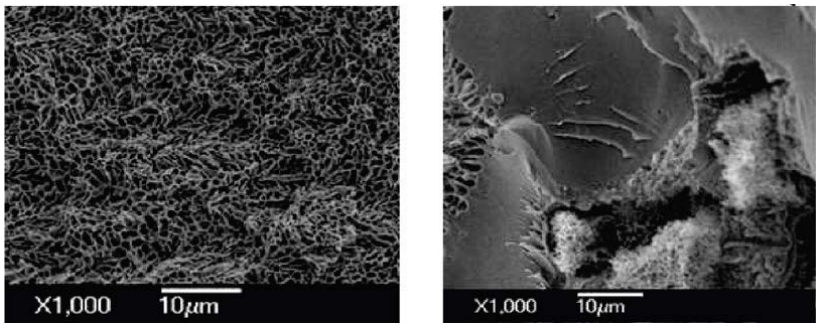

Figure 54. Scanning electron micrographs of poly(NIPAAm-co-HEMA-co-MAPLA) hydrogels 30s and 1d after transition at 37 °C demonstrating loss of porosity during thermal transition. From [265].

It is well known that infection of implantable devices is a tremendous clinical problem. Because infected devices account for nearly half of all nosocomial infections, substantial research is ongoing to develop material and controlled release systems for implantables that will be resistant to bacterial adhesion or survival.[324-326] Because of their life-sustaining nature, infection of cardiovascular implants such as vascular grafts, pacemakers, and ventricular assist

devices (VADs) has particularly dangerous repercussions. Studies show that the frequency of infected devices can reach as high as 40% in VADs and 4% in the other cardiovascular implants.[327] Given that about 450,000 vascular grafts are implanted every year in the United States leading to 16,000 infected devices, and that the estimated cost of treatment per infected device is $40,000, it is apparent that preventing and treating infected devices is of significant concern. These types of infections can be particularly difficult to treat through administration of intravenous antibiotics because they may reside on the outside of the device – for example in pacemaker and VAD pockets – where blood does not readily contact. Treatments for these infections generally require difficult surgical intervention involving irrigation and debridement and even placement of a muscle or omental flap over the infected device to increase vascular access to the infected device.[328-330] In some cases polymethylmethacrylate beads that were designed for orthopedic applications and are impregnated with antibiotic have been implanted into infected device pockets for local antibiotic delivery.[331, 332] However, studies show only a small portion of loaded antibiotic is delivered and adequate inhibitory concentrations do not extend beyond a few days.[333] The ability to deliver a material to the outside of such infected implants that would provide controlled release of antibiotic for longer periods would be beneficial. Thermoresponsive materials inherently have the ability to be delivered through injection where a fluid material could coat a device and fill infected cavities, thus making the procedure less invasive.

Short-term drug delivery has many other applications in the cardiovascular system, especially for the release of proteins or other signaling molecules to aid in regeneration. If the primary purpose of the therapy is drug delivery, the release behavior of the material would be more beneficial than a material with robust mechanical properties. Shorter drug delivery durations may be particularly useful in the early period following infarction where a host of processes cause necrosis, apoptosis, and fibrosis in the myocardium. There are many different chemical cues that can help rescue the myocardium if given during the first few weeks, when most of the tissue damage occurs. Examples of such signals that have been useful during this stage include heat shock proteins, p38 MAP kinase inhibitor, antioxidants, and IGF1, among others.[278, 306, 334-336] After myocardial rescue is complete, prolonged release of some of these agents may no longer be needed and so degradation of the injected carrier would be worthwhile.

We aimed to develop a material based on the poly(NIPAAM-co-HEMA-co-MAPLA) that is used for cardiac applications but that would show minimal network collapse while maintaining its thermoresponsiveness. The material should be better able to deliver drug and degrade over a shorter duration. To this end we used atom transfer radical polymerization (ATRP) to make a block copolymer that incorporated a balance of hydrophilic and hydrophobic moieties and studied the material and drug delivery characteristics of this material.

6.3.2 Materials and Methods

All chemicals were purchased from Sigma-Aldrich unless otherwise stated. NIPAAm was purified by recrystallization from hexane and vacuum-dried. 2-Hydroxyethyl methacrylate (HEMA) was purified by vacuum distillation. Vancomycin, sodium methoxide (NaOCH3), poly(vinyl alcohol), methacryloyl chloride, copper (II) bromide, 2-bromoisobutyryl bromide, triethylamine, linear chain poly(ethylene glycol) (PEG, M_n 3,400), and 4-arm star polymer PEG (M_n 10,000, PEGworks) were used as received. ^{125}I-BSA (Perkin Elmer) was reconstituted according to manufacturer instructions.

6.3.2.1 Synthesis of methacrylate polylactide (MAPLA)

MAPLA was synthesized as reported above – **Figure 29**.[265] Polylactide-monomethyl ether (HOPLA-OCH_3) was synthesized by ring opening polymerization by dissolving lactide in dichloromethane to which $NaOCH_3$ initiator in methanol was added. After 2 h of reaction at 0°C, the polymer solution was rinsed with 0.1 M HCl and deionized water, the organic phase was dried with $MgSO_4$ and removed by rotary evaporation. MAPLA was formed by dropping methacryloyl chloride in an HOPLA-OCH_3 solution in dichloromethane containing triethylamine, followed by reaction overnight at 0°C. Following reaction, precipitates were removed, the organic phase was dried and removed by rotary evaporation, leaving raw MAPLA product. MAPLA was purified by flash chromatography. NMR confirmed the synthesis of MAPLA with an average of 2.8 PLA units per MAPLA monomer.

6.3.2.2 Synthesis of ATRP macroinitiators

Linear or 4-arm PEG were activated with 2-bromoisobutyryl bromide to make the ATRP macroinitiator – **Figure 55**. Briefly, PEG was dissolved in dichloromethane to which triethylamine and then 2-bromoisobutyryl bromide were added under vigorous stirring at room temperature. After 48 hr, precipitates were removed from the sample by filtration, the sample was washed once each with 0.2 M Na_2CO_3, 0.1 M HCl and deionized water, the organic phase was dried with $MgSO_4$ and removed by rotary evaporation. Finally, the sample went through repeated steps of dissolving in warm ethanol, precipitating the polymer when cooled to 4 °C, and then centrifuging while cooled to collect and discard the supernatant. This was completed until the product was a white color and the supernatant was clear. The sample was then dried overnight in a vacuum oven before use.

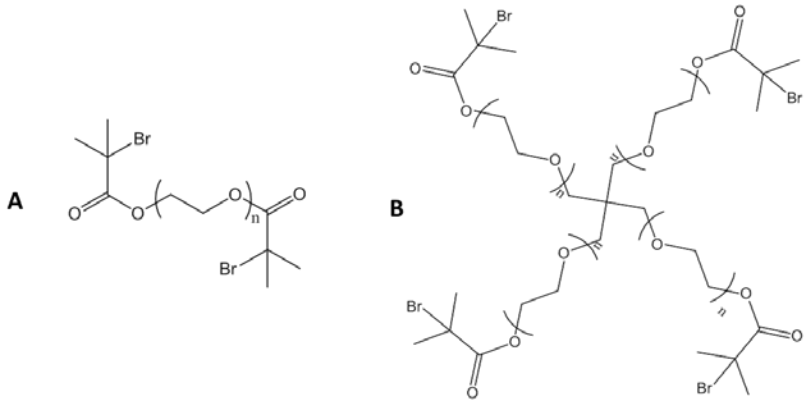

Figure 55. Macroinitiators for ATRP chemistry. Linear PEG (MW=3.4k) and 4-arm star PEG (MW=10k) were activated with bromoisobutyrl bromide to form PEG-BBr_2 (A) and $(PEG\text{-}BBr)_4$ (B).

6.3.2.3 ATRP of thermoresponsive block copolymers

A dry, hot schlenk flask was prepared by repeated applications of argon and vacuum. In 40 ml of methanol were added 0.0001 mole PEG macroinitiator, the ligand 1,8-dimethyl-1,4,8,11-tetraazacyclotetradecane, NIPAAm, HEMA, and MAPLA – **Figure 56**. The molar ratio of 1,8-dimethyl-1,4,8,11-tetraazacyclotetradecane to the –Br end groups of the macroinitiator was 6:1. Using 2g of NIPAAm, the HEMA and MAPLA were added to have a molar ratio of NIPAAM:HEMA:MAPLA of 80:10:10 as before. The solution went through repeated freeze-

pump-thaw cycles to remove oxygen and was maintained under an argon atmosphere. After degassing, the copper (II) bromide catalyst was added and the reaction proceeded at 45 °C for 48 hrs. After reaction, the methanol was removed by rotary evaporation and the product was dissolved in DCM. Aluminum oxide beads were repeatedly mixed into the solution to bind impurities and copper, and removed by centrifugation until the solution became colorless. Rotary evaporation removed the dichloromethane to form a solid product which was twice dissolved in THF and precipitated once in hexane and once in diethyl ether and then dried. The final product was a hydrophilic block flanked by hydrophobic moieties as shown in **Figure 57**. Before use the polymer was dissolved in PBS at 15-20 wt%.

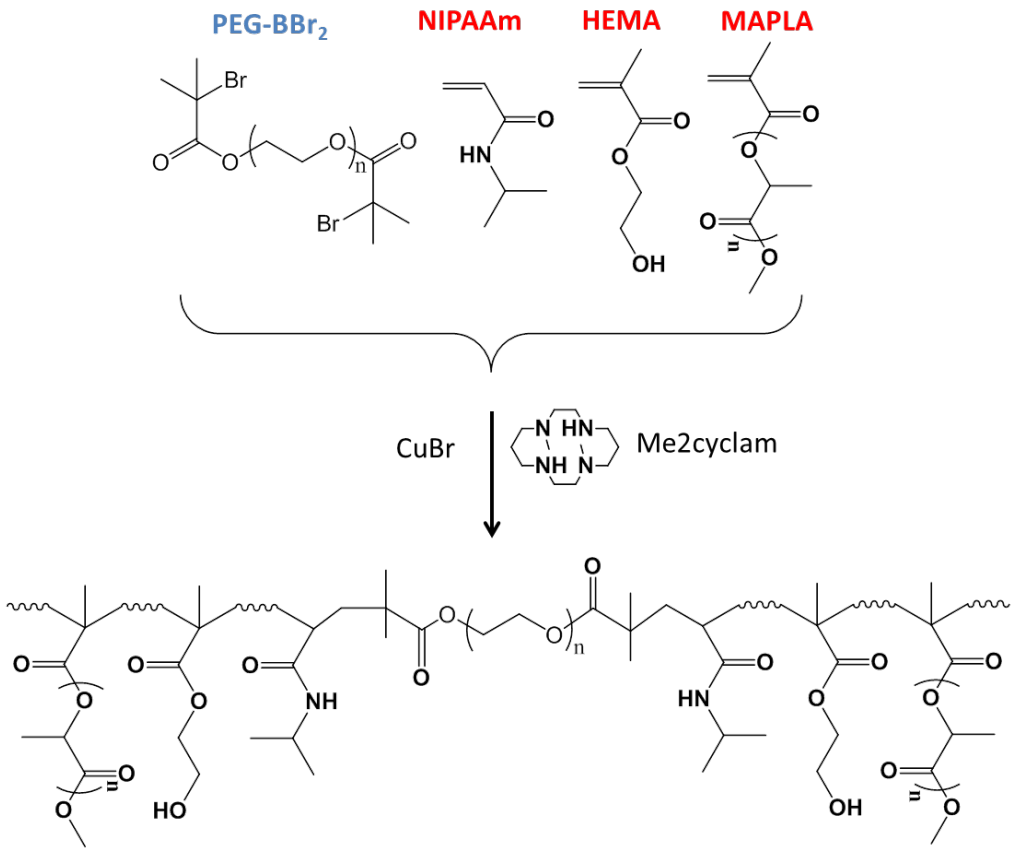

Figure 56. Scheme of ATRP synthesis of the linear block copolymer.

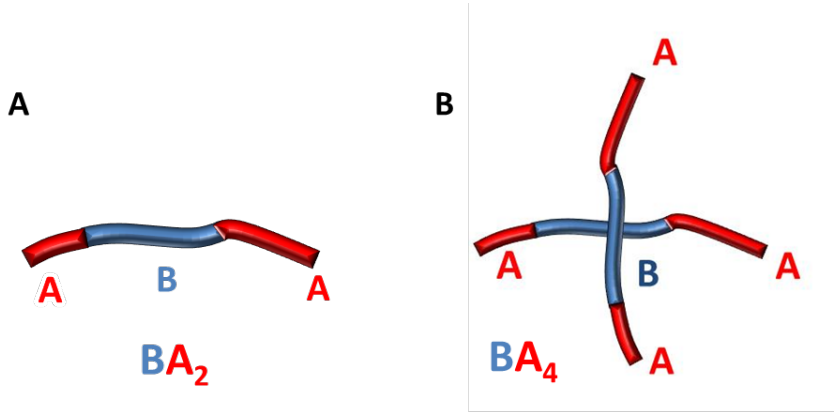

Figure 57. Representation of the linear (A) and star-shaped (B) block copolymers where the hydrophilic block, B=PEG is flanked by the hydrophobic blocks, A=poly(NIPAAm-co-HEMA-co-MAPLA).

6.3.2.4 Material characterization

The molecular weight of samples was determined using gas permeation chromatography. The gelation properties were assessed using parallel plate rheometry. Water content was determined by freeze drying gelled samples, where the weights of the sample before and after drying were used to determine original water content. Sample degradation was conducted in PBS at 37 °C.

6.3.2.5 Bacterial culture

Methicillin-resistant stapholococcus aureus was cultured in trypticase soy broth under agitation overnight. The bacterial solution was diluted by a factor of 50 and allowed to return to the growth phase for 2 more hr. This culture was diluted to a 1:10 working dilution for bacterial studies. The actual number of cells present in the working dilution was determined by plating serial dilutions of the working solution on trypticase soy agar plates and counting colony forming units after overnight growth.

6.3.2.6 Drug delivery studies

Vancomycin or ^{125}I-BSA was dissolved into block copolymer solutions or poly(NIPAAM-co-HEMA-co-MAPLA) at concentrations of 20 mg/ml and 0.5 mg/ml, respectively. 0.5 ml samples were allowed to gel at 37 °C and then were maintained in warm PBS. Releasate was collected at designated time points and the amount of released drug was measured by UV spectroscopy at

280 nm or by gamma counter for vancomycin and ^{125}I-BSA, respectively. For activity of released vancomycin, releasates were diluted to 2.5 ug/ml (just above the mean inhibitory concentration [MIC] of vancomycin for MRSA which was determined to be 2 ug/ml) and were mixed with MRSA solutions for 6 hr at 37 °C. After incubation the number of MRSA cells present was determined using a luminescence assay (BacTiter Glo, Promega). The luminometer readings were verified by correlation to the number of colony forming units that grew from solutions of known bacterial load.

6.3.3 Results and discussion

The block copolymer hydrogels were able to form a gel under 37 °C and did not demonstrate significant collapse of the network upon thermal transition. The general properties of the materials are shown in **Table X**. The onset of gel transition was at 25 °C and 30 °C for the linear and star copolymers, respectively.

Table X. Material Properties of Block Copolymers

Block copolymer type	B Block	Molecular weight (Da)	Gel property and water content at 37 °C	Full dissolution (PBS at 37°C)
BA_2	PEG (3.4k)	24,000	White color, 84%	2 weeks
BA_4	4-arm PEG (10k)	48,000	White color, 84%	3 weeks

The release of ^{125}I-BSA from these two materials is shown in **Figure 58**. The amount of protein released during the first 3 hr after gel transition was 11.1 ± 1.0 % and 17.7 ± 2.0 % for the linear and star-shaped block copolymers, respectively, compared to 78.0 ± 2.1% for the previous poly(NIPAAM-co-HEMA-co-MAPLA) hydrogel used for cardiac injection. The release profile demonstrated a diffusion-controlled system characterized by a gradual decrease in release at each subsequent time point until exhaustion of the loaded protein.

Release of vancomycin from these block copolymer gels also showed a diffusion-controlled system that delivered antibiotic over 1 to 2 weeks – **Figure 59**. In comparison the release of vancomycin from poly(NIPAAm-co-HEMA-co-MAPLA) gels is also shown. The initial release at 3 hr was 33.1 ± 5.1% and 15.7 ± 0.8% for the linear and star-shaped block copolymers, respectively, compared to 46.2 ± 2.8% for the cardiac gel. Following the initial release, the concentration of antibiotic in the releasate at each time point in the block copolymers was higher than the MIC for MRSA. In contrast, after gel formation very little vancomycin was released from the poly(NIPAAm-co-HEMA-co-MAPLA) gel during the subsequent 2 week. The antibiotic that was released from the star copolymer was bioactive as demonstrated by its ability to inhibit MRSA survival in solution when diluted to just above the MIC – **Figure 60**. Releasate from control gels without loaded antibiotic had no ability to inhibit MRSA growth.

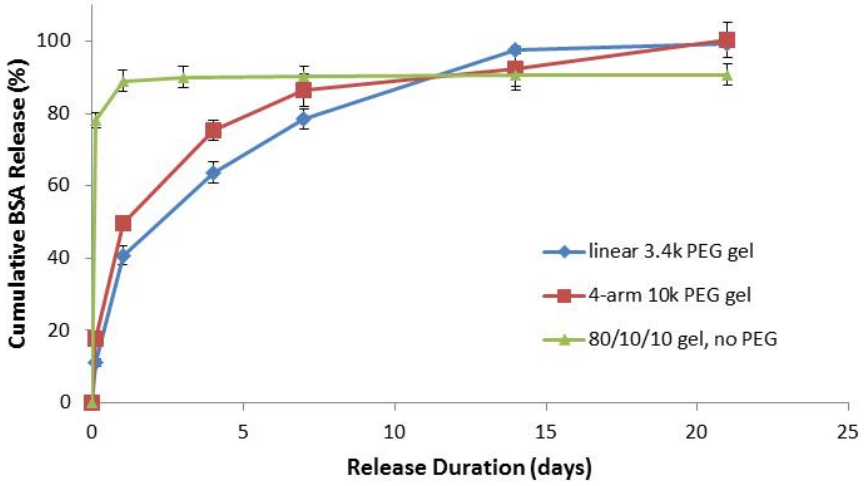

Figure 58. Release profiles of BSA from linear and star-shaped copolymers compared to the poly(NIPAAm-co-HEMA-co-MAPLA) gel without PEG. The initial release of protein is significantly reduced when a PEG block is incorporated into the copolymer.

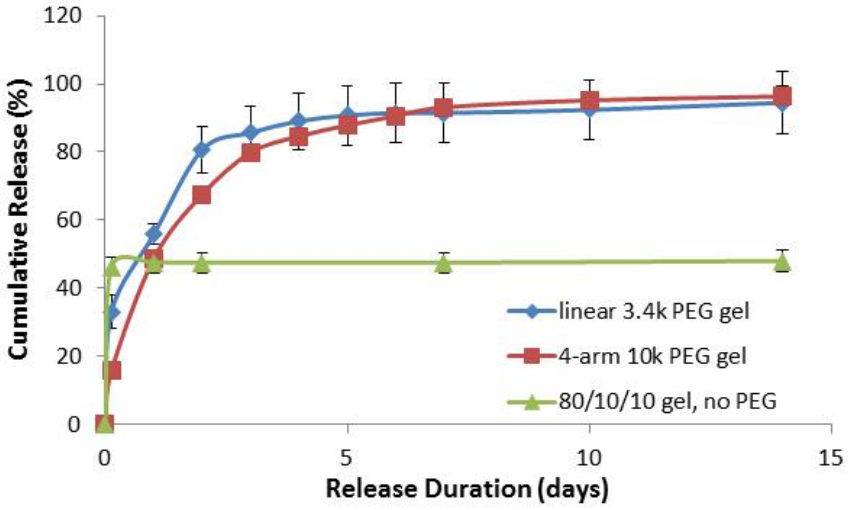

Figure 59. Release of vancomycin from block copolymer gels and the poly(NIPAAm-co-HEMA-co-MAPLA) gel that did not have a PEG block. After an initial release the non-PEG gel releases very little antibiotic.

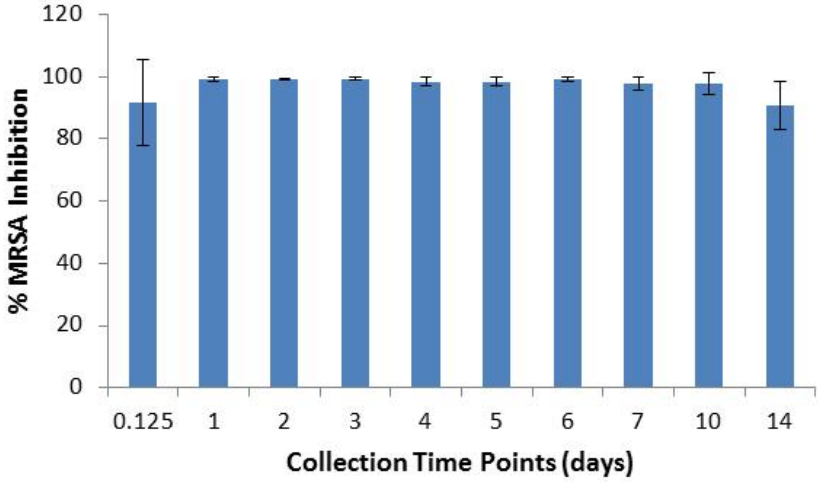

Figure 60. Inhibition of methicillin-resistant staphylococcus aureus by releasate from 4-arm star copolymers loaded with vancomycin.

A relatively short duration of drug delivery from cardiovascular biomaterials may be appropriate or even advantageous in some situations. A material that will deliver its payload and degrade within a few weeks may have higher clinical efficacy and a reduced risk of chronic inflammation. The newly developed block copolymers using ATRP chemistry are one example where a substantial adaptation of the material previously used for intramyocardial injection may prove to be useful for shorter term drug delivery needs in applications where strong mechanical properties are of lesser importance. These applications may include therapeutic angiogenesis, myocardial rescue, or even cell delivery.

The material developed using hydrophilic PEG blocks between the thermoresponsive blocks consisting of NIPAAm, HEMA, and MAPLA was able to form a gel below body temperature without substantial collapse. The fine balance between affinity for water and repulsion of it allows the material to maintain its volume without either collapsing or requiring a transition temperature higher than 37 °C. The ultimate effect of this balance in these materials is a gel network with increased water content which allows for simple diffusion of drug from the matrix. In contrast to the cardiac gels, these materials did not exhibit the substantial drug losses seen just after gel transition. Not only did the initial release decrease, but the amount of drug released at each time point over the next several days was more substantial, presumably due to the higher water flux through the open gel network.

One area of promise in the field of injectable materials is their ability to co-deliver a cell of interest to an injection site. It has been widely observed that cells injected into a tissue, especially one as mechanically active as the heart, do not remain, survive, or engraft at the injection site in significant numbers.[337-339] In cases where cells have been simultaneously delivered with material to act as an in situ scaffold the cell survival and engraftment has increased substantially.[78, 79, 87] The requirements for a scaffolding material would be to allow a favorable cell environment with adequate mass transfer for nutrient supply to cells throughout the material. These block copolymers may be useful candidates for a material to deliver cells to the heart due to their high water content. While lacking mechanical strength relative to its poly(NIPAAm-co-HEMA-co-MAPLA) precursor, because the primary purpose of this material would be for cell delivery, trading some mechanical strength for greater porosity may be reasonable.

In determining the potential benefit of these new gels, the clinical applications of the material need to be investigated. As mentioned previously, infected cardiovascular implants are a significant problem in clinical practice. To further investigate the ability of this material to treat infected cardiovascular devices, a reasonable experiment may involve coating materials used for vascular grafts with this antibiotic-loaded gel in vitro as either prophylaxis against bacterial innoculation or as treatment once a bacterial biofilm has already deposited. Prophylactic delivery of such a material at the implant site during cardiovascular surgery may prove to be a more effective means of preventing implant related infections than systemic delivery of antibiotic in the post-operative period.

Where short term delivery of protein is needed this material may be loaded with protein to be delivered to the infarct zone soon after infarction. One relevant protein for this type of approach may be IGF1 which could act as a cell survival cue to salvage myocardium in the days to weeks following injury, when cell death is most prevalent. The sol-gel nature of this material means that systems could be devised to deliver it through non-invasive techniques such as endovascular catheterization. This may reasonably be done at the time of balloon angioplasty or stent placement which is often performed early after a heart attack.

There are many ways in this these newly developed block copolymers could be used and adapted. As relating to controlled release, functionalization of the polymer to include peptide sequences, conjugating moieties, or particle systems may be applied to change the rates at which drugs are released. The full field of modifications to hydrogel systems that has been reported over several decades is at the engineer’s disposal when considering directions to pursue. Additional applications of this material beyond the cardiac environment may also be pursued. For example, antibiotic delivery in other wound environments or protein delivery for various regenerative medicine applications could be investigated.

7.0 FINAL SUMMARY

As heart disease remains a significant problem throughout the world, finding new and better ways to treat it is always of value. Biomaterials-based approaches have been gaining recognition in recent years for their ability to ameliorate the effects seen after MI. The research presented above discusses new developments in two of those biomaterial approaches: implantation of a cardiac patch and intramyocardial biomaterial injection. Both approaches have shown success in animal models. Historically, results are generally improved when appropriate signaling molecules are loaded into the materials for controlled release after implantation. The delivery rates for these drugs can have an influence on their effectiveness. Especially in the case of more advanced systems involving spatial or temporal control, it is important to understand and adjust the controlled release system before implantation.

Inherent with either a patch or injection technique are certain benefits and disadvantages. For example, using a cardiac patch allows for a greater variety of materials and processing methods to be used. In the case of material injection, the material is limited by its ability to be injectable through a small gauge needle and form a stable implant in situ. In contrast, materials used as a patch can be formed before implantation to provide specific architectures, porous networks, and mechanical properties. The synthesis and processing can involve harmful chemicals that would not be possible in vivo, so long as they are removed before implantation. Formed patches can also be treated in vitro before implantation, for example with cells or proteins, to increase their functionality. This provides numerous control points to the engineer and allows many specific design parameters to be specified. Another advantage to a patch method is that large areas of the heart can be patched continuously. Injected material has been shown to have a local effect on myocardial wall stress around the injection sites. This makes choosing the injection locations and layout important. In the case of a large patch there is likely to be a more widespread benefit throughout the ventricular wall.

The injection of material into the heart wall directly has some distinct advantages over a patch approach. One major benefit can be found in the method of delivery. Whereas patch implantation will generally require an open-chest procedure to have enough access to the epicardial surface for material deployment, intramyocardial injection may be done less invasively through a keyhole incision or endovascular approach. Because major surgery is highly demanding on a weakened heart and infection risk is increased with larger incisions, this could make the delivery safer as well as decrease the morbidity and recovery time following injection. Another advantage to an injection approach is that the material may interact more freely with the native tissue which allows for better cellular infiltration and communication between the material and the host. It has been shown with patch implantation, for example, that host cells may have difficulty in penetrating or surviving in epicardial patches presumably due to the decreased nutrient access. Injectable materials, which tend to be gel-like, are also generally porous with high water content to allow for better nutrient transfer for cellular ingrowth or to support cells loaded into the material before injection.

Poly(ester urethane) urea has been shown to be a valuable patch material. The elastomeric properties and degradation profile make it useful in cardiovascular and other applications. We showed that when loaded with a gene-inducing molecule, RSL1, this material provides long-term drug delivery from polymer films. The released inducer is bioactive as determined by its ability to cause expression of GFP in cells stably transfected with the corresponding gene induction system. Cells grown on RSL1-loaded films expressed GFP proportional to the amount of RSL1 loaded. When films and porous scaffolds were differentially loaded with regions of high RSL1 content and regions without the inducer, the expression of GFP in cells cultured on the material generally mirrored the RSL1 loading pattern. Delivery of gene inducing molecules in 3D patterns has important applications in tissue engineering as it can allow the formation of tissue substitutes with complex cellular architectures. Tissues such as cardiac muscle and blood vessels, which are formed by specific organizations of cells and proteins, may be fabricated by combining appropriately transfected cells and scaffolds that present the inducer in specific spatial patterns as described in this research. Furthermore, cells grown on inducer-loaded scaffolds would continue to receive their directions for gene expression whether being cultured in vitro or after implantation in vivo. This approach is novel because it allows the scaffold, once appropriately loaded with inducer, to independently direct cell fate or

behavior in the absence of any additional cues to the system. This approach has not been investigated before and may lead to a new paradigm for both in vitro and in vivo tissue engineering.

A more common approach to aiding in tissue regeneration after patch implantation would be the controlled release of growth factors from the material. We show that growth factors IGF1 and HGF can be loaded into the patch and are released in a bioactive form as shown by in vitro cellular response to releasates. It was interesting to observe that the proteins were released over a long time period with multiple phases of fast and slow release. This complex profile has not been observed previously and may be related to the segmented nature of the polyurethane. An important observation was that the release rates were much different when scaffolds were soaked in solutions that contained the enzyme lipase. This enzyme degrades the material in a way that helps mimic the in vivo environment that would be seen following patch implantation. In this case it was shown that while polymer mass fraction in the scaffold did influence the delivery rates as had been shown with scaffolds in PBS, the effect was much smaller in the presence of enzyme. Most studies of drug delivery from biomaterials use a saline environment to simulate sink conditions that would be experienced in vivo. However, sink conditions are only part of the complex milieu experienced by implanted materials. This research clearly shows that information gained from in vitro testing of drug delivery systems may not accurately describe what the devices will ultimately experience upon implantation, especially in the case of degradable materials. The lessons learned from this research, while useful for the dynamic cardiac environment discussed here, has broad applications for drug delivery studies throughout the field of controlled release.

Another important biomaterials-based therapy for heart disease, delivering material into the wall of an infarcted ventricle, has been under considerable investigation in recent years. The properties of the materials used are increasingly appreciated as a necessary component to the success or failure of a material in this application. We developed a strong, thermoresponsive material that can be injected into the heart and degrades over at least 5 months. The ability to release growth factors from this material may be able to augment the regeneration and benefit that is seen upon injection of material alone. We showed that the significant volume collapse of the material during thermal transition leads to loss of much of the loaded model protein BSA

during the first few hours. By adjusting the chemistry and providing a means of binding the protein to the polymer we are able to better encapsulate the growth factors so they can be released more steadily over time. We were also able to load degradable microparticles that encapsulate protein into the gel network to provide a second depot of drug delivery. When particles are loaded into the hydrogel their burst release diminishes significantly, leading to later-stage release of drugs. Combining the gel with the microparticles allows one protein to be directly loaded into the gel and be released mostly during the early period following gelation while proteins loaded into microparticles inside the gel are released later – forming a sequential release profile. It is important to note that the system described here has multiple control points and allows for independent adjustment of both of the drug delivery reservoirs: gel or microparticles. This system thus becomes a useful foundation for multifaceted systems where more drugs and various delivery rates are desired. These types of complex release systems may be especially useful for aiding regeneration in target tissues where the complexity of signaling molecule delivery is increasingly appreciated.

After using model protein we demonstrate the ability of this gel-microparticle drug delivery system to release important growth factors bFGF and IGF1 in a sequential manner. We hypothesize that earlier bFGF delivery from the gel phase will be able to encourage angiogenesis in infarcted tissue and thus create a healthier microenvironment to which cardiac stem cells can survive, proliferate, and differentiate due to the signals of subsequent IGF1 release from loaded microparticles in the gel. We demonstrated that a sequential release profile can be obtained from this system and that the released protein retains its bioactivity in vitro. When growth factor-loaded gels are injected into infarcted myocardium it was seen that the tissue growth factor levels are elevated for at least two weeks. After intramyocardial injection of the new thermoresponsive gel without any growth factors we show the material alone is able maintain cardiac function for at least 16 weeks and significantly reduce negative remodeling of the heart seen during that time. Histological evaluation showed that many macrophages, smooth muscle cells, and blood vessels were present in the infarct zone at the study endpoint. The presence of growth factors loaded into the gel was not able to improve upon any of the functional, geometric, or histological properties seen from injection of plain gel. This points to a primary role of the material to improve cardiac function and cellular environment where added growth factors are insufficient to provide further benefits. More drug delivery strategies may need to be employed to see increased effect in this

system. Additionally, continued research into the mechanisms by which appropriate biomaterials elicit improvements in tissue environments is justified by the results we have shown here.

The lessons learned from the research just described have led to more improvements and investigation. For example, as the release of bFGF was unable to cause additional angiogenesis in vivo after release from the injectable gel, a different growth factor, VEGF, is being considered. Early evidence suggests it may be released with less suspected damage than was bFGF. The positive results seen from injection of the thermoresponsive material into infarcted rat hearts has led to its application in the large animal swine model of infarction. A pilot study has been completed that shows the infarcts can be created, material injected, and the cardiac anatomy imaged successfully. Chronic studies that will show efficacy relevant to future human applications will begin shortly. Finally, we showed previously that most growth factor is released from the injectable gel during the first few hours due to significant gel collapse. To ameliorate this concern we have developed a new material that uses the previous polymer as one block within a block copolymer structure. The applications for this material include intramyocardial injection, primarily as a depot for drug delivery, or as a means to treat infection in cardiovascular implants. The ability to release active antibiotic in a clinically relevant time frame from this material was demonstrated.

Regular clinical application of these therapies has not been fully realized and will require more research and optimization to make common human use a reality. While there have been few instances of patch materials being used in humans, material injection therapy is only beginning in the clinical environment. The research explained above illuminates some of the technical challenges that must be addressed to move through the necessary regulatory processes. The governing body for medical devices in the United States, the Food and Drug Administration (FDA), is responsible for guaranteeing that both safety and efficacy are demonstrated before device approval. While the safety of patch application has largely been confirmed, the safety of intramyocardial material injection remains to be fully proven. For example, approval will require a demonstration that a material can be injected without embolization in the blood stream, can be localized to the desired tissue, and does not migrate over time. When considering the growing number of materials used for patch and injection therapy there is specific safety testing of in vivo biocompatibility according to international standards that must be completed for FDA approval.

As the FDA does not approve a material, but rather applications, the soundness of the selected materials must also be proven in the context of cardiac failure. It is no surprise that common implanted materials such as collagen were among the first used in these applications as their previous approval in other devices may lead to a quicker regulatory approval in the context of patch and injection therapy.

The efficacy of the treatments must also be proved in a way that demonstrates improvement over current treatment options. In animal models this benefit has been demonstrated with some material systems but often large animal models have not been investigated. Acquiring more data in large animals will be necessary to move this work to the clinic. Many patch and injectable materials are useful as drug or cell carriers. As has been discussed here, the inclusion of these moieties can improve efficacy, however they do add complexity to the device and the regulatory pathway. As the changes in drug delivery properties have been shown to be influenced heavily by in vivo degradation, appropriate pre-clinical characterization becomes even more difficult. When drugs or cells are included in a treatment that is primarily a materials-based therapy the product becomes a "combination device" for regulatory approval. This requires approval of the device not only from a materials perspective but also from a biological or pharmaceutical perspective. The way in which with FDA handles such combination products is evolving but currently involves significant additional testing and time. As the FDA works to streamline the regulatory process the final clinical application of these products will become more common.

The benefits of application of biomaterials for cardiovascular disease have been shown in the settings of both cardiac patch and intramyocardial biomaterial injection. The complexities of drug delivery from both material types have been shown using large and small proteins and a small molecule. In each case described above we find a system with completely different release properties than the others – whether it be very long release times, cycling periods of fast and slow release, or sequential delivery of multiple factors. The overall theme is that each system requires independent testing and understanding of what dictates the release kinetics before in vivo use. It cannot necessarily be taken for granted that simple changes of drug types or material properties within a controlled release system will result in substantially similar results. As the field of implantable biomaterials continues to expand with better materials, the need for a drug

delivery component to the material in each application should be considered and the properties of controlled release will require investigation in order to have a successful product.

BIBLIOGRAPHY

1. Lloyd-Jones, D., R. Adams, M. Carnethon, G. De Simone, T.B. Ferguson, K. Flegal, et al. Heart disease and stroke statistics 2009 update: a report from the American Heart Association statistics committee and stroke statistics subcommittee. Circulation 2009;119:e21-e181.

2. Boland, L.L., A.R. Folsom, P.D. Sorlie, H.A. Taylor, W.D. Rosamond, L.E. Chambless, et al. Occurrence of unrecognized myocardial infarction in subjects aged 45 to 65 years (the ARIC study). Am J Cardiol 2002;90(9):927-31.

3. Gheorghiade, M. and R.O. Bonow. Chronic heart failure in the United States: a manifestation of coronary artery disease. Circulation 1998;97(3):282-9.

4. Pfeffer, M.A. and E. Braunwald. Ventricular remodeling after myocardial infarction. Experimental observations and clinical implications. Circulation 1990;81(4):1161-72.

5. Mann, D.L. and M.R. Bristow. Mechanisms and models in heart failure: the biomechanical model and beyond. Circulation 2005;111(21):2837-49.

6. Lloyd-Jones, D.M., M.G. Larson, E.P. Leip, A. Beiser, R.B. D'Agostino, W.B. Kannel, et al. Lifetime risk for developing congestive heart failure: The Framingham Heart Study. Circulation 2002;106(24):3068-72.

7. Khand, A., I. Gemmel, A.L. Clark, and J.G.F. Cleland. Is the prognosis of heart failure improving? J Am Coll Cardiol 2000;36(7):2284-6.

8. Jessup, M. and S. Brozena. Heart failure. N Engl J Med 2003;348(20):2007-18.

9. Hannan, E.L., M.J. Racz, B.D. McCallister, T.J. Ryan, D.T. Arani, O.W. Isom, et al. A comparison of three-year survival after coronary artery bypass graft surgery and percutaneous transluminal coronary angioplasty. J Am Coll Cardiol 1999;33(1):63-72.

10. Hannan, E.L., M.J. Racz, G. Walford, R.H. Jones, T.J. Ryan, E. Bennett, et al. Long-term outcomes of coronary-artery bypass grafting versus stent implantation. N Engl J Med 2005;352(21):2174-83.

11. Flaherty, J.D., C.J. Davidson, and D.P. Faxon. Percutaneous coronary intervention for myocardial infarction with left ventricular dysfunction. The American Journal of Cardiology 2008;102(5, Supplement 1):38G-41G.

12. Nelson, G.S., R.D. Berger, B.J. Fetics, M. Talbot, J.C. Spinelli, J.M. Hare, et al. Left ventricular or biventricular pacing improves cardiac function at diminished energy cost in patients with dilated cardiomyopathy and left bundle-branch block. Circulation 2000;102(25):3053-9.

13. Flather, M.D., S. Yusuf, L. Kober, M. Pfeffer, A. Hall, G. Murray, et al. Long-term ACE-inhibitor therapy in patients with heart failure or left-ventricular dysfunction: a systematic overview of data from individual patients. ACE-Inhibitor Myocardial Infarction Collaborative Group. Lancet 2000;355(9215):1575-81.

14. van Zwieten, P.A. Current and newer approaches in the drug treatment of congestive heart failure. Cardiovasc Drugs Ther 1997;10(6):693-702.

15. John, R., H.A. Rajasinghe, J.M. Chen, A.D. Weinberg, P. Sinha, D.M. Mancini, et al. Long-term outcomes after cardiac transplantation: an experience based on different eras of immunosuppressive therapy. Ann Thorac Surg 2001;72(2):440-9.

16. Goldstein, D.J., M.C. Oz, and E.A. Rose. Implantable left ventricular assist devices. N Engl J Med 1998;339(21):1522-33.

17. Simon, M.A., J. Watson, J.T. Baldwin, W.R. Wagner, and H.S. Borovetz. Current and future considerations in the use of mechanical circulatory support devices. Annu Rev Biomed Eng 2008;10:59-84.

18. Christman, K.L. and R.J. Lee. Biomaterials for the treatment of myocardial infarction. J Am Coll Cardiol 2006;48(5):907-13.

19. Holmes, J.W., T.K. Borg, and J.W. Covell. Structure and mechanics of healing myocardial infarcts. Annu Rev Biomed Eng 2005;7:223-53.

20. Gupta, K.B., M.B. Ratcliffe, M.A. Fallert, L.H. Edmunds, Jr., and D.K. Bogen. Changes in passive mechanical stiffness of myocardial tissue with aneurysm formation. Circulation 1994;89(5):2315-26.

21. Schwinger, R.H., M. Bohm, A. Koch, U. Schmidt, I. Morano, H.J. Eissner, et al. The failing human heart is unable to use the Frank-Starling mechanism. Circ Res 1994;74(5):959-69.

22. White, H.D., R.M. Norris, M.A. Brown, P.W. Brandt, R.M. Whitlock, and C.J. Wild. Left ventricular end-systolic volume as the major determinant of survival after recovery from myocardial infarction. Circulation 1987;76(1):44-51.

23. Tischler, M.D., J. Niggel, D.T. Borowski, and M.M. LeWinter. Relation between left ventricular shape and exercise capacity in patients with left ventricular dysfunction. J Am Coll Cardiol 1993;22(3):751-7.

24. Pfeffer, M.A. and J.M. Pfeffer. Ventricular enlargement and reduced survival after myocardial infarction. Circulation 1987;75(5 Pt 2):IV93-7.

25. Tonnessen, T. and C.W. Knudsen. Surgical left ventricular remodeling in heart failure. Eur J Heart Fail 2005;7(5):704-9.

26. Starling, R.C., M. Jessup, J.K. Oh, H.N. Sabbah, M.A. Acker, D.L. Mann, et al. Sustained benefits of the CorCap Cardiac Support Device on left ventricular remodeling: three year follow-up results from the Acorn clinical trial. Ann Thorac Surg 2007;84(4):1236-42.

27. Klodell, C.T., Jr., J.M. Aranda, Jr., D.C. McGiffin, B.K. Rayburn, B. Sun, W.T. Abraham, et al. Worldwide surgical experience with the Paracor HeartNet cardiac restraint device. J Thorac Cardiovasc Surg 2008;135(1):188-95.

28. Gummert, J.F., A. Rahmel, T. Bossert, and F.W. Mohr. Socks for the dilated heart. Does passive cardiomyoplasty have a role in long-term care for heart failure patients? Z Kardiol 2004;93(11):849-54.

29. Blom, A.S., J.J. Pilla, R.C. Gorman, 3rd, J.H. Gorman, R. Mukherjee, F.G. Spinale, et al. Infarct size reduction and attenuation of global left ventricular remodeling with the CorCap cardiac support device following acute myocardial infarction in sheep. Heart Fail Rev 2005;10(2):125-39.

30. Fukamachi, K. and P.M. McCarthy. Initial safety and feasibility clinical trial of the myosplint device. J Card Surg 2005;20(6):S43-7.

31. Kashem, A., S. Kashem, W.P. Santamore, D.L. Crabbe, K.B. Margulies, D.B. Melvin, et al. Early and late results of left ventricular reshaping by passive cardiac-support device in canine heart failure. J Heart Lung Transplant 2003;22(9):1046-53.

32. Sartipy, U., A. Albage, and D. Lindblom. The Dor procedure for left ventricular reconstruction. Ten-year clinical experience. Eur J Cardiothorac Surg 2005;27(6):1005-10.

33. Batista, R. Partial left ventriculectomy--the Batista procedure. Eur J Cardiothorac Surg 1999;15 Suppl 1:S12-9; discussion S39-43.

34. Callegari, A., S. Bollini, L. Iop, A. Chiavegato, G. Torregrossa, M. Pozzobon, et al. Neovascularization induced by porous collagen scaffold implanted on intact and cryoinjured rat hearts. Biomaterials 2007;28(36):5449-61.

35. Simpson, D., H. Liu, T.-H.M. Fan, R. Nerem, and S.C. Dudley. A tissue engineering approach to progenitor cell delivery results in significant cell engraftment and improved myocardial remodeling. Stem Cells 2007;25(9):2350-7.

36. Li, R.-K., Z.-Q. Jia, R.D. Weisel, D.A.G. Mickle, A. Choi, and T.M. Yau. Survival and function of bioengineered cardiac grafts. Circulation 1999;100(suppl 2):II-63-II-69.

37. Xiong, Q., K.L. Hill, Q. Li, P. Suntharalingam, A. Mansoor, X. Wang, et al. A fibrin patch-based enhanced delivery of human embryonic stem cell-derived vascular cell transplantation in a porcine model of postinfarction left ventricular remodeling. Stem Cells 2011;29(2):367-375.

38. Zhang, G., Y. Nakamura, X. Wang, Q. Hu, L.J. Suggs, and J. Zhang. Controlled release of stromal cell-derived factor-1 alpha in situ increases c-kit+ cell homing to the infarcted heart. Tissue Eng 2007;13(8):2063-71.

39. Tan, M.Y., W. Zhi, R.Q. Wei, Y.C. Huang, K.P. Zhou, B. Tan, et al. Repair of infarcted myocardium using mesenchymal stem cell seeded small intestinal submucosa in rabbits. Biomaterials 2009;30(19):3234-40.

40. Krupnick, A.S., D. Kreisel, F.H. Engels, W.Y. Szeto, T. Plappert, S.H. Popma, et al. A novel small animal model of left ventricular tissue engineering. The Journal of Heart and Lung Transplantation 2002;21(2):233-43.

41. Giraud, M.-N., R. Flueckiger, S. Cook, E. Ayuni, M. Siepe, T. Carrel, et al. Long-term evaluation of myoblast seeded patches implanted on infarcted rat hearts. Artificial Organs 2010;34(6):E184-E192.

42. Siepe, M., M.-N. Giraud, M. Pavlovic, C. Receputo, F. Beyersdorf, P. Menasché, et al. Myoblast-seeded biodegradable scaffolds to prevent post–myocardial infarction evolution toward heart failure. The Journal of Thoracic and Cardiovascular Surgery 2006;132(1):124-31.

43. Fujimoto, K.L., K. Tobita, W.D. Merryman, J. Guan, N. Momoi, D.B. Stolz, et al. An elastic, biodegradable cardiac patch induces contractile smooth muscle and improves cardiac remodeling and function in subacute myocardial infarction. J Am Coll Cardiol 2007;49(23):2292-300.

44. Fujimoto, K.L., K. Tobita, J. Guan, R. Hashizume, K. Takanari, C.M. Alfieri, et al. Placement of an Elastic Biodegradable Cardiac Patch on a Subacute Infarcted Heart Leads to Cellularization With Early Developmental Cardiomyocyte Characteristics. Journal of Cardiac Failure 2012;18(7):585-95.

45. Fujimoto, K.L., J. Guan, H. Oshima, T. Sakai, and W.R. Wagner. In vivo evaluation of a porous, elastic, biodegradable patch for reconstructive cardiac procedures. Ann Thorac Surg 2007;83(2):648-54.

46. Piao, H., J.-S. Kwon, S. Piao, J.-H. Sohn, Y.-S. Lee, J.-W. Bae, et al. Effects of cardiac patches engineered with bone marrow-derived mononuclear cells and PGCL scaffolds in a rat myocardial infarction model. Biomaterials 2007;28(4):641-9.

47. Jin, J., S.I. Jeong, Y.M. Shin, K.S. Lim, H.s. Shin, Y.M. Lee, et al. Transplantation of mesenchymal stem cells within a poly(lactide-co-ε-caprolactone) scaffold improves cardiac function in a rat myocardial infarction model. European Journal of Heart Failure 2009;11(2):147-53.

48. Zachary, I. and R. Morgan. Therapeutic angiogenesis for cardiovascular disease: biological context, challenges, prospects. Heart 2010;97:181-9.

49. Simons, M., R.O. Bonow, N.A. Chronos, D.J. Cohen, F.J. Giordano, H.K. Hammond, et al. Clinical trials in coronary angiogenesis: issues, problems, consensus : an expert panel summary. Circulation 2000;102(11):e73-86.

50. Ferrara, N. and K. Alitalo. Clinical applications of angiogenic growth factors and their inhibitors. Nat Med 1999;5(12):1359-64.

51. Ma, J., J. Ge, S. Zhang, A. Sun, J. Shen, L. Chen, et al. Time course of myocardial stromal cell–derived factor 1 expression and beneficial effects of intravenously administered bone marrow stem cells in rats with experimental myocardial infarction. Basic Research in Cardiology 2005;100(3):217-23.

52. Abbott, J.D., Y. Huang, D. Liu, R. Hickey, D.S. Krause, and F.J. Giordano. Stromal cell–derived factor-1α plays a critical role in stem cell recruitment to the heart after myocardial infarction but Is not sufficient to induce homing in the absence of injury. Circulation 2004;110(21):3300-5.

53. Wall, S.T., J.C. Walker, K.E. Healy, M.B. Ratcliffe, and J.M. Guccione. Theoretical impact of the injection of material into the myocardium: a finite element model simulation. Circulation 2006;114(24):2627-35.

54. Wenk, J.F., S.T. Wall, R.C. Peterson, S.L. Helgerson, H.N. Sabbah, M. Burger, et al. A method for automatically optimizing medical devices for treating heart failure: designing polymeric injection patterns. J Biomech Eng 2009;131(12):10111-7.

55. Mukherjee, R., J.A. Zavadzkas, S.M. Saunders, J.E. McLean, L.B. Jeffords, C. Beck, et al. Targeted myocardial microinjections of a biocomposite material reduces infarct expansion in pigs. Ann Thorac Surg 2008;86(4):1268-76.

56. Rowley, J.A., G. Madlambayan, and D.J. Mooney. Alginate hydrogels as synthetic extracellular matrix materials. Biomaterials 1999;20(1):45-53.

57. Alsberg, E., K.W. Anderson, A. Albeiruti, R.T. Franceschi, and D.J. Mooney. Cell-interactive alginate hydrogels for bone tissue engineering. J Dent Res 2001;80(11):2025-9.

58. Augst, A.D., H.J. Kong, and D.J. Mooney. Alginate hydrogels as biomaterials. Macromol Biosci 2006;6(8):623-33.

59. Kong, H.J., K.Y. Lee, and D.J. Mooney. Decoupling the dependence of rheological/mechanical properties of hydrogels from solids concentration. Polymer 2002;43:6239–46.

60. Drury, J.L., R.G. Dennis, and D.J. Mooney. The tensile properties of alginate hydrogels. Biomaterials 2004;25(16):3187-99.

61. Stokke, B.J., K.I. Draget, O. Smidsrod, Y. Yuguchi, H. Urakawa, and K. Kajiwara. Small-angle x-ray scattering and rheological characterization of alginate gels. 1. Ca-alginate gels. Macromolecules 2000;33(5):1853-63.

62. Bouhadir, K.H., K.Y. Lee, E. Alsberg, K.L. Damm, K.W. Anderson, and D.J. Mooney. Degradation of partially oxidized alginate and its potential application for tissue engineering. Biotechnol Prog 2001;17(5):945-50.

63. Tonnesen, H.H. and J. Karlsen. Alginate in drug delivery systems. Drug Dev Ind Pharm 2002;28(6):621-30.

64. Simmons, C.A., E. Alsberg, S. Hsiong, W.J. Kim, and D.J. Mooney. Dual growth factor delivery and controlled scaffold degradation enhance in vivo bone formation by transplanted bone marrow stromal cells. Bone 2004;35(2):562-69.

65. Landa, N., L. Miller, M.S. Feinberg, R. Holbova, M. Shachar, I. Freeman, et al. Effect of injectable alginate implant on cardiac remodeling and function after recent and old infarcts in rat. Circulation 2008;117(11):1388-96.

66. Tsur-Gang, O., E. Ruvinov, N. Landa, R. Holbova, M.S. Feinberg, J. Leor, et al. The effects of peptide-based modification of alginate on left ventricular remodeling and function after myocardial infarction. Biomaterials 2009;30(2):189-95.

67. Yu, J., K.L. Christman, E. Chin, R.E. Sievers, M. Saeed, and R.J. Lee. Restoration of left ventricular geometry and improvement of left ventricular function in a rodent model of chronic ischemic cardiomyopathy. J Thorac Cardiovasc Surg 2009;137(1):180-7.

68. Hao, X., E.A. Silva, A. Mansson-Broberg, K.H. Grinnemo, A.J. Siddiqui, G. Dellgren, et al. Angiogenic effects of sequential release of VEGF-A165 and PDGF-BB with alginate hydrogels after myocardial infarction. Cardiovasc Res 2007;75(1):178-85.

69. Mihardja, S.S., R.E. Sievers, and R.J. Lee. The effect of polypyrrole on arteriogenesis in an acute rat infarct model. Biomaterials 2008;29(31):4205-10.

70. Yu, J., Y. Gu, K.T. Du, S. Mihardja, R.E. Sievers, and R.J. Lee. The effect of injected RGD modified alginate on angiogenesis and left ventricular function in a chronic rat infarct model. Biomaterials 2009;30(5):751-6.

71. Garner, B., A. Georgevich, A.J. Hodgson, L. Liu, and G.G. Wallace. Polypyrrole-heparin composites as stimulus-responsive substrates for endothelial cell growth. J Biomed Mater Res 1999;44(2):121-9.

72. Leor, J., S. Tuvia, V. Guetta, F. Manczur, D. Castel, U. Willenz, et al. Intracoronary injection of in situ forming alginate hydrogel reverses left ventricular remodeling after myocardial infarction in swine. J Am Coll Cardiol 2009;54(11):1014-23.

73. Lee, D.S., P.C. Austin, J.L. Rouleau, P.P. Liu, D. Naimark, and J.V. Tu. Predicting mortality among patients hospitalized for heart failure: derivation and validation of a clinical model. JAMA 2003;290(19):2581-7.

74. Breen, A., T. O'Brien, and A. Pandit. Fibrin as a Delivery System for Therapeutic Drugs and Biomolecules. Tissue Eng Part B Rev 2009.

75. Jackson, M.R. Fibrin sealants in surgical practice: An overview. Am J Surg 2001;182(2 Suppl):1S-7S.

76. Sierra, D.H. Fibrin sealant adhesive systems: a review of their chemistry, material properties and clinical applications. J Biomater Appl 1993;7(4):309-52.

77. Sierra, D.H., A.W. Eberhardt, and J.E. Lemons. Failure characteristics of multiple-component fibrin-based adhesives. J Biomed Mater Res 2002;59(1):1-11.

78. Christman, K.L., H.H. Fok, R.E. Sievers, Q. Fang, and R.J. Lee. Fibrin glue alone and skeletal myoblasts in a fibrin scaffold preserve cardiac function after myocardial infarction. Tissue Eng 2004;10(3-4):403-9.

79. Christman, K.L., A.J. Vardanian, Q. Fang, R.E. Sievers, H.H. Fok, and R.J. Lee. Injectable fibrin scaffold improves cell transplant survival, reduces infarct expansion, and induces neovasculature formation in ischemic myocardium. J Am Coll Cardiol 2004;44(3):654-60.

80. Christman, K.L., Q. Fang, M.S. Yee, K.R. Johnson, R.E. Sievers, and R.J. Lee. Enhanced neovasculature formation in ischemic myocardium following delivery of pleiotrophin plasmid in a biopolymer. Biomaterials 2005;26(10):1139-44.

81. Huang, N.F., J. Yu, R. Sievers, S. Li, and R.J. Lee. Injectable biopolymers enhance angiogenesis after myocardial infarction. Tissue Eng 2005;11(11-12):1860-6.

82. Auger, F.A., R. Guignard, C.A. Lo´pez Valle, and L. Germain. Role and innocuity of Tisseel®, a tissue glue, in the grafting process andin vivo evolution of human cultured epidermis. British Journal of Plastic Surgery 1993;46(2):136-42.

83. Kim, I.Y., S.J. Seo, H.S. Moon, M.K. Yoo, I.Y. Park, B.C. Kim, et al. Chitosan and its derivatives for tissue engineering applications. Biotechnol Adv 2008;26(1):1-21.

84. Khor, E. and L.Y. Lim. Implantable applications of chitin and chitosan. Biomaterials 2003;24(13):2339-49.

85. Chenite, A., C. Chaput, D. Wang, C. Combes, M.D. Buschmann, C.D. Hoemann, et al. Novel injectable neutral solutions of chitosan form biodegradable gels in situ. Biomaterials 2000;21(21):2155-61.

86. Dang, J.M., D.D. Sun, Y. Shin-Ya, A.N. Sieber, J.P. Kostuik, and K.W. Leong. Temperature-responsive hydroxybutyl chitosan for the culture of mesenchymal stem cells and intervertebral disk cells. Biomaterials 2006;27(3):406-18.

87. Lu, W.N., S.H. Lu, H.B. Wang, D.X. Li, C.M. Duan, Z.Q. Liu, et al. Functional improvement of infarcted heart by co-injection of embryonic stem cells with temperature-responsive chitosan hydrogel. Tissue Eng Part A 2009;15(6):1437-47.

88. Yeo, Y., W. Geng, T. Ito, D.S. Kohane, J.A. Burdick, and M. Radisic. Photocrosslinkable hydrogel for myocyte cell culture and injection. J Biomed Mater Res B Appl Biomater 2007;81(2):312-22.

89. Dobaczewski, M., C. Gonzalez-Quesada, and N.G. Frangogiannis. The extracellular matrix as a modulator of the inflammatory and reparative response following myocardial infarction. J Mol Cell Cardiol 2009.

90. Juliano, R.L. and S. Haskill. Signal transduction from the extracellular matrix. J Cell Biol 1993;120(3):577-85.

91. Badylak, S.F., D.O. Freytes, and T.W. Gilbert. Extracellular matrix as a biological scaffold material: Structure and function. Acta Biomaterialia 2009;5(1):1-13.

92. Tomihata, K., K. Burczak, K. Shiraki, and Y. Ikada, Cross-Linking and Biodegradation of Native and Denatured Collagen, in Polymers of Biological and Biomedical Significance. 1993, American Chemical Society: Washington, DC. p. 275-86.

93. Barocas, V.H., A.G. Moon, and R.T. Tranquillo. The fibroblast-populated collagen microsphere assay of cell traction force--Part 2: Measurement of the cell traction parameter. J Biomech Eng 1995;117(2):161-70.

94. Semler, E.J., C.S. Ranucci, and P.V. Moghe. Mechanochemical manipulation of hepatocyte aggregation can selectively induce or repress liver-specific function. Biotechnol Bioeng 2000;69(4):359-69.

95. Shao, Z.Q., K. Takaji, Y. Katayama, R. Kunitomo, H. Sakaguchi, Z.F. Lai, et al. Effects of intramyocardial administration of slow-release basic fibroblast growth factor on angiogenesis and ventricular remodeling in a rat infarct model. Circ J 2006;70(4):471-7.

96. Dai, W., L.E. Wold, J.S. Dow, and R.A. Kloner. Thickening of the infarcted wall by collagen injection improves left ventricular function in rats: a novel approach to preserve cardiac function after myocardial infarction. J Am Coll Cardiol 2005;46(4):714-9.

97. Kofidis, T., J.L. de Bruin, G. Hoyt, D.R. Lebl, M. Tanaka, T. Yamane, et al. Injectable bioartificial myocardial tissue for large-scale intramural cell transfer and functional recovery of injured heart muscle. J Thorac Cardiovasc Surg 2004;128(4):571-8.

98. Kofidis, T., D.R. Lebl, E.C. Martinez, G. Hoyt, M. Tanaka, and R.C. Robbins. Novel injectable bioartificial tissue facilitates targeted, less invasive, large-scale tissue restoration on the beating heart after myocardial injury. Circulation 2005;112(9 Suppl):I173-7.

99. Zhao, Z.Q., J.D. Puskas, D. Xu, N.P. Wang, M. Mosunjac, R.A. Guyton, et al. Improvement in cardiac function with small intestine extracellular matrix is associated with recruitment of C-kit cells, myofibroblasts, and macrophages after myocardial infarction. J Am Coll Cardiol 2010;55(12):1250-61.

100. Singelyn, J.M., J.A. Dequach, S.B. Seif-Naraghi, R.B. Littlefield, P.J. Schup-Magoffin, and K.L. Christman. Naturally derived myocardial matrix as an injectable scaffold for cardiac tissue engineering. Biomaterials 2009;30:5409-16.

101. Seif-Naraghi, S.B., M.A. Salvatore, P.J. Schup-Magoffin, D.P. Hu, and K.L. Christman. Design and characterization of an injectable pericardial matrix gel: a potentially autologous scaffold for cardiac tissue engineering. Tissue Eng Part A 2010;16(6):2017-27.

102. Ifkovits, J.L., E. Tous, M. Minakawa, M. Morita, J.D. Robb, K.J. Koomalsingh, et al. Injectable hydrogel properties influence infarct expansion and extent of postinfarction left ventricular remodeling in an ovine model. Proc Natl Acad Sci U S A 2010;107(25):11507-12.

103. Zhang, S. Fabrication of novel biomaterials through molecular self-assembly. Nat Biotechnol 2003;21(10):1171-8.

104. Zhao, X. and S. Zhang. Molecular designer self-assembling peptides. Chem Soc Rev 2006;35(11):1105-10.

105. Narmoneva, D.A., R. Vukmirovic, M.E. Davis, R.D. Kamm, and R.T. Lee. Endothelial cells promote cardiac myocyte survival and spatial reorganization: implications for cardiac regeneration. Circulation 2004;110(8):962-8.

106. Holmes, T.C. Novel peptide-based biomaterial scaffolds for tissue engineering. Trends Biotechnol 2002;20(1):16-21.

107. Davis, M.E., J.P. Motion, D.A. Narmoneva, T. Takahashi, D. Hakuno, R.D. Kamm, et al. Injectable self-assembling peptide nanofibers create intramyocardial microenvironments for endothelial cells. Circulation 2005;111(4):442-50.

108. Hsieh, P.C., C. MacGillivray, J. Gannon, F.U. Cruz, and R.T. Lee. Local controlled intramyocardial delivery of platelet-derived growth factor improves postinfarction ventricular function without pulmonary toxicity. Circulation 2006;114(7):637-44.

109. Hsieh, P.C., M.E. Davis, J. Gannon, C. MacGillivray, and R.T. Lee. Controlled delivery of PDGF-BB for myocardial protection using injectable self-assembling peptide nanofibers. J Clin Invest 2006;116(1):237-48.

110. Segers, V.F., T. Tokunou, L.J. Higgins, C. MacGillivray, J. Gannon, and R.T. Lee. Local delivery of protease-resistant stromal cell derived factor-1 for stem cell recruitment after myocardial infarction. Circulation 2007;116(15):1683-92.

111. Hoffman, A.S. Hydrogels for biomedical applications. Adv Drug Deliv Rev 2002;54(1):3-12.

112. Zheng Shu, X., Y. Liu, F.S. Palumbo, Y. Luo, and G.D. Prestwich. In situ crosslinkable hyaluronan hydrogels for tissue engineering. Biomaterials 2004;25(7-8):1339-48.

113. Wang, D.-a., C.G. Williams, Q. Li, B. Sharma, and J.H. Elisseeff. Synthesis and characterization of a novel degradable phosphate-containing hydrogel. Biomaterials 2003;24(22):3969-80.

114. Li, J., X. Ni, and K.W. Leong. Injectable drug-delivery systems based on supramolecular hydrogels formed by poly(ethylene oxide)s and alpha-cyclodextrin. Journal of Biomedical Materials Research Part A 2003;65A(2):196-202.

115. Lee, B.H. and B.L. Vernon. In situ-gelling, erodible N-isopropylacrylamide copolymers. Macromol Biosci 2005;5(7):629-35.

116. Wu, D.Q., T. Wang, B. Lu, X.D. Xu, S.X. Cheng, X.J. Jiang, et al. Fabrication of supramolecular hydrogels for drug delivery and stem cell encapsulation. Langmuir 2008;24(18):10306-12.

117. Jiang, X.J., T. Wang, X.Y. Li, D.Q. Wu, Z.B. Zheng, J.F. Zhang, et al. Injection of a novel synthetic hydrogel preserves left ventricle function after myocardial infarction. J Biomed Mater Res A 2009;90(2):472-7.

118. Wang, T., X.J. Jiang, T. Lin, S. Ren, X.Y. Li, X.Z. Zhang, et al. The inhibition of postinfarct ventricle remodeling without polycythaemia following local sustained intramyocardial delivery of erythropoietin within a supramolecular hydrogel. Biomaterials 2009;30(25):4161-7.

119. Dobner, S., D. Bezuidenhout, P. Govender, P. Zilla, and N. Davies. A synthetic non-degradable polyethylene glycol hydrogel retards adverse post-infarct left ventricular remodeling. Journal of Cardiac Failure 2009;15(7):629-36.

120. Jeong, B., S.W. Kim, and Y.H. Bae. Thermosensitive sol-gel reversible hydrogels. Adv Drug Deliv Rev 2002;54(1):37-51.

121. Guan, J., Y. Hong, Z. Ma, and W.R. Wagner. Protein-reactive, thermoresponsive copolymers with high flexibility and biodegradability. Biomacromolecules 2008;9(4):1283-92.

122. Ma, Z., D.M. Nelson, Y. Hong, and W.R. Wagner. Thermally Responsive Injectable Hydrogel Incorporating Methacrylate-Polylactide for Hydrolytic Lability. Biomacromolecules 2010;11(7):1873-81.

123. Wang, F., Z. Li, M. Khan, K. Tamama, P. Kuppusamy, W.R. Wagner, et al. Injectable, rapid gelling and highly flexible hydrogel composites as growth factor and cell carriers. Acta Biomater 2010;6(6):1978-91.

124. Kim, S. and K.E. Healy. Synthesis and characterization of injectable poly(N-isopropylacrylamide-co-acrylic acid) hydrogels with proteolytically degradable cross-links. Biomacromolecules 2003;4(5):1214-23.

125. Stile, R.A. and K.E. Healy. Thermo-responsive peptide-modified hydrogels for tissue regeneration. Biomacromolecules 2001;2(1):185-94.

126. Fujimoto, K.L., Z. Ma, D.M. Nelson, R. Hashizume, J. Guan, K. Tobita, et al. Synthesis, characterization and therapeutic efficacy of a biodegradable, thermoresponsive hydrogel designed for application in chronic infarcted myocardium. Biomaterials 2009;30(26):4357-68.

127. Wu, D.Q., F. Qiu, T. Wang, X.J. Jiang, X.Z. Zhang, and R.X. Zhuo. Toward the development of partially biodegradable and injectable thermoresponsive hydrogels for potential biomedical applications. ACS Appl Mater Interfaces 2009;1(2):319-27.

128. Wang, T., D.Q. Wu, X.J. Jiang, X.Z. Zhang, X.Y. Li, J.F. Zhang, et al. Novel thermosensitive hydrogel injection inhibits post-infarct ventricle remodelling. Eur J Heart Fail 2009;11(1):14-9.

129. Ryan, L.P., K. Matsuzaki, M. Noma, B.M. Jackson, T.J. Eperjesi, T.J. Plappert, et al. Dermal filler injection: a novel approach for limiting infarct expansion. Ann Thorac Surg 2009;87(1):148-55.

130. Jacovella, P.F. Use of calcium hydroxylapatite (Radiesse) for facial augmentation. Clin Interv Aging 2008;3(1):161-74.

131. Richardson, T.P., M.C. Peters, A.B. Ennett, and D.J. Mooney. Polymeric system for dual growth factor delivery. Nat Biotech 2001;19(11):1029-34.

132. Chen, R.R., E.A. Silva, W.W. Yuen, and D.J. Mooney. Spatio-temporal VEGF and PDGF delivery patterns blood vessel formation and maturation. Pharm Res 2007;24(2):258-64.

133. Davis, M.E., P.C. Hsieh, T. Takahashi, Q. Song, S. Zhang, R.D. Kamm, et al. Local myocardial insulin-like growth factor 1 (IGF-1) delivery with biotinylated peptide nanofibers improves cell therapy for myocardial infarction. Proc Natl Acad Sci U S A 2006;103(21):8155-60.

134. Kadner, K., S. Dobner, T. Franz, D. Bezuidenhout, M.S. Sirry, P. Zilla, et al. The beneficial effects of deferred delivery on the efficiency of hydrogel therapy post myocardial infarction. Biomaterials 2012;33(7):2060-6.

135. Hayakawa, K., G. Takemura, M. Kanoh, Y. Li, M. Koda, Y. Kawase, et al. Inhibition of Granulation Tissue Cell Apoptosis During the Subacute Stage of Myocardial Infarction Improves Cardiac Remodeling and Dysfunction at the Chronic Stage. Circulation 2003;108(1):104-9.

136. Richardson, T.P., M.C. Peters, A.B. Ennett, and D.J. Mooney. Polymeric system for dual growth factor delivery. Nat Biotechnol 2001;19(11):1029-34.

137. Sakakibara, Y., K. Tambara, G. Sakaguchi, F. Lu, M. Yamamoto, K. Nishimura, et al. Toward surgical angiogenesis using slow-released basic fibroblast growth factor. European Journal of Cardio-Thoracic Surgery 2003;24(1):105-12.

138. Lin, C.C. and A.T. Metters. Hydrogels in controlled release formulations: network design and mathematical modeling. Adv Drug Deliv Rev 2006;58(12-13):1379-408.

139. Amsden, B. A model for osmotic pressure driven release from cylindrical rubbery polymer matrices. J Control Release 2003;93(3):249-58.

140. Lao, L.L., S.S. Venkatraman, and N.A. Peppas. A novel model and experimental analysis of hydrophilic and hydrophobic agent release from biodegradable polymers. J Biomed Mater Res A 2009;90(4):1054-65.

141. Rothstein, S.N. and S.R. Little. A "tool box" for rational design of degradable controlled release formulations. Journal of Materials Chemistry 2011;21(1):29-39.

142. Li, B., K.V. Brown, J.C. Wenke, and S.A. Guelcher. Sustained release of vancomycin from polyurethane scaffolds inhibits infection of bone wounds in a rat femoral segmental defect model. J Control Release 2010;145(3):221-30.

143. Batycky, R.P., J. Hanes, R. Langer, and D.A. Edwards. A theoretical model of erosion and macromolecular drug release from biodegrading microspheres. J Pharm Sci 1997;86(12):1464-77.

144. Khan, M. and T. Shefeeq. Role of mathematical modeling in controlled drug delivery. J Scientific Res 2009;1(3):539-50.

145. Siepmann, J. and A. Gopferich. Mathematical modeling of bioerodible, polymeric drug delivery systems. Adv Drug Deliv Rev 2001;48(2-3):229-47.

146. Guo, Q., P.T. Knight, and P.T. Mather. Tailored drug release from biodegradable stent coatings based on hybrid polyurethanes. J Control Release 2009;137(3):224-33.

147. Rothstein, S.N., W.J. Federspiel, and S.R. Little. A unified mathematical model for the prediction of controlled release from surface and bulk eroding polymer matrices. Biomaterials 2009;30(8):1657-64.

148. Amsden, B.G. Biodegradable elastomers in drug delivery. Expert Opin Drug Deliv 2008;5(2):175-87.

149. Woo, G.L.Y., M.L. Yang, H.Q. Yin, F. Jaffer, M.W. Mittelman, and J.P. Santerre. Biological characterization of a novel biodegradable antimicrobial polymer synthesized with fluoroquinolones. J Biomed Mater Res 2002;59(1):35-45.

150. Manning, M.C., K. Patel, and R.T. Borchardt. Stability of protein pharmaceuticals. Pharmaceutical Research 1989;6(11):903-18.

151. Frokjaer, S. and D.E. Otzen. Protein drug stability: a formulation challenge. Nat Rev Drug Discov 2005;4(4):298-306.

152. Ye, M., S. Kim, and K. Park. Issues in long-term protein delivery using biodegradable microparticles. Journal of Controlled Release 2010;146(2):241-60.

153. van der Walle, C.F., G. Sharma, and M. Ravi Kumar. Current approaches to stabilising and analysing proteins during microencapsulation in PLGA. Expert Opin Drug Deliv 2009;6(2):177-86.

154. Hatefi, A. and B. Amsden. Biodegradable injectable in situ forming drug delivery systems. Journal of Controlled Release 2002;80(1–3):9-28.

155. Harris, J.M. and R.B. Chess. Effect of pegylation on pharmaceuticals. Nat Rev Drug Discov 2003;2(3):214-21.

156. Kokai, L.E., H. Tan, S. Jhunjhunwala, S.R. Little, J.W. Frank, and K.G. Marra. Protein bioactivity and polymer orientation is affected by stabilizer incorporation for double-walled microspheres. J Control Release 2010;141(2):168-76.

157. Pérez, C., I.J. Castellanos, H.R. Costantino, W. Al-Azzam, and K. Griebenow. Recent trends in stabilizing protein structure upon encapsulation and release from bioerodible polymers. Journal of Pharmacy and Pharmacology 2002;54(3):301-13.

158. Fischbach, C. and D.J. Mooney. Polymers for pro- and anti-angiogenic therapy. Biomaterials 2007;28(12):2069-76.

159. Baker, R.E. and P.K. Maini. Travelling gradients in interacting morphogen systems. Math Biosci 2007;209(1):30-50.

160. Kennedy, T.E., H. Wang, W. Marshall, and M. Tessier-Lavigne. Axon guidance by diffusible chemoattractants: a gradient of netrin protein in the developing spinal cord. J Neurosci 2006;26(34):8866-74.

161. Haugh, J.M., F. Codazzi, M. Teruel, and T. Meyer. Spatial sensing in fibroblasts mediated by 3' phosphoinositides. J Cell Biol 2000;151(6):1269-80.

162. Schneider, I.C. and J.M. Haugh. Quantitative elucidation of a distinct spatial gradient-sensing mechanism in fibroblasts. J Cell Biol 2005;171(5):883-92.

163. Makanya, A.N., D. Stauffer, D. Ribatti, P.H. Burri, and V. Djonov. Microvascular growth, development, and remodeling in the embryonic avian kidney: the interplay between sprouting and intussusceptive angiogenic mechanisms. Microsc Res Tech 2005;66(6):275-88.

164. Raftery, L.A. and D.J. Sutherland. Gradients and thresholds: BMP response gradients unveiled in Drosophila embryos. Trends Genet 2003;19(12):701-8.

165. Veitia, R.A. and I. Salazar-Ciudad. Commonalities in fly embryogenesis and mammalian pituitary patterning. Trends Endocrinol Metab 2007;18(7):261-5.

166. Ennett, A.B., D. Kaigler, and D.J. Mooney. Temporally regulated delivery of VEGF in vitro and in vivo. J Biomed Mater Res A 2006;79(1):176-84.

167. Phillippi, J.A., E. Miller, L. Weiss, J. Huard, A. Waggoner, and P. Campbell. Microenvironments engineered by inkjet bioprinting spatially direct adult stem cells toward muscle- and bone-like subpopulations. Stem Cells 2008;26(1):127-34.

168. McDevitt, T.C., J.C. Angello, M.L. Whitney, H. Reinecke, S.D. Hauschka, C.E. Murry, et al. In vitro generation of differentiated cardiac myofibers on micropatterned laminin surfaces. J Biomed Mater Res 2002;60(3):472-9.

169. McDevitt, T.C., K.A. Woodhouse, S.D. Hauschka, C.E. Murry, and P.S. Stayton. Spatially organized layers of cardiomyocytes on biodegradable polyurethane films for myocardial repair. J Biomed Mater Res A 2003;66(3):586-95.

170. Kim, D.N., W. Lee, and W.G. Koh. Micropatterning of proteins on the surface of three-dimensional poly(ethylene glycol) hydrogel microstructures. Anal Chim Acta 2008;609(1):59-65.

171. Campbell, P.G., E.D. Miller, G.W. Fisher, L.M. Walker, and L.E. Weiss. Engineered spatial patterns of FGF-2 immobilized on fibrin direct cell organization. Biomaterials 2005;26(33):6762-70.

172. Campbell, P.G. and L.E. Weiss. Tissue engineering with the aid of inkjet printers. Expert Opin Biol Ther 2007;7(8):1123-7.

173. Hong, S., D. Lee, H. Zhang, J.Q. Zhang, J.N. Resvick, A. Khademhosseini, et al. Covalent immobilization of p-selectin enhances cell rolling. Langmuir 2007;23(24):12261-8.

174. Miller, E.D., G.W. Fisher, L.E. Weiss, L.M. Walker, and P.G. Campbell. Dose-dependent cell growth in response to concentration modulated patterns of FGF-2 printed on fibrin. Biomaterials 2006;27(10):2213-21.

175. Wright, D., B. Rajalingam, J.M. Karp, S. Selvarasah, Y. Ling, J. Yeh, et al. Reusable, reversibly sealable parylene membranes for cell and protein patterning. J Biomed Mater Res A 2007;85A(2):530-8.

176. Storrie, H. and D.J. Mooney. Sustained delivery of plasmid DNA from polymeric scaffolds for tissue engineering. Adv Drug Deliv Rev 2006;58(4):500-14.

177. Jang, J.H., T.L. Houchin, and L.D. Shea. Gene delivery from polymer scaffolds for tissue engineering. Expert Rev Med Devices 2004;1(1):127-38.

178. Godbey, W.T., K.K. Wu, and A.G. Mikos. Poly(ethylenimine) and its role in gene delivery. J Control Release 1999;60(2-3):149-60.

179. Huang, Y.-H., G.T. Zugates, W. Peng, D. Holtz, C. Dunton, J.J. Green, et al. Nanoparticle-delivered suicide gene therapy effectively reduces ovarian tumor burden in mice. Cancer Research 2009;69(15):6184-91.

180. De Laporte, L., A. Huang, M.M. Ducommun, M.L. Zelivyanska, M.O. Aviles, A.F. Adler, et al. Patterned transgene expression in multiple-channel bridges after spinal cord injury. Acta Biomaterialia 2010;6(8):1889-97.

181. Houchin-Ray, T., L.A. Swift, J.-H. Jang, and L.D. Shea. Patterned PLG substrates for localized DNA delivery and directed neurite extension. Biomaterials 2007;28(16):2603-11.

182. Laporte, L.D., Y. Yang, M.L. Zelivyanskaya, B.J. Cummings, A.J. Anderson, and L.D. Shea. Plasmid releasing multiple channel bridges for transgene expression after spinal cord injury. Mol Ther 2008;17(2):318-26.

183. Clackson, T. Regulated gene expression systems. Gene Ther 2000;7(2):120-5.

184. Alexander, H.K., E.P. Booy, W. Xiao, P. Ezzati, H. Baust, and M. Los. Selected technologies to control genes and their products for experimental and clinical purposes. Arch Immunol Ther Exp (Warsz) 2007;55(3):139-49.

185. Vilaboa, N. and R. Voellmy. Regulatable gene expression systems for gene therapy. Curr Gene Ther 2006;6(4):421-38.

186. Goverdhana, S., M. Puntel, W. Xiong, J.M. Zirger, C. Barcia, J.F. Curtin, et al. Regulatable gene expression systems for gene therapy applications: progress and future challenges. Mol Ther 2005;12(2):189-211.

187. Karzenowski, D., D.W. Potter, and M. Padidam. Inducible control of transgene expression with ecdysone receptor: gene switches with high sensitivity, robust expression, and reduced size. Biotechniques 2005;39(2):191-2, 194, 196, 198-200.

188. Kumar, M.B., D.W. Potter, R.E. Hormann, A. Edwards, C.M. Tice, H.C. Smith, et al. Highly flexible ligand binding pocket of ecdysone receptor. Journal of Biological Chemistry 2004;279(26):27211-18.

189. Palli, S.R., M.Z. Kapitskaya, M.B. Kumar, and D.E. Cress. Improved ecdysone receptor-based inducible gene regulation system. Eur J Biochem 2003;270(6):1308-15.

190. Guan, J., M.S. Sacks, E.J. Beckman, and W.R. Wagner. Synthesis, characterization, and cytocompatibility of elastomeric, biodegradable poly(ester-urethane)ureas based on poly(caprolactone) and putrescine. J Biomed Mater Res 2002;61(3):493-503.

191. Cho, Y.W., J. Lee, S.C. Lee, K.M. Huh, and K. Park. Hydrotropic agents for study of in vitro paclitaxel release from polymeric micelles. Journal of Controlled Release 2004;97(2):249-57.

192. Solomon, O.F. and I.Z. Ciuta. Determination of the intrinsic viscosity of polymer solutions by a simple determination of viscosity. J Appl Polym Sci 1962;6(24):683-6.

193. Li, Y., T. Ma, D.A. Kniss, L.C. Lasky, and S.T. Yang. Effects of filtration seeding on cell density, spatial distribution, and proliferation in nonwoven fibrous matrices. Biotechnol Prog 2001;17(5):935-44.

194. Stankus, J.J., J. Guan, K. Fujimoto, and W.R. Wagner. Microintegrating smooth muscle cells into a biodegradable, elastomeric fiber matrix. Biomaterials 2006;27(5):735-44.

195. Lessard, J., S.B. Aicha, A. Fournier, E. Calvo, E. Lavergne, M. Pelletier, et al. Characterization of the RSL1-dependent conditional expression system in LNCaP prostate cancer cells and development of a single vector format. Prostate 2007;67(8):808-19.

196. Hashizume, R., K.L. Fujimoto, Y. Hong, N.J. Amoroso, K. Tobita, T. Miki, et al. Morphological and mechanical characteristics of the reconstructed rat abdominal wall following use of a wet electrospun biodegradable polyurethane elastomer scaffold. Biomaterials 2010;31(12):3253-65.

197. Nieponice, A., L. Soletti, J. Guan, Y. Hong, B. Gharaibeh, T.M. Maul, et al. In vivo assessment of a tissue-engineered vascular graft combining a biodegradable elastomeric scaffold and muscle-derived stem cells in a rat model. Tissue Eng Part A 2010;16(4):1215-23.

198. Grad, S., L. Kupcsik, K. Gorna, S. Gogolewski, and M. Alini. The use of biodegradable polyurethane scaffolds for cartilage tissue engineering: potential and limitations. Biomaterials 2003;24(28):5163-71.

199. Rashid, S.T., B. Fuller, G. Hamilton, and A.M. Seifalian. Tissue engineering of a hybrid bypass graft for coronary and lower limb bypass surgery. FASEB J. 2008;22(6):2084-9.

200. Sharifpoor, S., R.S. Labow, and J.P. Santerre. Synthesis and characterization of degradable polar hydrophobic ionic polyurethane scaffolds for vascular tissue engineering applications. Biomacromolecules 2009;10(10):2729-39.

201. Guan, J., J.J. Stankus, and W.R. Wagner. Biodegradable elastomeric scaffolds with basic fibroblast growth factor release. J Control Release 2007;120(1-2):70-8.

202. Liu, J., Y. Xiao, and C. Allen. Polymer–drug compatibility: A guide to the development of delivery systems for the anticancer agent, ellipticine. Journal of Pharmaceutical Sciences 2004;93(1):132-43.

203. Ieda, M., J.-D. Fu, P. Delgado-Olguin, V. Vedantham, Y. Hayashi, B.G. Bruneau, et al. Direct reprogramming of fibroblasts into functional cardiomyocytes by defined factors. Cell 2010;142(3):375-86.

204. Takahashi, K. and S. Yamanaka. Induction of pluripotent stem cells from mouse embryonic and adult fibroblast cultures by defined factors. Cell 2006;126(4):663-76.

205. Takeuchi, J.K. and B.G. Bruneau. Directed transdifferentiation of mouse mesoderm to heart tissue by defined factors. Nature 2009;459(7247):708-11.

206. Wichterle, H., I. Lieberam, J.A. Porter, and T.M. Jessell. Directed differentiation of embryonic stem cells into motor neurons. Cell 2002;110(3):385-97.

207. Zhou, Q., J. Brown, A. Kanarek, J. Rajagopal, and D.A. Melton. In vivo reprogramming of adult pancreatic exocrine cells to [bgr]-cells. Nature 2008;455(7213):627-32.

208. Wescoe, K.E., R.C. Schugar, C.R. Chu, and B.M. Deasy. The role of the biochemical and biophysical environment in chondrogenic stem cell differentiation assays and cartilage tissue engineering. Cell Biochem Biophys 2008;52(2):85-102.

209. DeLise, A.M. and R.S. Tuan. Alterations in the spatiotemporal expression pattern and function of N-Cadherin inhibit cellular condensation and chondrogenesis of limb mesenchymal cells in vitro. Journal of Cellular Biochemistry 2002;87(3):342-59.

210. He, W., A. Nieponice, L. Soletti, Y. Hong, B. Gharaibeh, M. Crisan, et al. Pericyte-based human tissue engineered vascular grafts. Biomaterials 2010;31(32):8235-44.

211. Stankus, J.J., L. Soletti, K. Fujimoto, Y. Hong, D.A. Vorp, and W.R. Wagner. Fabrication of cell microintegrated blood vessel constructs through electrohydrodynamic atomization. Biomaterials 2007;28(17):2738-46.

212. Breier, G., U. Albrecht, S. Sterrer, and W. Risau. Expression of vascular endothelial growth factor during embryonic angiogenesis and endothelial cell differentiation. Development 1992;114(2):521-32.

213. Owens, G.K. Regulation of differentiation of vascular smooth muscle cells. Physiological Reviews 1995;75(3):487-517.

214. Reusch, H.P., S. Zimmermann, M. Schaefer, M. Paul, and K. Moelling. Regulation of raf by akt controls growth and differentiation in vascular smooth muscle cells. Journal of Biological Chemistry 2001;276(36):33630-7.

215. Deans, T.L., A. Singh, M. Gibson, and J.H. Elisseeff. Regulating synthetic gene networks in 3D materials. Proceedings of the National Academy of Sciences 2012;109(38):15217-22.

216. Cress, D.E. The need for regulatable vectors for gene therapy for Parkinson's disease. Experimental Neurology 2008;209(1):30-3.

217. Rehfeldt, F., A.J. Engler, A. Eckhardt, F. Ahmed, and D.E. Discher. Cell responses to the mechanochemical microenvironment--implications for regenerative medicine and drug delivery. Adv Drug Deliv Rev 2007;59(13):1329-39.

218. Wells, R.G. The role of matrix stiffness in regulating cell behavior. Hepatology 2008;47(4):1394-400.

219. Ramaswami, P., Wagner, WR, Cardiovascular Tissue Engineering, in An Introduction to Biomaterials, S. Guelcher, JO Hollinger, Editor. 2006, CRC Press: Boca Raton, FL. p. 461-84.

220. Skarja, G.A. and K.A. Woodhouse. In vitro degradation and erosion of degradable, segmented polyurethanes containing an amino acid-based chain extender. J Biomater Sci Polym Ed 2001;12:851-73.

221. Guan, J. and W.R. Wagner. Synthesis, characterization and cytocompatibility of polyurethaneurea elastomers with designed elastase sensitivity. Biomacromolecules 2005;6(5):2833-42.

222. Gogolewski, S. and G. Galletti. Degradable, microporous vascular prosthesis from segmented polyurethane. Colloid & Polymer Science 1986;264(10):854-8.

223. Hafeman, A., B. Li, T. Yoshii, K. Zienkiewicz, J. Davidson, and S. Guelcher. Injectable biodegradable polyurethane scaffolds with release of platelet-derived growth factor for tissue repair and regeneration. Pharmaceutical Research 2008;25(10):2387-99.

224. Hafeman, A.E., K.J. Zienkiewicz, E. Carney, B. Litzner, C. Stratton, J.C. Wenke, et al. Local delivery of tobramycin from injectable biodegradable polyurethane scaffolds. J Biomater Sci Polym Ed 2010;21(1):95-112.

225. Sivak, W.N., J. Zhang, S. Petoud, and E.J. Beckman. Incorporation of ionic ligands accelerates drug release from LDI-glycerol polyurethanes. Acta Biomater 2010;6(1):144-53.

226. Stankus, J.J., D.O. Freytes, S.F. Badylak, and W.R. Wagner. Hybrid nanofibrous scaffolds from electrospinning of a synthetic biodegradable elastomer and urinary bladder matrix. J Biomater Sci Polym Ed 2008;19(5):635-52.

227. Zhang, J., B.A. Doll, E.J. Beckman, and J.O. Hollinger. A biodegradable polyurethane-ascorbic acid scaffold for bone tissue engineering. J Biomed Mater Res A 2003;67A(2):389-400.

228. Rosenthal, N. and A. Musaro. Gene therapy for cardiac cachexia? Int J Cardiol 2002;85(1):185-91.

229. Schulze, P.C., J. Fang, K.A. Kassik, J. Gannon, M. Cupesi, C. MacGillivray, et al. Transgenic overexpression of locally acting insulin-like growth factor-1 inhibits ubiquitin-mediated muscle atrophy in chronic left-ventricular dysfunction. Circ Res 2005;97(5):418-26.

230. Hayashi, S., H. Aso, K. Watanabe, H. Nara, M.T. Rose, S. Ohwada, et al. Sequence of IGF-I, IGF-II, and HGF expression in regenerating skeletal muscle. Histochem Cell Biol 2004;122(5):427-34.

231. Machida, S. and F.W. Booth. Insulin-like growth factor 1 and muscle growth: implication for satellite cell proliferation. Proc Nutr Soc 2004;63(2):337-40.

232. Padin-Iruegas, M.E., Y. Misao, M.E. Davis, V.F. Segers, G. Esposito, T. Tokunou, et al. Cardiac progenitor cells and biotinylated insulin-like growth factor-1 nanofibers improve endogenous and exogenous myocardial regeneration after infarction. Circulation 2009;120(10):876-87.

233. Jin, H., J.M. Wyss, R. Yang, and R. Schwall. The therapeutic potential of hepatocyte growth factor for myocardial infarction and heart failure. Curr Pharm Des 2004;10(20):2525-33.

234. Duan, H.F., C.T. Wu, D.L. Wu, Y. Lu, H.J. Liu, X.Q. Ha, et al. Treatment of myocardial ischemia with bone marrow-derived mesenchymal stem cells overexpressing hepatocyte growth factor. Mol Ther 2003;8(3):467-74.

235. Ueda, H., T. Nakamura, K. Matsumoto, Y. Sawa, and H. Matsuda. A potential cardioprotective role of hepatocyte growth factor in myocardial infarction in rats. Cardiovasc Res 2001;51(1):41-50.

236. Ellison, G.M., D. Torella, S. Dellegrottaglie, C. Perez-Martinez, A. Perez de Prado, C. Vicinanza, et al. Endogenous cardiac stem cell activation by insulin-like growth factor-1/hepatocyte growth factor intracoronary injection fosters survival and regeneration of the infarcted pig heart. Journal of the American College of Cardiology 2011;58(9):977-86.

237. Aoki, M., R. Morishita, Y. Taniyama, I. Kida, A. Moriguchi, K. Matsumoto, et al. Angiogenesis induced by hepatocyte growth factor in non-infarcted myocardium and infarcted myocardium: up-regulation of essential transcription factor for angiogenesis, ets. Gene Ther 2000;7(5):417-27.

238. Pulavendran, S., M. Rajam, C. Rose, and A.B. Mandal. Hepatocyte growth factor incorporated chitosan nanoparticles differentiate murine bone marrow mesenchymal stem cell into hepatocytes in vitro. IET Nanobiotechnol 2010;4(3):51.

239. Kato, N., K. Nakanishi, and K. Nemoto. Efficacy of HGF gene transfer for various nervous injuries and disorders. Cent Nerv Syst Agents Med Chem 2009;9(4):300-6.

240. Guan, J., K.L. Fujimoto, M.S. Sacks, and W.R. Wagner. Preparation and characterization of highly porous, biodegradable polyurethane scaffolds for soft tissue applications. Biomaterials 2005;26(18):3961-71.

241. Kricker, J.A., C.L. Towne, S.M. Firth, A.C. Herington, and Z. Upton. Structural and functional evidence for the interaction of insulin-like growth factors (IGFs) and IGF binding proteins with vitronectin. Endocrinology 2003;144(7):2807-15.

242. Liu, X.J., Q. Xie, Y.F. Zhu, C. Chen, and N. Ling. Identification of a nonpeptide ligand that releases bioactive insulin-like growth factor-I from its binding protein complex. J Biol Chem 2001;276(35):32419-22.

243. Singh, M., B. Shirley, K. Bajwa, E. Samara, M. Hora, and D. O'Hagan. Controlled release of recombinant insulin-like growth factor from a novel formulation of polylactide-co-glycolide microparticles. J Control Release 2001;70(1-2):21-8.

244. Bussolino, F., M.F. Di Renzo, M. Ziche, E. Bocchietto, M. Olivero, L. Naldini, et al. Hepatocyte growth factor is a potent angiogenic factor which stimulates endothelial cell motility and growth. J Cell Biol 1992;119(3):629-41.

245. Gu, F., R. Neufeld, and B. Amsden. Sustained release of bioactive therapeutic proteins from a biodegradable elastomeric device. J Control Release 2007;117(1):80-9.

246. Gu, F., R. Neufeld, and B. Amsden. Osmotic-driven release kinetics of bioactive therapeutic proteins from a biodegradable elastomer are linear, constant, similar, and adjustable. Pharm Res 2006;23(4):782-9.

247. Hirose, K., A. Marui, Y. Arai, T. Nomura, S. Inoue, K. Kaneda, et al. Sustained-release vancomycin sheet may help to prevent prosthetic graft methicillin-resistant Staphylococcus aureus infection. Journal of Vascular Surgery 2006;44(2):377-82.

248. Li, B., J.M. Davidson, and S.A. Guelcher. The effect of the local delivery of platelet-derived growth factor from reactive two-component polyurethane scaffolds on the healing in rat skin excisional wounds. Biomaterials 2009;30(20):3486-94.

249. Cui, F., D. Cun, A. Tao, M. Yang, K. Shi, M. Zhao, et al. Preparation and characterization of melittin-loaded poly (dl-lactic acid) or poly (dl-lactic-co-glycolic acid) microspheres made by the double emulsion method. J Control Release 2005;107(2):310-9.

250. Cometa, S., I. Bartolozzi, A. Corti, F. Chiellini, E. De Giglio, and E. Chiellini. Hydrolytic and microbial degradation of multi-block polyurethanes based on poly([var epsilon]-

caprolactone)/poly(ethylene glycol) segments. Polymer Degradation and Stability 2010;95(10):2013-21.

251. Santerre, J.P., K. Woodhouse, G. Laroche, and R.S. Labow. Understanding the biodegradation of polyurethanes: From classical implants to tissue engineering materials. Biomaterials 2005;26(35):7457-70.

252. Labow, R.S., E. Meek, and J.P. Santerre. Hydrolytic degradation of poly(carbonate)-urethanes by monocyte-derived macrophages. Biomaterials 2001;22(22):3025-33.

253. Labow, R.S., E. Meek, and J.P. Santerre. Model systems to assess the destructive potential of human neutrophils and monocyte-derived macrophages during the acute and chronic phases of inflammation. J Biomed Mater Res 2001;54(2):189-97.

254. Peng, H., J. Ling, J. Liu, N. Zhu, X. Ni, and Z. Shen. Controlled enzymatic degradation of poly(caprolactone)-based copolymers in the presence of porcine pancreatic lipase. Polymer Degradation and Stability 2010;95(4):643-50.

255. Labow, R.S., D.J. Erfle, and J.P. Santerre. Neutrophil-mediated degradation of segmented polyurethanes. Biomaterials 1995;16(1):51-9.

256. Labow, R.S., D. Sa, L.A. Matheson, D.L.M. Dinnes, and J. Paul Santerre. The human macrophage response during differentiation and biodegradation on polycarbonate-based polyurethanes: Dependence on hard segment chemistry. Biomaterials 2005;26(35):7357-66.

257. Tang, Y.W., R.S. Labow, I. Revenko, and J.P. Santerre. Influence of surface morphology and chemistry on the enzyme catalyzed biodegradation of polycarbonate-urethanes. J Biomater Sci Polym Ed 2002;13:463-83.

258. Carrascosa, C., I. Torres-Aleman, C. Lopez-Lopez, E. Carro, L. Espejo, S. Torrado, et al. Microspheres containing insulin-like growth factor I for treatment of chronic neurodegeneration. Biomaterials 2004;25(4):707-14.

259. Lam, X.M., E.T. Duenas, A.L. Daugherty, N. Levin, and J.L. Cleland. Sustained release of recombinant human insulin-like growth factor-I for treatment of diabetes. Journal of Controlled Release 2000;67(2-3):281-92.

260. Tambara, K., G.U. Premaratne, G. Sakaguchi, N. Kanemitsu, X. Lin, H. Nakajima, et al. Administration of control-released hepatocyte growth factor enhances the efficacy of skeletal myoblast transplantation in rat infarcted hearts by greatly increasing both quantity and quality of the graft. Circulation 2005;112(9 Suppl):I129-34.

261. Gutowska, A., B. Jeong, and M. Jasionowski. Injectable gels for tissue engineering. The Anatomical Record 2001;263(4):342-9.

262. Kretlow, J.D., L. Klouda, and A.G. Mikos. Injectable matrices and scaffolds for drug delivery in tissue engineering. Advanced Drug Delivery Reviews 2007;59(4-5):263-73.

263. Yu, L. and J. Ding. Injectable hydrogels as unique biomedical materials. Chem Soc Rev 2008;37(8):1473-81.

264. Stile, R.A., W.R. Burghardt, and K.E. Healy. Synthesis and characterization of injectable poly(N-isopropylacrylamide)-based hydrogels that support tissue formation in vitro. Macromolecules 1999;32(22):7370-9.

265. Ma, Z., D.M. Nelson, Y. Hong, and W.R. Wagner. Thermally responsive injectable hydrogel incorporating methacrylate-polylactide for hydrolytic lability. Biomacromolecules 2010;11(7):1873-81.

266. Lee, B.H., B. West, R. McLemore, C. Pauken, and B.L. Vernon. In-situ injectable physically and chemically gelling NIPAAm-based copolymer system for embolization. Biomacromolecules 2006;7(6):2059-64.

267. Cui, Z., B.H. Lee, C. Pauken, and B.L. Vernon. Manipulating degradation time in a N-isopropylacrylamide-based co-polymer with hydrolysis-dependent LCST. Journal of Biomaterials Science, Polymer Edition 2010;21:913-26.

268. Overstreet, D.J., H.D. Dhruv, and B.L. Vernon. Bioresponsive copolymers of poly(N-isopropylacrylamide) with enzyme-dependent lower critical solution temperatures. Biomacromolecules 2010;11(5):1154-9.

269. Chen, J.P. and T.H. Cheng. Thermo-responsive chitosan-graft-poly(N-isopropylacrylamide) injectable hydrogel for cultivation of chondrocytes and meniscus cells. Macromol Biosci 2006;6(12):1026-39.

270. Vernengo, J., G.W. Fussell, N.G. Smith, and A.M. Lowman. Evaluation of novel injectable hydrogels for nucleus pulposus replacement. Journal of Biomedical Materials Research Part B: Applied Biomaterials 2008;84B(1):64-9.

271. Ibusuki, S., Y. Fujii, Y. Iwamoto, and T. Matsuda. Tissue-engineered cartilage using an injectable and in situ gelable thermoresponsive gelatin: fabrication and in vitro performance. Tissue Engineering 2003;9(2):371-84.

272. Babensee, J.E., L.V. McIntire, and A.G. Mikos. Growth factor delivery for tissue engineering. Pharmaceutical Research 2000;17(5):497-504.

273. Sinha, V.R. and A. Trehan. Biodegradable microspheres for protein delivery. Journal of Controlled Release 2003;90(3):261-80.

274. Hoare, T.R. and D.S. Kohane. Hydrogels in drug delivery: progress and challenges. Polymer 2008;49(8):1993-2007.

275. Holland, T.A., Y. Tabata, and A.G. Mikos. In vitro release of transforming growth factor-[beta]1 from gelatin microparticles encapsulated in biodegradable, injectable oligo(poly(ethylene glycol) fumarate) hydrogels. Journal of Controlled Release 2003;91(3):299-313.

276. Patel, Z., H. Ueda, M. Yamamoto, Y. Tabata, and A. Mikos. In vitro and in vivo release of vascular endothelial growth factor from gelatin microparticles and biodegradable composite scaffolds. Pharmaceutical Research 2008;25(10):2370-8.

277. DeFail, A.J., C.R. Chu, N. Izzo, and K.G. Marra. Controlled release of bioactive TGF-[beta]1 from microspheres embedded within biodegradable hydrogels. Biomaterials 2006;27(8):1579-85.

278. Lee, J., C.Y. Tan, S.-K. Lee, Y.-H. Kim, and K.Y. Lee. Controlled delivery of heat shock protein using an injectable microsphere/hydrogel combination system for the treatment of myocardial infarction. Journal of Controlled Release 2009;137(3):196-202.

279. Park, M.-R., C. Chun, S.-W. Ahn, M.-H. Ki, C.-S. Cho, and S.-C. Song. Sustained delivery of human growth hormone using a polyelectrolyte complex-loaded thermosensitive polyphosphazene hydrogel. Journal of Controlled Release 2010;147(3):359-67.

280. Holland, T.A., Y. Tabata, and A.G. Mikos. Dual growth factor delivery from degradable oligo(poly(ethylene glycol) fumarate) hydrogel scaffolds for cartilage tissue engineering. Journal of Controlled Release 2005;101(1-3):111-25.

281. Holland, T.A., E.W.H. Bodde, V.M.J.I. Cuijpers, L.S. Baggett, Y. Tabata, A.G. Mikos, et al. Degradable hydrogel scaffolds for in vivo delivery of single and dual growth factors in cartilage repair. Osteoarthritis and Cartilage 2007;15(2):187-97.

282. Peattie, R.A., E.R. Rieke, E.M. Hewett, R.J. Fisher, X.Z. Shu, and G.D. Prestwich. Dual growth factor-induced angiogenesis in vivo using hyaluronan hydrogel implants. Biomaterials 2006;27(9):1868-75.

283. Buket Basmanav, F., G.T. Kose, and V. Hasirci. Sequential growth factor delivery from complexed microspheres for bone tissue engineering. Biomaterials 2008;29(31):4195-204.

284. Tengood, J.E., K.M. Kovach, P.E. Vescovi, A.J. Russell, and S.R. Little. Sequential delivery of vascular endothelial growth factor and sphingosine 1-phosphate for angiogenesis. Biomaterials 2010;31(30):7805-12.

285. Kim, B.S., J.M. Oh, K.S. Kim, K.S. Seo, J.S. Cho, G. Khang, et al. BSA-FITC-loaded microcapsules for in vivo delivery. Biomaterials 2009;30(5):902-9.

286. Ahmed, B., M.Z. Kamal, and R.H. Khan. Alkali-induced conformational transition in different domains of bovine serum albumin. Protein and Peptide Letters 2004;11:307-15.

287. Nelson, D.M., Z. Ma, K.L. Fujimoto, R. Hashizume, and W.R. Wagner. Intra-myocardial biomaterial injection therapy in the treatment of heart failure: materials, outcomes and challenges. Acta Biomaterialia 2011;7(1):1-15.

288. Laham, R.J., F.W. Sellke, E.R. Edelman, J.D. Pearlman, J.A. Ware, D.L. Brown, et al. Local perivascular delivery of basic fibroblast growth factor in patients undergoing coronary bypass surgery : Results of a phase I randomized, double-blind, placebo-controlled trial. Circulation 1999;100(18):1865-71.

289. Iwakura, A., M. Fujita, K. Kataoka, K. Tambara, Y. Sakakibara, M. Komeda, et al. Intramyocardial sustained delivery of basic fibroblast growth factor improves angiogenesis and ventricular function in a rat infarct model. Heart Vessels 2003;18(2):93-9.

290. Crotts, G. and T.G. Park. Preparation of porous and nonporous biodegradable polymeric hollow microspheres. Journal of Controlled Release 1995;35(2-3):91-105.

291. Yang, Y.-Y., H.-H. Chia, and T.-S. Chung. Effect of preparation temperature on the characteristics and release profiles of PLGA microspheres containing protein fabricated by double-emulsion solvent extraction/evaporation method. Journal of Controlled Release 2000;69(1):81-96.

292. Mao, S., J. Xu, C. Cai, O. Germershaus, A. Schaper, and T. Kissel. Effect of WOW process parameters on morphology and burst release of FITC-dextran loaded PLGA microspheres. International Journal of Pharmaceutics 2007;334(1-2):137-48.

293. Ruvinov, E., J. Leor, and S. Cohen. The promotion of myocardial repair by the sequential delivery of IGF-1 and HGF from an injectable alginate biomaterial in a model of acute myocardial infarction. Biomaterials 2011;32(2):565-78.

294. Brazel, C.S. and N.A. Peppas. Pulsatile local delivery of thrombolytic and antithrombotic agents using poly(N-isopropylacrylamide-co-methacrylic acid) hydrogels. Journal of Controlled Release 1996;39(1):57-64.

295. Huang, X. and T.L. Lowe. Biodegradable thermoresponsive hydrogels for aqueous encapsulation and controlled release of hydrophilic model drugs. Biomacromolecules 2005;6(4):2131-9.

296. Roberts, M.J., M.D. Bentley, and J.M. Harris. Chemistry for peptide and protein PEGylation. Adv Drug Deliv Rev 2002;54(4):459-76.

297. Rane, A.A. and K.L. Christman. Biomaterials for the treatment of myocardial infarction: A 5-year update. Journal of the American College of Cardiology 2011;58(25):2615-29.

298. Ifkovits, J.L., E. Tous, M. Minakawa, M. Morita, J.D. Robb, K.J. Koomalsingh, et al. Injectable hydrogel properties influence infarct expansion and extent of postinfarction left ventricular remodeling in an ovine model. Proceedings of the National Academy of Sciences 2010;107(25):11507-12.

299. Tous, E., J.L. Ifkovits, K.J. Koomalsingh, T. Shuto, T. Soeda, N. Kondo, et al. Influence of injectable hyaluronic acid hydrogel degradation behavior on infarction-induced ventricular remodeling. Biomacromolecules 2011;12(11):4127-35.

300. Rane, A.A., J.S. Chuang, A. Shah, D.P. Hu, N.D. Dalton, Y. Gu, et al. Increased infarct wall thickness by a bio-Inert material is insufficient to prevent negative left ventricular remodeling after myocardial infarction. PLoS ONE 2011;6(6):e21571.

301. Hughes, G.C., S.S. Biswas, B. Yin, R.E. Coleman, T.R. DeGrado, C.K. Landolfo, et al. Therapeutic angiogenesis in chronically ischemic porcine myocardium: comparative effects of bFGF and VEGF. The Annals of Thoracic Surgery 2004;77(3):812-8.

302. Laham, R.J., M. Rezaee, M. Post, D. Novicki, F.W. Sellke, J.D. Pearlman, et al. Intrapericardial delivery of fibroblast growth factor-2 induces neovascularization in a porcine model of chronic myocardial ischemia. J Pharmacol Exp Ther 2000;292(2):795-802.

303. Garbern, J.C., E. Minami, P.S. Stayton, and C.E. Murry. Delivery of basic fibroblast growth factor with a pH-responsive, injectable hydrogel to improve angiogenesis in infarcted myocardium. Biomaterials 2011;32(9):2407-16.

304. Wang, H., X. Zhang, Y. Li, Y. Ma, Y. Zhang, Z. Liu, et al. Improved myocardial performance in infarcted rat heart by co-injection of basic fibroblast growth factor with temperature-responsive Chitosan hydrogel. The Journal of Heart and Lung Transplantation 2010;29(8):881-7.

305. Wu, J., F. Zeng, X.-P. Huang, J.C.Y. Chung, F. Konecny, R.D. Weisel, et al. Infarct stabilization and cardiac repair with a VEGF-conjugated, injectable hydrogel. Biomaterials 2011;32(2):579-86.

306. Suleiman, M.S., R.J. Singh, and C.E. Stewart. Apoptosis and the cardiac action of insulin-like growth factor I. Pharmacol Ther 2007;114(3):278-94.

307. Urbanek, K., M. Rota, S. Cascapera, C. Bearzi, A. Nascimbene, A. De Angelis, et al. Cardiac stem cells possess growth factor-receptor systems that after activation regenerate the infarcted myocardium, improving ventricular function and long-term survival. Circulation Research 2005;97(7):663-73.

308. Cheng, K., K. Malliaras, D. Shen, E. Tseliou, V. Ionta, J. Smith, et al. Intramyocardial injection of platelet gel promotes endogenous repair and augments cardiac function in rats with myocardial infarction. J Am Coll Cardiol 2012;59(3):256-64.

309. Tengood, J.E., R. Ridenour, R. Brodsky, A.J. Russell, and S.R. Little. Sequential delivery of basic fibroblast growth factor and platelet-derived growth factor for angiogenesis. Tissue Engineering Part A 2011;17(9-10):1181-9.

310. Anderson, J.M., A. Rodriguez, and D.T. Chang. Foreign body reaction to biomaterials. Seminars in Immunology 2008;20(2):86-100.

311. Brown, B.N., B.D. Ratner, S.B. Goodman, S. Amar, and S.F. Badylak. Macrophage polarization: An opportunity for improved outcomes in biomaterials and regenerative medicine. Biomaterials 2012;33(15):3792-802.

312. Sunderkötter, C., K. Steinbrink, M. Goebeler, R. Bhardwaj, and C. Sorg. Macrophages and angiogenesis. Journal of Leukocyte Biology 1994;55(3):410-22.

313. Badylak, S.F., J.E. Valentin, A.K. Ravindra, G.P. McCabe, and A.M. Stewart-Akers. Macrophage phenotype as a determinant of biological scaffold remodeling. Tissue Eng Part A 2008;14(11):1835-42.

314. Singelyn, J.M., P. Sundaramurthy, T.D. Johnson, P.J. Schup-Magoffin, D.P. Hu, D.M. Faulk, et al. Catheter-deliverable hydrogel derived from decellularized ventricular extracellular matrix increases endogenous cardiomyocytes and preserves cardiac function post-myocardial infarction. Journal of the American College of Cardiology 2012;59(8):751-63.

315. Carmeliet, P. and D. Collen. Molecular basis of angiogenesis: role of VEGF and VE-Cadherin. Annals of the New York Academy of Sciences 2000;902(1):249-64.

316. Henry, T.D., B.H. Annex, G.R. McKendall, M.A. Azrin, J.J. Lopez, F.J. Giordano, et al. The VIVA trial: vascular endothelial growth factor in ischemia for vascular angiogenesis. Circulation 2003;107(10):1359-65.

317. Kwon, J.S., I.K. Park, A.S. Cho, S.M. Shin, M.H. Hong, S.Y. Jeong, et al. Enhanced angiogenesis mediated by vascular endothelial growth factor plasmid-loaded thermo-responsive amphiphilic polymer in a rat myocardial infarction model. Journal of Controlled Release 2009;138(2):168-76.

318. Elçin, Y.M., V. Dixit, and G. Gitnick. Extensive in vivo angiogenesis following controlled release of human vascular endothelial cell growth factor: implications for tissue engineering and wound healing. Artificial Organs 2001;25(7):558-65.

319. Zarafshani, Z., T. Obata, and J.-F.o. Lutz. Smart PEGylation of trypsin. Biomacromolecules 2010;11(8):2130-5.

320. Yockman, J.W., A. Kastenmeier, H.M. Erickson, J.G. Brumbach, M.G. Whitten, A. Albanil, et al. Novel polymer carriers and gene constructs for treatment of myocardial ischemia and infarction. Journal of Controlled Release 2008;132(3):260-6.

321. Patronik, N.A., T. Ota, M.A. Zenati, and C.N. Riviere. A miniature mobile robot for navigation and positioning on the beating heart. Robotics, IEEE Transactions on 2009;25(5):1109-24.

322. Chapman, M.P., J.L. Lopez Gonzalez, B.E. Goyette, K.L. Fujimoto, M. Zuwei, W.R. Wagner, et al. Application of the HeartLander crawling robot for injection of a thermally sensitive anti-remodeling agent for myocardial infarction therapy. in Engineering in Medicine and Biology Society (EMBC), 2010 Annual International Conference of the IEEE. 2010.

323. Klocke, R., W. Tian, M.T. Kuhlmann, and S. Nikol. Surgical animal models of heart failure related to coronary heart disease. Cardiovascular Research 2007;74(1):29-38.

324. Hetrick, E.M. and M.H. Schoenfisch. Reducing implant-related infections: active release strategies. Chemical Society Reviews 2006;35(9).

325. Hong, Y., K. Fujimoto, R. Hashizume, J. Guan, J.J. Stankus, K. Tobita, et al. Generating elastic, biodegradable polyurethane/poly(lactide-co-glycolide) fibrous sheets with controlled antibiotic release via two-stream electrospinning. Biomacromolecules 2008;9(4):1200-7.

326. Schmidmaier, G., M. Lucke, B. Wildemann, N.P. Haas, and M. Raschke. Prophylaxis and treatment of implant-related infections by antibiotic-coated implants: a review. Injury 2006;37(2, Supplement):S105-12.

327. Darouiche, R.O. Treatment of infections associated with surgical implants. New England Journal of Medicine 2004;350(14):1422-9.

328. Holman, W.L., B.K. Rayburn, D.C. McGiffin, B.A. Foley, R.L. Benza, R.C. Bourge, et al. Infection in ventricular assist devices: prevention and treatment. The Annals of Thoracic Surgery 2003;75(6, Supplement):S48-S57.

329. Hutchinson, O.Z., M.C. Oz, and J.A. Ascherman. The use of muscle flaps to treat left ventricular assist device infections. Plastic and Reconstructive Surgery 2001;107(2):364-73.

330. Manahan, M.A., N.H. Goldberg, and R.P. Silverman. Successful salvage of ventricular-assist devices in the setting of pump pocket infection. Annals of Plastic Surgery 2006;57(4):435-9.

331. Holman, W.L., R.J. Fix, B.A. Foley, D.C. McGiffin, B.K. Rayburn, and J.K. Kirklin. Management of wound and left ventricular assist device pocket infection. The Annals of Thoracic Surgery 1999;68(3):1080-2.

332. McKellar, S.H., B.D. Allred, J.D. Marks, C.G. Cowley, D.C. Classen, S.C. Gardner, et al. Treatment of infected left ventricular assist device using antibiotic-impregnated beads. The Annals of Thoracic Surgery 1999;67(2):554-5.

333. van de Belt, H., D. Neut, D.R.A. Uges, W. Schenk, J.R. van Horn, H.C. van der Mei, et al. Surface roughness, porosity and wettability of gentamicin-loaded bone cements and their antibiotic release. Biomaterials 2000;21(19):1981-7.

334. Engel, F.B., P.C. Hsieh, R.T. Lee, and M.T. Keating. FGF1/p38 MAP kinase inhibitor therapy induces cardiomyocyte mitosis, reduces scarring, and rescues function after myocardial infarction. Proc Natl Acad Sci U S A 2006;103(42):15546-51.

335. Seshadri, G., J.C. Sy, M. Brown, S. Dikalov, S.C. Yang, N. Murthy, et al. The delivery of superoxide dismutase encapsulated in polyketal microparticles to rat myocardium and protection from myocardial ischemia-reperfusion injury. Biomaterials 2010;31(6):1372-9.

336. Sy, J. and M. Davis. Delivering regenerative cues to the heart: cardiac drug delivery by microspheres and peptide nanofibers. Journal of Cardiovascular Translational Research 2010;3(5):461-8.

337. Hamdi, H., A. Furuta, V. Bellamy, A. Bel, E. Puymirat, S. Peyrard, et al. Cell delivery: intramyocardial injections or epicardial deposition? a head-to-head comparison. The Annals of Thoracic Surgery 2009;87(4):1196-203.

338. Zhang, G., Q. Hu, E.A. Braunlin, L.J. Suggs, and J. Zhang. Enhancing efficacy of stem cell transplantation to the heart with a PEGylated fibrin biomatrix. Tissue Eng Part A 2008;14(6):1025-36.

339. Muller-Ehmsen, J., P. Whittaker, R.A. Kloner, J.S. Dow, T. Sakoda, T.I. Long, et al. Survival and development of neonatal rat cardiomyocytes transplanted into adult myocardium. J Mol Cell Cardiol 2002;34(2):107-16.